UNIVERSITÀ DEGLI STUDI DI PALERMO
DOTTORATO IN PROGETTAZIONE MECCANICA
DIPARTIMENTO DELL' INNOVAZIONE INDUSTRIALE E DIGITALE (DIID)-
INGEGNERIA CHIMICA, GESTIONALE, INFORMATICA, MECCANICA
SSD ING-IND/13 MECCANICA APPLICATA ALLE MACCHINE

HEALTH MONITORING, FAULT DETECTION AND DIAGNOSIS IN INDUSTRIAL ROTATING MACHINERY BY ADVANCED VIBRATION ANALYSIS

IL DOTTORE
Karamoko Diarrassouba

IL COORDINATORE
Prof. Salvatore Gaglio

IL TUTOR
Prof. Marco Cammalleri

IL TUTOR AZIENDALE
Ing. Franco Porzio
SKF Solution Factory-Italy

CICLO XXVI
ANNO CONSEGUIMENTO TITOLO 2017

SOMMARY

Acknowledgment

I would like to express my gratitude to my doctoral advisor Prof. Marco Cammalleri for his patience, guidance and invaluable support throughout the realisation of this research.

My sincere gratitude to SKF Italy, in particular to Ing. Roberto Tomasi, Ing. Luca Lemma and Ing. Georgio Beato. My sincere gratitude to my company tutor, Ing. Franco Porzio, to the Ing. Francesco Caracciolo and to all those who supported me in this research.

Grand part of my research work was held during the weekend and holidays. I therefore thank my family, especially my wife Diarrassouba Kitungwa Euphrasie for her understanding, her be patient and her support.

Ultimately, I would like to dedicate this PhD work to my Mother and the memory of my Father.

Liste of Symbols

a	*Vibration acceleration*
A	*the mixing matrix (q×k) consisting of unknown mixture coefficientsi*
A_{Sup_DE}	*Axial direction on support drive end*
α	*Bearing Contact angle*
Λ	*degree of asperity interaction*
B	*separation matrix*
b_d	*Bearing ball diameter*
b_n	*Bearing Ball Number*
$BPFI$	*Inner race defect frequency*
$BPFO$	*Outer race defect frequency*
BSF	*Ball defect frequency*
σ_b	*RMS roughness of the ball and.*
σ_r	*RMS roughness of the raceway*
σ	*vibration overall value standard deviation*
C	*Basic dynamic load rating*
C_0	*basic static load rating*
$C_{single\ bearing}$	*Basic dynamic load rating of single angular contact ball bearing*
$C_{0\ Single\ bearing}$	*basic static load rating of single angular contact ball bearing*
D	*bearing bore diameter*
d_1	*Distance between centrifugal force F and the support NDE*
d_2	*Distance between centrifugal force F and the support DE*
d_3	*Distance between correction plan and the support DE*
l	*Distance between the support NDE and the support DE*
e	*the eccentricity in the disc*
f	*Vibration frequency*
f(t)	*forced vibration function*
Δf	*frequency resolution*

F	*excitation force amplitude*
f_n	*natural frequency*
f_{max}	*Spectrum maximum frequency*
f_M	*Analog signal frequency*
f_s	*Sampling frequency*
f_u	*Lubrication factor, the rate of lubricated system speed to the diametrical load*
F_r	*radial load angular contact ball bearings*
F_a	*axial load*
F'_r	*radial load on single row deep groove load*
FTF	*Fundamental cage frequency*
F_I	*Centrifucal force create by the correction mass m_1 in two plane static balancing*
F_{II}	*Centrifucal force create by the correction mass m_2 in two plane static balancing*
gE	acceleration enveloping
h	*the lubricant film thickness*
H_{Sup_DE}	*Horizontal direction on support drive end*
H_{Sup_NDE}	*Horizontal direction on support non drive end*
ω	*the spin speed of the rotor*
ω	*angular natural frequency*
ω_F	*excitation force angular frequency*
ω_s	*spin component*
φ_F:	*excitation force initial phase shift*
φ	*initial phase shift*
P	*load*
K	*MRC Bearing Division of SFK Industries factor*
k	*Stiffness of the structure*
l_1	*Distance between centrifugal force P_I and G the point intersection between the rotor axe and the rotation axe*
l_2	*Distance between centrifugal force P_{II} and G the point intersection between the rotor axe and the rotation axe*
m	*mass*

M	*The moment due to couple unbalance*
M_s	*twisting moment required to cause slip*
m_c	*correction mass of the unbalance in a Single Plane*
m_1	*correction masse m_1 of unbalance in Two plane balancing*
m_2	*correction masse m_2 of unbalance in Two plane balancing*
N_l	*number of lines (or discrete values)*
N	*Shaft rotation speed in rpm*
n	*Number of blades*
N_{planes}	*the number of flexible modes need to be balanced*
p	*Number of balancing planes*
p_d	*Rolling Bearing pitch diameter*
$P_{\ bearing\ pair}$	*Equivalent dynamic load on pair angular row angular contact ball bearings*
$P_{\ single\ bearing}$	*Equivalent dynamic load on angular single row angular contact ball bearing*
P_u	*Equivalent dynamic load on single bearing*
P_I	*Centrifucal force create by the correction mass m_1 in Couple unbalance*
P_{II}	*Centrifucal force create by the correction mass m_2 in Couple unbalance*
Q_i	*oil quantity needed on the pump support to ensure good lubrication*
$Q_{oil\ -sump}$	*total annual oil consumed*
$Q_{oil\ -mixt}$	*Amount of annual oil consumed of oil mist generator*
$Q_{oil-dispersed}$	*amount of annual oil dispersed in the environment*
$Q_{\ generator}$	*Annual oil mist quantity consumed by generator*
n	*number of balancing speed*
n_i :	*number of times oil change for considerate machine i, during one year*
η	*Lubricant viscosity*
q	*Number of sensors*
r_i	*monthly amount of oil mist condensed in the piping distribution system.*
$R(t)$	*the noise measured vectors which size is q*
r_1	*Distance between the masse m_1 and the rotor rotation axe*
r_2	*Distance between the masse m_2 and the rotor rotation axe*

$\vec{R}_I$	*Centrifugal force create by the correction mass m_1 in dynamic unbalance*
$\vec{R}_{II}$	*Centrifugal force create by the correction mass m_2 in dynamic unbalance*
R_{NDE}	*the reaction force to the unbalance force on the NDE support*
R_{DE}	*the reaction force to the unbalance force F on the DE support*
R'_{NDE}	*the reaction force on the NDE support after adding correction mass*
R'_{DE}	*the reaction force on the DE support after adding correction mass*
[C]	*The matrix of influence coefficient*
$S(t)$	*Signal sources vectors which size is k*
$\tilde{S}(t)$	*Recovered signals vector*
$s(t)$	*Analog signal*
U	*is the unbalance with a unit of kg-m or g-mm*
u_{t1}	*test unbalance in the balancing plane 1*
u_i	*Amount oil mist condenses in the supports of the pump and collected in container*
μ	*Stribeck curve with coefficient of friction,*
ū	*vibration mean value*
t	*time*
T	*Vibration period*
T_{ex}	*external temperature*
T_h	*Housing external temperature*
$T_{r:}$	*Outer Race /housing temperarure*
T_b	*ball temperature*
V	*Velocity*
v	*Vibration velocity*
V_{Sup_DE}	*Vertical direction on support drive end*
V_{Sup_NDE}:	*Vertical direction on support non drive end*
{W}	*the vector initial vibrations which size is $q \times n$*
X	*the frequency pertinent to the rotational speed of the shaft used for the spectra evaluation*
X_a	*amplitude of harmonic oscillation*

$X(t)$	*Vibration amplitude function*
X_{RMS}	*amplitude of harmonic oscillation root mean square value*
X_{mean}	*amplitude of harmonic oscillation mean value*
$X_{pk\text{-}pk}$	*amplitude of harmonic oscillation peak-to-peak value*
X_F	*amplitude of forced vibration*
$x_F(t)$	*Forced Vibration amplitude function*
X'	*Radial direction of Eddy Probe sensor*
$Y(t)$	*recovered signals vectors*
Y'	*Radial direction of Eddy Probe sensor*
z	*Entire number*
Z	*Unbalance correction force*

Liste of Acronyms ond Abreviations

ADC	*Analogue to Digital Converter*
AE	*Acoustic Emission*
BECBM	***B** : single row bearing with a 40° contact angle, **E**: Optimized internal design; **CB**: Bearing for universal matching, two bearings arranged back-to-back or face-to-face have Normal axial internal clearance.; **M**: Machined brass cage,*
BSS	*Blind Source Separation*
CHP	*Coupling Hub fitted to the Pump*
CSA	*Cyclic Spectral Analysis*
DADs	*Data Acquisition Devices*
DE	*Driver End*
DES	*Non Drive End Support*
ECP	*Eddy Current Probe*
ESP	*Envelope Signal Processing*
FFT	*Fast Fourier Transform*
HPI	*Hydrocarbon Processing Industry*
ICM	*Influence Coefficient method*
ICA	*Independent Component Analysis*
MSCP	*Multi-stage Centrifugal Pump*
NDE	*Non Drive End*
OML	*Oil Mist Lubrication*
NDES	*Non Drive End Support*
OEL-TWA	*Time-Weighted-Average Occupational Exposure Limit*
RMS	*Root Mean Square*
SCFM	*Standard Cubic Feet Per Minute*
SPB	*Single Plane Balancing*
SRB	*Support Radial Bearing*
STB	*Support Thrust Bearing*
WT	*Wave let Transform*

Introduction

The rotating machinery are fundamentals components in industrials plants. The rotating machines meanly used in industrial process are pumps, compressors, turbines, expanders, engines, motors, generators, fans, blowers, gearboxes. They are becoming more and more sophisticated because of informatics and electronic applications.

Indeed, Computer technology, automation and general electronic applications have become the characteristic of our era, where high technology allows important advantages in terms of economy, productivity, quality and safety by quickly outdated company that does not adapting to the new pace of growth and innovation. The rotating machine then becomes more and more sophisticated, expensive, delicate maintenance to maximize to decrease the depreciation costs. It grows accordingly the importance of a correct control to eliminate faults and stops. An accurate forecast of the possible damage and then the machine stops it is therefore essential, otherwise serious damage to the entire plant productivity.

In this context, vibration analysis is a tool for detecting and then diagnosing machine malfunctions. The operation of the machines generates forces which will often cause the subsequent failures (rotating forces, turbulence, shocks, instability…). The forces in their turn cause vibrations which will damage the structures and components of the machines. The analysis of these vibrations will make possible to identify the forces as soon as they appear before they have caused irreversible damage. It will also make possible, after analysis, to deduce the origin and to estimate the risks of failure.

The rotating machines are multicomponent machinery. However, on the basis of their operating principle, a rotating machine can be represented in a simplified manner by a rotor mounted on two bearings through a shaft as shown in Fig. 0.1. In the case of a biaxial (or triaxial) rotating machinery, it can be represented by two (or three) rotors mounted each on two bearings through its own shaft.

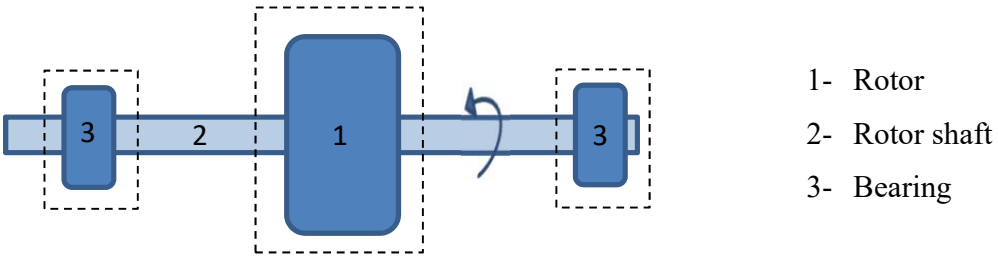

***Figure 0.1**: Rotative machine Semplificate Schema nomo axial*

The rotor and the bearings are fundamental components for the correct operation of the rotating machine. The majority of failures encountered during the life of a machine are related to these two components.

- The bearings can be mainly of two types: rolling bearings and fluid film bearings (or sliding bearing). The first type is the most widespread while the second is used for applications where the stresses are more burdensome and, at the same time, where it is required less clutter. In the same load effects, the film fluid bearings are less bulky than rolling bearings. The bearings which undergo all the vibrations of the rotating machine are the most delicate components. So the bearings, especially those in rolling, are frequently subject to damage.
- The rotor to function well must be well balanced around its axis of rotation. But unfortunately, this is not always the case for various reasons which may be related to manufacturing errors, defects or mounting of the rotor changes during the phases of use. As a result, an imbalance arises that creates high stress capable, in many cases, to bring the machine to damage in a short time.

This thesis will address the issue of multi-component machine monitoring and fault diagnosis using advanced vibration analysis articulated mainly around the issues related to bearings and rotor.

The chapter 1 presents a generality on vibration analysis applied to rotating machinery monitoring and rotating machine main faults.

In the chapter 2, we present a review of rolling element bearing vibration detection. This review is mainly based on bearing failure modes, bearing vibration measurement. In the second part we descript the approaches for analysing the vibration signature for diagnosis of bearing faults in (complex) rotating machines. We mean Blind Source Separation (BSS) approach and cyclic spectral analysis approach. In the third part, a cyclic we present an experimental study, basing on enveloped acceleration method, on a machine bearing failure, i.e. a liquid ring compressor which is an hypercritical in oil refinery plant.

In the chapter 3, the performances of pure oil mist lubrication and conventional oil bath lubrication are been compared. This study is based on a petroleum industrial plants where pumps are been retrofitted

from conventional oil bath lubrication to pure oil mist in order to improve the lubrication performance so to increase bearing life and reduce the oil consumption.
First a comparison of oil consumption has been done. Second the comparative study has been done in terms vibration level and spectrum analysis related to rolling bearings operating load and rotation speed for each pumps. And third, to assess the oil mist lubrication reliability, a new parameter based on rolling bearing dimension, load and rotation speed has set up. This parameter has been compared to with a common industries applicability parameter.

In the chapter 4, a method for on-site and quick balancing of rotating machine such as multi-stage centrifugal pump, is proposed. It permits to reduce the number of unscheduled maintenance that requires the removing of rotor and others part of this machine. The proposed approaches are based on the method of influence coefficients which is recognized for its efficiency and for its ease of implementation in industrial context. The first part presents the rotors and rotating parts unbalance causes and an overview of basics theory of balancing of rotors. It presents also the theoretical basis of the study. The unbalances in the rigid and flexible rotors. The theoretical development of Influence coefficient method for the flexible rotor balancing and its application. The second part describes the on-site balancing approach of Multi-Stage Centrifugal Pump (MSCP). The Problem definition and the description of theoretical approach for the resolution, the assumption of hypotheses to overcome the inaccessibility of pumps rotors for on-site balancing. The description of the two systems considered for the application of the theoretical approach for resolution. In the thirds part, this document present the experimental study, application to industrial multi-stage pump. The balancing process of the pump based on the coupling hub are shown. The two different approaches for the two systems considered for balancing are studied and the results are then compared. These results allow to judge the effectiveness of such approaches to balancing multi-stage centrifugal pump in the industrial field.

Chapter 1

Generality on vibration analysis applied to rotating machinery monitoring and rotating machine main faults.

1 Generality on vibration analysis applied to rotating machinery monitoring and rotating machine main faults.

Vibration analysis is one of the most used method in rotating machines condition monitoring. This stems from the fact that oscillation is an inherent characteristic of rotating machines and different components of these types of machinery such as shafts, bearings and gears produce vibration energy with different characteristics. Any deterioration in the condition of such components can affect their vibratory attributes and manifest itself in the vibration signature. This allows diagnosis of machine faults by analyzing the vibration signature of the system. Vibration diagnostics is described in more detail in [1, 2].

A number of transducer types exist for measuring machinery noise and vibration, including proximity probes, velocity transducers, accelerometers, acoustic emission transducers, microphones, and lasers. The measurement of machine casing acceleration is the most common method used for bearing fault detection. This is normally achieved by mounting a piezoelectric accelerometer externally on the machine casing, preferably near or on the bearing housing, or on a portion of the casing where a relatively rigid connection exists between the bearing support and the transducer. This will allow the bearing vibration to transmit readily through the structure to the transducer. Accelerometers have the advantage of providing a wide dynamic range and a wide frequency range for vibration measurement. They have been found to be the most reliable, versatile and accurate vibration transducer available.

In this chapter, we present a review of rolling element bearing vibration detection. This review is mainly based on bearing failure modes, and bearing vibration measurement. In the second part we descript the Approaches for analysing the vibration signature for diagnosis of bearing faults in (complex) rotating machines. We mean Blind Source Separation (BSS) approach and cyclic spectral analysis approach. In the third part, we present an experimental study on a machine bearing failure.

1.1 Vibration Analysis applied to Rotating Machinery Monitoring

Vibration analysis is part of a predictive maintenance policy of industrial production tools. The objectives of such approach are to reduce the number of stops on sensitive; reliable production tools; increase its availability rate; better manage the stock of spare parts, etc.

Condition monitoring systems are of two types: periodic and permanent.

- In a periodic monitoring system (also called an off-line condition monitoring system), machinery vibration is measured (or recorded and later analyzed) at selected time intervals in the field; then an analysis is made either in the field or in the laboratory.

- In a permanent monitoring system (also called an on-line condition monitoring system), machinery vibration is measured continuously at selected points of the machine and is constantly compared with acceptable levels of vibration. The permanent monitoring system can be costly, so it is usually used only in critical applications [3].

There are two technologies enabling a vibration monitoring:

- By direct measurement of the displacement of the rotating parts (machines shafts). Performed using eddy current sensors. The technology used is heavy. A common application is the monitoring of hydraulic bearings machines (Oil corner). This monitoring is almost always done on-line that is to say in real time. The sensors measure the movement of shaft and thus permit the immediate triggering of alarms in case of malfunction;

- By measuring the acceleration undergone by fixed machine parts (casings). The instruments used are, in this case, much more accessible to small structures. Using an accelerometer connected to a data collector, the technician collects the vibration transmitted to the casings of the machines. This technique can be used both for on-line monitoring and for the periodic monitoring. It is the most common method used for bearing fault detection.

In turbo machinery in heavy industry both technologies often are used in order to achieve an efficient vibration monitoring of its production facilities.

1.1.1 Machine Maintenance

1.1.1.1 Role of Maintenance

The role of maintenance is not only to repair damaged equipment, but to prevent its damage. Moreover, we want the machines to work efficiently, reliably and safely. Goal of the maintenance can be expressed through three interrelated requirements:

- Achieve maximum productivity:
    - Ensure continuous and satisfactory operation of the machine throughout its proposed lifetime – or even longer.
    - Achieve higher machine utilization with minimal downtimes for maintenance and repairs.
    - Continually improve the production process.
- Optimize machine performance – Smooth and efficiently running machines cost less and produce higher quality products.
- Ensure operation safety. Each of you may imagine a car example – when you neglect maintenance, your car will not only be unreliable, but can also be dangerous.

1.1.1.2 Maintenance Types

Equipment maintenance is essential for long-term trouble-free operation. In the course of technological development, several types of maintenance have been established: Breakdown (run to failure), preventive (planned), condition based maintenance, proactive reliability maintenance; reliability centred maintenance. Assessing the reliability of systems and/or components and determining the maintenance requirements to ensure that maximum reliability is achieved.

The application of those types of maintenance depends on a number of circumstances that must be considered. Basic maintenance tasks are listed in the paragraph above. In considering them, however, costs should always be considered together with safety.

A) Breakdown (Run-to-Failure) Maintenance

The premise is simple – run a machine without performing any maintenance on it until it breaks down. There are a number of machines in a plant that should actually be maintained in this fashion. These are machines that typically cost more to maintain than replace and that have little or no impact on production, safety, or the environment and perhaps have a stand-by. In other words, the risk associated with failure is low.

B) Preventive (Planned) Maintenance

For more expensive equipment with more costly operation, the method with *periodic* maintenance inspections or repairs has been established, which is called *preventive maintenance*. Equipment that receives routine and/or necessary maintenance will run longer, better, and more reliably at a lower cost.

Preventive maintenance is also referred to as scheduled, planned or time based maintenance and the aim is to prevent failures and extend life through cleaning, inspection, routine replacement of lubricants and filters, and scheduled repairs or overhauls based on experience or history.

This maintenance philosophy is very good for scheduling and planning, however getting the optimum interval correct is not always easy. Another issue with this type of maintenance is that of maintenance induced failures. This is where every time an engineer stops and works on a machine, the higher the potential to cause a problem with the machine.

C) Predictive Maintenance

A machine is repaired when its condition requires a repair rather than at predetermined intervals. Of course, it is necessary to know this condition, and therefore watch the machine in operation, i.e. to perform monitoring and diagnostics. This approach helps us to avoid unplanned shutdowns and failures. The key idea is *the right information at the right time*. The main requirements are that good accurate data is collected and properly trained staff are available to analyse the readings and make informed decisions about the condition of the equipment. Maintenance is applied only to those machines that require attention and only when needed. Much of the time, condition monitoring is performed while the machinery is running, avoiding downtime.

If we know which part of the equipment requires replacement or repair, we can order spare parts, arrange it for staff, etc., and perform shutdown at the appropriate time. Such a planned shutdown is shorter and less costly than a shutdown forced by a failure of equipment or even an accident. An

increase of equipment lifetime, increased safety, fewer accidents with negative consequences for the environment, optimized management of spare parts, etc. are other advantages of predictive maintenance.

D) Proactive Reliability Maintenance

Run-to-failure, preventive, and condition based programmes are all reactive. In practice, a good maintenance programme blends all of these practices to provide the best mix of machine availability, cost, and acceptable equipment risk. Proactive maintenance is planned and directs actions aimed at eliminating or reducing the sources of failures through craftsmanship and the use of the highest quality components and parts available.

In fact, if a problem source can be identified and corrected, or prevented in the first place, the machine, if properly operated, should provide significantly longer service and present fewer maintenance problems. Some examples of proactive maintenance include monitoring contamination levels in the lubricants, monitoring the physical & chemical properties of the lubricants, as well as improving balance and alignment conditions.

Like any other philosophy, a continuous improvement approach should be adopted and the basic steps to this continuous improvement cycle are shown in Fig.1.1.

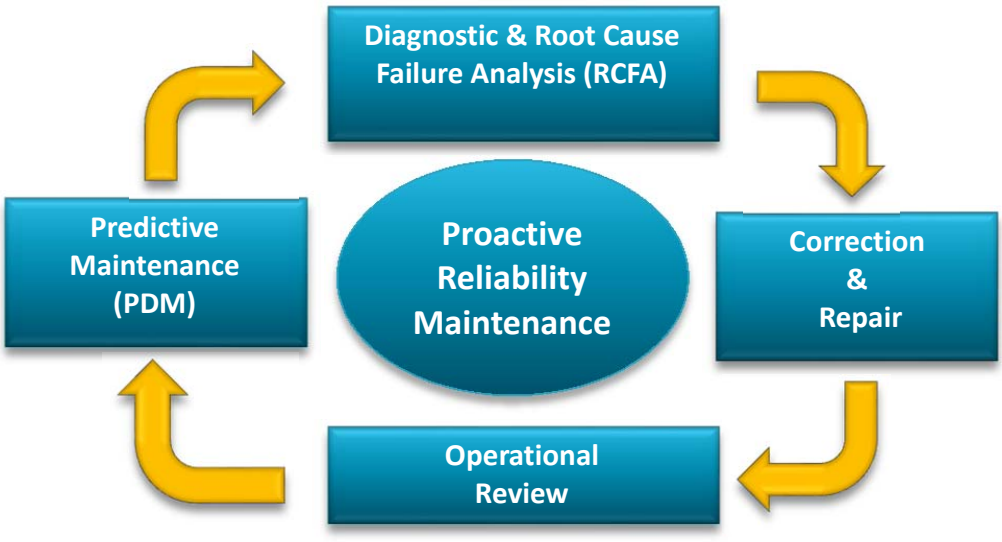

Figure 1.1: *The Proactive Reliability Maintenance Cycle.*

There are also other modern maintenance methods such as Reliability Centred Maintenance, which is used in aviation, and others.

When predictive and proactive maintenance is applied, it is necessary to determine the current condition of the machine. Maintenance process can be divided into five stages:

1. **Determining the initial condition -** A thorough measurement of the machine is performed at the time when it is in good state, which provides the basic reference values for subsequent comparison.
2. **Monitoring -** On the machine, points are defined at which vibrations are measured at regular time intervals. Usually the overall value of vibration is measured. This activity can be carried out by a trained worker without diagnostic knowledge.
3. **Detection -** Data obtained through monitoring are simply quantitatively evaluated. For each measured quantity, alarm limits are set. Exceeding the programmed alarm limit means warning about a problem.
4. **Analysis (diagnostics itself) -** After detecting the problem, detailed measurements and analyses (evaluation of the trend, FFT analysis, phase analysis, etc.) are carried out allowing a clearer view of the problem and its underlying cause.
5. **Recommendation -** Once the basic cause of the problem has been detected, economically acceptable corrective actions can be recommended and implemented.

E) Condition Monitoring Techniques

Condition Monitoring (or Predictive Maintenance) is the science and technology related to assessing machine performance and/or condition (health) based on the following:

- Periodic, continuous, or semi-continuous data acquisition from samples, sensors, etc.
- Application of the appropriate tests or related diagnostic techniques
- Analysis and validation of the data
- The making of the results into meaningful recommendations for appropriate maintenance action, leading to a reduction in cost and an increase in machine reliability

There are probably six accepted condition monitoring techniques

- *Vibration Analysis***:** Electronic data collectors and associated software allow both trending and analysis of routinely collected data
- *Lubrication Management:* Analysis of oils and greases to identify wear and save money by replacement only when needed. Another technique usually incorporated into LM is *magnetic chip detectors***,** which consist in Ferrous debris monitoring using magnetic plugs in lubrication oil scavenge lines.
- *Acoustic Emission (AE):* Can be used to diagnose bearing wear, rubbing, electrical discharges, leaking or passing valves, etc.
- *Infrared Thermography***:** Used for many years, primarily for detection of electrical circuit faults. It is now used for a wide variety of applications
- *Motor Current Analysis:* Motor Current Analysis for detection of broken rotor bars in squirrel cage induction motors. Partial discharge detection in motor and generator stator windings
- *Airborne Ultrasound***:** Can be carried out by contact or non-contact measurement and is used very successfully in conjunction with other techniques, or as a stand-alone technique.

Other parameters that can be measured include *Temperature Monitoring* (e.g., bearings & motor windings), *ultrasonic flow measurement* **(** Use of ultrasonic techniques to determine pump performance and fluid systems' flow characteristics); *Electronic Process Variable Logging* (flows, pressures, PH levels, etc. Plant process parameters' log-sheets replaced with electronic data collectors and software enabling central data handling and trending plus plant and machinery performance calculations)

Virtually any machine health or operability parameter that you can reliably and accurately measure can be used as an input to a condition based maintenance programme. Some of the previously mentioned techniques provide earlier detection of machinery problems than others do. However, not all changes are necessarily indications of a problem. It may be the situation that one single measurement shows a change but nothing else does and this may simply be the result of a process or operational change.

1.1.2 Vibration Measurements and Analysis

Vibration signal involves information about the cause of vibration and through its analysis using different methods, an emerging or developing fault can be detected. For rotating machines, this is usually the method that covers most possible faults. Vibration diagnostics is described in more [1, 2].

1.1.2.1 Excitation Force and Vibration Response

A vibration is a dynamic phenomenon, during which a body is subjected to stresses of compression, tension or torsion with periodic character. The vibrations then intervene in elastic bodies under varying forces.

Basic problem of the application of each type of diagnosis is the fact that we analyse only the response to the acting causes that are essential to establish the method of repair. In the case of vibration diagnostics, this response is represented by vibrations, the character of which depends on the applied force. Common types of excitation force are: periodical, impulse, random

A) Periodical excitation force

The simplest case of periodic force is a harmonic force. In engineering practice, harmonic force is very rare, but most of the real forces occurring in rotating machinery can be expressed as a sum of harmonic forces. Therefore, it is possible to describe the properties of periodic force and its influence on the vibration response using harmonic force and response. If a harmonic force acts on a flexibly supported body, the steady movement of the body is also harmonic with the same angular frequency ω_F, but generally with different amplitude (see Fig. 1.2). This vibration is called *forced vibration* f.

$$\mathrm{f}\,(t) = F.sin(\omega_F t + \varphi_F) \qquad \text{(Eq. 1.1)}$$

where :

F : excitation force amplitude [N]

ω_F : excitation force angular frequency [rad/s]

t: time [s]

φ_F excitation force initial phase shift,

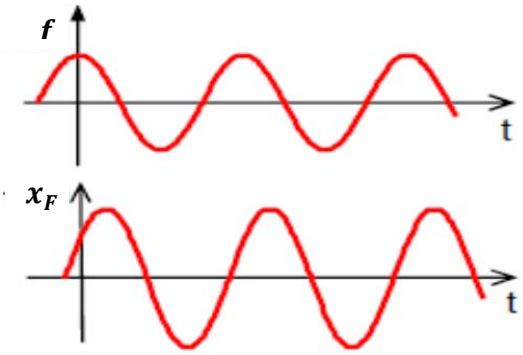

Figure 1.2: *Forced Vibration Caused by Harmonic Excitation Force*

Displacement of such a vibration can be expressed as:

$$x_F(t) = X_F.sin(\omega t + \varphi_F - \varphi) \qquad \text{(Eq. 1.2)}$$

where :

x : amplitude of forced vibration

$(\varphi_F - \varphi)$: lag between the displacement and the acting force

B) Impulse Excitation Force

When an impulse force is acting on the body, it diverts the body from the equilibrium position which causes subsequent free vibration on one or more of its natural frequencies (see Fig. 1.3). In technical practice, we use intentional impulse excitation performing "bump test" or a modal test. The unintentional impact excitation is associated with defects in rolling bearings (see section 1.3).

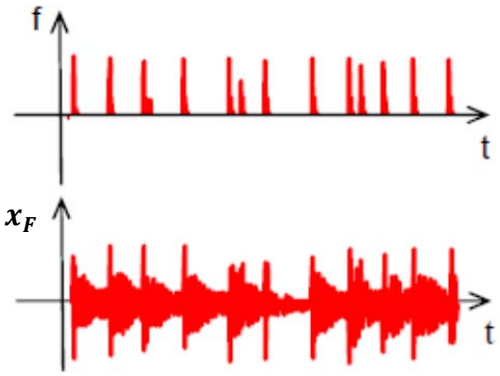

Figure 1.3: *Free Vibration Caused by Impulse Excitation Force*

C) Excitation force of random waveform

When random force acts on a body, the response is also random (see Fig. 1.4). Moreover, similarly to impulse excitation, natural frequencies can be excited (any abrupt change in force would excite the free vibration on natural frequencies). It should be realized that the random excitation is always present, mostly as noise only, but occasionally it should be considered even in the standard vibration diagnostics, e.g. when unwanted turbulence flow occurs.

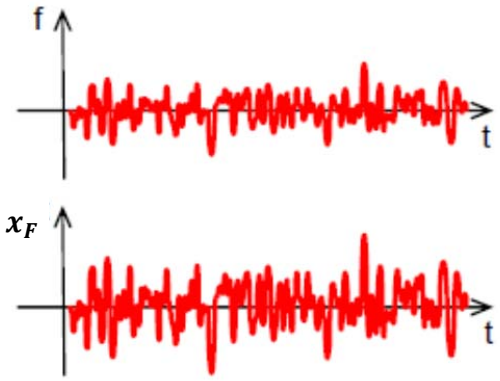

Figure 1.4: *Vibration Excited by Force of Random Waveform*

1.1.2.2 Resonance and Natural Frequency

Consider the following simple spring-mass system. If the mass is displaced and released, it will undergo a decaying oscillation as illustrated. The frequency of this oscillation is known as the natural frequency and its value depends on the stiffness of the spring and the magnitude of the mass.

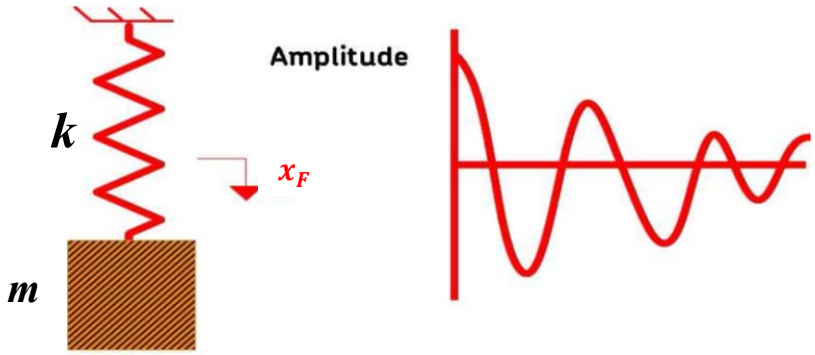

Figure 1.5: *Decay of vibration over time*

If a sinusoidal force is now applied to the mass at a low frequency, it will move in response to the force. Provided that the frequency is sufficiently low, the inertia of the mass will have little effect on the amplitude of vibration, which will be controlled simply by the stiffness of the spring. In other words, the displacement will be equal to the compression and extension of the spring caused by the applied force of the same amplitude. At the opposite extreme, if the mass is driven with a very high frequency force, its amplitude will be controlled by the inertia of the mass, and the effect of the spring will be negligible.

In between these two extremes there exists a frequency, often called a *Natural Frequency*, where the amplitude of vibration is magnified by a factor that can be from about 5 to 1,000. At this frequency, the resistance to movement/vibration due to the spring stiffness and the inertia of the block are equal in magnitude but in opposite directions, thus cancelling their effect. The only resistance to movement/vibration comes from the system's damping. Highly damped systems display a low amplification factor, whilst systems with low damping can display very large amplification factors.

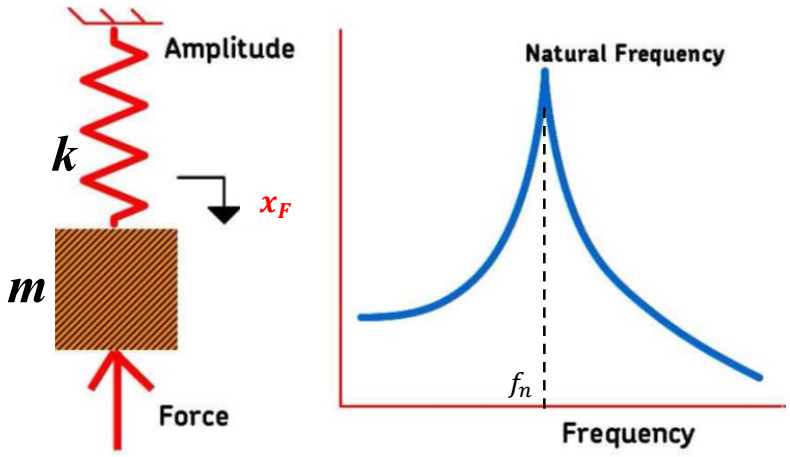

Figure 1.6: *Illustration of the natural frequency*

The phenomenon known as *"resonance"* occurs if one of the fundamental exciting frequencies (or harmonics of these) is close to the natural frequency of the structure. As noted earlier, this phenomenon is fundamental to all aspects of vibration analysis. With rotating shafts, the phenomenon is known as the "critical speed" and this where is the actual rotating speed of the shaft coincides with the natural frequency of the shaft. This is defined in ISO 2041 as "a *characteristic speed at which resonances of a*

system are excited." This phenomenon can also introduce localised errors in vibration measurement (for example, if an accelerometer is fitted to a resonant bracket).

Natural frequencies are present in every structure, shaft, component and assembled system. The vibration that is seen when a natural frequency is excited will depend on how close the vibration frequency is to the natural frequency. The closer the exciting frequency is to the natural frequency, the higher the vibration levels will be. This will also be affected by the stiffness, the mass and the damping characteristics of the structure. As can be seen in Fig. 1.6, at the natural frequency very high amplitudes of vibration will be seen.

$$f_n = \frac{1}{2\pi}\sqrt{\frac{k}{m}} \qquad \text{(Eq. 1.3)}$$

There are methods of controlling the amount of vibration that is experienced when a system is experiencing resonance and these include changing the mass, changing the stiffness or by improving the damping characteristics. However, before attempting to alter any of these, the exact natural frequency must be confirmed and analysis carried out to prove that resonance is indeed the problem.

1.1.2.3 Basic Quantities Describing the Oscillatory Movement

In mechanics, movement can be described by displacement, velocity or acceleration. We consider first the vibration amplitude defined by the displacement *x*, which have as unit of measure the length, generally in microns *[μm]*. If a mass of *m* is supported on a spring of stiffness *k*, after being displaced from its equilibrium position, it performs harmonic oscillating motion. If damping is neglected, the mass oscillates with natural frequency and the course of displacement is a sine wave with amplitude of $\boldsymbol{X_a}$ (see Fig. 1.7), thus:

$$x(t) = X_a \sin(\omega t - \varphi) \quad \text{(Eq. 1.4)}$$

Where:

X_a: amplitude of harmonic oscillation [m]

ω : angular natural frequency [rad/s]

φ : initial phase shift (is determined by the initial displacement)

It important underline that in technical practice, frequency f expressed in hertz (i.e. in number of complete cycles per second) is used more often than angular frequency ω expressed in radians per second. They are related by le relation (Eq.1.5). Reciprocal value of a frequency f is a period T (Eq.1.4).

$$f = \frac{\omega}{2\pi} \quad [\text{Hz}] \qquad \text{(Eq. 1.5)}$$

$$T = \frac{1}{f} = \frac{2\pi}{\omega} \quad [\text{s}] \qquad \text{(Eq. 1.6)}$$

Other characteristics, rather than amplitude, are often used to describe the harmonic signal (see Figure. 1.7), namely (Note: **x** here can mean any quantity, not just the displacement):

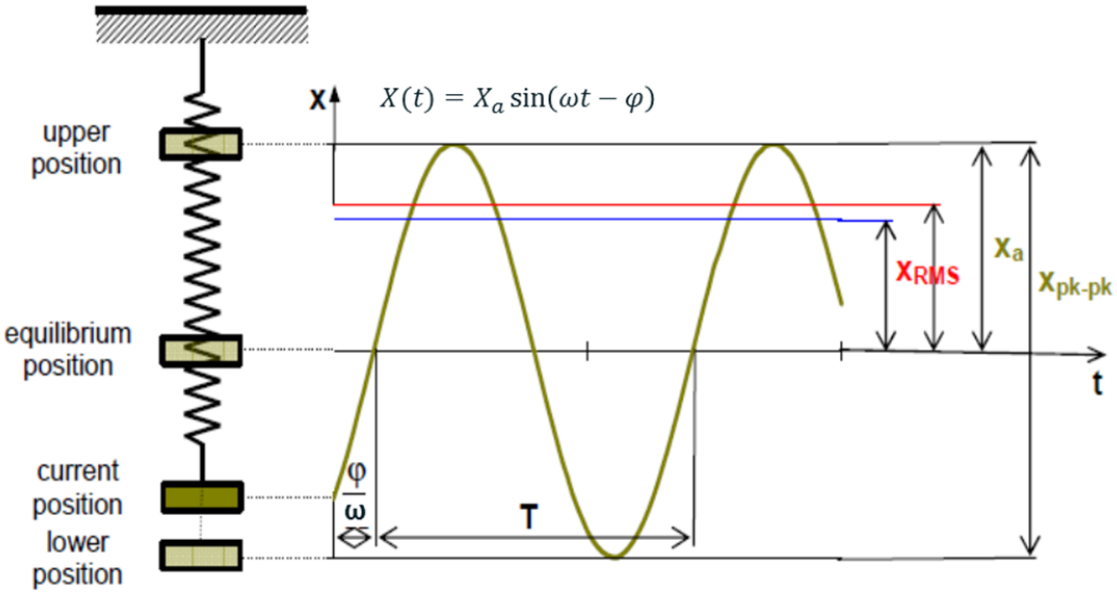

***Figure 1.7** : Quantities for Harmonic Motion Description*

peak value (= amplitude for harmonic signal)	X_a
rms (Root Mean Square) *value* = 0,707 × amplitude	$X_{RMS} = \frac{X_a}{\sqrt{2}}$
mean value = 0,637 × amplitude	$X_{mean} = 0{,}637 \cdot X_a$
peak-to-peak value = 2 × amplitude	$X_{pk-pk} = 2 \cdot X_a$

In addition to displacement, velocity (generally in $m.s^{-1}$) and acceleration (generally in $m.s^{-2}$) are others ways of measuring the vibration amplitude. These variables are linked by mathematical relationships. From this perspective, it does not matter which variable is chosen to describe the vibrational behaviour, it is just a matter of scale and time shift (phase). In fact, the speed is the first derivative with respect to time of the displacement (Eq.1.7) and the acceleration is in turn the first derivative with respect to time of the speed (Eq.1.8).

$$v = \frac{dx}{dt} = X_a\, \omega \cos(\omega t - \varphi) \quad [mm/s] \qquad \text{(Eq. 1.7)}$$

$$a = \frac{dv}{dt} = \frac{d^2x}{dt^2} = -X_a\, \omega^2 \sin(\omega t - \varphi) \quad [g;\ m\ s^{-2}] \qquad \text{(Eq. 1.8)}$$

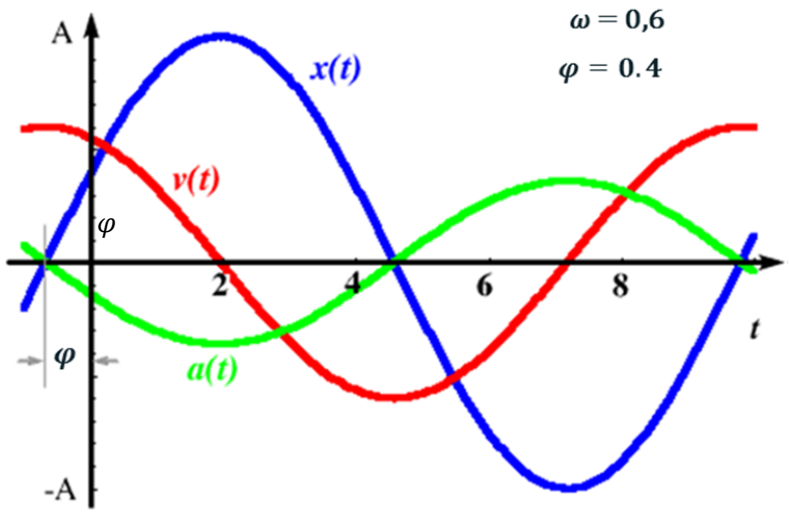

Figure1.8: *Relations between Displacement, Velocity and Acceleration*

Note that *x(t)* and a(t) are out of phase by 180°, or π radians, while x(t) and v(t) are out of phase by 90°, or $\frac{\pi}{2}$ radians.

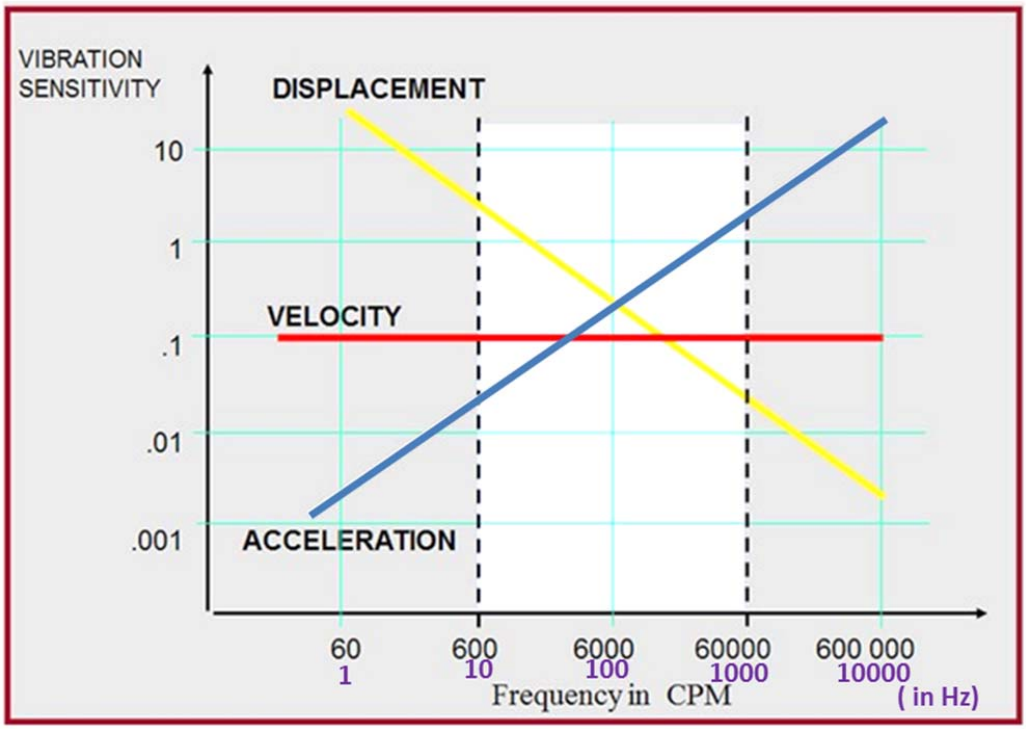

Figure. 1.9 *: Measurement Limitations*

The Fig. 1.9 indicates why velocity is used for common measurements in the frequency range 600 to 60000 CPM (10 Hz to 1000 Hz), acceleration is preferred for higher frequencies and displacement is preferred for lower frequencies. If a constant amount of vibration at all frequencies is considered, the deflection decreases with increasing vibration frequency and acceleration increases. Frequency range of interest is one of the factors that determine the type of measured value. If the measured frequency range includes high frequencies (such as gear mesh frequencies), the best choice would be to measure acceleration. Conversely, if the measurement frequency is limited to the running speed, the best choice would be measuring displacement or velocity (depending on application). When measuring the velocity of vibration, there is no need to care about the frequency (speed) at which the value was measured; when measuring the other two variables, it is necessary to indicate at what rotational speed (frequency) the value was measured. Otherwise, it is not possible to assess the condition of the machine.

1.1.2.4 Vibration Analysis (Frequency Analysis) - Fourier Transform

- **Principle of Frequency Analysis**

The vibration that follows a sinusoidal development is very simple. But, in a real system, there may be numerous types of excitation force such as periodical, impulse, random (as mention above), etc… Instead of simple sinusoidal signal, it detects a complex signal not easily interpretable, thus not allowing to identify the different causes of vibration. Fortunately all the perturbations mentioned above are separable in a simple signal of sinusoidal type obviously at different frequencies.

From the intuitive point of view, we can think to perform a rotation of the signal in time and to display the frequency domain. Basic consideration about more detailed analysis of vibration is shown in Fig.1.10. Each waveform consists of contributions from individual vibrating parts, usually having different frequencies. Frequency analysis is a tool that is capable to identify these individual contributions directly.

At this point, we must rely on the help of mathematics in order to decompose the signal into its simplest components. Frequency analysis is performed by Fourier transform (by its decomposition into Fourier series). All procedures related to the frequency analysis, which will be discussed below, are implemented in analyzers that are used in vibration diagnostics. There are different types of analyzers - operational or laboratory, with one or more channels - but the principle of their operation is always the same.

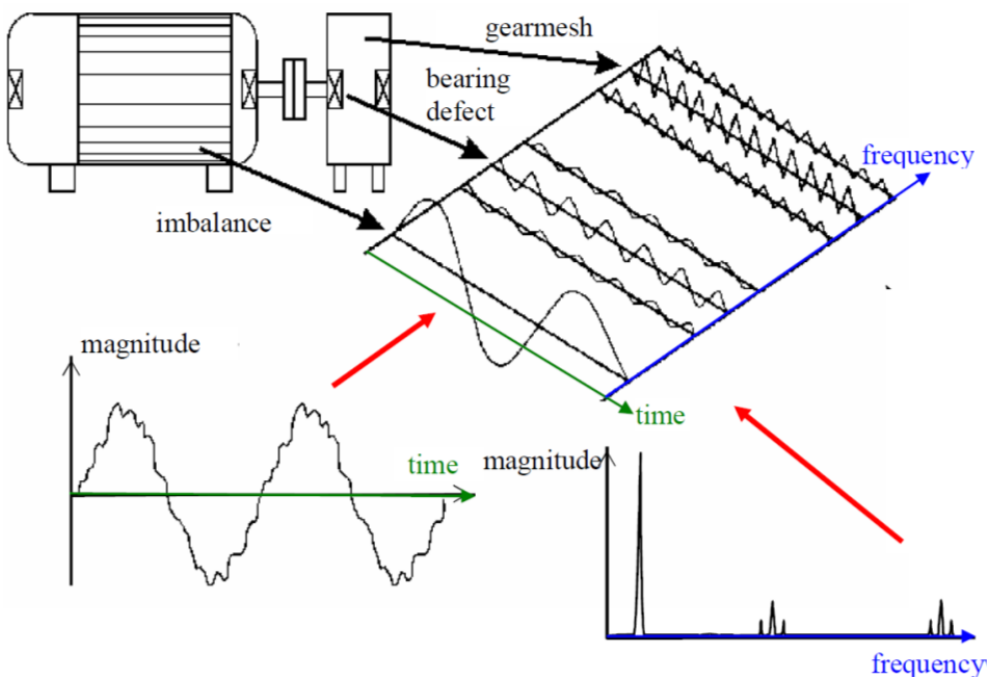

***Figure. 1.10**: Principle of Frequency*

- **Fourier Transform**

Function *x(t)*, periodical in time *T*, can be expressed as an infinite progression

$$x(t) = \frac{a_0}{2} + \sum_{i=1}^{\infty}[a_i \cos(\omega t) + b_i \sin(\omega t)]; \qquad \omega = \frac{2\pi}{T}, \qquad \text{Eq.19-a}$$

This expression means that the original function *x(t)* can be composed from (infinite) number of sinusoids of different amplitudes, frequencies of which are multiplies of the fundamental frequency ω.

Coefficients a_i and b_i are Fourier or spectral coefficients of the function *x(t)* and can be computed using expressions:

$$a_i = \frac{2}{T} \cdot \int_0^T \mathrm{x(t)} \cdot \cos(i\omega t)dt\,; \qquad b_i = \frac{2}{T} \cdot \int_0^T \mathrm{x(t)} \cdot \sin(i\omega t)dt\,; \qquad \text{Eq.19-b}$$

When working with measured vibration signals, a function is considered as periodical in the measured time interval **T**, though it is mostly not the case and additional adjustments of the signal are needed in order not to commit errors (see leakage, chapter 3.3). Current analyzers for processing measured signals do not work with a continuous waveform, but the measured signal passes to the analyzer

through the A/D (analog/digital) converter, which records the waveform as a sequence of **N** discrete values with regular spacing in the time interval ***T***. This procedure is called *discretization*. Discrete function ***x (t)***, which is defined on the set of N_l different instants of time t_k *(k = 1, N_l),* can be written as a finite Fourier series:

$$x_k\big(=\ x(t_k)\big) = \frac{a_0}{2} + \sum_{i=1}^{N_l/2}\left(a_i \cos\left(\frac{2\pi\omega t_k}{T}\right) + b_i \sin\left(\frac{2\pi\omega t_k}{T}\right)\right);\ k = 1, N_l \qquad \text{Eq.19-c}$$

Fourier coefficients are often represented in the form of amplitudeac_i and phase Φ_i:

$$\mathrm{c}_{\,i} = \sqrt{a_i^2 + b_i^2} \text{ and } \quad \Phi_i = \tan^{-1}\left(-\frac{b_i}{a_i}\right) \qquad \text{Eq.19-d}$$

Then, the finite Fourier series can be written as:

$$x_k\big(=\ x(t_k)\big) = \frac{a_0}{2} + \sum_{i=1}^{N_l/2}\left(c_i \cdot \cos\left(\frac{2\pi\omega t_k}{T}\right) + \varphi_i\right) \qquad \text{Eq.19-e}$$

This form of Fourier transform is called the discrete Fourier transform (DFT). The resulting Fourier series, a set of sinusoids from which the original waveform can be composed, is called a frequency spectrum. By Fourier transform, the original information about vibration in the time domain, where the individual events are mixed, is transformed into the frequency domain, in which each physical phenomenon (imbalance, damaged teeth, etc.) is represented by a single line wave of the corresponding frequency, i.e. by a frequency or spectral line.

There is a basic relationship between the length of the sample *T*, the number of discrete values N_l, *sampling frequency* $\boldsymbol{f_s}$, frequency range and *spectral resolution*. This is dealt in the following section (1.1.1.3 – B). An algorithm called *Fast Fourier Transform (FFT)* is used in up to date analyzers, where N_l is an integer power of number 2.

1.1.3 Data Acquisition & Signal Processing in industrial field

This section will deal with the types of instrumentation used for measuring vibration from rotating machinery. In industrial field The instrumentation typically consists of two main parts, which are the transducer and the data processing device, such as a portable data collector, or an on-line system.

Condition monitoring requires good quality vibration data, since important decisions about whether or not to run machines will be made on the basis of such data. Usually, it is a priority that there are clear trends of the vibration levels over several measurements. This requires accurate data to be collected in a consistent manner. Therefore, when selecting transducers and instruments, several factors need to be considered to ensure that the most representative data is collected.

1.1.3.1 Instrumentation for Vibration Condition Monitoring

A large number of devices are available for reading the output of the transducers previously considered. These range from simple handheld meters that read overall vibration as condition indicator through to very sophisticated On-line systems.

Handheld Meters – Condition indicators: Simple handheld meters measure the overall vibration level and perhaps an overall enveloped reading to provide an indication of machinery condition. The information that they contain is not detailed enough for analysis. Devices can be standalone with devices that simply provide a go/no-go status or linked to a computer to provide trending**.**

Protection Systems: Protection systems are usually the most costly systems to purchase and install. They are generally used where the failure of the monitored equipment is critical to the operation of the plant, e.g. turbines in power generation industry. These systems will continuously monitor the machine and shut it down if unacceptable vibration level, or other process parameter change is encountered. However, these systems are not used as condition monitoring systems. They generally provide an initial alarm but if the alarm is ignored, or the readings change too quickly, they simply act to stop the machine in a safe manner. The protection system will work on overall values or filtered values only and are not used for viewing spectral data or trending readings on a month to month basis. The buffered outputs from the system can be used in conjunction with portable data collectors or on-line systems to perform regular condition monitoring using transducers such as accelerometers or proximity probes.

Portable Systems- These systems usually comprise of a data collector and a software package. The equipment that is to be monitored will be entered into the database and for each item of equipment, the location and set-up for each measurement is specified. The machines will normally be assembled into routes (also known as Lists, or tours depending on the software package being used). These routes are then loaded to the data collector as required; this is often referred to as Upload & Download.

On-Line Surveillance Systems: On-line systems replace the portable data collector with data acquisition systems that automatically collect and store the data. This allows for data to be collected far more frequently than could be achieved with a portable system. However, a significant cost in such a system is the associated wiring that is required to connect the transducers to the system. To reduce this cost, most systems will place a monitoring unit in the vicinity of the machine. The transducers are then wired back to the unit. The on-line system performs all the same functions that the portable system does. Often, machine mimic diagrams will show the layout of the machine and alarm status will update as data is collected, perhaps by the mimic changing color, or an alarm being set off. These systems have simultaneous and continuous acquisition, but often only store data at preset intervals, i.e., weekly or daily, when there are changes in speed/condition and on alarm status/triggering. On-line Surveillance systems will monitor the equipment, continuously if required, and will then alert the users that a measurement has exceeded its pre-set alarm limits. These systems do not have shutdown protection and will not trip the machine if the readings go out of specification.

Troubleshooting: If problems are found on a machine, more sophisticated instrumentation may be required to diagnose the problem. In particular, very valuable data can be collected from certain machines during the run up and run down periods, providing there is sufficient time to do so. A typical modern portable system may have 16 or more input channels that can acquire data simultaneously. These systems are commonly controlled using a dedicated laptop PC, with all data being stored on the laptop hard drive for post processing and analysis as required. These types of instruments are extremely useful for carrying out run up/run down/coast down tests and can also be used for determine cause of machine trips.

- **Transducers/Sensors**

Transducers/Sensors measure the mechanical vibrations and convert them into proportional electrical signals that are then processed by the instruments into the vibration signals that we can interpret. The transducers are placed at strategic points on the machines in order to monitor its condition. The transducers can be further sub-divided into two main categories for measuring absolute (casing) vibration, or relative vibration.

Accelerometers and velocity transducers measure the absolute motion of the vibrating surface and are sometimes referred to as “Seismic Transducers.” Proximity probes, or eddy current probes measure the relative vibration based on a particular reference point.

- **Accelerometers**

Accelerometers are the most widely used transducer for vibration measurement, because of their relative simplicity, robustness, and reliability. The accelerometer measures acceleration and the construction of a typical accelerometer is as illustrated in Fig.1.11.

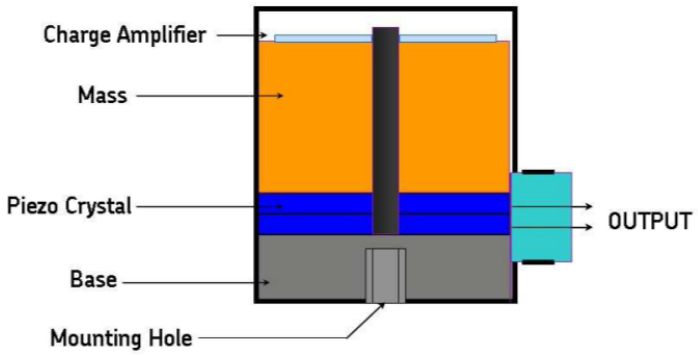

***Figure 1.11**: Typical Accelerometer Design*

A mass of a few grams is supported on a piezoelectric crystal. The characteristics of the piezoelectric material are such that if it is compressed, it generates an electrical charge. This charge can be picked up on the surface of the crystal and amplified into a usable signal.

Traditionally, this was done by means of a remote charge amplifier. However, modern accelerometers for condition monitoring often have the amplifier already incorporated inside the transducer. Such an accelerometer is known as an Integrated Circuit Piezoelectric (ICP) accelerometer, or more recently, some have been renamed as Integrated Electronic Piezoelectric (IEPE). This is also known as signal condition.

The amplifier circuit in an ICP accelerometer is powered through its connecting cable by a constant current supply from the analyser or data collector. The signal is returned through the same cable as a voltage varying proportionally to the acceleration to which the transducer is subjected.

The piezoelectric material can set a temperature limit on the accelerometer, normally of around 250 °C. However, with integral electronics, the maximum temperature at which the amplifier will function is typically 125 °C. For this reason, this type of accelerometer is not suitable for measuring casing vibration at specific locations on certain types of machinery (e.g., hot end of a gas turbine). However, if

the accelerometer uses a separate charge amplifier, then its temperature range can also be increased to around 250 °C. Other general characteristics of an accelerometer include:

- Frequency range between 0.1 Hz and 30 kHz
- Mass ranges from 10 g to 200 g

All accelerometers have a useful frequency range and this is determined by the deviation of the amplitude. On transducer specification sheets, this is typically defined as ± 5%; ± 10% or ± 3dB. The diagram shown in Fig. 1.12 illustrates this.

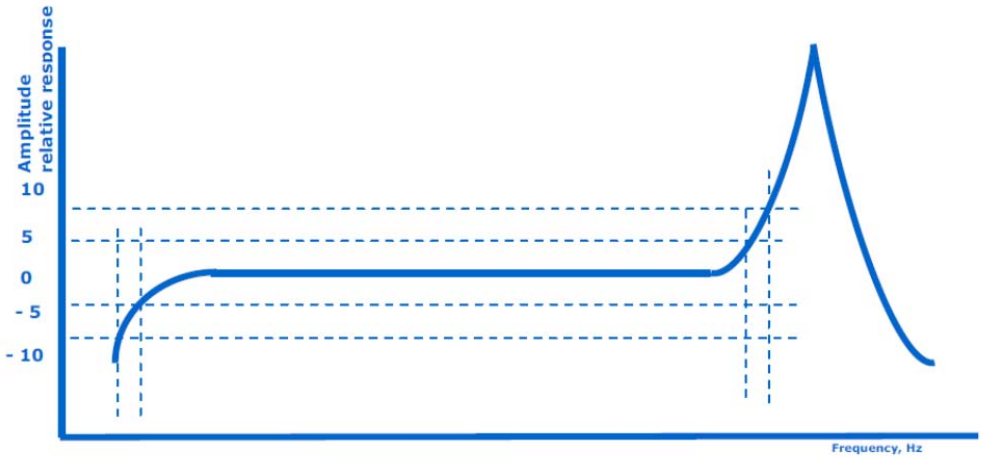

Figure 1.12: *Typical Accelerometer Output Curve*

- **Velocity Transducers**

There are essentially two types of velocity transducer, which are the moving coil type and the piezoelectric type. The moving coil type comprises of a magnetic element within the casing and a coil on a compliant suspension, or vice versa. Vibration causes relative motion of the magnets over the coil, resulting in a very strong voltage being generated. This type of transducer is no longer normally used for condition monitoring routines because they can be big and heavy, however they can still be found on some balancing machines. This is illustrated in Fig. 1.13.

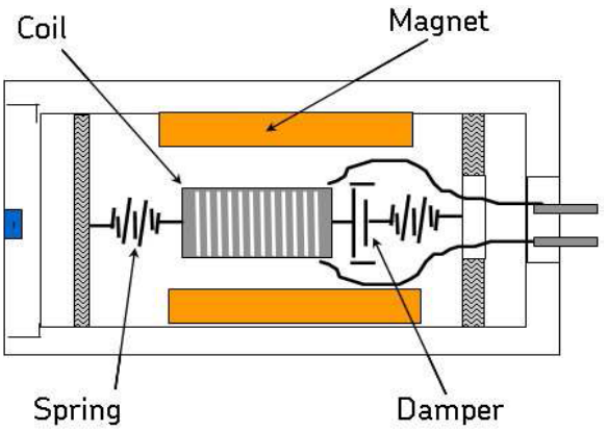

Figure 1.13: *Typical velocity transducer design*

The natural frequency of the moving assembly in the transducer above is generally about 3 Hz, giving it a minimum low frequency range of 10 Hz. The upper frequency limit is normally about 1 kHz. Therefore this transducer can provide an accurate velocity signal between 10 Hz to 1 kHz and satisfies the requirements of ISO standards.

However, the actual base size can become a problem for horizontal locations with magnets or studs. Also, the fact that there are moving parts within this transducer and that the coil is supported in springs can lead to problems as the transducers age. It has been known in the past that the springs sag and the coil rubs along the magnets causing wear. Care must also be taken to ensure that the natural frequency is not excited by low frequency vibration or impacts, as spurious results will be produced when the moving component reaches its limit of linear movement or bounces.

Compared with accelerometers, velocity transducers are generally much larger in size and weight; they have much lower natural frequencies and are inherently less reliable because of the moving parts.

In the past, velocity transducers were a less expensive option than accelerometers for obtaining velocity signals. Where there is still a requirement to obtain a velocity signal from a fixed transducer, piezoelectric velocity transducers are now available. The piezoelectric velocity transducer is simply the original accelerometer design, but with an additional circuit already built into the transducer that integrates the amplified signal to velocity, as illustrated below. These were introduced by Bently Nevada in 1991 and have been trademarked as “Velomitors”, however most users simply refer to these

as piezoelectric velocity transducers. An example of a piezo-electric velocity transducer is shown in Fig.1.14.

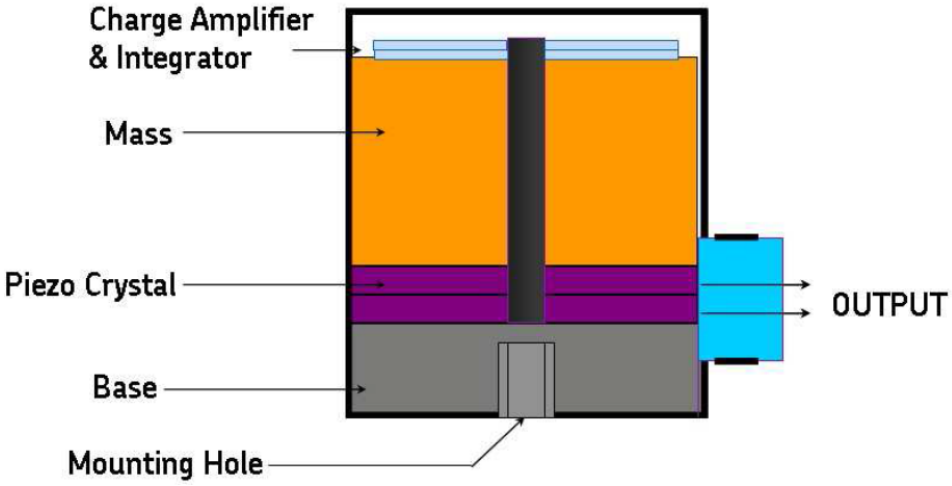

Figure 1.14: *Typical piezoelectric velocity design*

- **Transducer Mounting Methods**

The method for mounting the sensor depends on access, convenience, and economic considerations, as well as technical requirements. Generally speaking, the mounting method will influence the frequency response (accuracy vs. frequency) of the sensor. In most cases, there will be a change in the high frequency response characteristics of the mounted sensor.

Ideally, the sensor (transducer) should be permanently mounted on the machine component using a stud integral with the transducer base and fitted in a tapped hole by tightening to a nominal torque specified by the manufacturer. This, however, is not economically feasible for most industrial applications, since it requires as many transducers as there are points to sample. There are several other mounting methods that are commonly used, some of which are shown in Fig.1.15. The most common mounting techniques are listed below and rated from best to the least desirable:

- Stud *(screw)* mounted and torque directly to machine (preferred)
- Adhesively mounted
- Adhesively mounted “quick-fit” stud (good)

- Magnetically mounted on a good surface (acceptable)
- Handheld probe, or stinger (last resort)

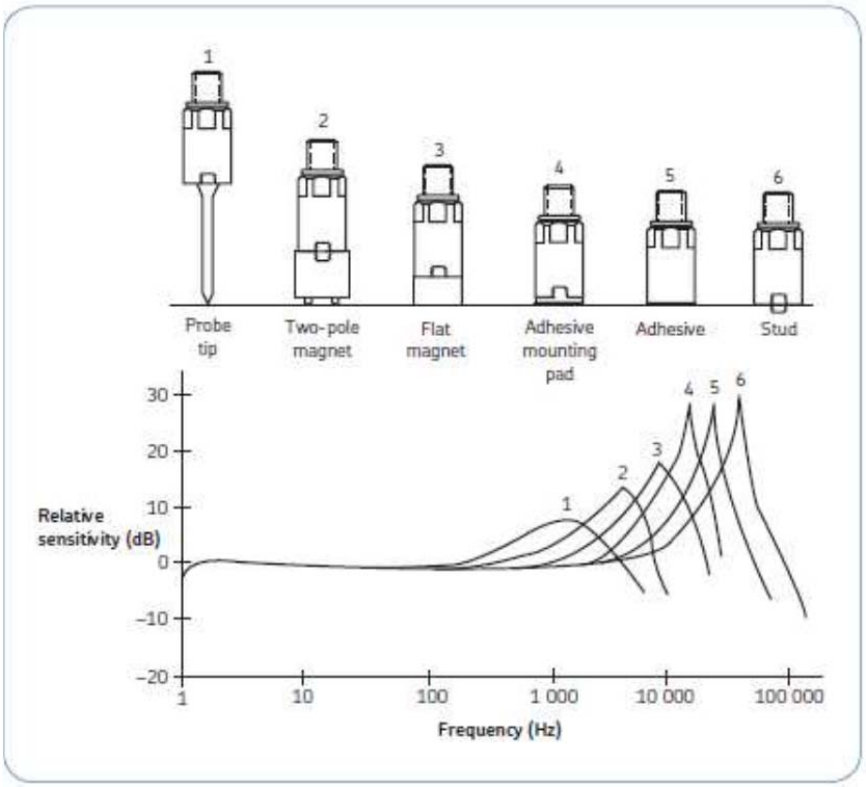

Figure 1.15: *Types of transducer mounting methods*

o Displacement Transducers

There are several types of sensors to measure displacement, distance or position. The oldest type is probably a contact mechanical slider; nowadays, the often used type is a noncontact sensor based on eddy currents - proximity probe which operates on the base of change of Foucault currents - the resistance of the material changes due to the change in distance. Other types, such as laser, ultrasonic, capacitive or inductive sensors, also exist. Displacement sensors are quite complex systems; so, they are only used for shaft vibration measurement - they measure vibrations of shaft relative to a part of stator, usually relative to the bearing housing.

The proximity probe based on eddy currents measures the distance between the sensor tip and a conductive surface. The measuring system comprises the sensor and the proximitor (see Fig.1.16). The oscillator in proximitor generates high-frequency alternating current that passes through a coil embedded in the sensor tip and creates high-frequency electromagnetic field around the tip of the sensor. Bias voltage used to be -10 Vdc, but may be up to -24 Vdc (depending on the manufacturer); an alternating component has a frequency of about 1.5 MHz (depending on the manufacturer). The electromagnetic field in the coil induces *eddy (Foucault) currents* in the conductive material. These eddy currents absorb energy from the system, resulting in the change in impedance of the coil. Instant distance to the target surface would modulate itself onto this wave and then is demodulated. With respect to the high frequency of the electromagnetic field, the entire measurement is strongly dependent on the total resistance (all of ohmic, inductive and capacitive resistance). Cables leading the high frequency signal are produced in strict tolerances of electrical values and their length cannot be modified. Any damage to the cable or the shield threatens the quality of measurements. After affecting the carrier wave and eddy current by the variable distance of the target surface during the vibration, the signal is led back to the demodulator. Then - now already low frequency- the signal is led to the evaluation unit. Fig. 1.17 shows a typical installation and orientation of an eddy current probe system.

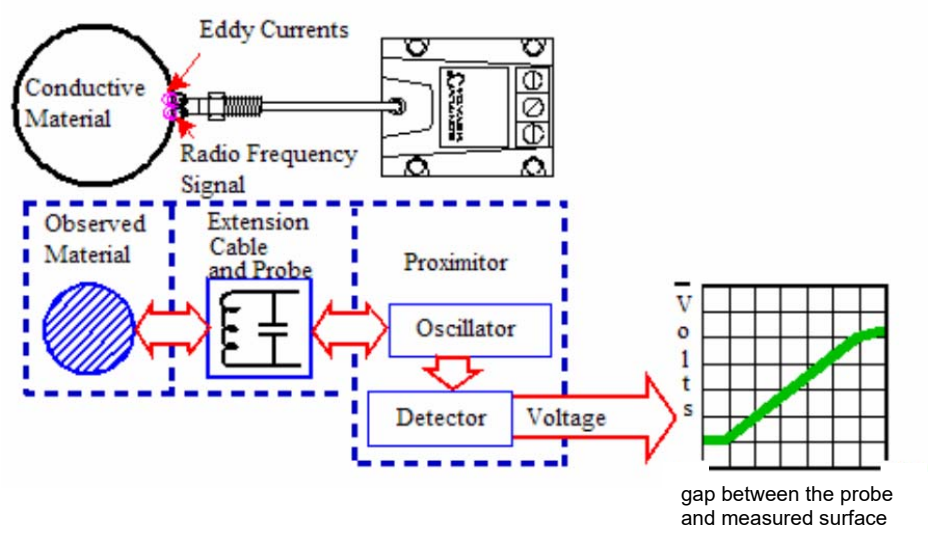

Figure: 1.16:- *Scheme of the Proximity Probe System Based on Eddy Currents*

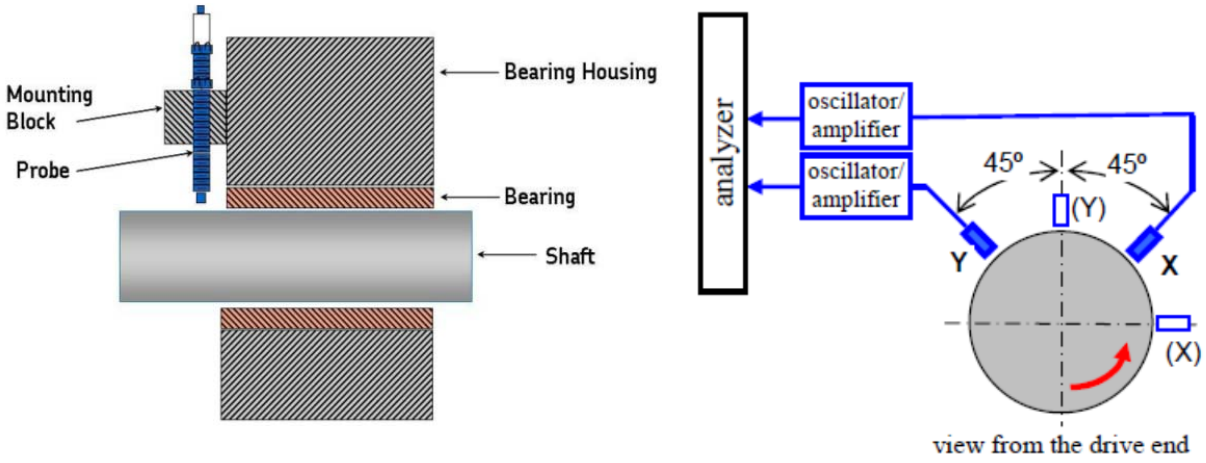

Figure 1.17: *Typical installation of, and typical orientation of Proximity Probes*

Since the magnetic field is disturbed by the proximity of a metal surface, then the sensitivity of the probe will be affected by the electrical and magnetic properties of the shaft material. This is an important factor calibrating the probes because the optimum gap setting for the probe is determined by the shaft material output curve. The variation of the output curves for some common target materials is shown in Fig. 1.18.

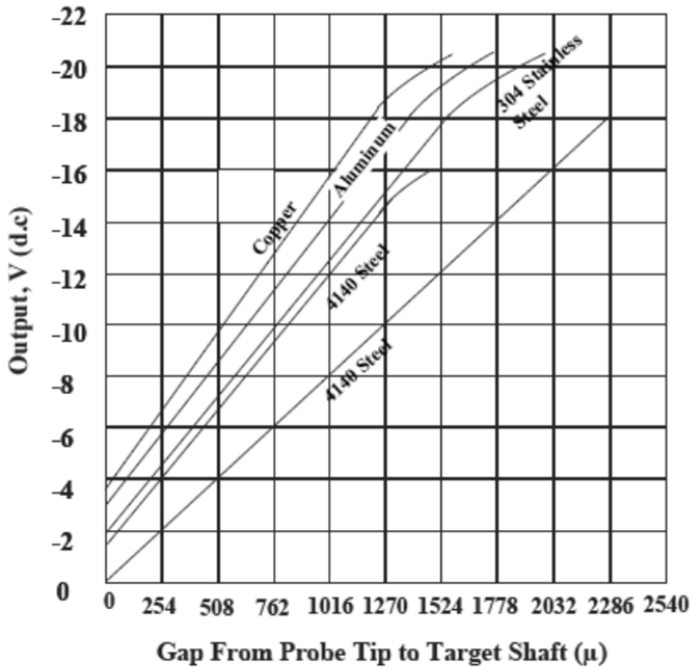

Figure 1.18: *Eddy Current Probe Output Curves for Common Materials*

- **FFT Spectrum Analyser**

We have seen in previous chapters the theoretical foundations on which the *FFT* is based. Here we see in practice what is the internal process of the analyzer operation when it is connected to the sensor to make a measurement, because even when you have set the tool, sometimes it is prompted for parameters that may be unknown. The signal transformation process from the time domain to the frequency can be schematized as below:

For little more details , basic scheme of the analyser used for vibration measurements is in Fig.1.19. The analogue signal from the vibration sensor passes through the input amplifier, anti-aliasing filter and A/D converter, where it is digitized and enters the data buffer. From the buffer it can be displayed either as a time waveform or can be further processed by the Fourier transform to obtain frequency spectrum.

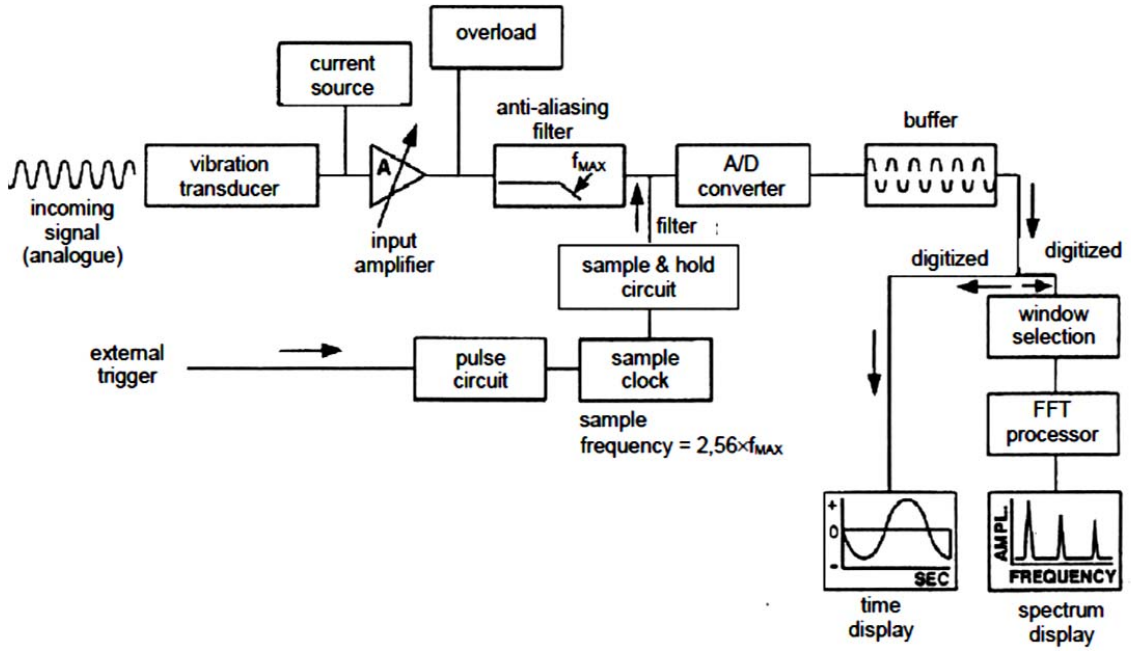

***Figure 1.19**: Vibration Analyser Scheme*

o Analog section and sampling

The sampling is the first step of analog-digital conversion process of a signal. It involves taking samples from an analog signal and continuous in time every $\boldsymbol{T_s}$ seconds. The value of $\boldsymbol{T_s}$ is said sampling interval (or length of the sample), while $\Delta\boldsymbol{f}$ is the frequency resolution. The result is an analog signal in discrete time, which is subsequently quantized, encoded and made accessible to any digital computer.

There is a basic relationship between $\boldsymbol{T_a}$ (total acquisition time), the number of lines (discrete values) N_l *sampling* (or *capture*) *frequency* $\boldsymbol{f_s}$, frequency range and *spectral resolution*. Spectrum frequency range is 0- $f_{\max}$, where $\boldsymbol{f_{max}}$ is the *Nyquist frequency* and $\Delta\boldsymbol{f}$ is the frequency resolution (sampling frequency or spacing between frequency lines):

$$\Delta f = \frac{1}{T_a} = \frac{f_{max}}{N_l} \qquad \text{(Eq. 1.10)}$$

$$f_{max} = \frac{f_s}{2} = \frac{N_l}{T_a} \qquad \text{(Eq. 1.11)}$$

An algorithm called Fast Fourier Transform (FFT) is used in up to date analysers, where N_l is an integer power of number 2.

o Aliasing

Aliasing is a phenomenon which consists of a signal misinterpretation by the analyzer when the sampling frequency is too small to realistically capture a fast action. The principle of the Aliasing Error (or stroboscopic effect) is clearly seen in Fig.1.20. It can be seen for example in a movie in which the wheels (it is best seen on carriage wheels) rotate unrealistically slowly or even reversely with respect to the corresponding direction.

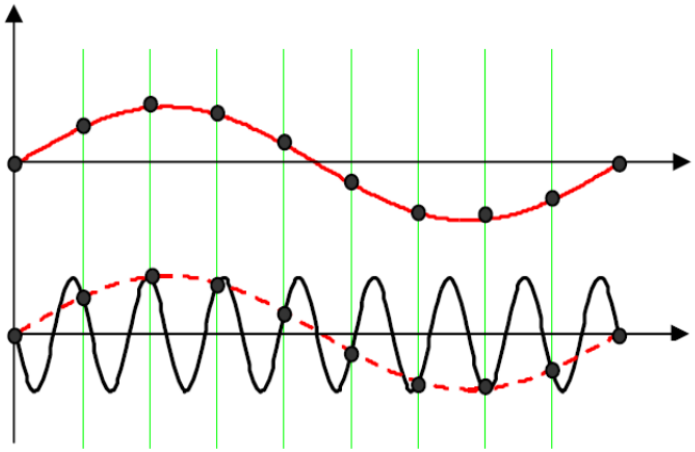

***Figure 1.20**: Principle of the Aliasing*

If the sampling frequency is f_s, then the signal of frequency f and the signal of frequency $(f_s - f)$ are indistinguishable after discretization. The highest frequency f_{max}, which may be contained in the spectrum, is $\frac{f_s}{2}$. The part of the signal which has frequency components above $\frac{f_s}{2}$ appears reflected in the range $\mathbf{0 - \frac{f_s}{2}}$. These high frequency components, thus, act as if they were (*alias*) of low-frequency and they create an indistinguishable mixture with the real low-frequency components.

Nyquist and Shannon developed in 1949 the sampling theorem that puts some restrictions on the content of the signal in the time domain in relation to the sampling frequency.

This theorem states that: since an analog signal ***s(t)*** whose frequency band is limited by frequency f_M, and since $n \in Z$, the signal ***s(t)*** can be uniquely reconstructed from its samples ***s(nΔt)*** taken at frequency $f_s = \frac{1}{\Delta t}$ if $\boldsymbol{f_s > 2f_M}$.

From this theorem, the solution to the Aliasing Error problem is to use an anti-aliasing filter (a low pass filter with a steep falling edge), which removes the components higher than half the sampling frequency of the original signal. The filter is an analogue device that is an integral part of up to date analysers. It should be inserted before the signal is discretized. Characteristics of the filter is steep, but not perfectly perpendicular, and therefore, the upper part of the spectrum is also removed (typically, the frequency range from $0.8 \cdot \frac{f_s}{2}$ to $\frac{f_s}{2}$ is removed). For this reason, the 2048 point transform does not result in the full 1024-line spectrum, but only the first 800 lines are used. The requirement for the correct sampling frequency can also be expressed as: $f_s = 2{,}56 \cdot f_{max}$.

o Analogic Digital Converter and Memory

The next step in the sampled signal to the digital conversion or digital signal is performed by the analog-to-digital converter which is a circuit capable of transforming the signal from the "sample & hold" in a binary number (formed by a number of bits) , proportional to the amplitude of the sample. The converters are generally used in the analyser 10, 12, or 14 bits. This means that the length of the word is the element characterizing the dynamics of the instrument. The signal sampled and converted into digital form, is transferred to a memory circuit, dimensioned according to the number of samples on which you want to operate using the *FFT* algorithm.

o Leakage

Fourier transform assumes a periodic function. But real signals from vibration often do not have the period significantly marked, neither the course of the signal in different periods is exactly the same. Consequently, the spectrum of such a signal can be distorted (this distortion is called leakage), unless the signal is appropriately adjusted.

To minimize the effects of leakage, weighting windows are used. The original signal is treated as if through a window of an appropriate shape (mathematically this means convolution of the original signal and the weighting function in the time domain and multiplication of the original signal and weighting function in the frequency domain).

Fig.1.21 shows the principle of the leakage and a window suitable for its suppression. If the signal entering the Fourier transform is periodic (i.e. periodic in the measurement time *T*, which in Fig.1.21 left means that an integer number of sine waves enters the transform), there is no need to use any weighting window (in analysers, Rectangular window is set, which actually means no window). In case of a simple sine wave, the result of the transformation is a single spectral line, which corresponds to reality. Another situation occurs when the signal entering the Fourier transform is not periodic (Fig.1.21 right). It can be seen that the signal is actually the same as in the case of the left, but the measuring time is different, and this produces a non-periodicity. In this case, the transform algorithm tries to model the resulting discontinuity, and the only way it can do this is by (infinitely) many other sine waves. Result of the transformation here is not the only spectral line with the corresponding frequency, but the energy "leaked" into many other spectral lines. It is obvious that such a spectrum

does not testify much about the original signal. In addition, when there are more "spread" lines, important diagnostic information (e.g. a weak signal from rolling bearings) can be hidden in the increased threshold.

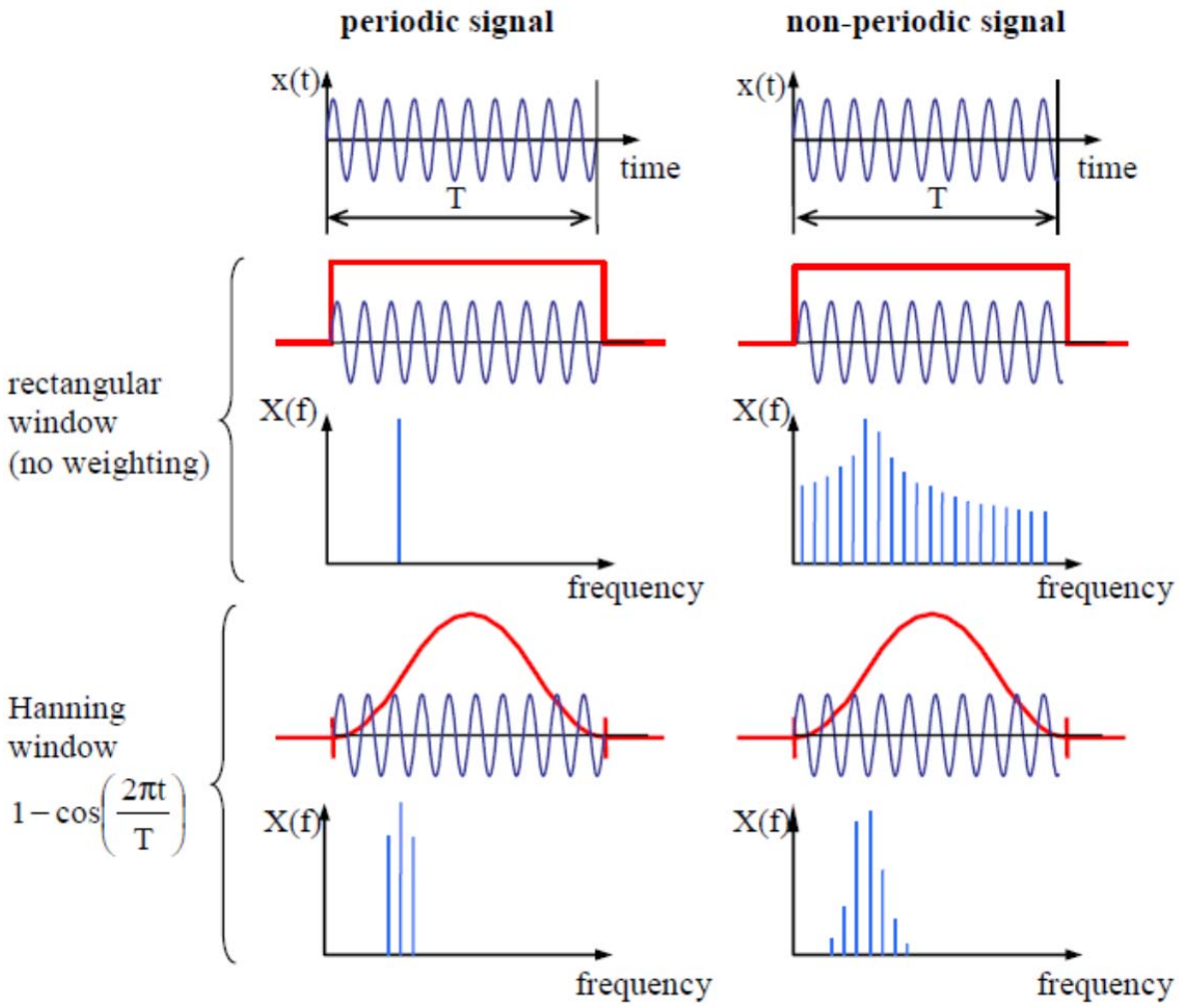

Figure 1.21: *Influence of Signal Periodicity and Weighting Windows to the Leakage [6]*

To minimize the effects of leakage, *Hanning window* is used when measuring steady signals. The point is that the signal was suppressed at their ends to zero, thereby removing the signal discontinuities and creating a signal that is closer to the real periodic signal. The result of using Hanning window is shown in Fig. 1.21. In the case where the signal was periodic, the result got worse (instead of one spectral line there are three lines), but in case of non-periodic signal the result is substantially improved - there are just a few spectral lines.

In addition to the most often used Hanning and rectangular windows, other types of windows are used in diagnostics as well:

- *Flat Top* window - It is used for transducer calibration; it does not distort the signal magnitude (Hanning window would decrease the signal magnitude a bit, which does not matter in operational measurements).
- *Transient window* - It is a rectangular window but shorter in time than the measurement period *T*. It is used for shortly acting signals, e.g. for impact excitation signal.
- *Exponential* window - It is used for measuring the response to impact excitation.

- **Signal Processing & FFT**

FFT algorithm is implemented in all up to date vibration analysers, eliminating the need of the user to have a good grasp of it. However, it is necessary to know basic principles to be able to avoid mistakes and to set efficiently transformation parameters. So before data acquisition, whether for a detailed analysis or for routine predictive maintenance checks, it is necessary to define or specify the FFT spectral parameters. These parameters include:

1. *Measurement Parameters*: Displacement, velocity, or acceleration
2. *Units and Scale:* Metric or Imperial and in RMS, Peak, or Peak-to-Peak
3. *Maximum Frequency (F_{max}):* The *maximum* range of vibration frequencies to be analysed
4. *Frequency Units*: Hz or cpm
5. *Number of Lines of Resolution (NLOR):* The resolution of spectral frequencies
6. *Number of Spectral Averages:* How many FFT's are taken and amplitude-averaged to improve statistical accuracy by minimizing the influence of random and transient events

- **Selecting the Right Measurement Parameter**

The choice of selecting vibration displacement, velocity, or acceleration for measurement (based on the vibration frequencies anticipated) has already been covered.

- **Units and Scale**

The selection of the measurement unit (Hz or cpm) and scale type (RMS, Pk, or Pk-Pk) should be compatible for comparison or assessment to a particular standard or to an online monitoring/ protection panel.

- **Selecting f_{max}**

Perhaps the most important decision that must be made in obtaining an FFT is selecting the frequency range of interest. This is commonly referred to as the f_{max}. The selected f_{max} must be high enough to include all significant, problem related defect frequencies. However, if the f_{max} is set too high, then the frequency resolution will be too low for a given number of lines. Lines of resolution will be discussed later. Therefore, the f_{max} should be selected after careful consideration of the possible defect related frequencies.

It must be noted that most commonly used accelerometers have a limited useful upper frequency range and often their mounting method will reduce this range significantly.

Therefore, where high frequency vibration readings are required, an appropriate accelerometer type and mounting method must be selected.

Most *FFT* analysers and data collectors allow the user to select any f_{max} within their limits, which can range from 2 Hz up to 40 kHz.

- **Selecting the Number of Lines of Resolution**

The next important decision that you must make when taking an *FFT* is selecting the number of lines of resolution. The decision will not only determine the resolution of frequency data presented, but will also determine the amount of time required to acquire the data (time window), as well as the amount of instrument and computer memory required to store the data.

Most *FFT* analysers and data collectors offer 25, 50, 100, 200, 400, 800, 1,600, and 3,200 lines of resolution. The latest designs have 12,800 lines and more. Most *FFT*'s taken for predictive maintenance checks and general machinery analysis are taken using 800 or more lines of resolution.

The equation below illustrates the concept of lines of resolution. The selected frequency range (f_{max}) is divided by the selected number of lines. For example, assume that 400 lines of resolution (N_l) was

chosen for an *FFT* with an f_{max} of 2 kHz. This means that the entire frequency range from 0–2,000 Hz will be divided into 400 lines, sometimes called frequency "bins."

The significance of the number of lines of resolution (N_l) selected is that, along with the selected $f_{\max}$, it determines the "resolution" of the frequency data presented in the *FFT*. In other words, in this example, each of the 400 lines or bins would be 5 Hz wide. And since each bin is 5 Hz wide, it is quite possible that more than one vibration frequency could be present within a single bin. However, on the *FFT* display it would appear as a single peak or as a single vibration component.

Generally speaking:

- increasing f_{max} with the same number of lines gives worse resolution
- decreasing f_{max} with the same number of lines gives better resolution
- increasing the number of lines with the same f_{max} gives better resolution
- decreasing the number of lines with the same f_{max} gives worse resolution
- the better the frequency resolution, the longer it takes to obtain the *FFT* reading and the more memory it requires to store.

- **Number of Spectral Averages and Averaging**

Given that the measured vibration signal is not deterministic but its character is probabilistic, the signal should be averaged in order to base the diagnostic assessment on reliable data. Generally, the more volatile the signal is and the more contaminated with noise, the more samples of the signal should be used.

Most applications in vibration diagnostics use averaging *in the frequency domain*. The principle is that spectra obtained by Fourier transform of the measured time period of signal are averaged. The analyser usually offers several types of such averaging:

- *linear (arithmetic)* where all measurements have the same weight
- *exponential* where new measurements are of greater weight
- *peak hold* – no averaging is performed, but maximum peak values of the individual spectral lines are stored.

Another parameter that is set in analyser is the number of averages. Four to eight averages are typically set for steady-state, but it is advisable to set more averages at first and observe, since when the

spectrum obtained is stable and unchanged. Depending on this, the number of averages should be set. For transient actions, e.g. run-up or coast-down, the peak-hold option and a large number of averages can be used to catch the entire transient process.

Further, the averaging can be set in analyser either to

- *Continuous* where the measurement is still in progress and the actual spectrum is computed from the given number of averages; the older measurements are forgotten and replaced by newer ones; or to
- *Finite* where, after starting the measurement, the finite number of averages is captured and the spectrum is computed and then the measurement is stopped.

The last parameter concerning averaging that is set in analyser is the amount of Overlap. It is the way in which the samples of the continuous time signal are input to the analysis. If the time needed to process the signal sample in the analyser is less than the length of the sample, averaging with the overlap is possible. Overlapping means that a part of the previous signal sample together with a new portion of the signal are taken for the FFT processing rather than the entire new signal sample.

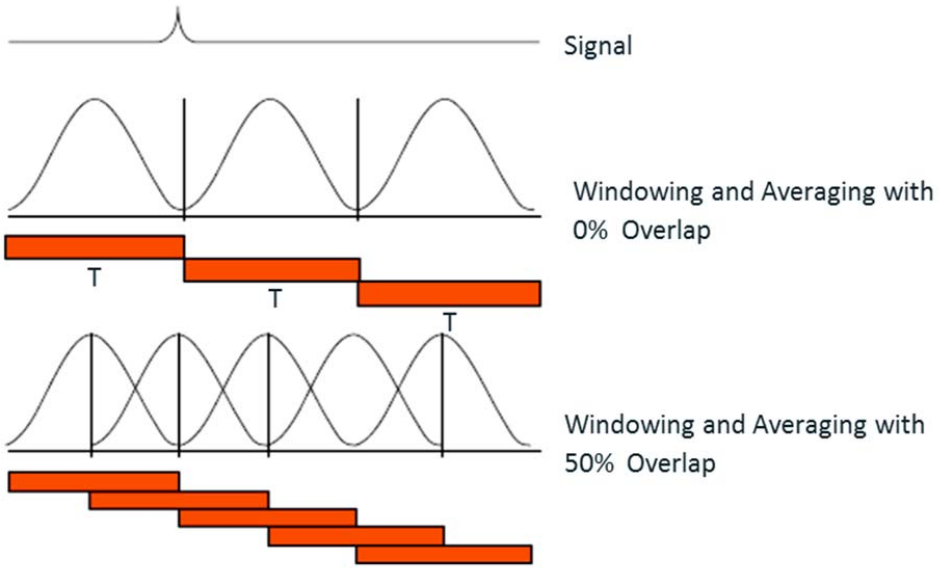

***Figure 1.22**: Averaging without Overlapping (0% Overlap) and with 50 % Overlap*

In Fig.1.22 there is one example where the signal only consists of one pulse. If we average the result, use the window function and we are unlucky, the signal will fall in the region where the window sets the values to zero and in the resulting FFT we will never see this pulse. That‘s why there is an

overlapping procedure which overcomes this problem. It no longer calculates averages one after another, but takes some part of the time signal, which is already calculated and uses it again for calculation. There could be any number for overlap, but usually there is 25%, 50%, 66.7% and 75% overlapping. 50% overlapping means that the calculation will take half of the old data. Now all data will be for sure shown in the resulting FFT. With 66.7% and higher overlapping, every sample in the time domain will count exactly the same in the frequency domain, so if it‘s possible, we should use this value for overlapping to get mathematically correct results.

There are four types of spectral averaging that are available, however only two will be discussed in this course. These are: Linear and Synchronous Time

- ***Linear Averaging***

Linear averaging is a useful method to obtain repeatable data for routine trending purposes. In many cases, the amplitudes of fundamental and passing frequencies are fairly constant and by taking more than one set of data, any random vibrations or spurious events will be averaged out. This is a quick and easy way of improving the signal to noise ratio without too much time or additional effort being added.

- ***Synchronous Time Averaging***

Amplitudes of the corresponding time domain samples are algebraically added for each record and then divided by the number of records. The result is that the desired repeating synchronous waveform components remain intact while all other non-synchronous waveform components tend towards zero. In other words - everything that is not related to the rotation of the measured part of the machine, e.g. signals from adjacent vibrating machines or signals from machine part behind the gearbox, will trickle away. This method requires reflective tape fitted to the shaft and an external trigger connected to the data collector. Usually a larger number of samples are collected and therefore this is not an everyday practice. This method is usually only carried out when a detailed analysis is required.

- **Dynamic Range**

The dynamic range is the ratio between the largest and smallest amplitude signals that a particular analyser can accommodate simultaneously. The amplitudes of the signals are proportional to the output voltages of the transducers, usually in milli-volts. The dynamic range in analogue systems is usually

limited by electrical noise. This is usually not a concern with respect to the transducer itself, but filters, amplifiers, recorders, etc., all add to the noise level and the result may be surprisingly high. In digital systems, the dynamic range is dependent on the analogue to digital converter (ADC) amplitude resolution, normally expressed in bits. The relationship between the number of bits used to sample an analogue signal and the dynamic range (if one bit is used for the sign) is as follows:

6 x (number of bits – 1) = Dynamic Range (db)

Therefore, a dynamic signal analyser with 16 bits of resolution will have a dynamic range of 90 db, but any analogue (electrical) noise or incorrect input range will reduce the dynamic range.

1.1.3.2 Methods of Spectra Analysis

The aim of diagnostics is to assess the machinery condition and, based on deviations from the expected state, to presume emerging machine faults. For this purpose, spectra obtained by Fourier transform of the time record of vibration are commonly used. In addition to vibration measurements and monitoring of the measured values, additional information about the machine is necessary:

- basic technical data (power, operational rotational speed, number of blades, number of teeth ...)
- operation history (downtimes, operating modes ...)
- maintenance history (routine repairs, overhauls, lubrication ...)
- faults in the past

- **Significant Frequencies**

To be able to read various information about a machine from a spectrum, it is worth to know which frequencies would likely occur in such a spectrum (rotational, gear-mesh, bladepass, from bearings, etc.). The spectrum usually contains a number of discrete lines and sometimes areas of the increased noise. It is appropriate to divide the spectrum into areas, in which various symptoms occur:

- Usually, the spectra evaluation process starts with identification of the frequency pertinent to the rotational speed of the shaft - rotational frequency for which the notation *1X* is used.

- Further, the integral multiplies of this rotational frequency (*2X, 3X* ...) are identified - they are also called *harmonics*.

- Spectrum is divided into three main areas (see Figure 1.23):
    - ***area below rotational frequency (<1X)*** - This area is called *subsynchronous* and if any peaks occur in it, they tend to be dangerous (e.g. journal bearing oil whirl).
    - ***area from rotational frequency up to ten times of it (1X to 10X)***- the area of low-frequency events related to the rotation. Symptoms of all the basic mechanical faults (unbalance, misalignment, looseness, etc.) usually occur in this area.
    - ***area above 10X*** - the area of high-frequency events. Symptoms of roller bearing defects, gear faults, etc. occur in this area.

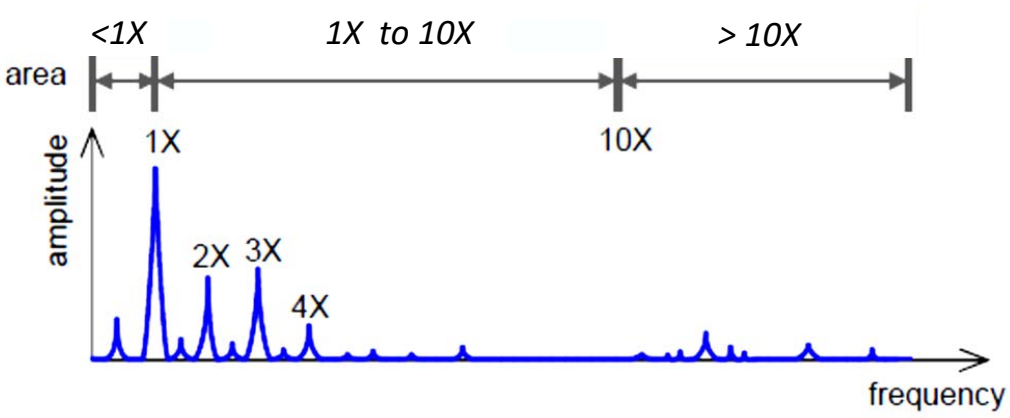

Figure 1.23*: Dividing the Spectrum into Significant Areas*

o Vibration global value

The vibration global value or Overall vibration is generally the first indices following in machine the condition monitoring. Overall vibration is a total vibration energy measured within a specific frequency rang. A higher than normal overall value provide a quick indication that something is causing the machine or component to vibrate more. For a vibration point defined with a specific f_{max} and specific number of lines (N_l), The frequency range of the spectrum took account to measure the overall vibration is to 0 to f_{max}. The method used to calculate the global value ($F_{Overall}$) is a function of several variables (as the following type of function : $F_{Overall} = G(F_1, F_2, F_3, \dots, F_{N_l})$ where $F_1, F_2, F_3, \dots, F_{N_l}$ are the peak values corresponding to the lines. This method should also allow to prevail the highest amplitudes that are more significant than lower amplitudes that are not indicative of a fault.

- **Trend diagrams**

A powerful help, easy to get and precise in result, is the ability to create trend graphs. It shows that the variation in time of the observed variables, then evaluating the progressive course and the extent of the variation. When possible, the creation of these graphs, it should be as a rule. But we must always make sure that, both the time interval considered, both the resolution of the data are adequate to provide the desired information.

- **Reference Spectrum and Monitoring of Changes**

It is in fact to note that the assessment of changes in a machine is not only based on comparison with normal pre-set values, but also and especially on the analysis of signature of normal or baseline vibration. As complicated and comprising many details not well definable, a spectrum presents a variety of peaks which may vary in time in function of changes of the machine operating conditions. Therefore its persistence over time will surely be index of constant operation, while its change will deepen the exact meaning of the individual components and then to trace the actual cause of the change in operating conditions.

In Fig.1.24 above, there is an example of a baseline spectrum, beneath there is a situation when the basic rotational frequency *1X* has changed and is significantly higher than normal. This indicates that the vibration signal is periodically changed once per shaft rotation. A typical cause for such behaviour use is either unbalance or misalignment.

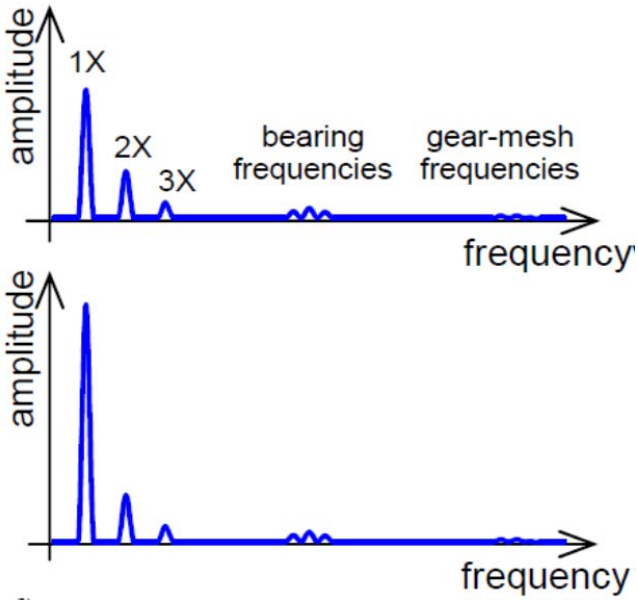

Figure. 1.24: *Baseline Spectrum and Changes in Spectra while Fault Development*

o Waterfall Diagrams

Another diagnostic tool for quick visual comparison of spectra is waterfall (cascade) diagrams. They are used to compare spectra from steady operation during a longer period of time (see Fig. 1.25). Gradual or sudden change in some frequency components is clearly visible.

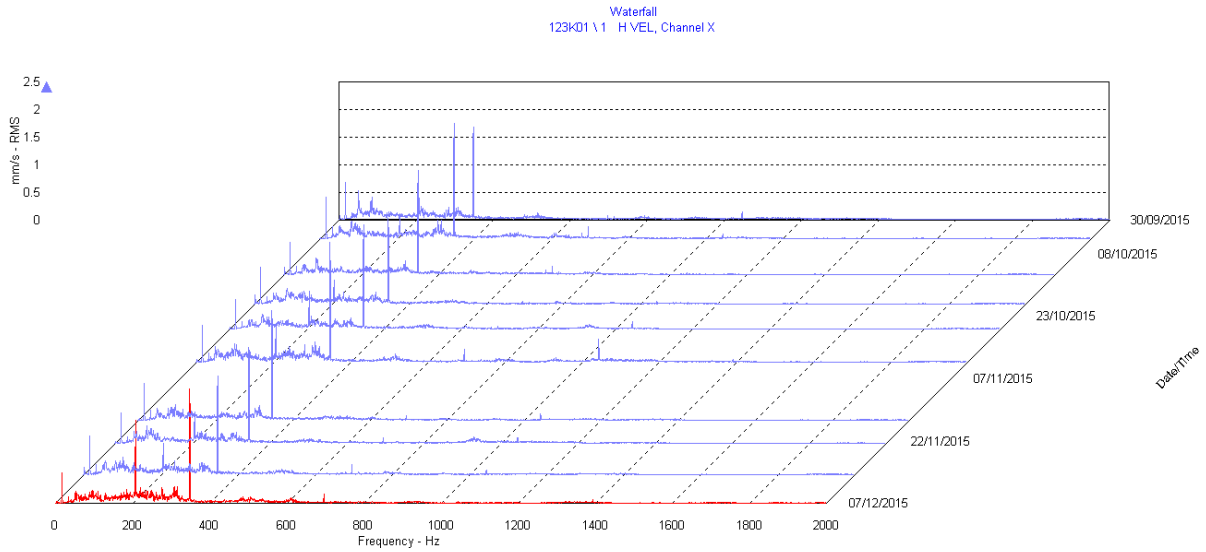

Figure 1.25: *Waterfall Diagrams*

1.2 Rotating machine Main Faults

This paragraph presents an overview of main defects that may be encountered on conventional rotating machines. We can distinguish defects in rotors and rotating parts, defects related to the deterioration of support and problems of flow-related vibration [7].

1.2.1 Rotors and rotating parts faults

1.2.1.1 Unbalance

Unbalance occurs in a rotating machinery when the mass centerline and the geometric center do not coincide on each other. In fact , the centrifugal force is one of the basic excitation forces in rotating machinery. It originates from the fact that with a real product (rotor), it is not possible to achieve the centre of gravity to be exactly on the axis of rotation and this axis of rotation to coincide with the principal axis of inertia. There are three types of unbalances depending on how the mass is distributed on the rotor and how it will affect the position of the principal axis of inertia with respect to the axis of rotation: static, couple and dynamic unbalance (This topic is developed in chapter 3 so see in Fig. 3.1.1). The causes of this condition are:

- in design (some parts may be not perfectly symmetrical)
- technological (non-homogenous material)
- manufacturing (everything is produced in some tolerances, rotating parts exhibit runout)
- in mounting (namely with mounted rotors).

Unbalanced rotors generate vibrations which may damage their components. Important symptom of an unbalance in a spectrum is high vibration amplitude in radial directions at the rotational component (1X). The reason is that the centrifugal force caused by the unbalance rotates with the rotational frequency and causes forced vibrations with the same frequency. In order to extend the life of the machine, vibration due to unbalance must be reduced to acceptable level.

1.2.1.2 Misalignment and Deterioration of the Alignment state

Shaft misalignment has major implications for modern-day rotating equipment reliability. Although effective alignment techniques have been applied successfully on a wide range of equipment for some

time, deterioration of the alignment state can frequently occur due to, for example, changes in equipment operating conditions, foundation settlement and piping strain. Shaft misalignment is usually defined in terms of angular and parallel components (Fig.1.26 a and b). Real systems are subjected to the combined influence of the two misalignment effects as shown in Figure l.26-c.

More research studies have been done on misalignment problem [9; 10; 11; 12; 13] in order to understand the dynamic characteristics of these machinery faults. These works showed that the forcing frequencies due to shaft misalignment are even multiple frequencies of the motor rotational speed.

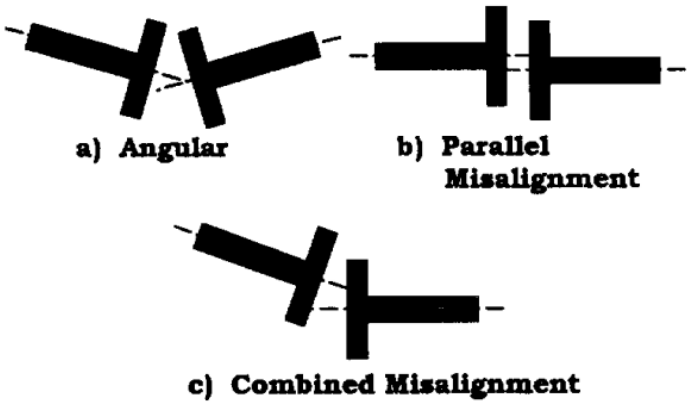

Figure 1.26: *Misalignment Types (Uncoupled State)*

Aligning rotors before assembling them, consist in the parallel and concentric coupling plates so as to align the axes of rotation. This requires that specific criteria are satisfied in both the horizontal and in the vertical plane. We then met two conditions: (1) rotation axes are confused, and (2) the reactions of the supports are those corresponding to own weight; each bearing carrying the expected share of the rotors weight. If the first condition is not satisfied, it creates an imbalance. If the support positions are not what they should be, then we have a misalignment. It can have a double effect:

- the misalignment inserts into the shaft alternating efforts, as the shaft rotates;

- It changes the supports stiffness and therefore the dynamic responses of the machine to these efforts, when the links are not linear, or when the rotors are not symmetrical [12;13].

Another consequence of edging, linked to the non-linear behavior of the bearings, is to alter the distribution of harmonic vibrations of the rotation frequency.

- **Angular Misalignment**

Angular misalignment is characterized by large axial vibration, which is out-of-phase, i.e. with the difference 180° over the coupling. In a typical case, large axial vibration is on both *1X* and *2X* components (see Fig. 1.27). But it is quite common that any of the components *1X, 2X* or *3X* dominates. These symptoms may also indicate the existence of the problems with the coupling. The considerable angular misalignment may excite many harmonics of rotational frequency.

- **Parallel Misalignment**

Misalignment, resulting from parallel shifting, has similar symptoms as an angular misalignment, but large vibration is in the radial direction. They are approximately out-ofphase, i.e. shifted by 180□□over the coupling. The *2X* component is often larger than the *1X*, but its size relative to the *1X* is often determined by the type and construction of the coupling (see Fig.1.27). When the angular or parallel misalignment is significant, it can generate either high amplitude peaks at several harmonics (*4X to 8X*) or even a lot of harmonics to a high frequency, which is similar to the mechanical looseness.

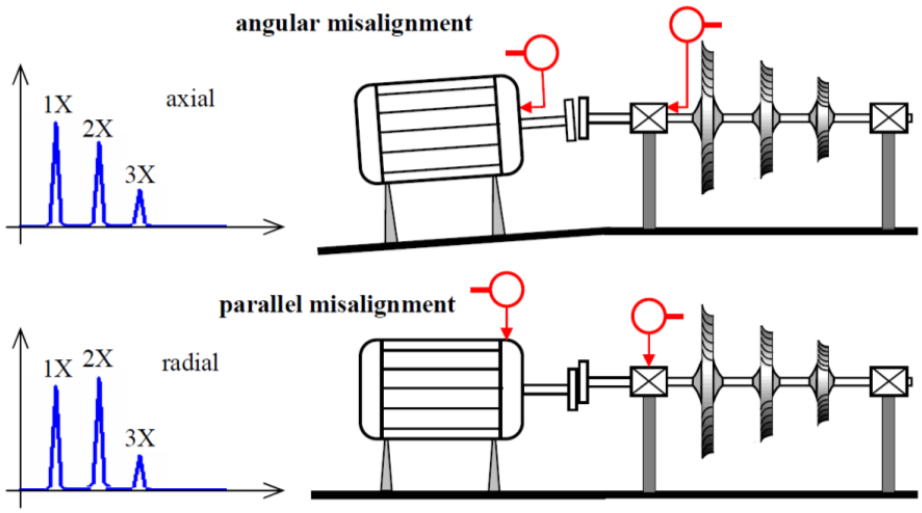

Figure 1.27: *Angular and Parallel Misalignment - Typical Spectrum and Phase Relations [6]*

Deterioration of the aligning results from deformations party fixed, body, massive, beam or bearing support due to: beams deformations up period on some machines, accidental blockage of vents, expansion disgruntled stators; cracking beams ...

1.2.1.3 Asymmetrical shaft

The behavior of a shaft having a stiffness dissymmetry for example, because of the presence of notches or coil (generators, motors, pins…) is particular. When the rotor rotates, the own weight of load is taken by the stiffness of the shaft, but the position of the shaft center will be even higher than the stiffness will be high. However, the stiffness varies with time. When the shaft made a rotation, stiffness varies twice per turn. The asymmetric rotors create efforts (thus vibration) at twice the rotation frequency (*2 X*).

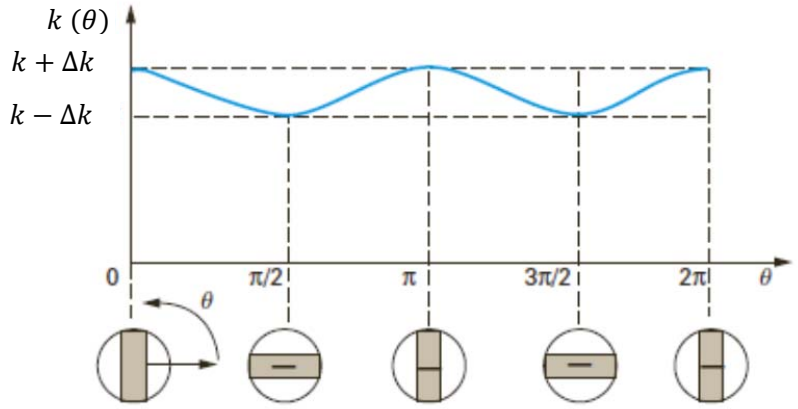

Figure 1.28: *Asymmetrical shaft: angular variation of the stiffness* ***k***

1.2.1.4 Shaft transversal cracking

A crack shaft has a stiffness that varies with the direction of the force, mainly the weight, and the reactions of support. So there is a certain analogy with the behavior of the asymmetric rotor. But this time, the arrow shaft will depend on whether the crack is in the up position (compressed fiber, crack closed) or low (fibre tense, crack open). The same movement is repeated for each revolution of the shaft, creating a periodic movement.

1.2.1.5 Couplings

Shaft couplings are critical parts of any transmission system, providing the smooth transmission of power from drive to driven equipment. They must transmit torque. They also sometimes allow the axial expansions of the machine, or the radial displacement. We will discuss a few defects that affect performance.

- **Plate Couplings**

The defects of this type of coupling are mainly: poor centering plates; a parallelism error (a non-perpendicularity of the plates with respect to the axis of rotation). Both defects create an imbalance and therefore vibrations at the rotation frequency *(1X)*.

- **Cardan or double cardan couplings**

A cardan is a joint designed to withstand considerable relative movements of the rotary axes of the driver and the driven machines. It acts like an asymmetrical shaft, and as such, it will lead efforts to frequency *2 X*.

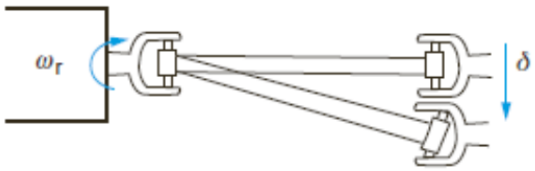

Figure 1.28: *cardan couplings*

- **Tooth couplings**

This type of coupling is often used if you want to allow large axial displacement between the driving machine and driven machine or a significant axial expansion of long rotors or shafts with large temperature variations. The first fault of these couplings results from poor slide prohibiting expansion. The upset shaft in its expansion will flex and unbalance will evolve with the expansion of the shaft. This type of fault may sometimes be revealed by removing the motor torque to enable the teeth to slip. Other more complex phenomena can be observed:

- Tooth defects (such as on the gears and having the same symptoms);
- Instabilities of lubricant blades centrifuged if they are thick.

1.2.1.6 Gear box

- **Tooth noise**

Incidents characteristics of the gears are related to damage of the dentition (teeth broken or damaged, uniform wear or not, pitting (fighting, chipping) localized or distributed, poor centering). We can also observe the fretting (in friction corrosion), which results in metal removal when the gear is poorly lubricated or that efforts are important. The vibrations of the gears are dominated by a force to each contact. It is in the frequencies nX (n is entire number) that contained the information, especially if there is too much clearance, or conversely too tight fitting. The localized defects (defect of a tooth) result in more by a pulse whenever the damaged tooth is in contact with another. There therefore occurrence of a line at the frequency of contacts of interest wheel.

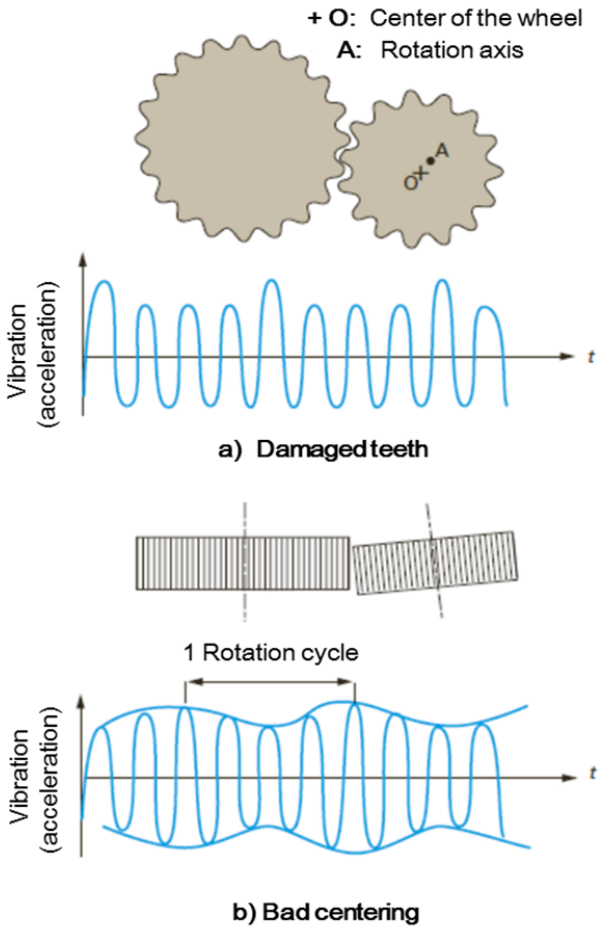

Figure 1.30 : *Vibrations of a gear [7]*

- **Poor centering**

One can observe a modulation of this effort if the wheels are not in focus. This modulation is manifested by the appearance in the vibrational spectrum of parallel lines around the frequency of teeth. The vibrations of a gearbox are a function of torque and radial forces [14].

1.2.1.7 Rolling Bearings Fault

Bearings are among the most stressed components of machines and a source of frequent failure. The defects that can meet there are: chipping, seizing, corrosion (which causes flaking), fake Brinnel effect, etc. All these defects have something in common: they result sooner or later in a loss of metal fragments. This argument is developed in Section 1.3.

1.2.1.8 Hydrodynamic journal bearings instabilities and default

Faults encountered on film fluid bearings are due primarily to an alteration of the pads. A bad lineage, high vibrations, especially interruption of lubrication or lack of uplift are some possible causes of destruction of babbitt (anti-friction alloy based on lead or tin). A difference of potential between the rotor and the bearing may induce pitting (especially on generators). The presence of particles in the oil can cause scratches the Babbitt.

- **Faults of Journal Bearings - Wear, Excessive Clearance**

Wear of the bearing causes an excessive clearance, which is usually reflected by the presence of harmonics of rotational frequency, particularly in the absolute vibration spectrum. On the contrary, in the relative vibration spectrum, a radial bearing with increased clearance will usually exhibit large $1X$ amplitude without the existence of harmonics. Symptoms of an excessive clearance in the bearing are similar to that of mechanical looseness. Bearing with correct clearance, but with loosed contact to the supporting structure, manifests itself similarly in vibration as a bearing with excessive clearance. Therefore, it is often difficult to distinguish between these two cases.

- **Hydrodynamic journal bearings instabilities**

Another problem of lubrication is that of self-excited vibrations that appear in a bearing when certain conditions are met.

- Too lightly loaded journal bearings (also called Film Fluid bearings), or whose radial clearance is too strong, may become unstable. Indeed, the behavior of a bearing is highly nonlinear. If the shaft is insufficiently loaded, that is to say, if the operating point of the bearing imposes too small eccentricity [7], the bearing becomes unstable and generates self-excited vibrations. Violent vibrations then occur at the half frequency of the rotation $\left(\frac{X}{2}\right)$. The evolution is so rapid and often the level is not stable. The dominant frequency of the vibration is the half frequency, it can be close to $\left(\frac{X}{3}\right)$ or $\left(\frac{X}{4}\right)$ if a critical speed of the rotor synchronizes the phenomenon.

- Oil Whirl is a case when the oil film causes the sub synchronous precession component of the rotor motion - oil wedge "pushes" the rotor around the shaft in the bearing with a frequency that is lower than the rotational frequency; the precession is forward. This instability appears at sub-synchronous frequency of about $0.40X$ to $0.48X$ and it is often quite strong. Oil whirl condition can be induced by several conditions including: Light dynamic and preload forces; excessive bearing wear or clearance; a change in oil properties (primarily shear viscosity); an increase or decrease in oil pressure or oil temperature; improper bearing design; change in internal damping (hysteretic, or material damping; or dry (coulomb) friction); gyroscopic effects - especially on overhung rotors having much overhang [8].

- Oil Whip is an instability which can occur when a machine is operated at above twice the rotor critical speed. When the rotor spins to twice the critical speed, the oil whirl frequency can be close to the rotor critical speed and, thus, can excite the resonance and cause excessive vibration. This instability causes transverse sub-harmonic vibration with frequency equal to the rotor critical speed during forward precession.

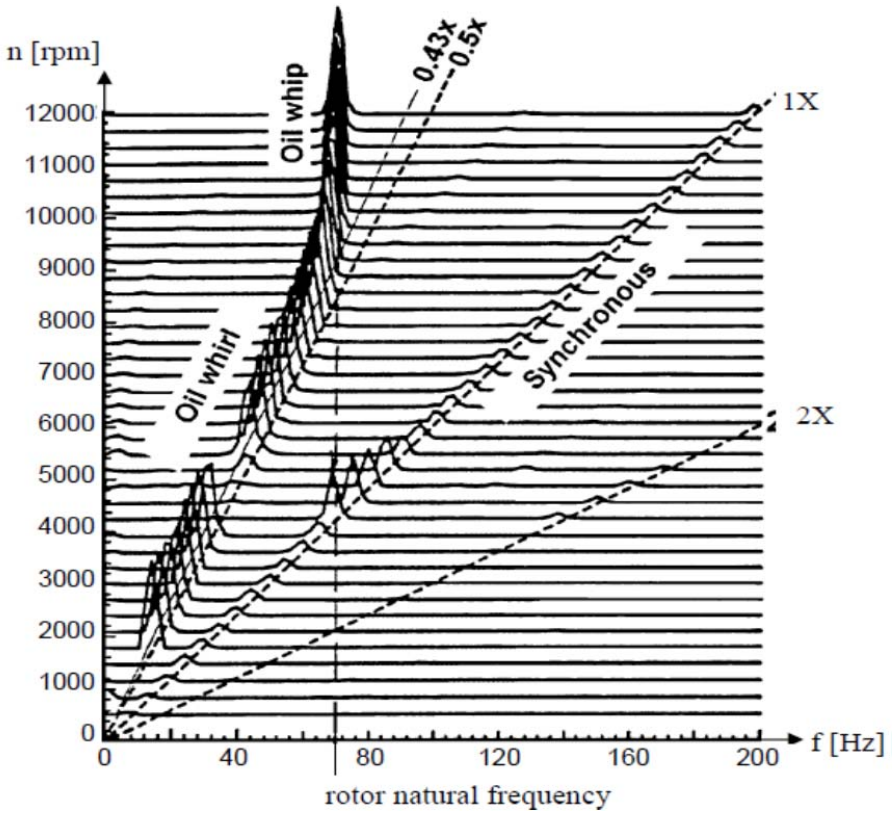

Figure 1.31: *Instabilities of Oil Film*

1.2.1.9 Clearance, Loosening, Poor fixation

This class of defects concerns machines fixations on their supports or solid. If installation fails, we can observe different phenomena.

- If there is clearance, the operation will not be linear and sinusoidal vibratory motion will be transformed into a periodic movement especially rich in harmonics that the signal will be distorted. Another consequence of the clearance may be to create shock, and in this case can be detected by methods similar to those used for the bearings or loose parts.

- If the fixation has an insufficient stiffness, that can highlight by deformed measures. The weak points of a structure appear as singularities of shape (excessive local deformation, vibration behavior asymmetries). Similarly we can highlight resonances structures or modifications of anchors in time by changing distorted.

1.2.1.10 Hydrodynamics Related Vibrations

Among the many phenomena affecting the vibration behavior of the pumps or hydraulic machines, there are those of hydrodynamic origin. In this report we will only few of them: hydraulic unbalance, gaskets, cavitation noise**.**

- **Hydraulic unbalance**

One may encounter in the pumps, a rotating force generated by the pressure asymmetries on the wheel. Indeed, during the manufacture of the blades, there are still differences in impeller geometric profile which are due to slight pressure asymmetries. The integral of the pressure asymmetries on the surface of the impeller creates hydraulic unbalance. This imbalance of a hydraulic pump varies with the operating conditions.

- **Gaskets**

The presence of gaskets in pumps has a beneficial effect on vibration dumping at critical speed of the rotor. But they behave as hydrodynamic bearings and create efforts even more important that the play are low. So we can meet similar instability phenomena to those observed on hydrodynamic bearings .

- **Cavitation noise**

Cavitation is the creation of cavities in the fluid when some areas are depressed. These cavities or bubbles disappear imploding in a very short time, creating intense pulse effects. The spectrum of vibrations due to cavitation is a broadband spectrum, which can range from a few Hz to over 300 kHz, since all structures are excited.

References

[1] ISO 13373-1: *"Condition monitoring and diagnostics of machines - Vibration condition monitoring - Part 1: General procedures. 2002"*; This standard was last reviewed* in 2012

[2] ISO 13373-2: "*Condition monitoring and diagnostics of machines - Vibration condition monitoring - Part 2: processing, presentation and analysis of vibration data"*. 2005

[3] Mao Kunli, Wu Yunxin, "*Fault Diagnosis of Rolling Element Bearing Based on Vibration Frequency Analysis*", IEEE Third International Conference on Measuring Technology and Mechatronics Automation (ICMTMA) 2011, 337.

[4] SKF, "*Basics of Condition Based Maintenance",* ISO 18436 Vibration Analysis Level 1, SKF May 2012.

[5] SKF; *" Data Acquisition & Signal Processing";* ISO 18436 Vibration Analysis Level 1, SKF May 2012.

[6] Alena Bilošová Jan Biloš; "*Vibration diagnostics*", Ostrava 2012.

[7] Jacques Morel; *"Surveillance Vibratoire Et Maintenance Prédictive",* Département surveillance diagnostic maintenance à EDF, Division recherches et développement

[8] James E. Berry P.E. *"Concentrated vibration signature analysis and related condition monitoring techniques",* Technical Associates of Charlotte, P.C. 2002 San Diego,CA

[9] Xu, M., Marsngoni, R.D. *"Vibration Analysis of a Motor Flexible Coupling Rotor System Subject to Misalignment and Unbalance, Part I: Theoretical Model and Analysis"*, Journal of Sound and Vibration Volume 176, Issue 5, 6 October 1994, Pages 663–679

[10] Sekhar, AS., Prsbhu, B.S. *"Effects of Coupling Misalignment on Vibrations of Rotating Machinery",* Journal of Sound and Vibration, Vol 185(4). pp666 - 671, 1995.

[11] Redmond.I, Hussain,K.M., "*Misalignment As a Source of Vibration in Rotating Shaft Systems"*, Proc. Intl. Modal Analysis Conf. (IMAC) XIX, Orlando, Feb. 2001.

[12] I. Redmond; *"Study of a misaligned flexibly coupled shaft system having nonlinear bearings and cyclic coupling*

stiffness—Theoretical model and analysis", Journal of Sound and Vibration 700-720, 2010

[13] Irvin Redmond; *"Shaft Misalignment and Vibration - A Model"* ; Dynamic Analysis Unit, Consulting Services Department, Saudi Arabian Oil Company, Dhahran, 2002.

[14] REMOND, VELEX et SABOT. *"Comportement dynamique et acoustique des transmissions par engrenages".* Publication CETIM n° 5B10, Senlis (1993)

Chapter 2

Rolling Element Bearing Vibration Detection and Diagnosis

2 Rolling Element Bearing Vibration Detection and Diagnosis

Abstract

Rolling element bearings are between the most common components to be found in industrial rotating machinery. They support and locate rotating shafts machines. Vibration produced by them can be complex and can result from geometrical imperfections during the manufacturing process, defects on the rolling surfaces or geometrical errors in associated components. Vibration (and Noise) is becoming more critical in all types of equipment since it is often perceived to be synonymous with quality and often used for predictive maintenance.

The key factors which are addressed in this chapter include bearing failure modes, vibration measurement, signal processing techniques (particularly envelop technique), and prognosis of bearing failure.

2.1 Introduction

The rolling element bearing is one of the most critical components that determine the machinery health and its remaining lifetime in modern production machinery. Robust predictive health monitoring tools are needed to guarantee the healthy state of rolling element bearing s during the operation. A Predictive Health Monitoring (PHM) tool indicates the upcoming failures which provide sufficient lead time for maintenance planning. The PHM tool aims to monitor the deterioration i.e. wear evolution rather than just detecting the defects. Its procedures contain detection, diagnosis and prognosis analysis, which are required to extract the features related to the faulty rolling element bearing and estimate the remaining useful lifetime. A recent study has been done by I. El-Thalji, E. Jantunen [15], where their presented a review of the PHM methods and explored their capabilities, advantages and disadvantage in monitoring rolling element bearings.

2.2 Bearing Failure Modes

The actual mode of bearing failure which occurs for any particular rotating machine can have a major influence on the resulting vibration which is measured externally. The normal service life of a rolling

element bearing rotating under load is determined by material fatigue and wear at the running surfaces. Premature bearing failures can be caused by a large number of factors, the most common of which are fatigue, wear, plastic deformation, corrosion, brinelling, poor lubrication, faulty installation and incorrect design [17; 18; 19]. Often there can be overlap between factors for a particular bearing failure or a bearing may start to fail in one particular mode which then leads on to other failure modes.

2.2.1 Fatigue

Fatigue wear can occur in surfaces that are dynamically loaded. Under elastic contacts, the fatigue process usually requires high number of cycles, while under plastic contact, a low-cycle fatigue mechanism can be expected. Fatigue damage begins with the formation of minute cracks below the bearing surface [20]. As loading continues, the cracks progress to the surface where they cause material to break loose in the contact areas. The actual failure can manifest itself as pitting, spalling or flaking of the bearing races or rolling elements. If the bearing continues in service, the damage spreads since the localised stresses in the vicinity of the defect are increased. The surface damage severely disturbs the rolling motion of the rolling elements which leads to the generation of short time impacts repeated at the appropriate rolling element defect frequency. As the damage spreads the periodic repetitive nature of the impacts will diminish as the motion of the rolling element becomes so irregular and disturbed that it becomes impossible to distinguish between individual impacts.

2.2.1.1 Wear

Wear is another common cause of bearing failure. It is caused mainly by dirt and foreign particles entering the bearing through inadequate sealing or due to contaminated lubricant. Solid, hard particles can cause local stress peaks and shorten the life of the bearing [21, 22, 23]. We can distingue the adhesive wear (smearing) and abrasive wear

- **Adhesive wear (smearing)**

Adhesive wear, just like most other lubrication-related damage, occurs between two mating surfaces. It is often a material transfer from one surface to another with friction heat, sometimes with a tempering or rehardening effect on the surface. This produces localized stress concentrations with potential spalling of the contact areas.

- **Abrasive wear**

abrasive wear is the progressive removal of material, which foreign particles roughen the surfaces in contact giving a dull appearance. Severe wear changes the raceway profile and alters the rolling element profile and diameter, increasing the bearing clearance. This type of wear occurs most of the time due to inadequate lubrication resulting mostly from the ingress of abrasive contaminant particles. Raceway material, but also rolling elements and cage material, is removed by abrasion. Most of the time, dull surfaces appear. However, some abrasive particles might act as polishing material and surfaces might become extremely shiny, all depending on the size, their hardness and in what stage. This is an accelerating process because wear particles will further reduce the lubrication ability of the lubricant and this destroys the micro geometry of the bearings. The rolling friction increases considerably and can lead to high levels of slip and skidding, the end result of which is complete breakdown [24]. A discussion on the effects of general wear on the resulting measured vibration can be found in [25, 26].

2.2.1.2 Plastic deformation

Plastic deformation of bearing contacting surfaces can be the result of a bearing subject to excessive loading while stationary or undergoing small movements. The result is indentation of the raceway as the excessive loading causes localised plastic deformation. In operation, the deformed bearing would rotate very unevenly producing excessive vibration and would not be fit for further service [24].

2.2.1.3 Corrosion

Corrosion damage occurs when water, acids or other contaminants in the oil enter the bearing arrangement. This can be caused by damaged seals, acidic lubricants or condensation which occurs when bearings are suddenly cooled from a higher operating temperature in very humid air. The result is rust on the running surfaces which produces uneven and noisy operation as the rust particles interfere with the lubrication and smooth rolling action of the rolling elements [24].

2.2.1.4 Brinelling

Brinelling manifests itself as regularly spaced indentations distributed over the entire raceway circumference, corresponding approximately in shape to the Hertzian contact area. Three possible causes of brinelling are:

- Static overloading which leads to plastic deformation of the raceways,
- When a stationary rolling bearing is subject to vibration and shock loads and,
- When a bearing forms the loop for the passage of electric current.

2.2.1.5 Lubrication

Inadequate lubrication is one of the common causes of premature bearing failure as it leads to skidding, slip, increased friction, heat generation and sticking. Under poor lubrication, rolling bearings may suffer from adhesive wear at roller ends and in micro slip zones. At the highly stressed region of Hertzian contact, the contacting surfaces will weld together, only to be torn apart as the rolling element moves on. The three critical points of bearing lubrication occur at the cage-roller interface, the roller-race interface and the cage-race interface [27, 28,29].

2.2.1.6 Electrical erosion

Electrical erosion are mainly caused by excessive voltage and current leakage.

- **Excessive voltage**

When an electric current passes through a bearing, i.e. proceeds from one ring to the other via the rolling elements, damage will occur. At the contact surfaces, the process is similar to electric arc welding (high current density over a small contact surface). The material is heated to temperatures ranging from tempering to melting levels. This leads to the appearance of discoloured areas, varying in size, where the material has been tempered, re-hardened or melted. Craters are formed where the material has been melted.

- **Current leakage**

Where current flows continually through the bearing in service, even at low intensity, the raceway surfaces become heat effected and eroded as many thousands of mini-craters are formed, mostly on the surface. They are closely positioned to one another and small in diameter compared to the damage from excessive voltage. Flutes (washboarding) will develop from craters over time, where they are found on the raceways of rings and rollers.

The extent of damage depends on a number of factors: current intensity, duration, bearing load, speed and lubricant. Also, the grease must be checked. Indeed in addition to bearing damage, the grease close to the damage will be carbonized, eventually leading to poor lubrication conditions and consequently to surface distress and spalling.

2.2.1.7 Faulty installation

Faulty installation can include such effects as excessive preloading in either radial or axial directions, misalignment, loose fits or damage due to excessive force used in mounting the bearing components [30].

2.2.1.8 Incorrect design

Incorrect design can involve poor choice of bearing type or size for the required operation, or inadequate support by the mating parts. Incorrect bearing selection can result in any number of problems depending on whether it includes low load carrying capability or low speed rating. The end result will be reduced fatigue life and premature failure.

2.2.2 Bearing Wear Evolution

Bearing wear evolution had been studied by different authors. We reported here some of those studies. Jantunen [46] and Yoshioka and Shimizu [47] observed two main stages of wear progress: steady state and instability. The steady-state stage is roughly stable. However, a clear offset in the root mean square (RMS) values of monitoring signals (vibration acceleration) is observed at instability stage, together with instability and rapid increase of these values before the final failure. Schwach and Guo [49] (using AE amplitude) and Harvey et al. [48] observed three stages of wear progress. Moreover, the instability stage is observed to follow a steep-offset propagation. Harvey et al. [48] observed that electrostatic charge measurement indicate the wear initiation as a region of high signal amplitude (with respect to normal signal state), where it disappears (i.e. goes back to normal single state) until the failure occurs.

Therefore, electrostatic measurement indicates instantaneous occurrences of wear mechanisms in the region of high signal amplitude rather than progressive stages.

Manoj et al. [50] observed that the 3rd harmonic of the roller contact frequency of vibration has very good correlation with wear and when the pitting takes place, the amplitude of the 3rd harmonic of contact frequency increases to nearly four to five times the amplitude of other harmonics. In the same manner, the frequency analysis of sound signal shows that the 3rd and 1st harmonics of roller contact frequency have good correlation with the wear trend. Zhi-qiang et al. [51] observed two stages of wear progress using vibration measurements. However, four stages of wear progress were observed using AE: running-in, steady-state, a stage of minor-instability due to distributed defects, and finally a stage of major-instability due to pitting and spalling.

2.2.3 Bearing Condition Monitoring Techniques

Even if our study is specifically focused on machinery condition monitoring technique basing on vibration analysis, we would like to present here others less successful monitoring techniques as mention above in the section 1.1.1.2. Actually, in addition to vibration, several experiments have been conducted to study others specific monitoring techniques such as AE, oil-debris, ultrasound, electrostatic, Shock-Pulse Measurements, etc. and their use in faulty rolling element bearings detection. We present the first two mentioned.

2.2.3.1 Acoustic Measurement

Acoustic emission is the phenomenon of transient elastic wave generation due to a rapid release of strain energy caused by relative motion of small particles under mechanical stresses [31]. The detection of cracks is the prime application of acoustic emission; therefore, this technique can be used as a tool for condition monitoring of bearing faults and shaft cracks. Interaction of rolling element bearing components and movement of bearing rollers over defects will produce acoustic emissions. The frequency content of acoustic emission is typically in the range of 100 kHz to 1 MHz, so AE is not influenced or distorted by imbalance and misalignment which are at low frequency ranges [32]. Typically, the accuracy of these methods depends on sound pressure and sound intensity data [33, 34].

2.2.3.2 Wear Debris Analysis

The use of wear particle examination as a diagnostic tool requires an estimate of the likely wear mechanisms and the regimes in which each of the contacts of interest operates [35].

In 2005 Halme [36] studied the condition monitoring of an oil-lubricated ball bearing in an accelerated bearing life test. He concluded that during a step from the steady state to the final phase of the life of a ball bearing, the most remarkable acceleration in a wear process was detected through the measured vibration acceleration responses, as well as through the amount of relatively large particles in the oil. In 2007, using a bearing test rig, Harvey et al. [37] studied the wear monitoring of a lubricated taper roller bearing with an artificial fault on the inner race. An accelerated test was run until a total damage occurred, and the wear particle responses were measured with electrostatic sensors and the vibrations were measured with acceleration sensors. When about 10 per cent of the calculated lifetime of the bearing was left, a first steady increase in the measured electrostatic responses was seen. When about 6 per cent of the life-time was left, both the electrostatic response and the vibration amplitude of the inner race fault frequency increased. When about 99 per cent of the calculated lifetime of the bearing had elapsed, a sharp increase occurred in all the measured parameters.

Several methods for the detection and analysis of wear particles in rolling bearings are available. The methods can be divided into off-line laboratory methods and continuous on-line or in-line methods. The wear particle detection techniques for in-line or on-line analyses have been listed in [38,39]. Some of methods for wear particle monitoring are: optical method, ferrography analysis, inductance based detection [40].

In inductance based detection, a coil is placed around a pipe with a flow of oil with particles, and metal particles are detected through an inductance change in the coil, which is different for ferrous and non-ferrous particles [41, 42]. Magnetic attraction of wear particles in oil can be used for sensing a particle flow past a magnetic sensor [41, 42].

Ferrography analysis: in this method, oil-borne particles are sedimented along a glass slide by the interaction of gravity and magnetic attraction. Based on the location and orientation, form, size, texture, and colour, wear particles and other particles can be identified under a light microscope [41, 42].

For the optical determination of the size distribution of particles in oil, one option is the Fraunhofer light diffraction technique (also known as forward scatter), by which an array of detectors ahead of a

light beam, passed through a mixture of oil and particles, detects the proportion of light diffraction caused by small and large particles. With the optical obscuration method, each particle casts a shadow when passing through a light beam, and a photo detector measures the drop in intensity at a reference surface [43, 44, 45].

2.2.3.3 Bearing Vibration Measurement

Analysis of vibrations from rolling bearings is typically based on the results of vibration acceleration and AE measurements, which are analysed in the time domain or in the frequency domain, or in both. Prior to sampling, the vibration signals are anti-alias filtered for preventing frequencies higher than half the sampling frequency so as to appear at the lower frequencies. Analyses in the frequency domain are based on spectrum analyses, which present the vibration data as a function of discrete frequency components. The spectrum is calculated by using fast Fourier transformation.

There are two types of defects: localized defects, distributed defects. Localized defects include cracks, pits and spalls on the rolling surfaces. Distributed defects include surface roughness, waviness, misaligned races and off-size rolling elements [4]. Since the abnormal vibration of rotary machines is the first sensory effect of rotary component failure, vibration analysis is widely employed in the industry. The fault vibration signal generated by the interaction between a damaged area and a rolling surface occurs regardless of the defect type. Consequently, a vibration analysis can be employed for the diagnosis of all types of faults, either localized or distributed.

- **Time Domain Technique and Statistical measures**

Time domain statistical parameters have been used as one-off and trend parameters in an attempt to detect the presence of incipient bearing damage. The signal processing methods were mainly based on statistical parameters such as RMS, mean, kurtosis (Ku), crest factor (CF), Impulse factor (IF), and Shape factor etc. (SF) [42,43, 44, 45]. These statistical parameters are defined in table1.1. Methods based on these parameters were applied with limits successes.

The simplest approach in the time domain is to measure the overall RMS level, which is a use to estimate the average power in system vibrations. The trending based on RMS value is one of the methods which can show the correlation between vibration acceleration and the rolling element bearing

wear over the whole lifetime [46, 52, 53, 54, 55, 56]. However this method has been applied with limited success for the detection of localized defects [90,91].

The kurtosis parameter had been proposed [57] for bearing defect detection. For an undamaged bearing with Gaussian distribution, the kurtosis value is close to 3. A value greater than 3 is judged by itself to be an indication of impending failure and no prior history is required. However, one disadvantage is that the kurtosis value comes down to the level of an undamaged bearing (i.e., 3) when the damage is well advanced. The kurtosis is sensitive to the rotational speed and the frequency bandwidth. Several studies [93, 94, 95,96,] have shown the effectiveness of kurtosis in bearing defect detection but in some cases [97, 98, 99] the method could not detect the incipient damage effectively. Kurtosis has not become a very popular method in industry for the condition monitoring of bearings.

As Kurtosis, the crest factors increase as the spikiness of the vibration increases. In this sense, it is very sensitive to the shape of the signal. However, the third central moment (Skewness) was found to be a poor measure of fault features in rolling bearings [68], in general skewness can be an effective measure for signals that are unsymmetrical i.e. non-linearity.

Another parameter is the shock pulse. The shock pulse method [92] principle is based on the fact that structural resonances are excited in the high frequency zone due to impulsive loading caused, for example, from spalling of the races or rolling elements and can be detected by a transducer whose resonant frequency is tuned to it. The shock pulse method uses a piezoelectric transducer having a resonant frequency based at 32 kHz (or more than this). The shock pulses caused by the impacts in the bearings initiate damped oscillations in the transducer at its resonant frequency. Measurement of the maximum value of the damped transient gives an indication of the condition of rolling bearings. Low-frequency vibrations in the machine, generated by sources other than rolling bearings, are electronically filtered out. The shock pulse value generated by good bearings due to surface roughness has been found empirically to be dependent upon the bearing bore diameter and speed. This value, called the initial value, is subtracted from the shock value of the test bearing to obtain a normalized shock pulse value. The maximum normalized shock value is a measure of the bearing condition. The shock pulse method has gained wide industrial acceptance and has been reported to be successful in the detection of rolling element bearing defects [3,5,34,39,43]. Some investigators [31,44,45] have reported that the method could not effectively detect defects at low speeds.

Table 2.1 : *Scalar indicators specific to bearing vibration detection (for a signal array X of i samples)*

Peak	$X_a = \frac{1}{2}\,(max(X_i) - \min(X_i))$	(Eq. 2.1)
Root mean square	$X_{RMS} = \sqrt{\frac{1}{Z}\sum_{i=1}^{Z} X_i^2}$	(Eq. 2.2)
Crest factor	$X_{CF} = \frac{X_a}{X_{RMS}}$	(Eq. 2.3)
Kurtosis	$X_{Kurtosis} = \frac{\frac{1}{Z}\sum_{i=1}^{Z}(X_i - \bar{X})^4}{{X_{RMS}}^4}$	(Eq. 2.4)
Shape Factor	$X_{SF} = \frac{X_{RMS}}{\frac{1}{Z}\sum_{i=1}^{Z}\lvert X_i\rvert}$	(Eq. 2.5)
Impulse factor	$X_{IF} = \frac{X_a}{\frac{1}{Z}\sum_{i=1}^{Z}\lvert X_i\rvert}$	(Eq. 2.6)

More advanced approaches of time-domain analysis are the parameter identification methods, where a time series modelling is applied to fit the waveform data to a parametric time series model and extract the features [60]. Baillie and Mathew [61] introduced the concept of an observer bank of autoregressive time series models for fault diagnosis of slow speed machinery under transient conditions, where a short set of vibration data is needed. Due to instantaneous variations in friction, damping, or loading conditions, machine systems are often characterised by non-linear behaviour. Therefore, techniques for non-linear parameter estimation provide a good alternative for extracting defect-related features hidden in the measured signals [62].

- **Frequency Domain Technique**

The frequency domain methods have been introduced to provide another way to detect the fault induced signals. FFT is commonly used method to transform the signal from time domain into its frequency components and produce a spectrum. However, it is often not clear enough method to observe the fault peaks, because of slip and masking by other stronger vibrations, beside the effects of harmonics of the defect frequencies and side bands [63]. Moreover, the FFT method is actually based on the assumption of periodic signal, which is not suitable for non- stationary signals. The output signals of running rolling element bearing contain non-stationary components due to the changes in the operating conditions and faults of the machine and bearing itself [64]. Time–frequency analysis is the most popular method to deal with non-stationary signals.

The Wigner–Ville distribution, the short time Fourier transform and Wave let transform (WT) represent a sort of compromise between the time and frequency based views of a signal and contain both time and frequency information. Mori. [65] applied the discrete wavelet transform to predict to the occurrence of spalling in rolling element bearings. Shibataetal. [66] used the WT to analyse the sound signals generated by bearings. Pengetal. [67] highlighted that Hilbert–Huang transform has good computational efficiency and does not involve challenges with the frequency resolution and the time resolution.

There are five basic motions that can be used to describe dynamics of bearing movements. Each motion generates a unique frequency, the five characteristics frequencies are shown in the table 1.2 in page 65 [68].

Although the fundamental frequencies generated by rolling bearings are expressed by relatively simple formulas they cover a wide frequency range and can interact to give very complex signals. This is often further complicated by the presence on the equipment of other sources of mechanical, structural or electro-mechanical vibration. For a stationary outer ring and rotating inner ring, the fundamental frequencies are derived from the bearing geometry [69, 70, 71].The bearing equations assume that there is no sliding and that the rolling elements roll over the raceway surfaces. However, in practice this is rarely the case and due to a number of factors the rolling elements undergo a combination of rolling and sliding. As a consequence, the actual characteristic defect frequencies may differ slightly from those predicted, but this is very dependent on the type of bearing, operating conditions and fits. Generally the bearing characteristic frequencies will not be integer multiples of the inner ring

2.2.3.4 Approaches for analyzing the vibration signature of the system

For improved and authentic fault diagnosis using vibration analysis techniques it is necessary that the acquired vibration signals be ‘clean’ enough that small changes in signal attributes due to an impending fault in any component can be detected. Unfortunately, this is not the case in common practice and vibration signals received from operating machinery are almost always cluttered with noise. In complex multi-component machines this problem is aggravated because vibration energy is generated by each individual component. Whenever it is necessary to monitor a specific component, vibration produced by other components affect the signal. One solution for this problem is to mount the vibration sensors as close as possible to the targeted components. Some restrictions such as complexity, manufacturer’s

warranty policy and inaccessibility constrain this approach and in a majority of cases sensors are placed on the innermost surface possible (i.e., casing) of the structure. As a consequence, the sensors collect vibration signals which are not uniquely generated from the targeted component, but also include contributions from many other components. The vibration signals collected by each sensor are in effect the combination of vibration energy produced by different components in addition to the noise. Dissipation of vibration energy through transmission path complicates the situation even further.

To tackle this problem, one of two alternative approaches can be adopted. One approach is to regard this case as a blind source separation (cocktail party) problem and take advantage of statistical and mathematical methods developed for this purpose, primarily independent component analysis (ICA), to separate signals coming from different sources. The other approach is to avoid making the effort to 'separate' the signals and relate them to different components (sources) and instead make use of the specification and characteristics of vibration signals; as envelop method.

2.2.4 Blind Source Separation (BSS) approach

Rotating machines are mainly multi-component system. As far as concern acquiring information from multi-component system, it is generally desired to have information about each component in isolation. However, this is not always possible and normally the acquired data is at best a mixture of signals produced by different components or sources in the system. Therefore, in order to consider the components individually mixed signals must be decomposed into elements pertaining to the system components. This is the subject of a subfield in signal processing entitled 'source separation'. Cases abound where either there is not enough available a priori information about the system or the mechanism of mixing is very complex. In such cases, the system can be considered a black box and the problem of separating sources is called blind source separation. BSS has been usefully applied in many fields and areas such as radio-communication, speech and audio processing and biomedical applications [72]. It has also been used to separate vibration signals in mechanical systems for the purpose of fault diagnosis. In the following sections we introduce the general model and a brief mathematical background of BSS.

2.2.4.1 General model

Blind source separation is a signal processing method to recover the signals produced by different individual sources from a number of observations of mixed source signals. The term "Blind" includes two facts: both the source signals and the mixing structure are unknown. For condition monitoring and fault diagnosis, the observed signals are usually the output of a set of sensors and linear combinations of the sources as shown in Fig.2.1.

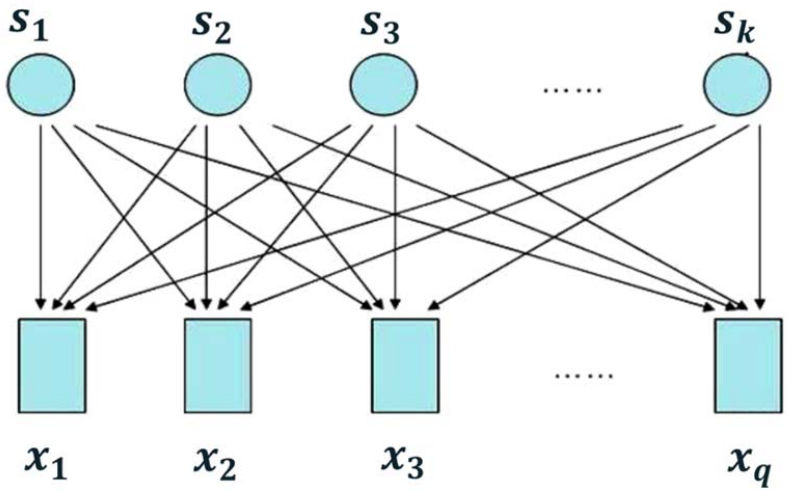

Figure 2.1: *Observed signals and sources.*

In this Fig.2.1 the S_1, S_2, S_3,…S_k denote the sources and the x_1, x_2, x_3,…x_q denote the observations (output of sensors).

In mathematical terms the general model for blind source separation can be described as follows:

If there are q zero-mean source signals at time t, $S(t) = [s_1(t), \dots, s_k(t)]$ that are assumed to be statistically independent, and $X(t) = [x_1(t), \dots, x_q(t)]$ denote the mixed signals received by q sensors and $R(t) = [r_1(t), \dots, r_q(t)]$ the noise measured vectors which size is p the data model can be written as:

$$X(t) = AS(t) + N = \sum_{i=1}^{q} a_{wi}(t)s_w(t) + R\,(t) \qquad \text{(Eq. 2.7)}$$

where A is the $q \times k$ mixing matrix consisting of unknown mixture coefficients, and it is always assumed that the sources are independent and the number of sensors is at least equal to the number of sources (i.e., $k \leq q$). Fig.2.22 symbolizes this relation.

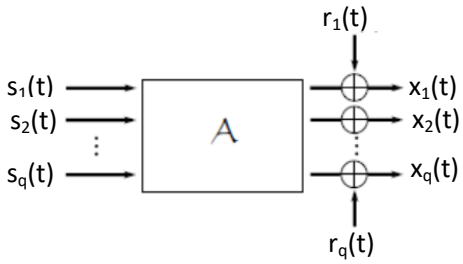

Figure 2.22 : *General model of the relation the sources - observations in the presence of noises.*

The primary technique for finding the unknown mixture coefficients (*A*) is Independent Component Analysis (ICA). A prerequisite for ICA to be applicable is that no more than one source can have a Gaussian distribution. This is because it is impossible to separate several Gaussian sources using ICA technique [73].

2.2.4.2 Independent Component Analysis (ICA)

The problem set by ICA may be summarized as follows. Given q realizations of X, it is desired to estimate both matrix A and the corresponding realizations of S. However, because of the presence of the noise R, it is in general impossible to recover exactly S. Since the noise R is assumed here to have an unknown distribution, it can only be treated as a nuisance, and the ICA cannot be devised for the noisy model above (Eq. 2.7), Instead, it will be assumed that:

assuming the mixing matrix A is invertible and the sources S_i (t) (i=1,2,…k) are statistically independent. The assumption of independence between the sources is physically plausible because they have different origins. The kernel of BSS is to find a $q*k$ separation matrix B and the recovered signals are given by the following equation (Eq. 2.8):

$$\tilde{S}(t) = BX(t) = BAS(t) = CS(t) = Y(t) \qquad \text{(Eq. 2.8)}$$

If matrix B could make the matrix C be an identity matrix, it could be concluded that the source signals have been separated perfectly. But in realty this is very difficult to be achieve. Therefore in practical, ICA consists in finding an estimation of the sources by determining matrix B such that a given objective function defined for components of Y becomes minimum.

The general model of BSS could be shown as Fig.2.3.

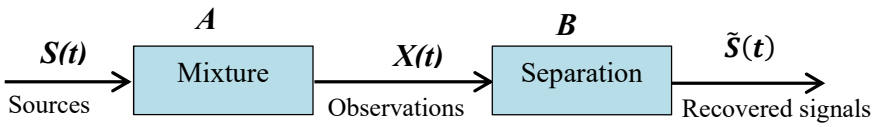

***Figure 2.3**: BSS general model.*

Regardless of what criterion is used, there are always two dominant ambiguities and indeterminacies associated with ICA.

- First, the original labeling of the sources is unknown. This means that, because both **S** and A are unknown, the order of the terms can be freely permutated. It is a result of the fact that the mathematical independency is insensitive to permutation of the sources.
- The second ambiguity is that the actual scale of the sources cannot be determined. The reason for this is that any scalar multiplier in one of the sources s_i can always be canceled by dividing the corresponding column a_i of A by the same scalar. This is also due to insensitivity of mathematical independency to the scaling factor.

Several objective functions based on different estimation criteria exist for ICA. Some of the most important criteria include: maximization of non-Gaussianity [74], minimization of mutual information [74] and maximum likelihood estimation [75]. A brief description of these criteria is provided below.

- **Maximization of non-Gaussianity and minimization of mutual information**

Random variables are known to be Gaussian or normally distributed. There is a general consensus that a mixture of two or more independent variables tends towards randomness or Gaussianity. Consequently, by distancing from Gaussianity or by maximizing 'non-Gaussianity', one may approach independency. One of the main measures of non-Gaussianity is 'negentropy'. Negentropy is derived from 'entropy' and serves as its converse. In the same manner, it is known that the more variables are unstructured and mixed, the higher is the entropy or the 'mutual information'. Therefore, it can be stated that negentropy ties the two criteria of maximization of non-Gaussianity and minimization of mutual information together and provides a measure for evaluating independency.

- **Maximum likelihood estimation**

The method of maximum likelihood corresponds to many well-known estimation methods in statistics. In general, for a fixed set of data and underlying statistical model, the method of maximum likelihood selects the set of values of the model parameters that maximizes the likelihood function. Intuitively, this maximizes the "agreement" of the selected model with the observed data, and for discrete random variables it indeed maximizes the probability of the observed data under the resulting distribution. In this method, it is first assumed that the sources are independent and identically distributed at different times. This is not an essential assumption and is referred to as a working assumption. In order to derive a likelihood function, the probability density functions of the sources are needed while they are unknown. In this case, they are assumed to be known up to a scaling factor.

2.2.4.3 Convolutive mixtures and frequency domain analysis

In literature certain data model pertains to the case where the mixing mechanism is assumed to be linear and instantaneous. This assumption is too simplistic for the majority of real applications. The mixing model in most cases is more consistent with a general linear mixtures, i.e. a convolutive mixtures. In the case of convolutive mixtures the data model can be rewritten as follows:

$$X(t) = A\ (t) * S(t) + R(t) \qquad \text{(Eq. 2.9)}$$

Where $*$ denotes the convolution product and *A (t)* represents the matrix impulse responses of the filters associated with each relationship between a source and an observation. The well-known convolution relation is written in a representation to continuous time:

$$A\ (t) * S(t) = \int_{-\infty}^{+\infty} A(\tau)S(t-\tau)d\tau \qquad \text{(Eq. 2.10)}$$

and for discrete-time signals:

$$A\ (z) * S(z) = \sum_{w=-\infty}^{+\infty} A(w)S(z-w) \qquad \text{(Eq. 2.11)}$$

The instantaneous mixtures, where each component of the matrix *A* filter of the Eq.2.7 does not present memory and summary to a simple factor, real or complex in the most general case. *A* is in this case a scalar matrix real or complex.

The convolutive mixture in which filters mix include terms from memory. *A (z)* then corresponds to a matrix of impulse responses of filters, with which is associated a transfer functions matrix denoted by *A (z)*. As *A* is the mixing matrix consisting of unknown mixture coefficients. In this case, solving the inverse problem is not as straightforward as it was for the instantaneous data model. Certain methods have been suggested to solve the convolutive mixture model in its general form. However, such methods are very limited [76]. Fortunately, a convolutive mixing model in the time domain becomes an instantaneous model when brought into the frequency domain. To be more precise, when data is represented using the joint time-frequency domain, at each frequency bin the mixing model is instantaneous and existing methods for instantaneous mixtures can be employed with minor modifications. Since data in the frequency domain are complex valued, instantaneous ICA methods must be modified for consistency with complex data. This can be simply done by taking a conjugate transpose wherever matrix transposition is needed throughout computations. After performing separation at each frequency bin, the resulting separated signals are transformed back from frequency domain to time domain and the source signals are recovered.

2.2.4.4 Final consideration on the application of BSS in fault diagnosis

In the literature various studies had been done on the application of BSS in separation of vibration signals as applied to fault diagnosis in rotating machinery. Each one of these studies used its own assumption and is based on determinate method and criterion involving time domain and frequency domain [77, 78, 79, 80, 81, 82,83, 84, 85]. Others studies ongoing might give interesting development in the future. However, despite these studies, the application of BSS in fault diagnosis in rotating machinery remain only at the laboratory level. He has not had successful in practice. In fact, this approach is not yet mature enough to be applied to industrial scale.

The approach which is applied in industrial scales with success is the one which make use of the specification and characteristics of vibration signals. This approach is developed in the following section.

2.2.5 Cyclic spectral analysis approach in diagnosis of bearing faults in complex machinery

Bearing faults are known to produce vibration with recurring impulsiveness in the energy which is referred to as cyclostationarity. Cyclic Spectral Analysis (CSA) is a powerful tool to measure the cyclostationarity of a signal in different frequency ranges. For this tool to be effective in applications related to complex machinery, two requirements are identified. One requirement is that the tool must be capable of detecting defects from a weak signal as it passes and attenuates through its transmission path. The other requirement is that it must allow robust, attainable and consistent trending. Also the feature being tracked must be consistent in the sense that its value bears some correspondence to the severity of the faults.

2.2.5.1 Bearing faults and cyclostationarity

There are five basic motions that can be used to describe dynamics of bearing movements. Each motion generates a unique frequency, the five characteristics frequencies. These frequencies for the common case where only the inner race of the bearing is rotating are listed in table 2.2.

Table 2.2: *Characteristic frequencies of bearing faults*

Shaft rotational frequency	$X = \frac{N}{60}$	(Eq. 2.12)
Inner race defect frequency	$BPFI = \frac{b_n}{2} X \left[1 + \left(\frac{b_d}{p_d}\right) cos\alpha\right]$	(Eq. 2.13)
Outer race defect frequency	$BPFO = \frac{b_n}{2} X \left[1 - \left(\frac{b_d}{p_d}\right) cos\alpha\right]$	(Eq. 2.14)
Ball defect frequency	$BSF = \frac{p_d}{b_d} X \left[1 - \left(\frac{b_d}{p_d}\right)^2 (cos\alpha)^2\right]$	(Eq. 2.15)
Fundamental cage frequency	$FTF = \frac{1}{2} X \left[1 - \left(\frac{b_d}{p_d}\right) cos\alpha\right]$	(Eq. 2.16)

b_n = Number of balls; **α**= Contact angle; p_d = pitch diameter; b_d = ball diameter; *N*= rotational speed in rpm

It is important to note that these frequencies don't represent bearing's natural frequencies (the bearing's natural frequencies are dependent on the design, geometry and material among many other factors and it is not possible to establish a general formulation for all bearings). Characteristic frequencies of bearing faults depend upon the bearing geometry and shaft speed. The procedure for obtaining each one of these formulas is briefly: if any defective point is considered on any of the main bearing components (i.e., rolling element, outer and inner races), then based on the geometry of the bearing components and kinematic concepts the frequency of any possible contact between that point and other components is calculated. The most common bearing problem is the outer race defect in the load zone; inner race faults are the next most common. It is very rare to see a fault at the bearings ball spin frequency or *BSF* because the ball material is the hardest. The gage frequency fault is mainly linked to poor lubrication.

It should be clear from the previous paragraph that bearing frequencies are produced by striking of a defective point of a bearing component on other component. Such striking results in excitation (ringing) of the bearing assembly at its natural frequencies. The striking itself occurs at rates equal to the characteristic frequencies (easily computable) and creates impulses in the signal. The ringing effect, on the other hand, occurs at natural frequencies of the bearing components in the shape of a random stationary signal at normally higher frequencies (usually unknown). The combination of these two phenomena creates vibration with repetitive bursts of energy. To be more accurate, vibration signals produced by a bearing defect are modulated signals; vibration energy at natural frequencies of the bearing (carrier frequency) is modulated with characteristic frequencies of the bearing (modulation frequency). Such signals in signal processing terminology are entitled cyclostationary.

It is clear, according to what mentioned above, typical spectral (*FFT)* analysis directly applied to vibration signal is not a strong tool for detecting bearing anomalies as it gives the averaged spectral representation (spectrum) based on stationarity assumptions. In fact, spectral analysis is only capable of detecting bearing defects when they are greatly developed and in presence of little noise. In such cases the modulation frequency and its harmonics are visible on the spectrum. An alternative for typical spectral analysis is to use spectrogram or any other joint time-frequency representation. In this case, the repetitive bursts of energy occurring at higher frequencies (ringing frequencies of the bearing component) are observable throughout the spectrogram. The duration between successive bursts is equal to the inverse of any one of the characteristic frequencies depending on the case.

These methods are very representative and appropriate for analysis purposes. On the other hand, they are not suitable for an automated diagnosis system since it is difficult to establish a robust trending and alarming scheme. For all these reasons envelope analysis is the method widely used for bearing fault detection.

- **Classic technique of bearing analysis**

The Fig.2.3 shows an overview of classic technique of bearing analysis. Unfiltered time signal, filtered time signal, and envelop are presented with their respective spectrum.

Supposing to be interested to analysis the bearing defect in high frequency as which highlighted in red in the spectrum of the unfiltered time signal. This spectrum shows a large energy load dominated by phenomena that occur with low frequencies; the part of the energy load concerning the high frequencies is not well visible in the spectrum.

In the filtered signal spectrum, we see only the part of the energy load concerning the high frequencies, but the level of detail is not sufficient for its interpretation. In the spectrum of envelop the energy load concerning the high frequencies is more clear and the detail level is sufficient for its interpretation.

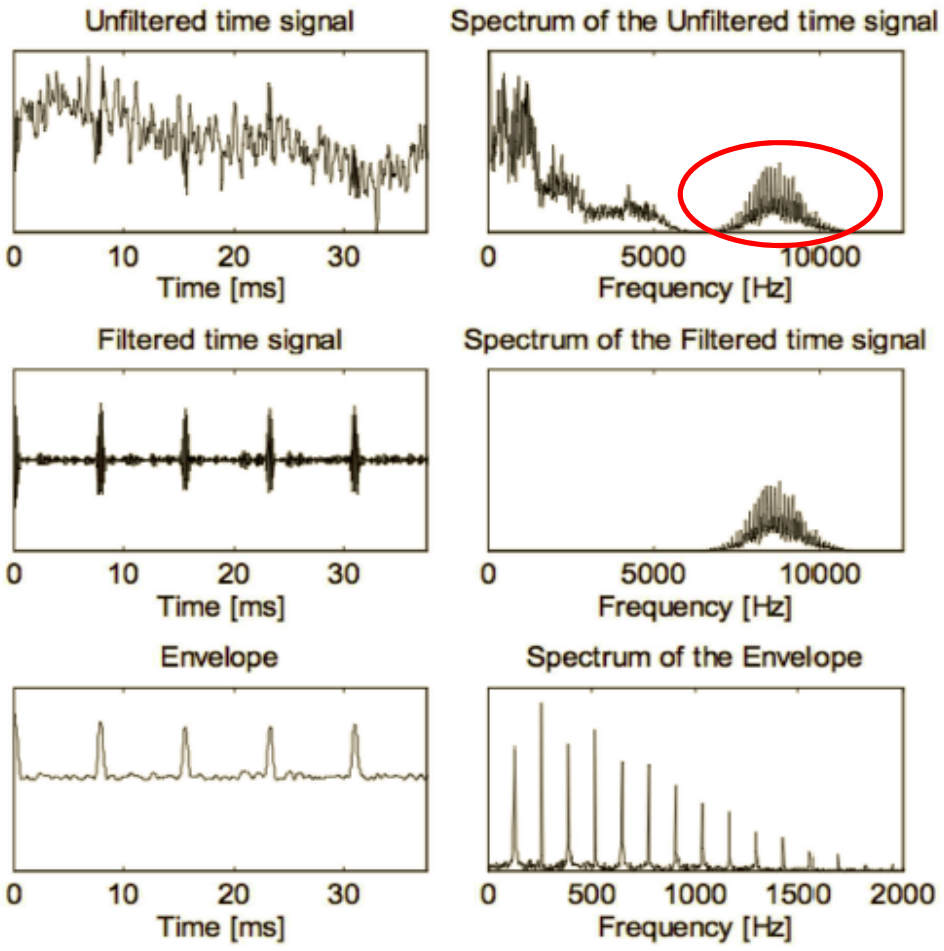

***Figure 2.3**: Comparison of signals Unfiltered signal, filtered signal, and envelop*

2.2.5.2 Envelope analysis

Envelope analysis is a powerful method widely used for bearing fault detection. Enveloping addresses the problem of isolating small but significant impulse perturbations that are summed, during measurement, with larger, low frequency, stationary vibration signals, such as imbalance and misalignment. These small impulse signals come from the accelerometer response to impulsive forces from bearing race defects, from roll flat spots, and even from felt joint connectivity. The envelope method separates a repetitive impulse from a complex vibration signal by using a band pass filter that rejects low frequency components that are synchronous with vibration.

Analysis of the enveloping process begins with the source of the vibration signal. As the elements of the bearing interact with each other and with defects, forces are coupled to the machine casing, producing vibration. Each time the interaction between bearing elements and a superficial defect excites a structural resonance in the bearing support structure (causing it to ring). The impacts originating trains of impulsive forces that are vibration sources as shown in Fig.2.4.

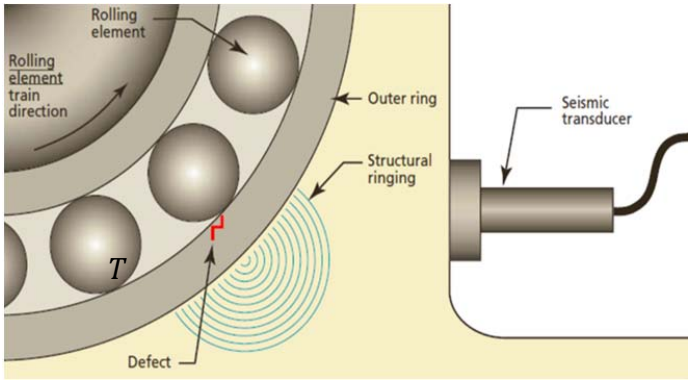

a) *Defect impact causes ringing of the machine structure*

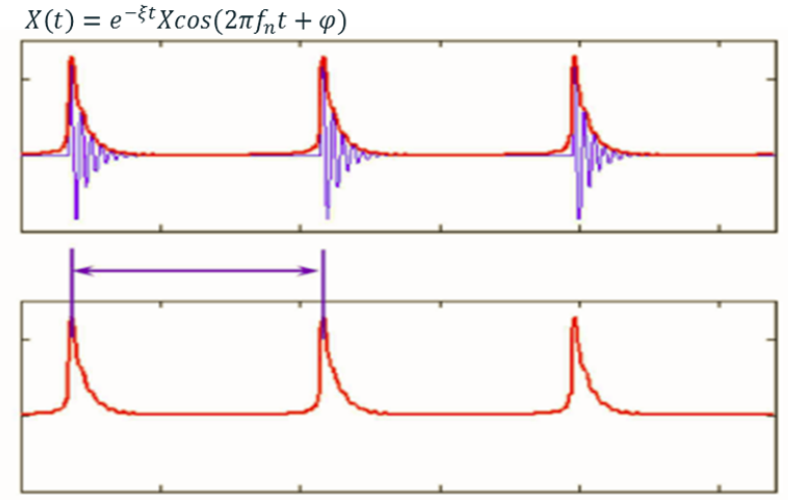

b) The natural resonance response modulated by the defect amplitude at the impact frequency

***Figure 2. 4**: Defect impact causes ringing of the machine structure at its natural frequencies.*

The amplitude of the ringing decays until the next impact, which re-excites the resonance. Thus, the defect amplitude modulates the natural resonance response at the impact frequency (Eq. 2.17).

$$X(t) = e^{-\xi t} X cos(2\pi f_n t + \varphi) \qquad \text{(Eq. 2.17)}$$

The defect related signal becomes part of the overall vibration of the machine. The fault frequency is the inverse of the periodicity T of the impulses train.

Actually, the rolling motion of the rolling elements is not perfect, because they are made of slips. This introduces a small random component within the characteristic of the defect period. The signal generated by a defect is *the second-order cyclostationary*.

- **Envelope Signal Processing**

Envelope Signal Processing (*ESP*) is a two stage demodulation technique, which extracts the high frequency range shown and obtains a signal containing the vibrations caused by the impacts.

The first stage of the process is to pass the signal through a band-pass filter to remove the low frequency vibration and the very high frequency random noise. This leaves the bursts of narrow band bearing signal that come from the impacts. The band of the filter should be centred on the resonant or carrier frequency. After filtering, the signal consists of the chosen resonant frequency with side frequencies that correspond to the defect frequency and its harmonics, and also the running speed and its harmonics.

The second stage of the process is the demodulation process. The filtered signal is rectified which produces a signal that consists of the defect frequency and its harmonics, the running speed and its harmonics, and side frequencies corresponding to the resonant frequency. The signal is then passed through a low-pass filter which smoothes the signal and removes the last traces of the resonant frequency. Finally, the enveloped signal is put through the *FFT* to produce the enveloped spectrum that contains fewer frequencies than the original signal. The *ESP* process is shown in Fig.2.5.

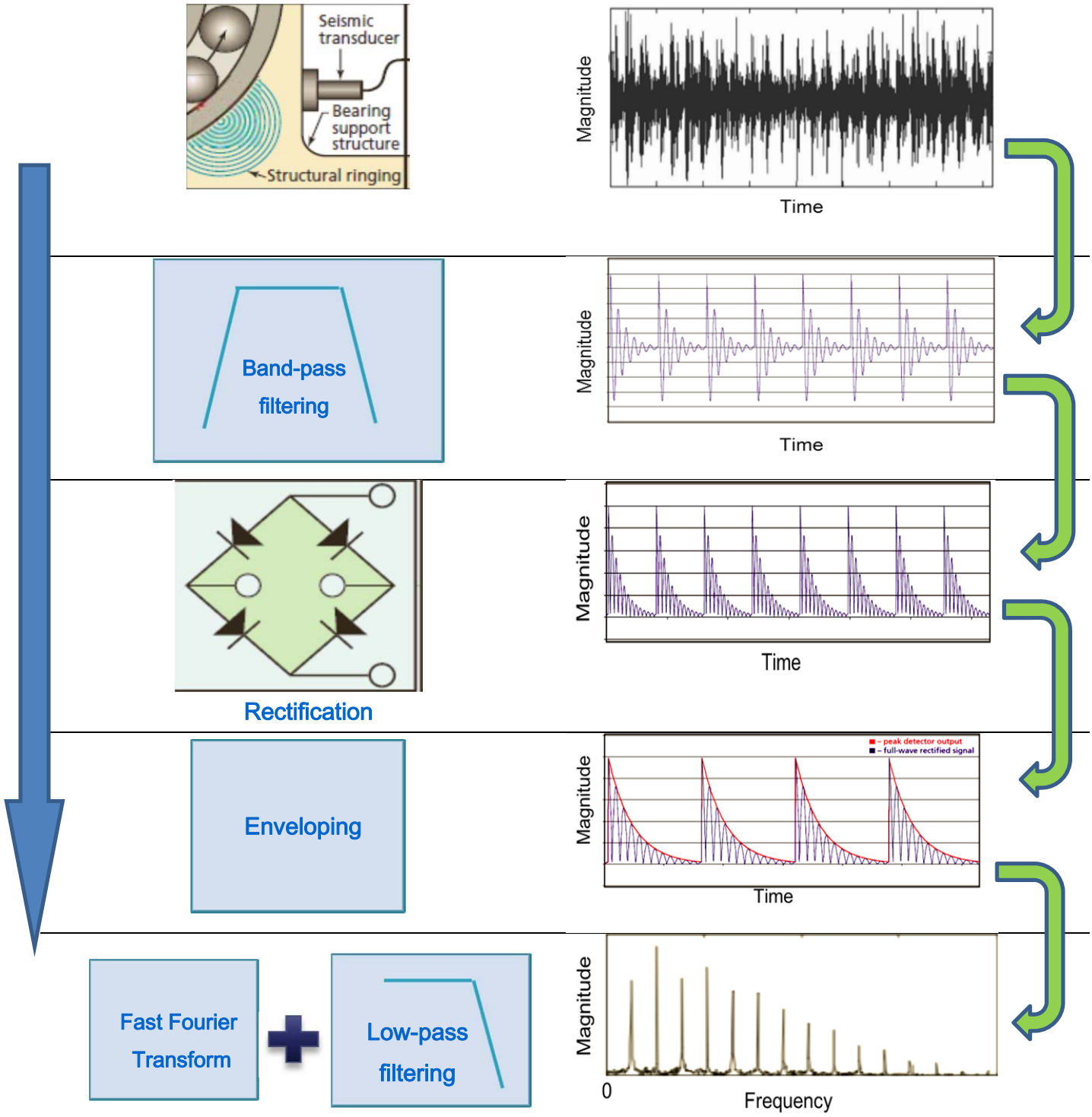

Figure 2.5: *The Envelope Signal Processing*

2.3 Experimental study on liquid ring compressor main failure

We have presented the method of vibration analysis, in particular of the envelope method for the detection of bearing damage. We now present here a practical case of application of this method in the problem solving of industrial machine failure.

In my capacity as SKF engineer specializing in vibrational analysis at an oil refinery, it has been brought to my attention a specific breaking problem for reasons not determined. And so in the context of the doctorate, I conducted, the investigations of a repeated failure problem of a liquid ring compressor. This liquid ring compressor is used to recover the gases from different processes of the oil refinery and to send them in the plants for the power production. This permit to keep very low the gases quantity send to the torch to be burnt. This machine is classified as a machine of high criticality for the refinery. its failure causes not only an important miss production, but also an environmental pollution that causes the protest of the local population and the refinery must pay heavy penalty.

An experimental investigation is done on a two stages liquid ring compressor bearing failure mode. It has been observed that once installed correctly and operate in regular process condition, compressor vibration are normal and stabile. However very often the vibration severity assessment (Envelop) values don't change gradually and progressively as in the case of bearing normal fatigue wear. But very often we note a brusque change in vibration serenity, witch spectrum shows a bearing failure. What happen? How this problem be solved? The Fig.2.6 shows the liquid ring compressor.

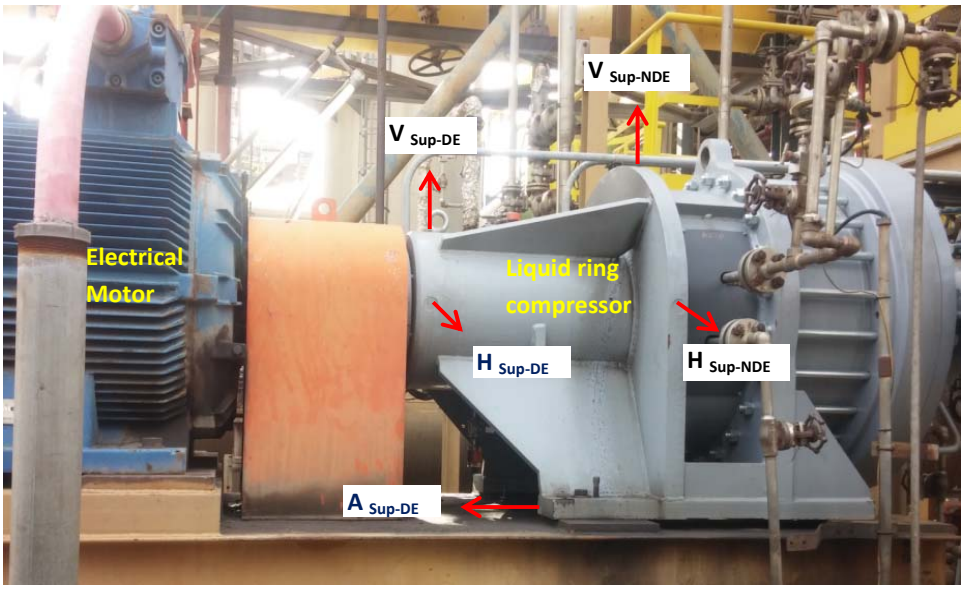

Vibration acquisition points

- **H** $_{Sup\_DE}$: Horizontal direction on support drive end
- **V** $_{Sup\_DE}$: Vertical direction on support drive end
- **A** $_{Sup\_DE}$: Axial diection
- **H** $_{Sup\_NDE}$: Horizontal direction on support non drive end
- **V** $_{Sup\_NDE}$: Vertical direction on support non drive end

Figure 2.6: *Liquid ring compressor and vibration acquisition points.*

The compressor is driven by an electrical motor witch rotation speed is 980 RPM. The compressor vibration is monitored once by week. For both of the supports, the vibration acquisition is made in horizontal and in vertical directions. In the following sections the liquid ring compressor working principle and their main failure will be descripted, and the main failure mode of compressor bearings will be studied.

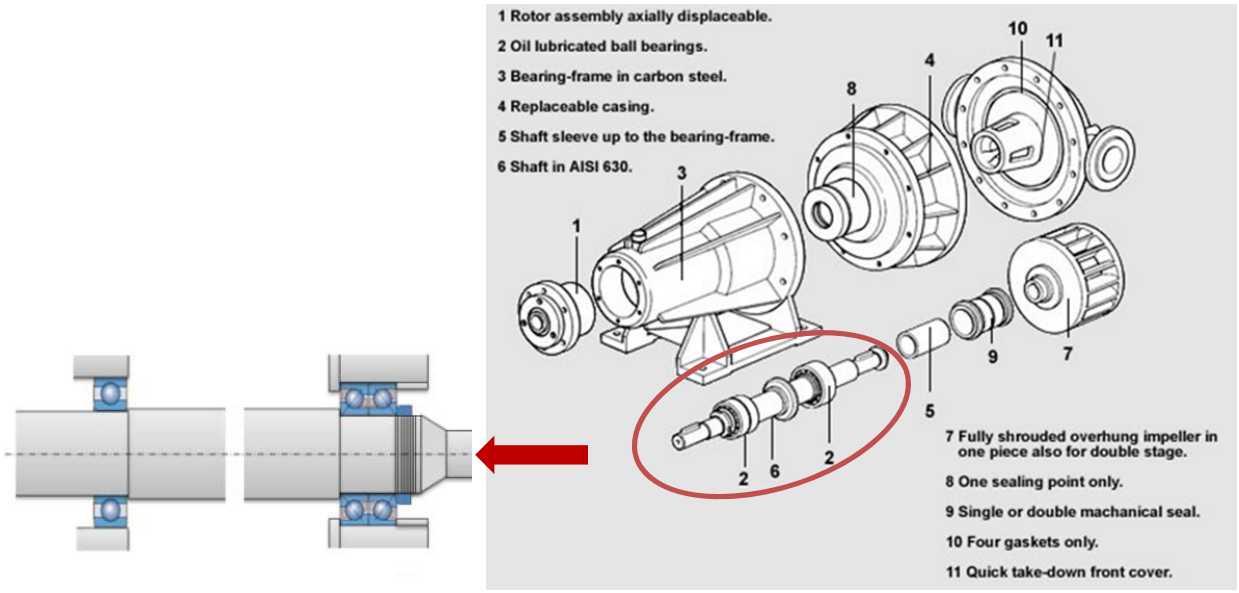

Figure 2.6: *Liquid ring compressor components*

2.3.1 Liquid ring compressor working principle and main failure

In a liquid ring compressor the casing is filled with the liquid, that is called “seal liquid” up to the rotor centerline. The process gas enters the compressor through its conical distributor that is fixed to the compressor front cover. During compressor start up the seal liquid will be centrifuged by the impeller rotation along the inner wall of the casing that has a double eccentricity shape. The conical distributor has two suction ports and two discharge ports, each of them opposite to the other. During the first quarter of turning, the gas is sucked to both suction chambers of the casing. During the second quarter of turning the gas is first compressed and then pushed out through the two discharge ports. During the third and the fourth quarter of turning the cycle is repeated. In this way for each complete turning of the impeller, the gas is sucked, compressed and pushed out twice. The radial forces originated, due to the gas compression, are therefore perfectly balanced.

This Liquid ring compressor is characterised by two main failure mode: impeller failure and angular bearing failure.

- **Bearing failure.**

This failure is the main objet of the experimental study , and will be developed in the following sections.

- **Impeller failure**

The work fluid of the compressor may be a gas in the normal condition of the processes. When this work fluid contain an amount of liquid, the compressor vibration increase and become irregular. The impeller under this irregular condition of the processes is solicited in abnormal mode. The vibration is severe as much as the liquid portion in the work fluid is higher. Therefore this irregular condition causes the failure of the impeller.

2.3.2 Vibration data acquisition

2.3.2.1 Definition of parameter measured

Considering the shaft rotational speed N= 980 RPM, the corresponding frequency is X =16,33 Hz.

The table 2.3, illustrates the frequencies ranges which must be observed to monitoring the different defaults.

- For the such as unbalance, misalignment, mechanical looseness,… the characteristic frequencies can be found from *1X* to *10X* . That mean from 16,33 to 163,3 Hz. As mention above (in section 1.1.2.3), when the frequencies ranges are from 10 to 1000 Hz the preferred vibration unit is the velocity. So the vibration point need to monitored the mentioned defaults will be set as velocity and the f_{max}*=1000 Hz*.
- The impellers has double stage, for each stage, the blades failure characteristic frequency are *nX* (where *n* is the number of blades) and its harmonics 2*nX, 3nX, 4nX* . The stage 1 has 21 blades, this mean the characteristic frequencies are from 326,6 to 653,2 Hz. And the stage 2 has 28 blades, that correspond to characteristic frequencies from 457,24 to 914,48 Hz. All those frequencies range are belong 1000 Hz the preferred vibration unit may be the Velocity. But since the maximum value of the stage 2 blades frequencies range (914,48 Hz) is very near to the limit and it might be useful to observe frequency over 1000 Hz, we will set another point in acceleration (g) and the maximum frequency is fixed *to* f_{max}*=5000* Hz.

Table 2.3: *Liquid ring compressor possible defaults*

Liquid ring compressor possible defaults	***Frequencies range***	***Vibration unit selected***
shaft rotational frequency X	16,33 Hz.	Velocity
Unbalance, misalignment, Mechanical Looseness,.. characteristic frequencies, is *1X* to *10X*	16,33 to 163,3 Hz.	Velocity
Impellers double stage failure characteristic frequencies For each stage , Blades failure characteristic frequency is calculated from the product of the frequency of rotation by the number of blades (*n*) of the impeller: *nX* and its related harmonic *2nX , 3nX , 4nX*	Stage 1 (n=21) 342,93 to 685,86 Hz Stage 2 (n=28): 457,24 to 914,48 Hz	Acceleration

- **Liquid ring compressor bearings characteristic frequencies.**

Table 2.4 report Liquid ring compressor bearings characteristic frequencies. In the spectrum each of them can be observed until the 4th harmonic. The highest of this frequency is *BPFI= 78,75* Hz (4th

harmonic=315 Hz) for radial bearing 6324 and *BPFI=113,4* Hz (4^{th} harmonic=453,6 Hz) for 7320 BECBM (BECBM is: *B single row bearing with a 40° contact angle; E optimized internal design; bearing for universal matching, i.e. two bearings arranged back-to-back or face-to-face which have a normal axial internal clearance; M machined brass cage).* The parameter indicated for bearing default monitoring is Acceleration Enveloping (gE**)** and the maximum frequency is fixed *to* f_{max}*=1000 Hz.*

Table 2.4 : *Liquid ring compressor Bearings characteristic frequencies.*

Bearing	6324	7320 BECBM (skf)
$BPFI$	78,75 Hz	113,4 Hz
$BPFO$	51,56 Hz	79,69 Hz
BSF	35,94 Hz	34,38 Hz
FTF	6,25 Hz	6,56 Hz

- **Definition of acquisition points**

After identifying liquid ring compressor possible defaults and their related frequencies range, we can define the acquisition points. A acquisition point is a machinery location at which measurement data is collected (sensor location to do vibration measurement). To make a good monitoring of the liquid ring compressor, it is necessary to define a sufficient number of vibration acquisition points. The acquisitions are made on both bearing housings. The table 2.5 report the defined points. They have been defined in total *9 points of acquisitions*. Each point aims to monitor certain types of problems, the chosen parameters (units, quantity ...) should be the most suitable to highlight the problems subjects.

***Table 2.5**: vibration acquisition points (See Fig. 2.6)*

	Point name	**Defaults / Problems assessed**	**Unity**	Quantity measured
1	H_{Sup-DE} _ Envelop	Bearings (7320 BECBM) default	Enveloped Acceleration (gE)	Peak to Peak
2	H_{Sup-DE} _ Velocity	Default developed from 1X to 10X	Velocity (mm/s)	RMS
3	H_{Sup-DE} _ Acceleration	Problem or default related to impellers blades	Acceleration (g = 9,8 m/s^2)	RMS
4	V_{Sup-DE} _ Velocity	Default developed from 1X to 10X	Velocity (mm/s)	RMS
5	A_{Sup-DE} _ Velocity	Default developed from 1X to 10X	Velocity (mm/s)	RMS
6	$H_{Sup-DNE}$ _ Envelop	Bearing default	Enveloped Acceleration (gE)	Peak to Peak
7	$H_{Sup-DNE}$ _ Velocity	Default developed from 1X to 10X	Velocity (mm/s)	RMS
8	$H_{Sup-DNE}$ _ Acceleration	Problem or default related to impellers blades	Acceleration (g = 9,8 m/s^2)	RMS
9	$V_{Sup-DNE}$ _ Velocity	Default developed from 1X to 10X	Velocity (mm/s)	RMS

These 9 points of acquisitions obviously can be classified in 3 categories considering the units: 5 points are setting in velocity, 2 in acceleration and 2 Enveloped acceleration. For each point category above defined, the same acquisition parameters are used.

2.3.2.2 Microlog analyser

The Microlog series data collector/ analyser is a lightweight, hand-held, data acquisition device and portable maintenance instrument, designed to enable to establish a comprehensive periodic condition monitoring program. The Microlog collects machinery vibration (and temperature measurements and performs detailed analyses in harsh industrial environments).

Figure 2.7: *SKF Microlog Analyzer GX and The @ptitude Analyst software*

- **The software SKF @ptitude Analyst for SKF Microlog Analyzer**

The @ptitude Analyst software works with Data Acquisition Devices (DADs) to assist machinery maintenance personnel in managing and analyzing their collected data. @ptitude analyst automatically uploads measurement data from DADs and performs the tedious clerical work required in sorting, storing, and pre-analyzing measurement data. @ptitude analyst is use to configure measurement points, for downloading measurement point setups to DADs, for database manipulation of collected data, and to graphically display and generate reports on collected measurement data. Exception Reports - @ptitude Analyst automatically compares current measurement values to past measurement values, and to pre-defined alarm values to detect changes from normal machinery conditions. Using hierarchy list alarm status indicators and detailed printed reports, @ptitude Analyst alerts maintenance personnel to

alarm conditions (exceptions from normal conditions). **Analysis** - @ptitude Analyst displays and prints various plots and reports for analyzing machinery condition. More information can be found in [87].

- **Accelerometers**

The sensor used for vibration measurements in ours experiment is the SKF industrial accelerometer CMSS 2200 / SN 21624. It is a kind of accelerometer shown above in Figure 1.38 (simply the original accelerometer design, but with an additional circuit already built into the transducer that integrates the amplified signal to velocity). It had the important advantage to allow to make vibration measurements acquisition in velocity, acceleration and Enveloped acceleration. The accelerometer environmental and dynamic specifications are reported in the table 2.6.

Table 2.6*: SKF industrial accelerometer CMSS 2200 Environmental and Dynamic Specifications*

Specifications Specifications conform to ISA-RP-37.2 (1 to 64) and are typical values referenced at 25 °C *(75 °F)*, 24 V DC supply, 4 mA constant current and 100 Hz.	
Environmental	• Temperature range: –50 to +120 °C *(–60 to +250 °F)*, operating temperature • Vibration limits: 500 g peak • Shock limit: 5 000 g peak
Dynamic	• Sensitivity: 100 mV/g • Sensitivity precision: ±5% at 25 °C *(75 °F)* • Acceleration range: 80 g peak • Amplitude linearity: 1% • Frequency range: - ±10%; 1,0 to 5 000 Hz - ±3 dB; 0,7 to 10 000 Hz • Resonance frequency: Mounted, minimum 22 kHz • Transverse sensitivity: ≤ 5% of axial

The accelerometer is mounted on a magnetic mounting bases (ideal solution when we need to take periodic vibration data for trending purposes) as shown is Fig.2.8. Accelerometer is connected to the Microlog analyser by a special cable. The connection cable seen in the Figure is coiled (extended 2,3 m), Model CMAC 107 for standard constant current accelerometers with 100 mV/g, MIL-SPEC connector.

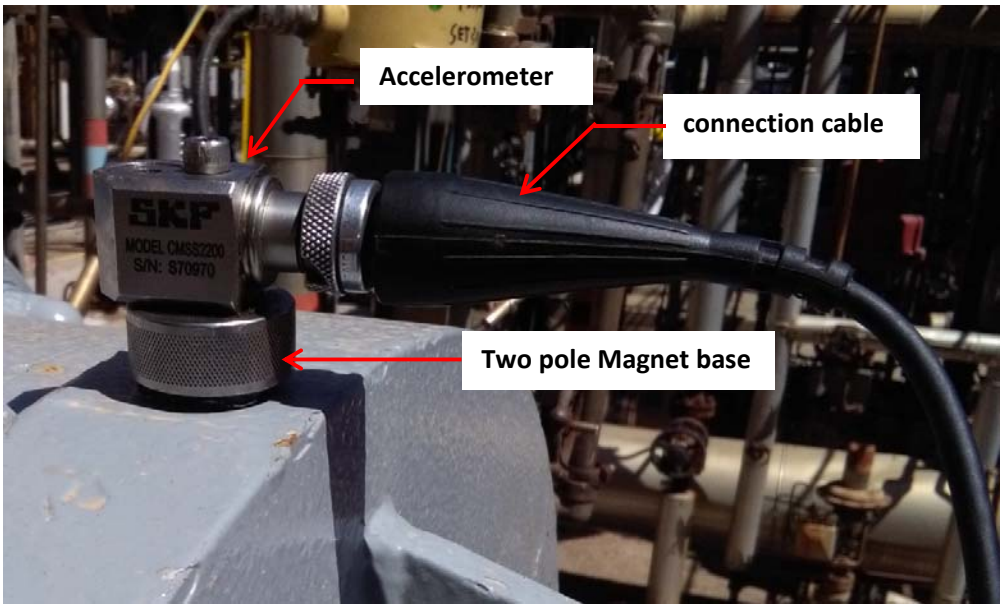

Figure 2.8: *Accelerometer and connection cable*

2.3.2.3 Parameters setting with @ptitude Analyst software

- **The point properties dialog allows us to enter all point information and settings.**
  - **General Tab**

Since SKF @ptitude Analyst software may work with different analyser (microlog, IMX, …) , different type of measure (vibration, temperature,…) and different accelerometer, the first step to define a new point properties is to specify those data. This specifications are made with "The point properties dialog's **General** tab". It allows you to enter the point name and description and displays the DAD / point Type information you previously entered. In the example shown in Fig.2.9, the DAD is Microlog, the type of application is vibration acquisition and analysis. The type of sensor used is an accelerometer. At this level, after specifying the application the point related unit may be indicated in this case mm/s (g or gE can be selected in alternative) .

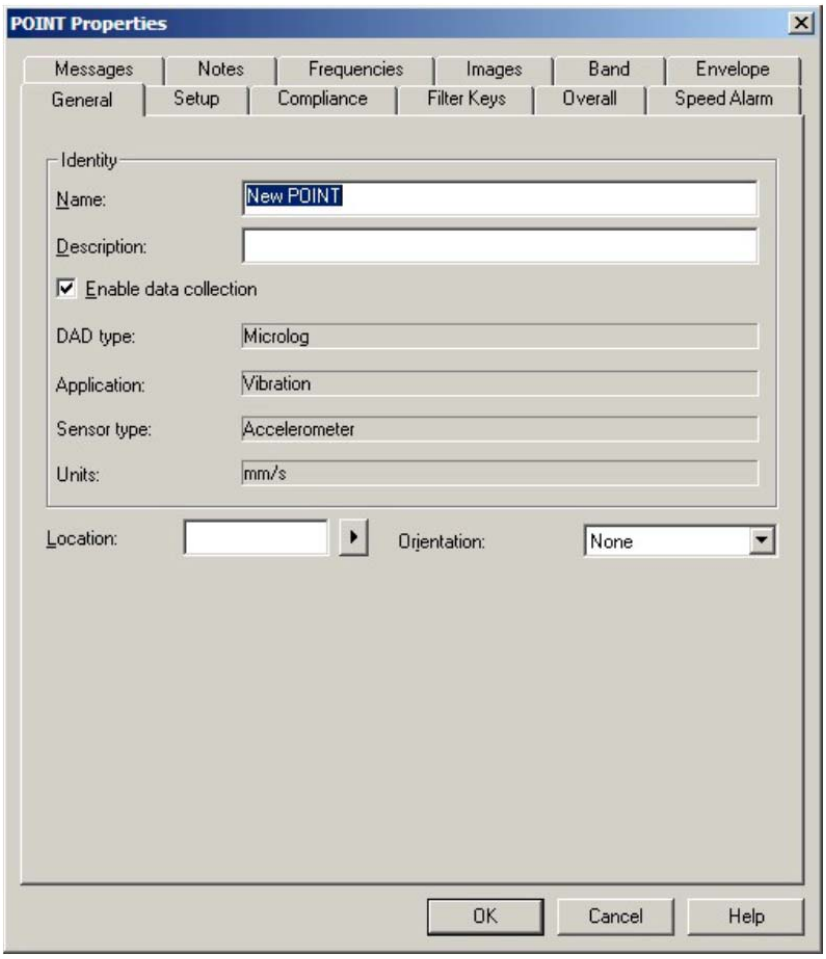

Figure 2.9: *The point properties Dialog's General Tab.*

- **Setup Tab (Microlog points)**

After General Tab setting, the next important step is to setup the microlog point. This is done through the "The Point Properties / Setup tab". This table displays depending :

- the point type.
- The sensor type and units.

In our case the **Setup** fields apply to points defined with the Microlog DAD, the sensor is accelerometer and units can be velocity (mm/s) , acceleration (g) or Enveloped acceleration (gE).

All possible **Setup** fields are defined below.

- **Setting of Microlog point in velocity**

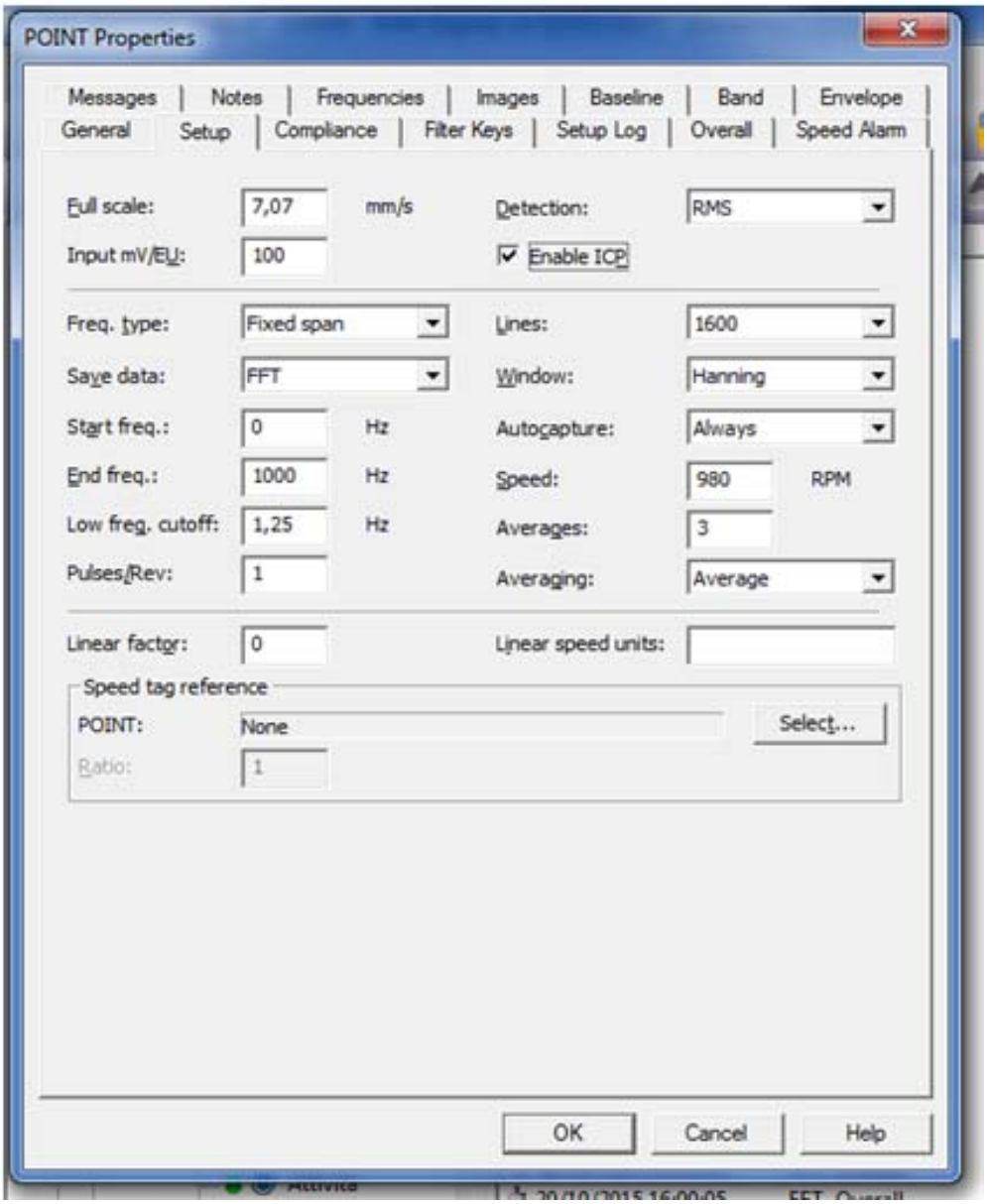

Figure 2.10 : *The POINT Properties Dialog's Microlog Setup Tab.: Velocity*

- **Setting of Microlog POINT in Acceleration**

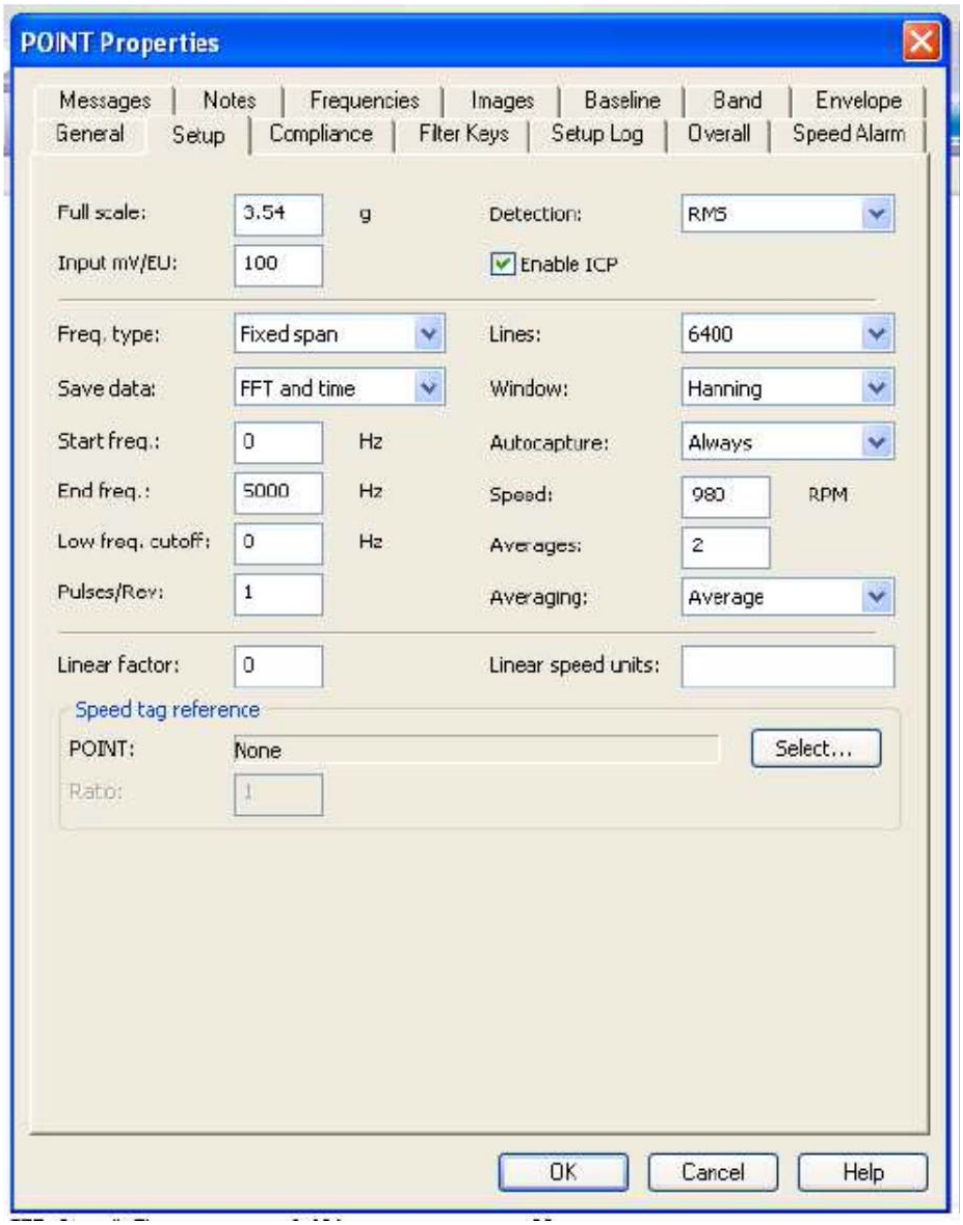

Figure 2.11: *The point properties Dialog's Microlog Setup Tab.*

- **Setting of Microlog Point in Enveloped Acceleration**

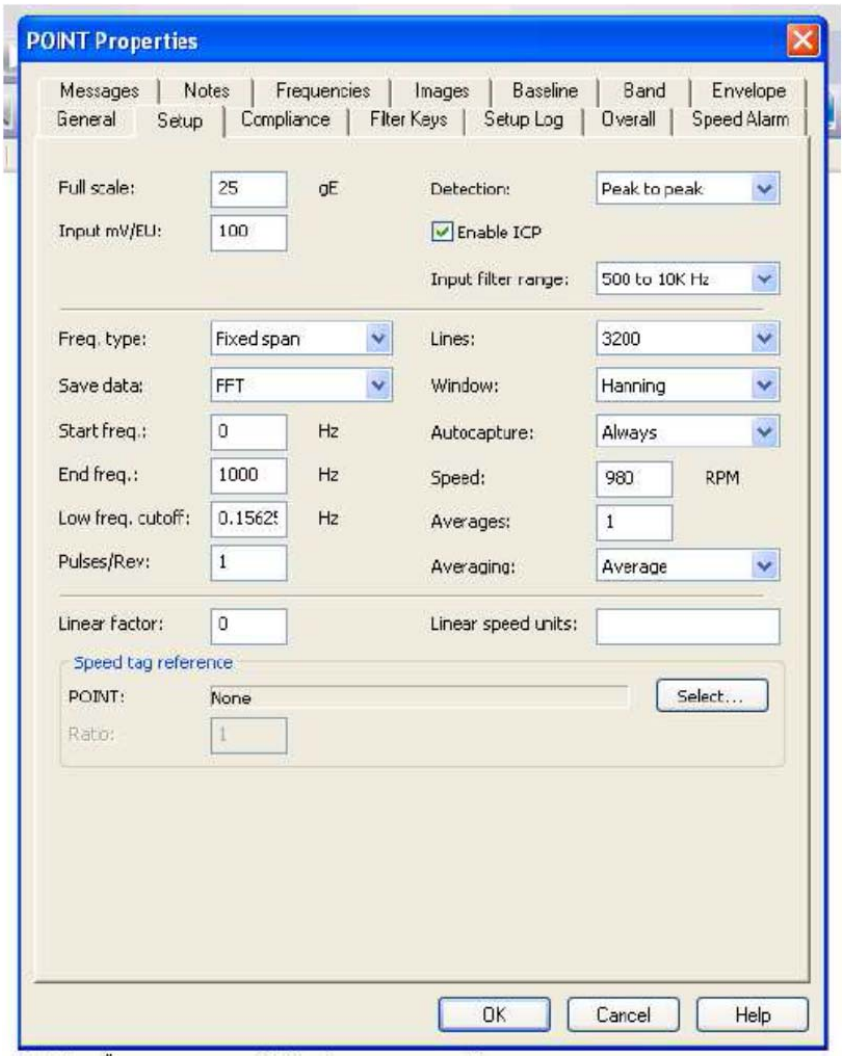

Figure 2.12: *The POINT Properties Dialog's Microlog Setup Tab.*

- **Enveloping filters selections**

The envelope method separates a repetitive impulse from a complex vibration signal by using a band pass filter that rejects low frequency components that are synchronous with vibration. Fig 2.13-a shows the optional filter selection of the SKF Condition Monitoring Microlog. Although there are signal enhancements that result from structural resonances, the envelope method is not solely dependent on local resonance to isolate rolling element defect signals. Filter criteria selection is based on suitable rejection of the low frequency sinusoids while

optimizing the passband of the defect harmonics. Fig 2.13-b provides a table of filter selections based on rotational speeds in an analysis range.

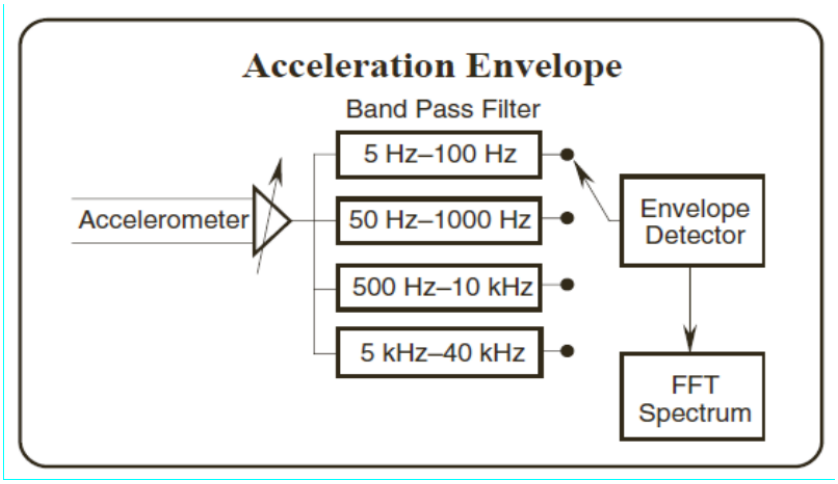

a)

Enveloping Settings Microlog

Filters	*Frequency Band*	*Speed Range*	*Analyzing Range*
E1	5 – 100 Hz	0 – 50 RPM	0 – 10 Hz
E2	50 – 1.000 Hz	25 – 500 RPM	0 – 100 Hz
E3	500 – 10.000 Hz	250 – 5000 RPM	0 – 1.000 Hz
E4	5.000 – 40.000 Hz	2500 – ...RPM	0 – 10.000 Hz

b)

Figure 2.13 : *Acceleration Envelope filters; a) Optimum filter options, b) Filter selection vs. speed/analysis range.*

2.3.2.4 Alarm setting for Detection

Data obtained through monitoring are simply quantitatively evaluated. For each measured quantity, alarm limits are set. Exceeding the programmed alarm limit means warning about a problem. Vibration severity limits can be defined basing on initial indication or basing on historical data. The table 2.7 report the alarm limits setting for Liquid ring compressor. This alarm limits are basing compressor on historical data initial.

Table 2.7: *Liquid ring compressor vibration alarm setting*

	Vibration Unity		**Detection**	**vibration severity basing on historical data**		
				Good (or satisfactory)	Alert	Unacceptable
2	Velocity	mm/s	RMS	0,01- 4	4,01 - 7	X > 7
3	Acceleration	g	RMS	0,01 - 2	2,01 – 3,5	X > 3,5
1	Enveloped Acceleration	gE	Peak to Peak	0,01 - 4	4,01 – 7	X > 7

To provide a warning that a defined value of vibration has been reached or a significant change has occurred at which remedial action may be necessary. In general, if an Alarm situation occurs, operation can continue for a period whilst investigations are carried out to identify the reason for the change in vibration and define any remedial action.

2.3.3 The main failure of Liquid ring compressor bearings.

It is well known that the most common causes for bearing failure are contamination and poor lubrication; however, excessive loading and bearing damage prior to operation-during assembly or handling-can also be culprits (section 1.2). The failure mode of the liquid ring compressors is first investigated in its initial asset (Asset 1). The Fig.2.14. shows the configuration of bearings asset. The free bearing is a Radial bearing 6324(SKF) and the fixed bearings are two angular contact ball bearings 7320 BECBM (SKF) arranged back-to-back. In this arrangement the axial load is not equally distributed on the bearing pairs in tandem [88].

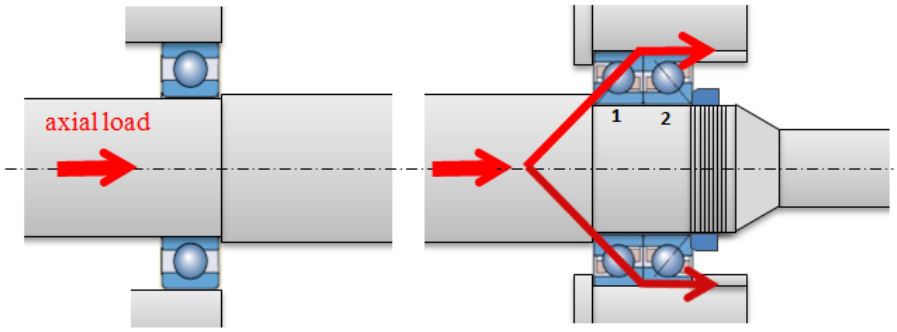

Figure 2.14: *Bearing system with a radial bearing and two angular bearings.*

2.3.3.1 Bearing Failure detection

Bearing state is monitored by the mean of vibration measure in Envelop. The characteristic frequencies of Asset1 bearings has been calculated and reported in the following table.

Table 2.8: *The characteristic frequencies of Asset1 bearings*

Bearing	6324	7320 BECBM
BPFI	78,75 Hz	113,4 Hz
BPFO	51,56 Hz	79,69 Hz
BSF	35,94 Hz	34,38 Hz
FTF	6,25 Hz	6,56 Hz

When a great and brusque change in compressor vibration overall value, it occurs become necessary make further investigation. As shows in Fig.2.15, we observed an increasing of vibration envelop value (gE) measured in horizontal direction on the support drive end ($\mathbf{H}_{\mathbf{Sup\_DE}}$).

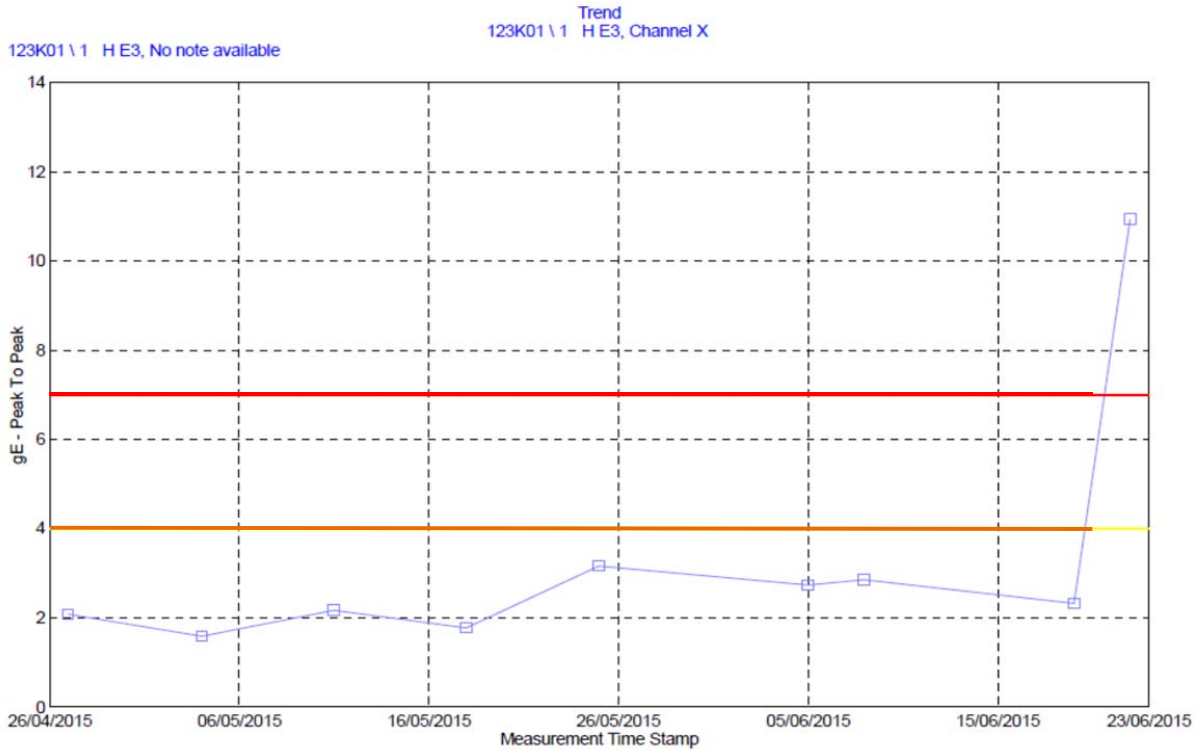

Figure 2.15: *Vibration trend of envelop value on support drive end*

The spectrum shows in the Fig. 2.16, highlights the presence of peaks of angular contact ball bearing 7320 BECBM inner ring defects frequencies ($BPFI = 113{,}4\ Hz$). Indeed in this figure, we can note that the higher peaks correspond $BFPI$ its second and third harmonics ($2 \times BPFI = 68{,}75$; $3 \times BPFI = 103{,}3$) as underline by la red lines. This means that, at this state, the inner ring is the bearing component more damaged.

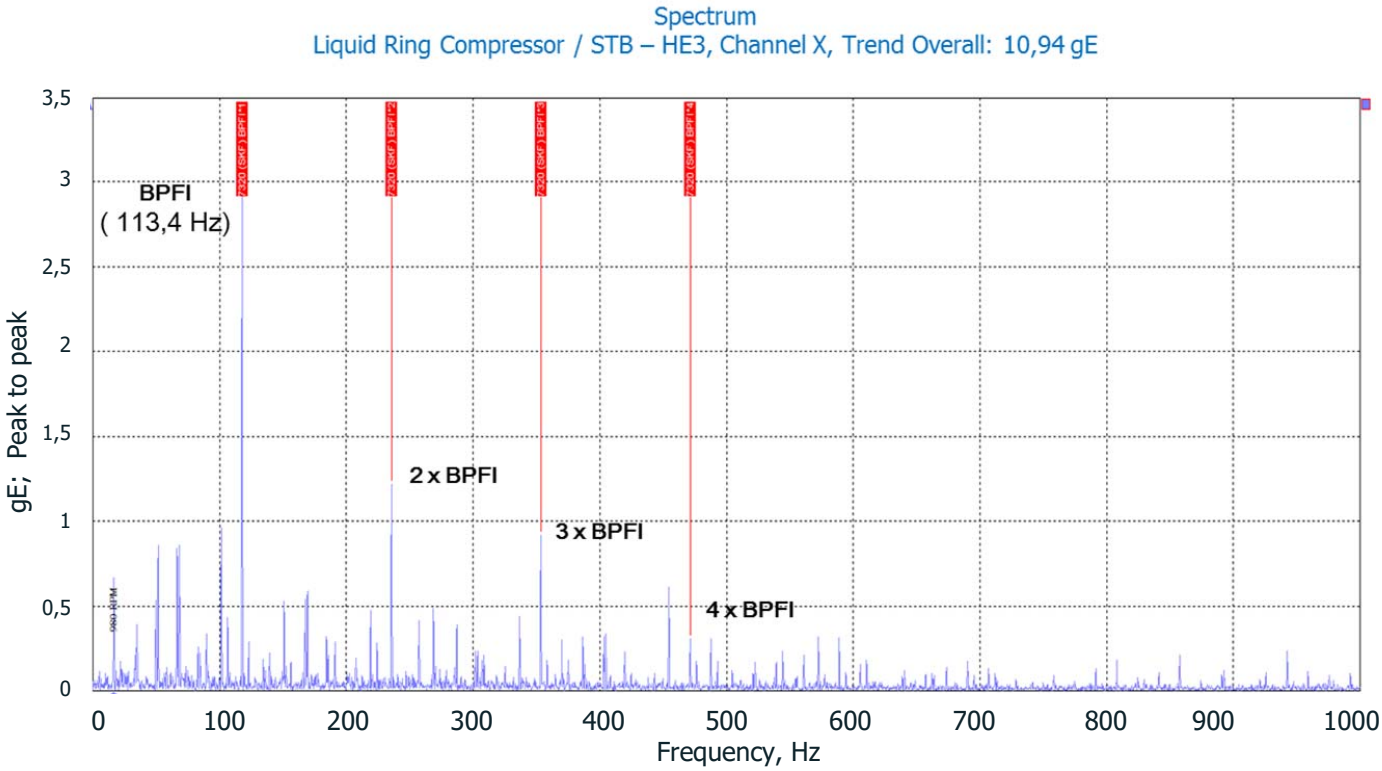

Figure 2.16: *Vibration envelop spectrum on support drive end*

2.3.3.2 Failure mode analysis

The machine has been stopped and disassembled as shown in Fig.2.17. The bearings had been analyzed. In order to analysis bearing damage to find clear indications point to the root cause, it is important to stop the machine on time. Indeed, once a bearing is damage, it gradually will further deteriorate. As soon as damage has occurred the elements will pass over the damaged and area and material is removed. If the machine is not stopped in time bearing damage analysis might become very difficult because the damage has progressed so far that it can be difficult, even impossible, to find the root cause. More on bearing damage can by find in the reference [89]. Good failure mode analysis pays dividends and should support the development of maintenance strategies.

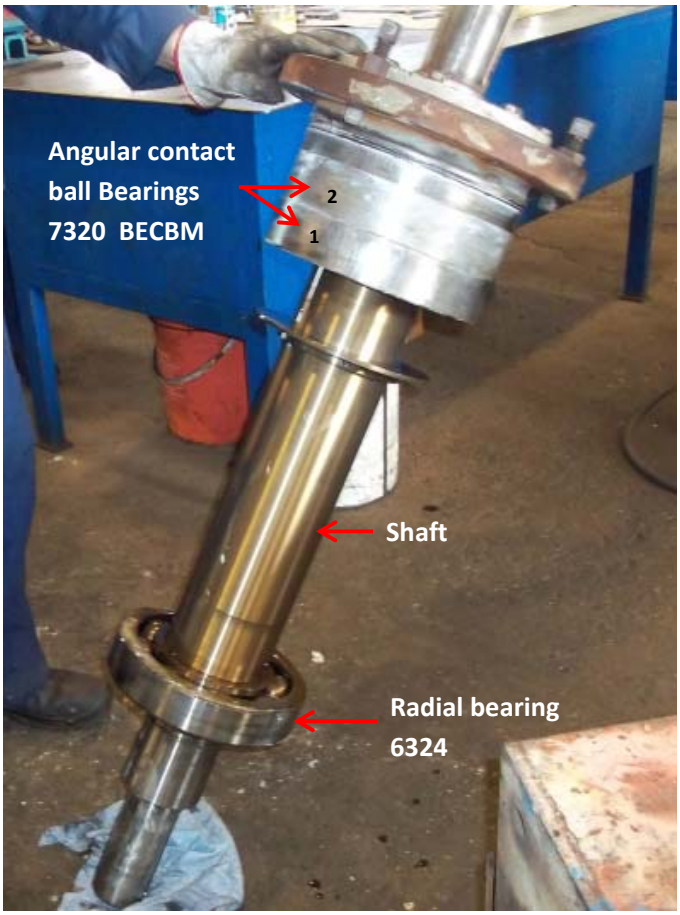

***Figure 2.17**: Shaft and bearing from compressor disassembled*

The two angular contact ball bearings 7320 BECBM (SKF) , arranged back-to-back, have been taken to pieces for analysis. One of them was more damage than the other. This is naturally due to the fact in this arrangement, the two bearing are not loaded equally by an (external) axial load. Indeed, only one of them is mainly loaded, this depend on the axial load direction [88]. In the presented case, the loaded and the more damage bearing is the bearing N° 1 (as indicated in Fig. 2.17).

All the machine bearings have been analysis to assess the damage state. The radial bearing (6324) have any beginning damage; this was predictable because its envelop vibration value didn't present any anomalies. The angular contact ball bearings (7320 BECBM) N°2 has beginning damage on the outer ring and inner ring. The bearing which analysis can give more information is the angular contact ball bearings (7320 BECBM) N°1. Its elements have been analysis.

Figure 2.18: *Bearing 7320BECBM Outer ring*

Outer ring and cage

The cage not have any evident damage. The outer ring have a beginning damage. As shown in the Fig.2.18 , the beginning of damage observed on the footprints of the outer ring track is due to the material of debts from others elements of the bearing.

Figure 2.19*:Bearing 7320BECBM (N°1) rolling elements (balls) damaged*

Rolling elements (ball) analysis

Some rolling elements (balls) have a beginning damage while others present marked damage, mainly located in only one point.

***Figure 2.20**: Bearing 7320BECBM (N°1) inner ring damaged*

Inner ring analysis

On the inner ring, it can be observed many points of damage on the rolling track. Some of them are more developed than others. This is due to the fact that the machine has not be stopped very early. On the Fig. 2.20, the damage points has been numerated . The N° 3 is the most developed and the most long, we think that this damage point result from the development of two different damage points. However, this damages state is useful.

It is very important noted that the damage point are more or less at the regular distance one from the other (we consider that the two initial damage point of N° 3 have the same distance). Those point may be correspond respectively to rolling elements position when occurred the damage. It mean that the damage happened when the compressor was stopped. It is due to an axial force.

2.3.3.3 Failure cause reconstruction and conclusion

Since the compressor vibration monitoring is done weekly, some "things strange" occurred between the date of penultimate measurement and that of the ultimate. Further investigation ensure that, during this period the compressor has been stopped and restarted. Indeed, the starting process of the liquid ring compressor is complex. And the initial axial force must be regulated correctly. If this not occurs during the restart, the axial force which is developed the instant before the rotation, is loaded on the angular bearings with the effect of "hammer blow" on the bearing, causing its damage.

This failure mode is a critical problem of this Liquid ring compressor. Even if , it is clear that the restart maneuvers must be performed by qualified operators for reduce a risk or bearing failure, this failure mode remains a critical problem. To overcome this problem a new bearing asset has been proposed.

2.3.3.4 Verification of the new asset of bearings to improve bearing load capacity

After highlighting the cause of the liquid ring compressor failure, here we are interested in the proposed new assets, that we have been called upon to monitor and verify.

Indeed, to reduce a risk of bearing failure during restate, an reengineering has been done to improve the compressor reliability, in particular its bearing asset load ratings or capacity load. Two new assets have been proposed one after another.

- **Definition of bearing Load ratings**

There is no standardized method for determining the load ratings of spherical plain bearings and rod ends, nor there is any standardized definition. As different manufacturers define load ratings differently, it is not possible to compare the load ratings of bearings produced by one manufacturer with those published by another manufacturer.

basic dynamic load rating *C*

The basic dynamic load rating C is used, together with other influencing factors, to determine the basic rating service life of spherical plain bearings and rod ends. As a rule it represents the maximum load which a spherical plain bearing or rod end can sustain at room temperature when the sliding contact surfaces are in relative motion. The maximum permissible load in any individual application should always be considered in relation to the desired service life. The basic dynamic load ratings quoted for SKF spherical plain bearings and rod ends are based on the specific load factor and the effective projected sliding surface.

The basic static load rating C_0

The basic static load rating C_0 represents the maximum permissible load which may be applied to a bearing when there is no relative movement of the sliding contact surfaces. Values of C_0 may be different for a spherical plain bearing and a rod end incorporating the corresponding bearing. For spherical plain bearings the basic static load rating represents the maximum load which the bearing can accommodate at room temperature without its performance being impaired as a result of inadmissible deformations, fracture or damage to the sliding contact surfaces. It is assumed that the bearing is adequately supported by the associated components of the bearing arrangement. In order to fully exploit the static load rating of a spherical plain bearing it is generally necessary to use shafts and housings of high-strength materials. The basic static load rating must also be considered when bearings

are dynamically loaded if they are also subjected to additional heavy shock loads. The total load in such cases must not exceed the basic static load rating.

The values for basic load ratings reported in the catalogue apply to single bearings. For angular contact ball bearing pairs mounted immediately adjacent to each other the following values apply:

- bearings in back-to-back ("O") or face to face and ("X") arrangement.

$$C = 1{,}62 \times C_{single\ bearing}$$

$$C_0 = 1{,}62 \times C_{0\ single\ bearing}$$

- bearings in a tandem arrangement.

$$C = 2 \times C_{single\ bearing}$$

$$C_0 = 2 \times C_{0\ single\ bearing}$$

A) Liquid ring compressor bearings new Asset 1

The liquid ring compressor bearings first new asset, asset 1; has been proposed as shown in Fig. 2.21. In this asset, in the free a radial bearing 6324(SKF) has been substituted by the free Double row angular contact ball bearing 3222 (SKF) with radial load capacity is higher. The fixed bearings are became three angular contact ball bearings 7320 BECBM (SKF) in order to increase le global axial load capacity. Indeed, respect to the initial asset, another bearing has been mounted in tandem arrangement with the bearing 1 (position of bearing damaged) in order to increase the axial load carrying capacity in a specific direction (abnormal axial load).

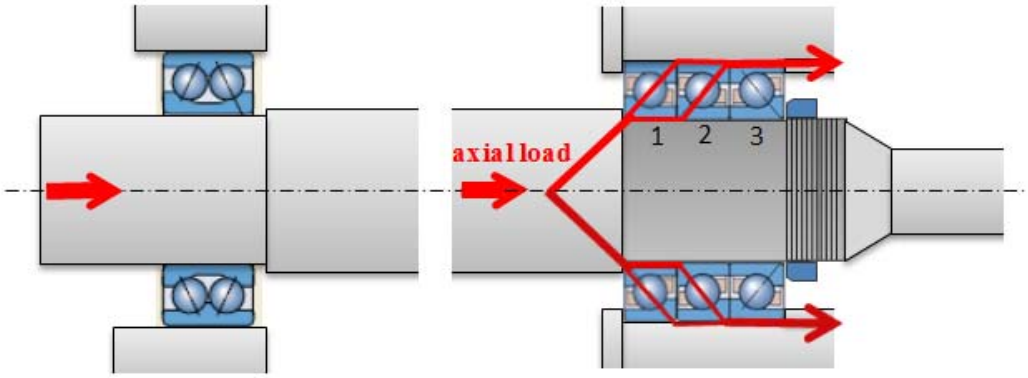

***Figure 2.21**: Bearing new system with a double bearing and three angular bearings.*

A tandem arrangement is used when the load carrying capacity of a single bearing is inadequate. When arranged in tandem, the load lines are parallel and the axial (and radial) loads may be equally shared by the bearings. However, the bearing set can accommodate axial loads in one direction only. If axial loads act in both directions, as in ours case of study, a third bearing, adjusted against the tandem pair, must be added. This is the raison why 3 angular contact ball bearings 7320 BECBM (SKF) in this new asset. The table 2.9 report the single bearings and set bearing load carrying capacity.

Table 2.9: *the single bearings and set bearings load carrying capacity.*

	Initial Asset		**New Asset 1**	
	Support No Diver end	Support Diver end	Support No Diver end	Support Diver end
Bearings	6324	7320 BECBM	3222	7320 BECBM
Bearings number by support	1	2	1	3
Bearing Arrangement	Single	Back-to-back	Single	Tandem (1 & 2) Back-to-back (2 &3)
Dynamic load rating C [kN] of single bearing	208	216	212	216
Static load rating C_0 [kN], of single bearing	186	208	212	208
Equivalent Dynamic load rating C [kN]	208	349,92	212	
Equivalent Static load rating C_0 [kN]	186	336,96	212	
Dynamic load rating C [kN] Bearings interested by the abnormal axial load	-	216	-	Tandem (1 and 2) 432
Static load rating C_0 [kN], Bearings interested by axial load	-	208	-	416

The Liquid ring compressor with a new bearings asset has been use in the production process and monitored. As mention above this new asset aim to reduce a risk of bearing failure due to abnormal impulse axial load during restate. But during it monitoring it has been verified some failure case on the Double row angular contact ball bearing.

Double row angular contact ball bearing failure

Fig.2.22 shows the spectrum of envelop vibration. We can observe that the highest peak are related to inner ring defect frequencies.

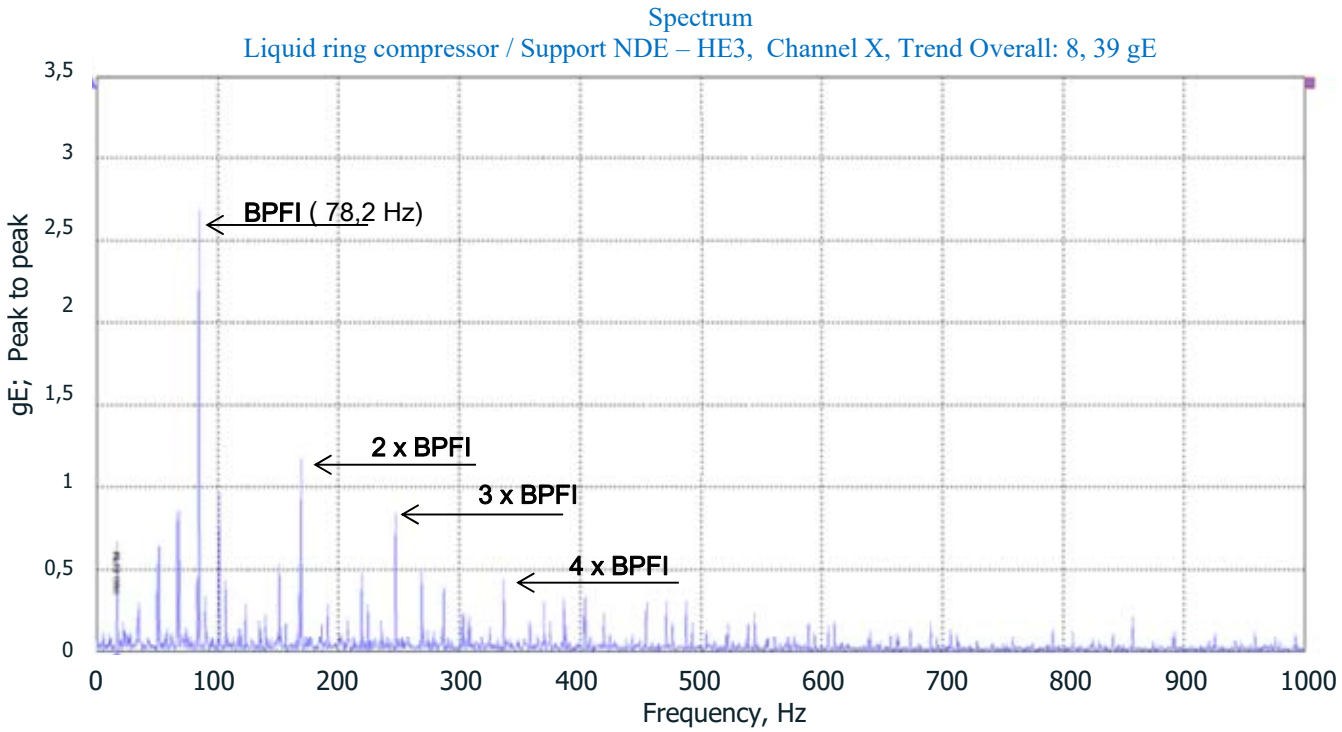

Figure 2.22: *Vibration envelop spectrum on drive end support, bearing 3322*

In the Fig 2.23, we make the RCFA . The Fig. 2.23-a, shows double row angular contact ball bearing 3322 inner ring damaged and this damaged has been descripted and analysis. Then it had been established that the failure of this bearing, happened only on the row A (as show in the fig.), is actually due to impulsive axial force (Fig.2.23-b). This is another anomaly failure, because this bearing has been mounted so that it can move itself in axial direction in the bearing housing and only support radial loads. This bearing is therefore not intended to support axial loads. To explain this failure; we presume that the outer ring of the bearing is being imputed during its axial sliding movement so subjecting the bearing to the impulsive axial load.

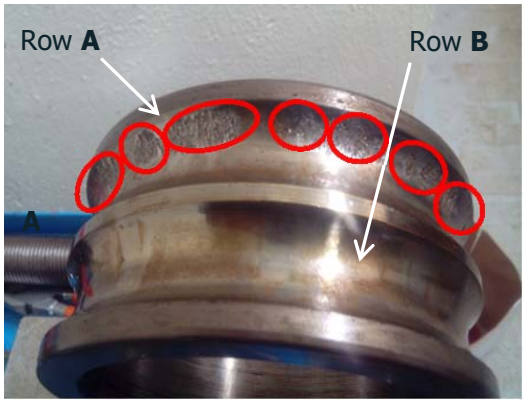

On the bearing 3322 inner ring.

Row A: it can be observed many points of damage on the rolling track. Some of them are more developed than others. This is due to an untimely stop of the machine. However, it can be observed that these damage points are separated each other by a distance more or less regular.

Row B: it can be observed no significant damage point on the rolling track.

a) *Double row angular contact ball bearing 3322 inner ring damaged*

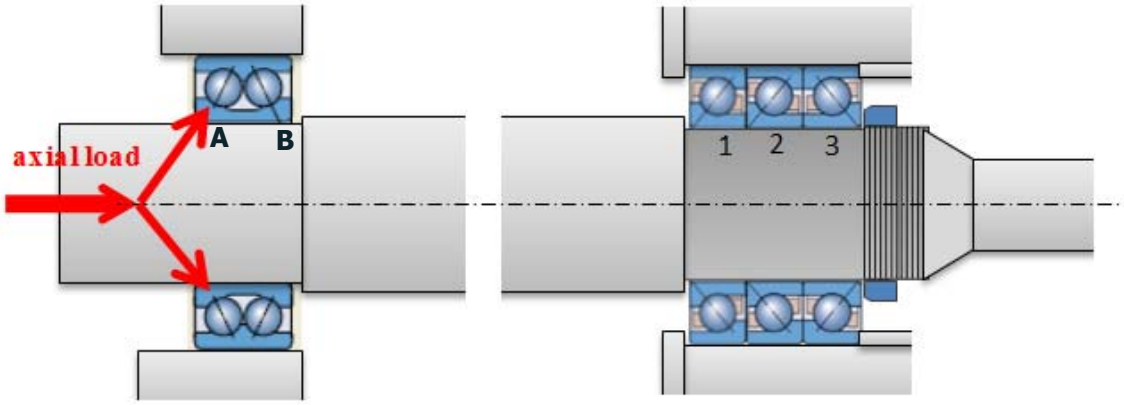

b) Abnormal action of axial loads on the bearing 3222 in the support radial loads

Figure 2.23: *Double row angular contact ball bearing 3222 inner ring damaged in the new asset 1*

B) Liquid ring compressor bearings new Asset 2

After the failure of the double row angular contact ball bearing 3322, a new asset (named asset2) has been proposed, as shown in Fig.2.24. This new asset 2 is obtained by the modification of new assets1. A radial bearing 6324(SKF) has replaced the double row angular contact ball bearing 3322 (SKF) in the free support. The fixed bearings remained the same.

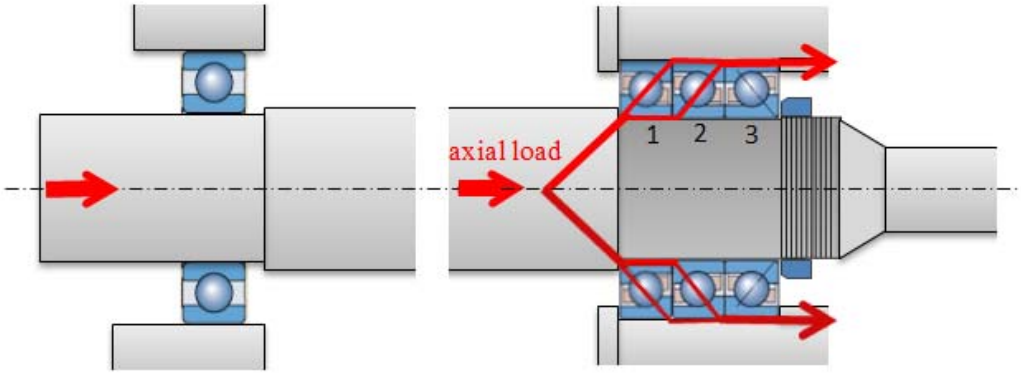

Figure 2.24 *: New bearing system, with a double bearing and three angular bearings.*

During the monitoring of new asset2, the envelop vibration global value have risen suddenly again, from 2,4 gE to 6,81 gE on the support DE. The spectrum is shown in Fig 2.25. The highest peaks are those related to the inner ring damage of the angular bearing 7320 BECBM. This means that also in this new asset 2, one bearing (bearing 1 or/and bearing 2) is damaged at least. It is sufficient to make unreliable the machine and needed the maintenance. The RCFA shown that the bearing damaged is the bearing 1 and the failure is also due to the abnormal axial load during the machine starting process.

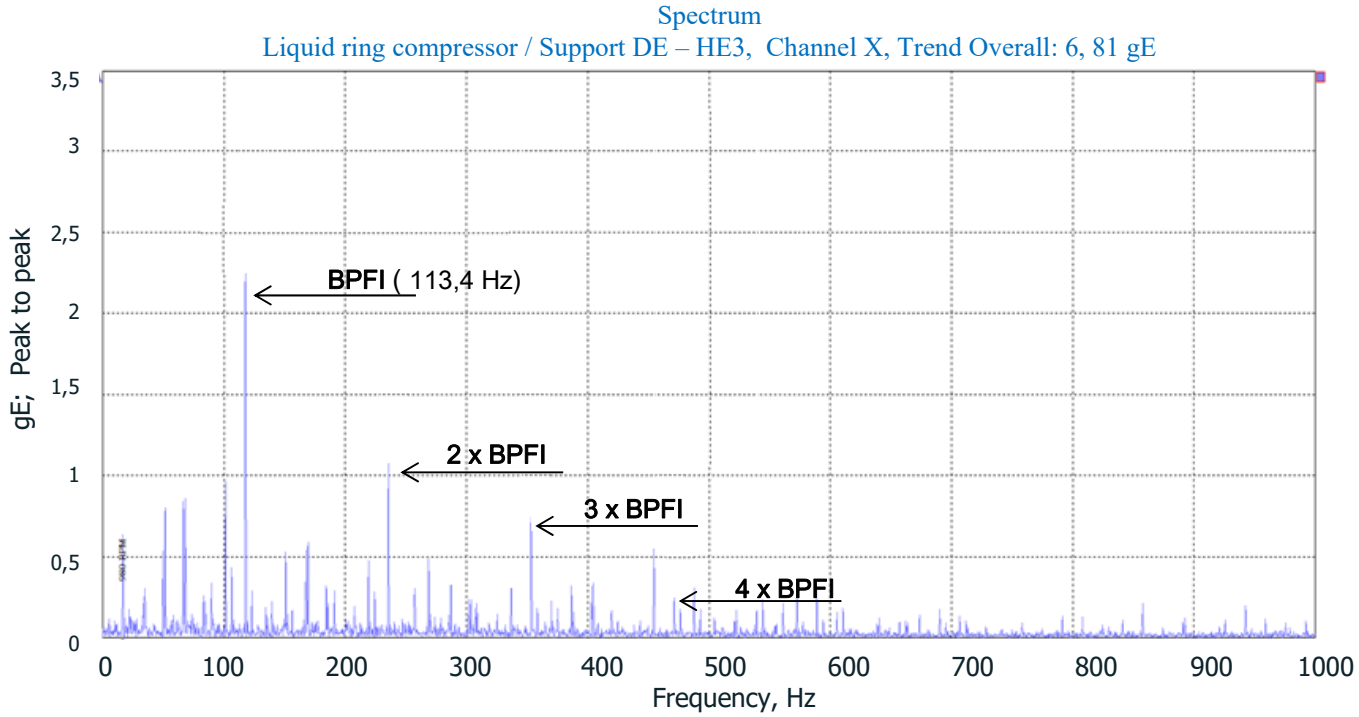

Figure 2.25: *Vibration envelop spectrum on drive end support, bearing 7320 BECBM*

2.3.3.5 Results and discussion

The ring liquid ring compressor had been investigated to found the cause of a improvise bearing failure. It has established after bearing damage analysis that this is caused during the restart by the axial force which is developed the instant before the rotation, and loaded on the angular bearings with the effect of “hammer blow” on the bearing. The change of the asset, reinforcing the load capacity of the bearings system, has not eliminated the risk of sudden rupture. The process of starting fluid compressor is complex and the error can happen to even the most experienced operators.

It is clear that the process of starting fluid compressor are the cause of bearings damage, since it represents the time at which the bearings are the most stressed by the axial load. It would be advisable to review the start-up process design, for the purpose of improve it and make this compressor more reliable.

2.3.4 Process problem evidence

As mention above, the liquid ring compressor is used to recover gas for use in torch and sends them in the plants for the power production. These gases may come from different systems, then the natures of the gases are different from a plant to another. To make the compressor work in the vicinity of its operating point, the flow must be adjusted according to the molecular mass of the gas in transit. If this adjustment is not done correctly or omitted for some reason there is a process problem. The process problem is not more than a fluid dynamic problem (for example stall) that creates abnormal stresses on the blades of the impeller, which, if not corrected in time leads to the breakage of them. A case of particularly heavy process problem for the impellers is the presence of liquid in the product in transit. This leads more rapidly to the impeller damage.

2.3.4.1 Measures for monitoring the process problem.

The vibration measurements are acquired weekly. and the occurrence of particular compressor noise.
The global values measured at different points of the compressor during an acquisition are reported in table 2.10.

***Table 2.10**: Global values measured at different points of the compressor*

	Measure Point name	Unity	Quantity measured	Vibration overall values
1	H $_{Sup-DE}$ _ Envelop	gE	Peak to Peak	3,82
2	H $_{Sup-DE}$ _ Velocity	mm/s	RMS	6,53
3	H$_{Sup-DE}$ _ Acceleration	g	RMS	1,68
4	V $_{Sup-DE}$ _ Velocity	mm/s	RMS	8,51
5	A $_{Sup-DE}$ _ Velocity	mm/s	RMS	2,24
6	H $_{Sup-DNE}$ _ Envelop	gE	Peak to Peak	8,78
7	H $_{Sup-DNE}$ _ Velocity	mm/s	RMS	3,18
8	H$_{Sup-DNE}$ _ Acceleration	g	RMS	3,03
9	V $_{Sup-DNE}$ _ Velocity	mm/s	RMS	3,31

- **Observation of the spectrum in Envelop acceleration units.**

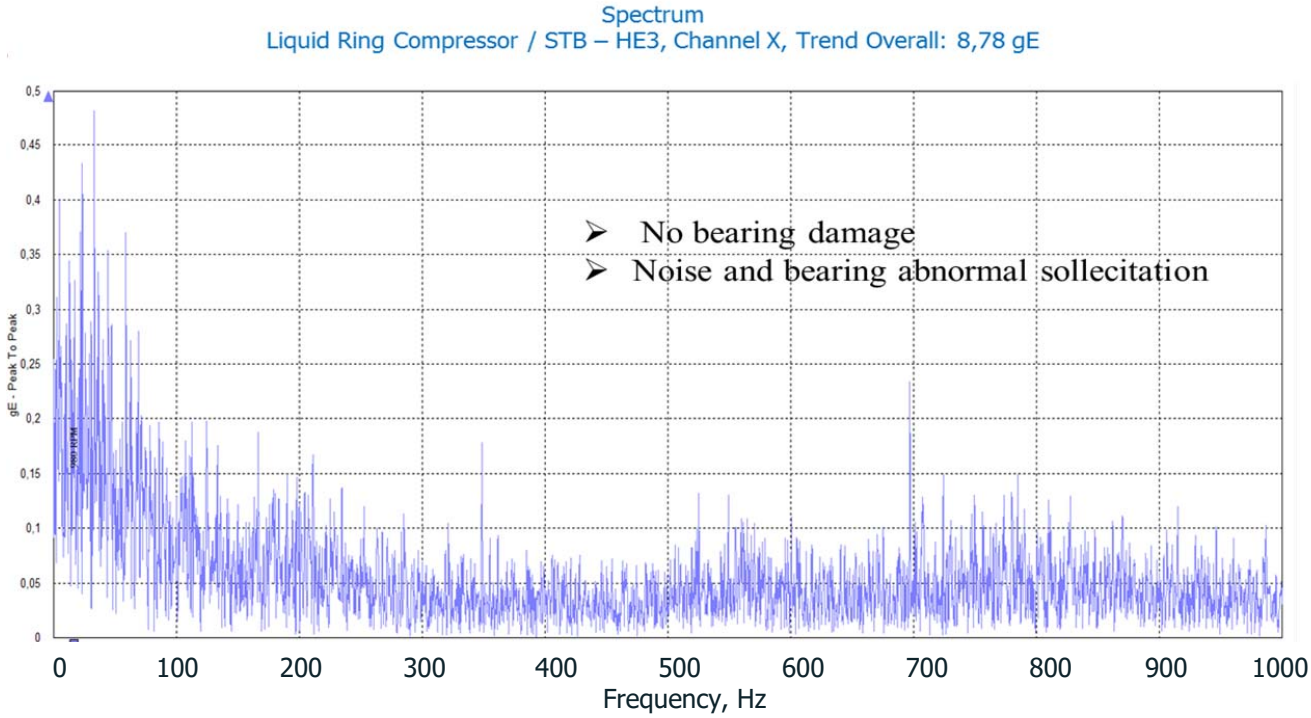

***Figure 2.24**: Vibration Spectrum of the point 2 (**H $_{Sup-DE}$ _ Envelop**)*

Fig.2.24 shows the spectrum of point 6 (H Sup-DNE _ Envelop). The overall value is 8,78 gE, we note the presence of noise but the spectrum doesn't present any bearing defect peak. Therefore we think that, at this moment, the bearing is not damage. But it is evident that the bearing is under abnormal stress that could cause its failure. We try to find the cause of this abnormal stress spectrum by another vibration unit: velocity or/ and acceleration units.

- **Observation of the spectrum in velocity units.**

The Fig. 2.25 shows the spectrum of the acquisition on the point 2 (**H $_{Sup-DE}$ _ Velocity**). It observes a peak amplitude 4.76 mm / s at the transition frequencies of the blades of the impeller first internship 1X. All other peaks are under 1mm / s. It also notes that beyond 1000hz, the spectrum is confused almost horizontal axis (the amplitude of peaks, even compressed 3X and 4X, are zero or nearly zero). This illustrates the fact that the measure vibration velocity units, are largely insusceptible to phenomena that occur at a frequency greater than 1000 Hz. The speed measurement is therefore recommended for phenomena observable from 10 to 1000 Hz as already indicated above (in section 1.1.2.3). To this vibration measurement point, it was sufficient to consider f_{max} = *1000 Hz.*

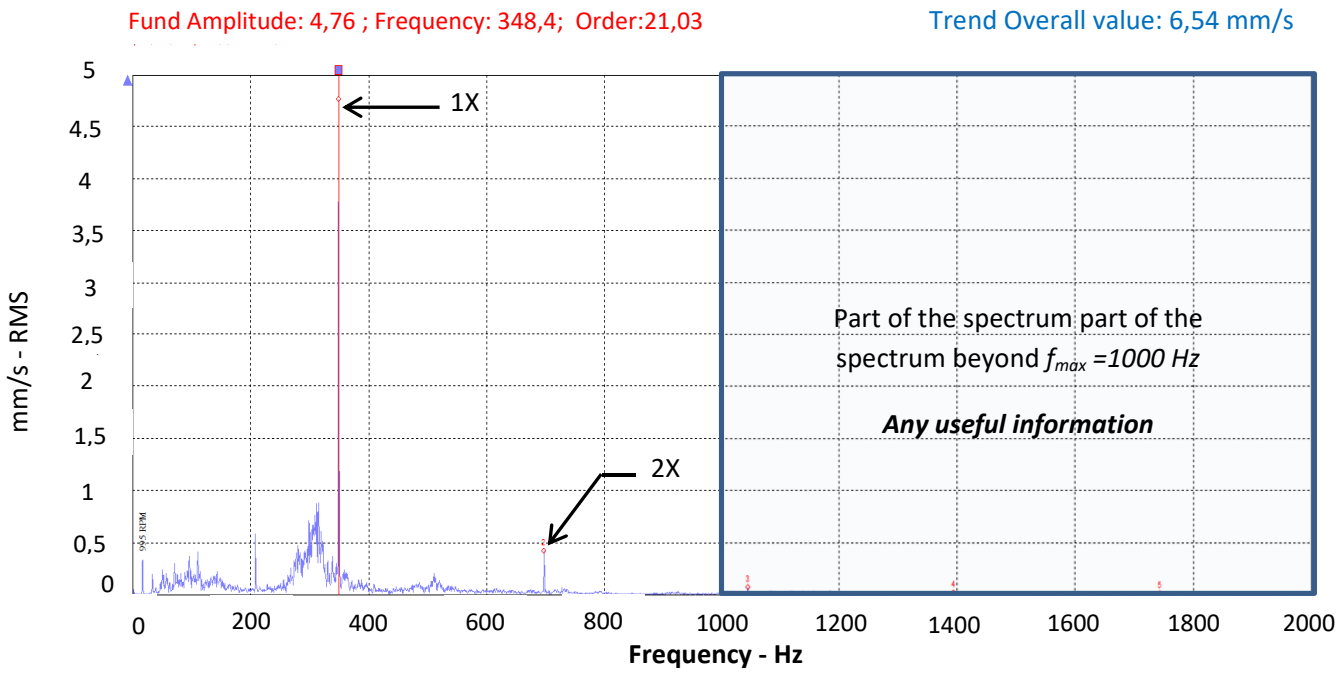

Figure 2.25**: Vibration Spectrum of the point 2 (**H $_{Sup-DE}$ _ Velocity)

- **Observation of the spectrum in acceleration units.**

The Fig.2.26 shows the spectrum of point 8 (H Sup-DNE _ Acceleration). Significant peaks are observed at frequencies *1X, 2X* and *3X* (1X being the transition frequencies of the blades of the impeller of the Stage 1). Between the frequencies 2500 and 4500 Hz, the spectrum highlights a noise phenomenon linked to the process. The spectrum allows to observe phenomena from 300 Hz to 4500 Hz (approximately), then up to very beyond 1000 Hz. This illustrates the fact that the measure vibration in acceleration units, are sensitive to phenomena that occur at a frequency greater than 1000 Hz. The extent to acceleration is therefore recommended for phenomena observable over 1000 Hz as already indicated above (in section 1.1 .2.3).

The evidence observed on the spectrum indicates an abnormal stress of the impeller blades due to a process problem. An appropriate process regulation returns to normal vibrations.

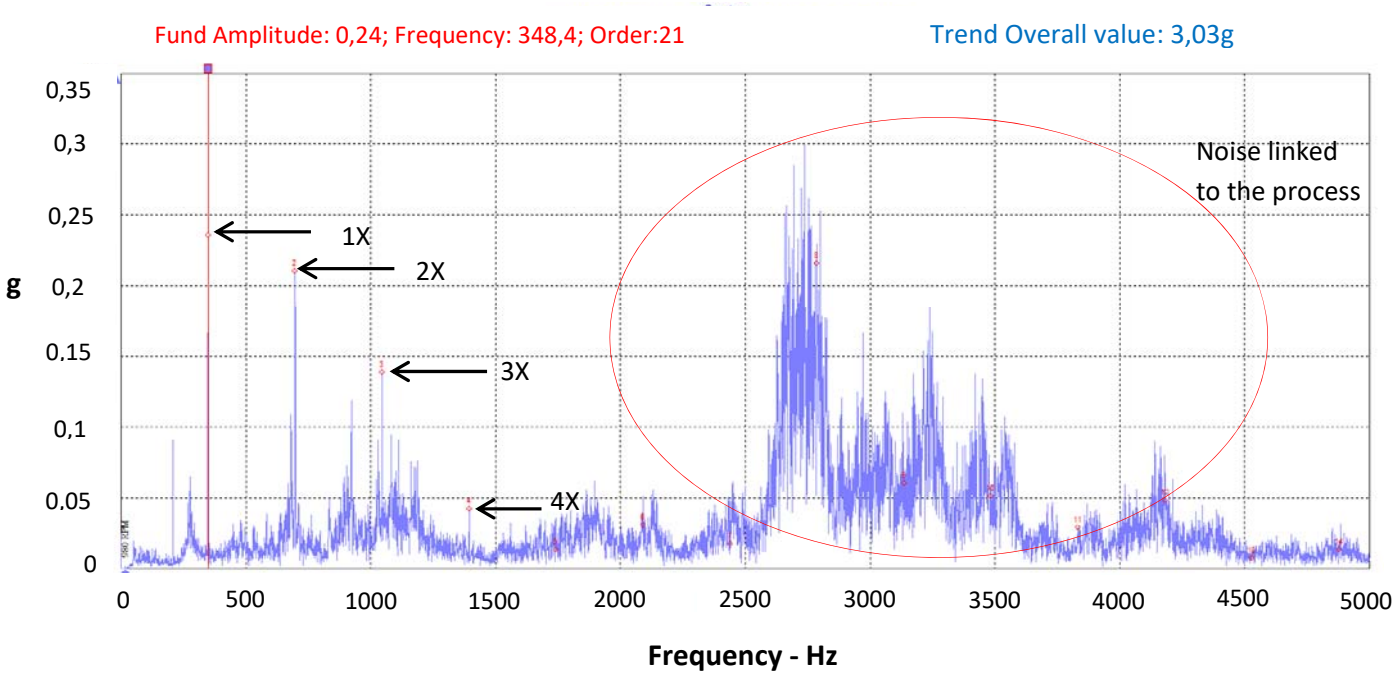

Figure 2.26 : *Vibration Spectrum of the point 8 (H Sup-DNE _ acceleration).*

2.3.4.2 Liquid ring compressor Impeller damaged

A case of particularly heavy process problem for the impellers is the presence of liquid in the product in transit (gas with high titre). This leads more rapidly to the impeller damage. The Fig.2.27 show an impeller damage.

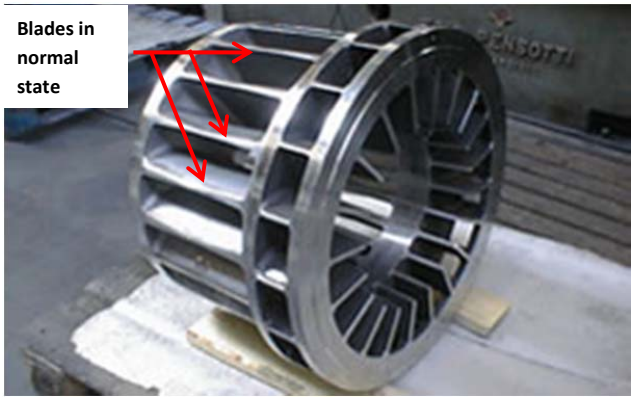

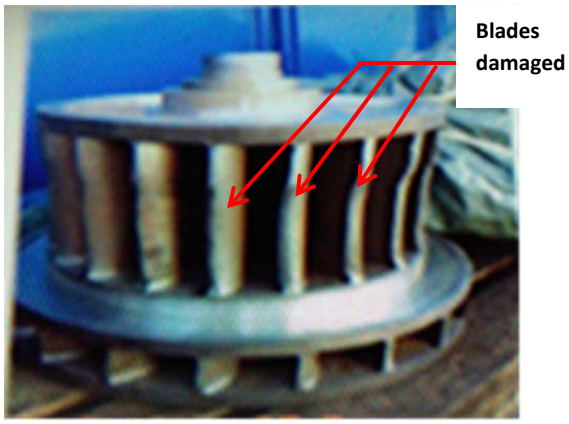

a)Liquid ring compressor Impeller normal state

b) Liquid ring compressor Impeller damaged by Process problem

***Figure 2.27**: Liquid ring compressor Impeller in normal state a) and Impeller damaged by Process problem b*

Conclusion

The bearing failure modes have been decrypted. It is well known that the most common causes for bearing failure are contamination and poor lubrication; however, excessive loading and bearing damage prior to operation-during assembly or handling- are others causes quite frequent.

From a review of studies on vibration measurement techniques for the detection of defects in rolling element bearings, it is seen that the emphasis is on vibration measurement methods. Vibration in the time domain can be measured through parameters such as overall RMS level, crest factor, probability density and kurtosis. Among these, RMS is the most effective; it is a powerful tool, the most used to estimate the average power in system vibrations. Vibration measurement in the frequency domain has the advantage that it can detect the location of the defect; a method widely used is Envelope analysis.

As far as concerned vibration analysis method it is seen that the emphasis is on two approaches: Cyclic spectral analysis and Blend Separation Source (BSS). Currently the most widely used is the first one that is also the most consolidated. However the second, introduced more recently in the analysis of vibration is the subject of more and more numerous research and applications.

A case of bearing failure has been studied. The liquid ring compressor had been investigated experimentally to found the cause of a improvise bearing failure. In this study the Envelope analysis efficiency to detect the location of the defect had been illustrated. After bearing damage, it has been established that this failure is caused during the restart by an abnormal axial force which is developed when the restart performance is not executed correctly.

Reference

[1] ISO 13373-1: *Condition monitoring and diagnostics of machines - Vibration condition monitoring* - Part 1: General procedures. 2002; This standard was last reviewed* in 2012

[2] ISO 13373-2: *Condition monitoring and diagnostics of machines - Vibration condition monitoring* - Part 2: processing, presentation and analysis of vibration data. 2005

[3] Mao Kunli, Wu Yunxin, "*Fault Diagnosis of Rolling Element Bearing Based on Vibration Frequency Analysis"*, IEEE Third International Conference on Measuring Technology and Mechatronics Automation (ICMTMA) 2011, 337.

[4] SKF, "*Basics of Condition Based Maintenance"*, ISO 18436 Vibration Analysis Level 1, SKF May 2012.

[5] SKF ; *" Data Acquisition & Signal Processing"*; ISO 18436 Vibration Analysis Level 1, SKF May 2012.

[6] ALENA BILOŠOVÁ JAN BILOŠ; *"Vibration diagnostics",* OSTRAVA 2012.

[7] Jacques MOREL ; *"Surveillance Vibratoire Et Maintenance Prédictive"*, Département surveillance diagnostic maintenance à EDF, Division recherches et développement

[8] James E. Berry P.E. *" Concentrated vibration signature analysis and related condition monitoring techniques"*, Technical Associates of Charlotte, P.C. 2002 San Diego,CA

[9] Xu, M., Marsngoni, R.D. "*Vibration Analysis of a Motor Flexible Coupling Rotor System Subject to Misalignment and Unbalance* , *Part I: Theoretical Model and Analysis"* , Journal of Sound and Vibration Volume 176, Issue 5, 6 October 1994, Pages 663–679

[10] Sekhar, AS., Prsbhu, B.S. *"Effects of Coupling Misalignment on Vibrations of Rotating Machinery",* Journal of Sound and Vibration, Vol 185(4). pp666 - 671, 1995.

[11] Redmond. I, Hussain,K.M., *"Misalignment As a Source of Vibration in Rotating Shaft Systems",* Proc. Intl. Modal Analysis Conf. (IMAC) XIX, Orlando, Feb. 2001.

[12] I. Redmond; *" Study of a misaligned flexibly coupled shaft system having nonlinear bearings and cyclic coupling stiffness — Theoretical model and analysis",* Journal of Sound and Vibration 700-720, 2010

[13] Irvin Redmond; *"Shaft Misalignment and Vibration - A Model"* ; Dynamic Analysis Unit, Consulting Services Department,

Saudi Arabian Oil Company, Dhahran, 2002.

[14] REMOND, VELEX et SABOT. *"Comportement dynamique et acoustique des transmissions par engrenages".* Publication CETIM n° 5B10, Senlis (1993).

[15] I. El-Thalji, E. Jantunen, *A summary of fault modelling and predictive health monitoring of rolling element bearings*, Mech. Syst. Signal Process. (2015),

[16] Mao Kunli, Wu Yunxin, "*Fault Diagnosis of Rolling Element Bearing Based on Vibration Frequency Analysis",* IEEE Third International Conference on Measuring Technology and Mechatronics Automation (ICMTMA) 2011, 337.

[17] R.M. Stewart, *"Application of signal processing techniques to machinery health monitoring"*. Noise and Vibration, Halsted Press, 1983, Chapter 23, pp 607-632.

[18] N.W. Sachs, *"Logical failure analysis in rolling element bearings".* Power Transmission Design, October 1992, pp 22-25.

[19] A.G. Herraty, "Bearing vibration - failures and diagnosis". Mining Technology, February 1993, pp 51-53.

[20] N. Tsushima, "Rolling contact fatigue and fracture toughness of rolling element bearing materials". JSME International Journal, Series C, Vol. 36, No. 1,1993, pp 1-8.

[21] Nikas, G., Sayles, R., and Ionnodes, E. Effects of debris in sliding/rolling elastohydrodynamic contacts. Proc. IMechE, Part J: J. Engineering Tribology, 1998, 212, 333–343. DOI: 10.1243/135065098154216.

[22] Dwyer-Joyce, R. S. Predicting the abrasive wear of ball bearings by lubricant debris.Wear, 1999, 233–235, 692–701.

[23] Ioannides, E. Contamination and the SKF new life theory for rolling bearings. NLGI Spokesman, 1990, 54, 14–19.

[24] Kerry, M., Peterson, L., Cagnasso, R.: *" An Atlas of railway axle bearing defects including guidelines on how to examine bearings and overhaul practice"* .SKF (2008).

[25] Kato, K. and Adachi, K. *"Wear mechanisms"*. In Modern tribology handbook (Ed. B. Bhusan), 2001 (CRC Press LLC, Boca Raton, Florida, USA).

[26] C.S. Sunnersjo, *"Rolling bearing vibrations - The effects of geometrical imperfections and wear"*. Journal of Sound and Vibration, Vol. 98, No. 4, 1985, pp 455-474.

[27] M.J. Hine, *"Absolute ball bearing wear measurements from SSME turbopump dynamic signals"*. Journal of Sound and Vibration, Vol. 128, No. 2,1989, pp 321-331.

[28] J.E. Keba, *"Component test results from the bearing life improvement program for the Space Shuttle Main Engine Oxidizer Turbopumps"*. Proceedings of the 3rd International Symposium on Rotating Machinery, Honolulu, HI, 1990, pp 303-318.

[29] Bowden, F. P. and Tabor, D. *"The friction and lubrication of solids"*. Part I, 1950/1971 (Clarendon Press, Oxford, UK).

[30] Manuale montaggio cuscinetti SKF.

[31] Y. H. Pao, R. R. Gajewski, and A. N. Ceranoglu, *"Acoustic emission and transient waves in an elastic plate,"* The Journal of the Acoustical Society of America, vol. 65, p. 96, 1979.

[32] N. Tandon and A. Choudhury, "A review of vibration and acoustic measurement methods for the detection of defects in rolling element bearings," Tribology International, vol. 32, pp. 469-480, 1999.

[33] N. Tandon, B.C. Nakra; *"Comparison of vibration and acoustic measurement techniques for the condition monitoring of rolling element bearings"*; Tribology International Vol 25, 1992, Pages 205–212

[34] Holroyd, T. and Randall, N., *"Use of acoustic emission for machine condition monitoring"*, British Journal of Non-Destructive Testing, Vol. 35, No. 2, pp. 75–78, 1993

[35] Williams, J. *" Wear and wear particles – some fundamentals"*. Tribol. Int., 2005, 30, 863–870.

[36] Halme, J. *" Condition monitoring of oil lubricated ball bearing using wear debris and vibration analysis"*. In Proceedings of the International Tribology Conference (AUSTRIB'02), Frontiers in tribology, Perth, Universityof Western Australia, 2–5 December 2002, vol. II, pp. 549–553.

[37] Harvey, T. J., Wood, R. J. L., and Powrie, H. E. G. *"Electrostatic wear monitoring of rolling element bearings"*. Wear, 2007, 263, 1429–1501.

[38] Hunt,T. M. *"Handbook of wear debris analysis and particle detection in liquids",* 1993 (Elsevier Applied science, London, UK).

[39] Roylance, B. J. and Hunt, T. M. "*The wear debris analysis handbook"*, 1999 (Coxmoor Publishing Company, Oxford, UK).

[40] J Halme ∗ and P Andersson; *" Rolling contact fatigue and wear fundamentals for rolling bearing diagnostics – state of the art"*, Proc. IMechE Vol. 224 Part J: J. Engineering Tribology, 2009.

[41] Toms, L. and Toms, A. *"Lubricant properties and test methods".* In Handbook of lubrication and tribology (Ed. G. Totten), vol. 1: application and maintenance, 2006, pp. 30.1–30.33 (Taylor & Francis Group, Boca Raton, Florida, USA).

[42] Archambault R.: *"Getting More Out of Vibration Signals: using the logarithmic scale",* Proceedings of the 1 st International Machinery Monitoring & Diagnostic Conference & Exhibit, Vol. 567, 1989.

[43] Ulieru D.: *"Diagnosis by Measurement of Internal Vibration and Vibration Analysis on Maintenance of Rotating Machinery such as Turbochillers, Proceedings,"* Annual Technical Meeting-Institute of Environmental Sciences, 2(1993) 525.

[44] Barkov A., Barkova N. and Mitchell J.S.: "*Condition Assessment and Life Prediction of Rolling Element Bearing" –* Part 1, Journal of Sound and Vibration, 29(6) (1995) 10.

[45] C.J. Li and J. Ma, *"Bearing localized defect detection through wavelet decomposition of vibrations".* Proceedings of the 46th Meeting of the Mechanical Failures Prevention Group, April 7-9,1992, Virginia Beach, Virginia, pp 53-62.

[46] E. Jantunen, *" How to diagnose the wear of rolling element bearings based on indirect condition monitoring methods"*, .J.COMADEM9 (3) (2006) 24–38.

[47] T. Yoshioka, S.Shimizu, *"Monitoring of ball bearing operation under grease lubrication using a new compound diagnostic system detecting vibration and acoustic emission"* Oct.,Tribol. Trans. 52 (6) (2009) 725–730.

[48] T. J. Harvey, R. J. K. Wood,.E. G. Powrie, *"Electrostatic wear monitoring of rolling element bearings",* Sep.,Wear 263 (2007) 1492–1501.

[49] D. Schwach, Y.Guo, *"A fundamental study on the impact of surface integrity by hard turning on rolling contact fatigue"* Dec.,Int.J.Fatigue 28(2006) 1838–1844

[50] V. Manoj, K. Manohar Shenoy, K.Gopinath, "*Developmental studies on rolling contact fatigue*" test rig Mar.,Wear264(2008)708–718

[51] Z. Zhi-qiang, L.Guo-lu, W.Hai-dou, X.Bin-shi, .Zhong-yu, Z.Li-na, *" Investigation of rolling contact fatigue damage process of the coating by acoustics emission and vibration signals"*, Mar.,Tribol.Int.47 (2012) 25–31.

[52] Z. Zhi-qiang,L.Guo-lu,W.Hai-dou,X.Bin-shi,P.Zhong-yu,Z.Li-na, " *Investigation of rolling contact fatigue damage process of the coating by acoustics emission and vibration signals"* Mar., Tribol. Int.47 (2012) –31.

[53] T.J.Harvey, R.J.K.Wood, H.E.G.Powrie, "*Electro static wear monitoring of rolling element bearings",* Sep., Wear 263 (2007) 1492–1501.

[54] E.D. Price, A.W. Lees, M.I.Friswell, B.J.Roylance, *"On line detection of subsurface distress by acoustic emissions",* Key Eng. Mater. 246–246 (2003) 451–460.

[55] T. Yoshioka, S.Shimizu, *" Monitoring of ball bearing operation under grease lubrication using a new compound diagnostic system detecting vibration and acoustic emission".* Oct.,Tribol. Trans. 52 (6) (2009) 725–730.

[56] Abhinay V. Dube, L.S.Dhamande, P.G.Kulkarni, "Vibration Based Condition Assessment of Rolling element Bearings With Localized Defects", International Journal of Scientific & Technology Research Volume 2, Issue 4, April 2013.

[57] S. Tyagi, "Transform preprocessing", .Sci.Eng. Technol. (2008)309–317.

[58] A. Djebala, N.Ouelaa, .Hamzaoui, "*Detection rolling*".,Meccanica 43 (3 2007) 339–348.

[59] C. Pachaud, R.Salvetas,C. ,Crest factor and Kurtosis contributions to identify defects inducing periodical impulsive forces, Mech. Syst. Signal Process.11(6)(1997)903–916.

[60] A. K. S. Jardine, D. Lin, D. Banjevic, "*A review on machinery diagnostics and prognostics implementing condition-based maintenance",* Mech. Syst. Signal Process. 20(7)(Oct.2006)1483–1510.

[61] D. C. Baillie, J. Mathew, *"A comparison of autoregressive modeling techniques for fault diagnosis of rolling element bearings".* Jan., Mech. Syst. Signal Process. 10(1)(1996)1–17.

[62] R. Yan, R. X. Gao, *" Approximate entropy as a diagnostic tool for machine health monitoring".* Feb., Mech. Syst. Signal Process. 21 (2007) 824–839.

[63] H. Ocak, K. a. Loparo, F. M Discenzo, *"Online tracking of bearing wear using wavelet packet decomposition and probabilistic modeling: a method for bearing prognostics".* May, J. Sound Vib. 302 (2007) – 961.

[64] Z. K. Peng, F. L. Chu, "*Application of the wavelet transform in machine condition monitoring and fault diagnostics: are view with bibliography"*, Mech. Syst. Signal Process. 18 (2004) 199 – 221.

[65] K. Mori, N. Kasashima, T.Yoshioka, Y. Ueno, *" Prediction of spalling on a ball bearing by applying the discrete wavelet transform to vibration signals".* Jul. , Wear 195 (1996) 162– 168.

[66] K. Shibata, A. Takahashi, T. Shirai, *"Fault diagnosis of rotating machinery through visualization of sound signals".* Mar.,Mech. Syst. Signal Process. 14(2) (2000) 229–241.

[67] W. Wei, L. Qiang, Z. Guojie, *"Novel approach based on chaotic oscillator for machinery fault diagnosis".* Oct., Measurement 41(8) (2008) 904 –911.

[68] Jayaswal Pratesh, Wadhwani A. K., Mulchandani K.B. *"Rolling Element Bearing Fault Detection via Vibration Signal Analysis".* The Icfai University of Journal of Science & Technology, Vol. 4, No.2, 2008, pp. 7-20.

[69] A. Palmgren, *Ball and Roller Bearing Engineering.* S.H. Burbank and Co. Inc., Philadelphia, 1947.

[70] Harris TA. *Rolling bearing analysis*. New York: John Wiley andSons, 1966

[71] P. Eschmann, L. Hasbargen and K. Weigand, *Ball and roller bearings - Theory, Design and Application*. John Wiley and Sons, 2nd Edition 1985.

[72] Deville, Y. *Towards industrial applications of blind source separation and independent component analysis.* in Proceedings of the First Workshop on Blind Source Separation and Independent Component Analysis (ICA'99). 1999. Aussois, France.

[73] Comon, P., *Independent component analysis. A new concept?* Signal Processing, 1994. **36**(3): p. 287-314.

[74] Comon, P., *Independent component analysis. A new concept?* Signal Processing, 1994. **36**(3):p. 287-314.

[75] Dinh Tuan, P. and P. Garat, *Blind separation of mixture of independent sources through a quasi-maximum likelihood approach.* IEEE Transactions on Signal Processing, 1997. **45**(7): p. 1712-25.

[76] Cornelius Scheffer, P.G., *Practical machinery vibration analysis and predictivemaintenance.*, ed. S. Mackay. 2004, Burlington: Newnes. 272.

[77] Gelle, G., M. Colas, and G. Delaunay, *Blind sources separation applied to rotating machinesmonitoring by acoustical and vibrations analysis.* Mechanical Systems and Signal Processing, 2000. **14**(3): p. 427-42.

[78] Gelle, G., M. Colas, and C. Servière, *Blind source separation: a tool for rotating machinemonitoring by vibrations analysis?* Journal of Sound and Vibration, 2001. **248**(5): p. 865-85.

[79] Ypma, A., A. Leshem, and R.P.W. Duin, *Blind separation of rotating machine sources:bilinear forms and convolutive mixtures.* Neurocomputing, 2002. **49**: p. 349-68.

[80] Servière, C. and P. Fabry, *Blind source separation of noisy harmonic signals for rotating machine diagnosis.* Journal of

Sound and Vibration, 2004. **272**(1-2): p. 317-339.

[81] Servière, C. and P. Fabry, *Principal component analysis and blind source separation of modulated sources for electro-mechanical systems diagnostic.* Mechanical Systems and Signal Processing, 2005. **19**(6): p. 1293-311.

[82] Antoni, J., *Blind separation of vibration components: Principles and demonstrations.* Mechanical Systems and Signal Processing, 2005. **19**(6): p. 1166-1180.

[83] Weiguo HUANG, Shuyou WU, Fangrang KONG, Qiang WU; " *Research on Blind Source Separation for Machine Vibrations";* Scientific research; Wireless Sensor Network, 2009, 1, 453-457

[84] A. Mahvash and Aouni A. Lakis; *A novel approach to evaluation of Vibration source separation based on spatial Distribution of sensors and fourier transforms*; Section of Applied Mechanics, Department of Mechanical Engineering, École Polytechnique de Montréal, Montréal H3T 1J4, Canada Thése Présentée En Vue De L'obtention Du Diplôme De Philosophiae Doctor, title: « Multi-Component Machine Monitoring And Fault Diagnosis Using Blind Source Separation And Advanced Vibration Analysis » 2011; p :13-30.

[85] Theodor D. Popescu; "*Blind separation of vibration components in machine monitoring"*; International Journal of Vehicle Noise and Vibration 2012; 8(1):14 - 26.

[86] Gardner, W., (1986). *Introduction to random processes with application to signals and systems*. New York: MacMillan.

[87] SKF @ptitude Analyst for SKF Microlog Analyzer User Manual; 2013 by SKF USA Inc.

[88] Group SKF; *" Rolling Bearings*"; General Catalogue, PUB BU/P1 10000/1 EN· February 2013

[89] W. Verhaert , G. de Wit, D. Reel; "*Advanced bearing Damage*"; SKF college; 2009.

[90] Miyachi T, Seki K. *"An investigation of the early detection of defects in ball bearings using vibration mnitoring — practical limit of detectability and growth speed of defects".* In: Proceedings of the International Conference on Rotordynamics, JSMEIFToMM, Tokyo, 14–17 September, 1986. p.403–8.

[91] Tandon N, Nakra BC. *"Detection of defects in rolling element bearings by vibration monitoring".* J Instn Engrs (India) — Mech Eng Div 1993;73:271–82.

[92] *The shock pulse method for determining the condition of antifriction bearings*, SPM Technical Information. Sweden: SPM Instruments AB.

[93] Martins LG, Gerges SNY. *" Comparison between signal analysis for detecting incipient bearing damage"*. In: Proceedings of the International Condition Monitoring Conference, Swansea, UK, 10–13 April, 1984. p.191–204.

[94] Stronach AF, Cudworth CJ, Johnston AB. *"Condition monitoring of rolling element bearings".* In: Proceedings of the International Condition Monitoring Conference, Swansea, UK, 10–13 April, 1984. p.162–77.

[95] Dyer D, Stewart RM. *"Detection of rolling element bearing damage by statistical vibration analysis".* Trans ASME, J Mech Design 1978;100(2):229–35.

[96] White MF. *"Simulation and analysis of machinery fault signals".* J Sound Vibr 1984;93:95–116.

[97] Mathew J, Alfredson RJ. *"The condition monitoring of rolling element bearings using vibration analysis".* Trans ASME, J Vibr, Acoust, Stress Reliab Design 1984;106:447–53.

[98] Kim PY. *"A review of rolling element bearing health monitoring (II): preliminary test results on current technologies. In: Proceedings of Machinery Vibration Monitoring and Analysis Meeting*", Vibration Institute, New Orleans, LA, 26–28 June, 1984. p.127–37.

[99] Gustafsson OG, Tallian T. Detection of damage in assembled rolling element bearings. ASLE Preprint 61-AM 3B-1. 16th ASLE, Philadelphia, PA, 1961. 39pp.

Chapter 3

Comparative study of rolling bearing vibration under oil bath lubrication and oil mist lubrication in centrifugal pumps

3 Comparative study of rolling Bearing vibration under oil bath lubrication and oil mist lubrication in centrifugal pumps

Abstract

The centrifugal pumps lubrication systems based on oil bath or oil circulation lubrication are the most diffused. However the use of oil mist lubrication has grown worldwide. In many petroleum industrial plants centrifugal pumps are retrofitting to pure oil mist in order to improve to lubrication quality so to increase bearing life. In the practice this improvement not happen for all the pumps retrofitted. This problem has been investigated with normal machine condition monitoring method with vibration analysis to ensure the evidences.

In this work, the performances of pure oil mist lubrication and conventional oil bath lubrication are been compared. This study is based on a petroleum industrial plants where pumps are been retrofitted from conventional oil bath lubrication to pure oil mist in order to improve the lubrication performance so to increase bearing life and reduce the oil consumption.

First an comparison of oil consumption has been done. We note that the consumption of oil mist lubrication system is higher about 24% than conventional oil sump lubrication system.

Second the comparative study has been done in terms of operating temperature, vibration level and spectrum analysis and oil analysis related to rolling bearings operating load and rotation speed for each pumps. We observe that the improvement of oil mist lubrication not happen for all the pumps and this is related to rolling bearing dimension, load and rotation speed.

In third to assess the oil mist lubrication reliability, set up a parameter, based on rolling bearing dimension, load and rotation speed. This parameter has been compared to SFK (different from SKF) industries applicability parameter.

3.1 Introduction

Rolling bearing operation is affected by friction, wear and lubrication mechanisms, fluid dynamics and lubricant rheology, material properties, and contact mechanics. Increased levels of vibrations due to surface degradation can be monitored by sensors. It's known that nearly 33% of rotating machine damages in process industries is due to the lubrication problems. To solve this problem or to reduce drastically its impact, several lubrication systems based on grease and oil exists. As far as concern oil lubrication, the systems based on oil bath or oil circulation lubrication are more diffused. However the use of oil mist lubrication has grown dramatically worldwide.

Oil-Mist is centralized lubrication system that continuously atomizes oil into small particles and then conveys and delivers the correct amount of the pressurized lubricant to the surfaces requiring lubrication. They proceeded cautiously, using "wet sump" or oil-mist purge techniques. The most common applications for oil mist lubrication in the Hydrocarbon Processing Industry (HPI) are pumps and motors [1]. The oil mist generator is the heart of the oil mist system. There are no moving parts in the oil mist generator; air is passed through a vortex or venture to atomize the oil into low micron-size particles, 1 to 3 micron [1, 2, 3]. The oil mist piping distribution system is the most important part of the entire package [1, 2, 3].

The applying of only pure mist oil can solve only part of rotating equipment lubrication problem across all industries. It had been necessary to develop both the methods of applying oil mist: dry sump or pure mist and wet sump or purge mist [2, 3, 4, 5]. The purge mist is similar to oil bath lubrication, in this application, oil mist acts only as a purge to prevent the intrusion of air borne contaminates and is not sufficient to provide prolonged lubrication, so it is necessary provide oil level.
A main different between oil bath lubrication and oil mist lubrication is the oil film thickness. The thin film causes an increasing of vibration levels on many machines. In what measure this increasing can be accepted?
The present study is based on a plants where pumps are been retrofitted from oil bath to pure oil mist. Comparison based on vibration levels and spectrum analyses between those

two kinds of lubrication is done in normal process industries. Connection between rolling bearing load and speed, and lubrication quality is fund out.

3.2 Review of oil mist lubrication application

Many articles, books, and conference papers describe application details and the overwhelmingly favorable experience with oil mist.
Oil Mist Lubrication (*OML*)technology was developed in Europe in 1938 for high speed spindles for the machining industry. Grease would not work and oil would cause the bearing to run too hot [6]. Oil mist has been lubricating rotating equipment in the HPI on a plant-wide basis since the late 1960s.

In 1987, H.P. Bloch, published "*Mist Lubrication Handbook",* which deal with several aspects link to oil mist application, in particular; description of oil system components and its function, lubricants for oil mist system and determination of the proper oil viscosity in function of the size, speed, and operating temperature of the bearing; calculation of oil mist flow for rolling bearing which depends on bearing type, and bearing preload factor. The author mentions that the applicability of oil mist is screened by using a rule of thumb from a formula quoted in literature issued by the MRC Bearing Division of SFK Industries: $K<10^9$. $K=DNP$, where D=bearing bore in mm, N= inner ring rpm, and P= load in pounds. If K does not exceed 10^9, oil mist is considered feasible [2]. In our study, we deal with rolling bearing vibration level variation under oil mist lubrication respect to oil bath lubrication. In effect, observing the prescription for a good oil mist lubrication [2], in some cases we observe a significant increase of the vibration levels in the envelope on the bearings. In our investigations we try to connect these change in addition to the parameters such that, the speed of rotation, diameter of the bearings, also to the load of the bearing.

In 1994, the tribological performance of *OML* (pure mist), as applied to rolling element bearings, was investigated by A. Shamim and C.F. Kettleborough. In the first part tests were conducted to compare the performances of oil mist and oil bath lubrication in terms

of operating temperature and friction with variation of load (0,56 kN ; 2,78 kN and 5 kN) and speed (1000 rpm, 1500 rpm, 2000 rpm). This test shows that oil mist lubricated bearing operate at lower temperatures (8 to10°C) and friction (20 to 25 percent). In the second part the two methods of lubrication were compared directly. Two extended comparative performance tests were conducted under endurance test conditions (18,9 kN thrust load and 2400 rpm), until one of the test bearings failed. An increase of 5°C above the normal operating temperature was use as failure criterion for the test bearings. And an increase of 50 percent of in the frictional load over the normal value was also taken as failure criterion for the test bearings. The operating temperature, frictional load and vibration of the tests bearings are been monitored throughout the duration of the experiment. The oil mist lubricated a high-precision angular contact test bearings ran cooler by about 10°C. Also the oil mist lubricated bearings had about 25 percent less friction. In both test, the oil sump lubrication failed earlier. The differences in temperature and friction between the two lubrication systems remained approximately constant throughout the tests until the happened the failure. In the third part, the endurance tests as defined above had studied to investigate the influence of oil mist lubrication on the life of rolling element bearings. Weibull and maximum likelihood analysis of endurance test data indicated that, in addition to savings in energy, oil mist lubrication provides better wear and fatigue protection to the test bearings compared to oil bath lubrication [7]. Differently, ours study concerned a normal petrochemical plant, where the machines bearings are monitored with the vibration criterion. In this plant we investigated the change in bearings vibration severity after the pumps have been retrofitted from conventional oil bath lubrication to pure oil mist. The bearing vibration severity became worse in some cases, even if new bearings were concerned. So we intend to assess the oil mist lubrication reliability, and set up a parameter based on rolling bearing dimension, bearing's load and rotation speed.

In 2001 Jeng, Y.-R., Gao, C.-C. made an investigation of the ball-bearing temperature rise under an oil-air [8]. Even if oil-air lubrications are based on the mixture of oil and air, is not perfectly equal to *OML* as described above. In oil-air lubrication, a quantity of oil metered volumetrically by a pump or distributor is pulled apart by a continuous air

flow in a tube and carried along the tube wall in the direction of compressed-air flow. The quantity of oil is fed into the air flow in pulses at a mixing point (mixing valve). A nearly continuous flow of oil is produced that leaves the outlet nozzle as fine drops and is fed to the rolling bearing without contact. In the investigation made, the operation parameters affecting the stability of the oil supply for an oil-air lubrication system were experimentally studied. A test rig for high-speed ball-bearings was also developed. Tests were conducted to study the effects of the preload, oil quantity, air flow rate and rotating speed on the bearing temperature rise. The operating conditions that provide a stable oil supply and low bearing temperature rise were established [8].

In 2002, K. Ramesh, S.H. Yeo, Z.W. Zhong, Akinori Yui, published their work on "Ultra-high-speed thermal behavior of a rolling element upon using oil–air lubrication". The total heat generation due to friction and gyro-induced torque were evaluated [9].
In the same 2002, they published "Ultra-high-speed grinding spindle characteristics upon using oil-air lubrication" [11].

In 2003, Douglas C. Branham, at 18th International Maintenance Conference presented in a document called "Improving Machinery Reliability with Oil Mist Technology" the results of oil mist application such 90% reduction in bearing failures when used in its pure form, 15 °C reduction in bearing temperatures. Oil mist reduces lubricant consumption by as much as 40% for once through systems. If a closed loop system is used, the oil consumption is reduced considerably [6]. However it hasn't been possible to find out the method used to evaluated the reduction of lubricants consumption. In our case of study, even if its conformed that oil mist reduces sensibility bearing temperatures in most case respect to oil bath lubrication, as far as concern oil consumption, the reduction are not confirm.

In 2008, H.P. Bloch, A. Shamim, published OIL MIST lubrication: Pratical Applications [37].

In 2011 Stanley I; Hans R. and Erwin V published they work on Comparison Between Oil-Mist and Oil-Jet Lubrication of High-Speed, Small-Bore, Angular-Contact Ball Bearings. They had conduced parametric tests with an optimized 35-mm-bore angular-contact ball bearing on a high-speed, high-temperature bearing tester Results from both oil mist lubrication and oil-jet lubrication systems used to lubricate the bearing were compared to speeds of 2.5×10^6 DN (rpm.mm). Lower bearing temperatures and higher power losses are obtained with oil-jet lubrication than with oil mist lubrication. Bearing power loss is a direct function of oil flow to the bearing and independent of oil delivery system [10].

Even if several articles have been written on oil mist lubrication application, very few of them are independent study. Our study deal with dynamic aspect which relate rolling bearing load, dimension and rotation speed in machine operating condition in an petrochemical plant.

3.3 Comparison of oil consumption between Oil Bath Lubrication (OBL) and Oil Mist Lubrication (OML) in the case studied

It interesting to compare the oil consumption of conventional oil sump lubrication and oil mist lubrication.

Oil Bath Lubrication

The simplest method of oil lubrication is the oil bath. The oil, which is picked up by the rotating components of the bearing, is distributed within the bearing and then flows back to a sump in the housing. Typically, the oil level should almost reach the center of the lowest rolling element when the bearing is stationary [36].

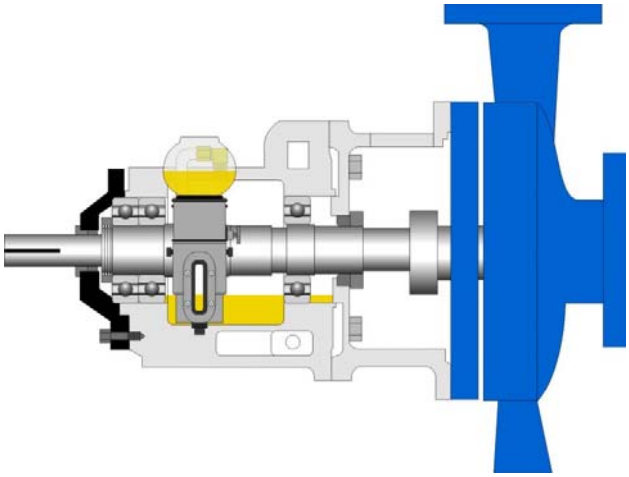

Figure 3.1: *Oil bath lubrication*

Oil mist lubrication

The figure illustrate pure oil mist lubrication and sump oil mist lubrication.

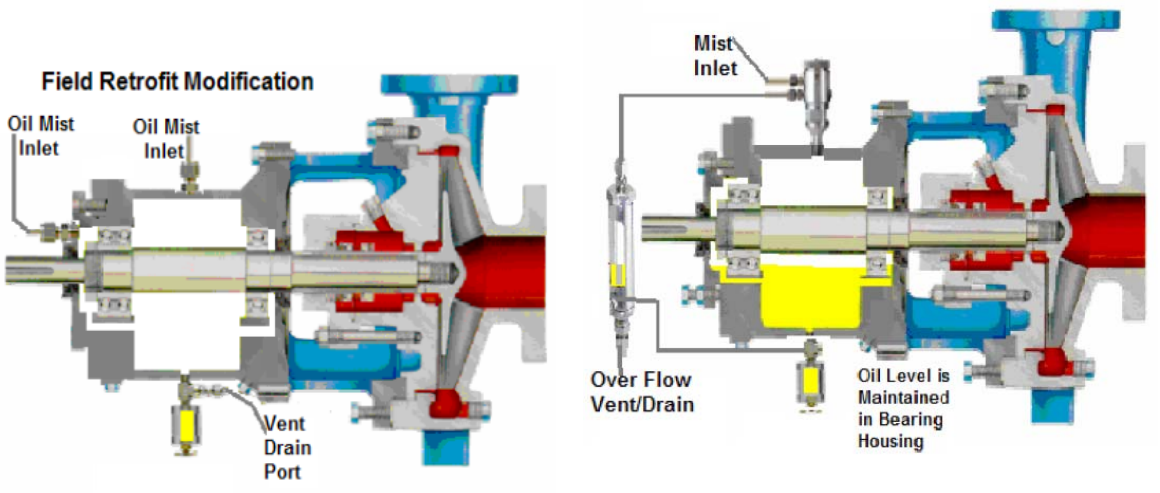

a) Application of pure oil mist *b) Application of purge mist.*

Figure 3.2: *Sample pure oil mist lubrication and Purge oil mist lubrication* [12].

In sump *OML* application, oil mist acts only as a purge to establish a positive pressure that prevent the intrusion of air borne contaminates. This extends oil change intervals [4]. It isn't required higher oil mist consumption respect to pure oil mist.

The number of machine retrofired is 41, in detail 4 turbines and 37 centrifugal pumps.

In detail 30 of them are retrofired to pure oil mist lubrication and 11 to sump oil mist lubrication.

a) *sump oil mist lubrication for turbine with film fluid bearing*

b) *sump oil mist lubrication for pumps rollers bearing*

***Figure 3.3** : Sump oil mist lubrication in the studied case plant*

The oil types used in the plant are mention is the table 1.

***Table 1:** lubrication oil type used*

Oil bath lubrication		**Oil mist Lubrication**	
Oil type	Number of Machine	Oil type	Number of machine
Mineral oil Iso 32 (Haydn 32)	31	Synthetic oil ISO 68 (Anderol 68)	41
Mineral oil ISO 46 (Haydn 46)	6		
Synthetic oil ISO 68 (Anderol 68)	4		

3.3.1 Calculation of oil consumed.

3.3.1.1 Conventional oil Bath lubrication

This lubrication method implies to change the oil used at less each semester in general. But some of the need frequent oil change to ensure good lubrication. In practice, the

support of the machine is emptied from the used oil, and the new oil is injected into the support with a manual pump connected to a graduated container. A first amount is injected with a certain pressure in order to clean it from any residual particles. This amount may vary from pump to pump and according to the size and evidence discovered. However, on average, it corresponds to half of a quantity of oil needed to restore the level of oil in the support for each type of pump. The total oil consumed can be calculated according the equation (1):

$$Q_{oil-sump} = \sum_{i=1}^{41} n_i \left(Q_i + \frac{1}{2} Q_i \right) = \frac{3}{2} \sum_{i=1}^{41} n_i Q_i \qquad \text{(Eq.3.1)}$$

Where:

$Q_{oil\text{-}sump}$: total annual oil consumed,

Q_i : oil quantity needed on the machine support to ensure good lubrication (o support capacity)

½ Q_i : amount of oil used to clean the support of the machine i from residues of particles

n_i : number of times oil change for considerate machine i, during one year

3.3.1.2 Oil Mist Lubrication

Fig.3.4 presents a schematic closed oil mist lubrication system layout. Minimum *cubic feet/minute* of mist to be fed to each bearing is specified by U.S. Motors as D (inches shaft diameter) x R (rows of balls)/20 using mist of approximately 0.4 to 0.65 cubic inches of oil/hour/standard cubic feet per minute (SCFM) of air flow [35]. The Standard cubic feet per minute (SCFM) is the volumetric flow rate of a gas corrected to "standardized" conditions of temperature and pressure thus representing a fixed number of moles of gas regardless of composition and actual flow conditions.

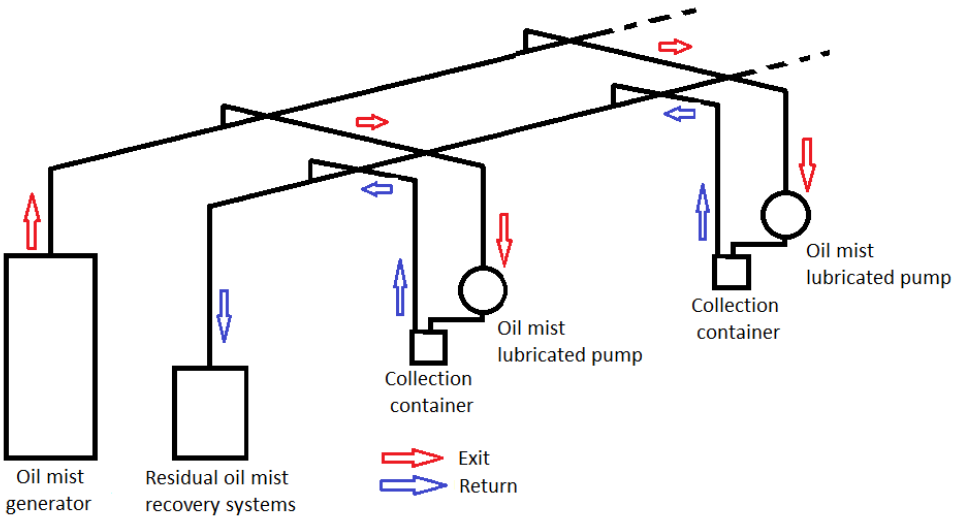

Figure 3.4: *Schematic closed Oil mist system layout. Sloped return headers lead back to the oil recovery units. Coalesced oil mist is collected in small containers at the edges of pump baseplates*

The mist value are converted to others international unities in the table 3.2.

Table 3.2*: Conversion in international unities*

cubic inches of oil/hour/ standard cubic feet per minute (SCFM) [in3/h /SCFM]	***international unities***
0.4	$166 \cdot \frac{air\ liters}{oil\ cm^3 hour}$
0.65	$269 \cdot \frac{air\ Liters}{oil\ cm^3 hour}$

In the present study the mist used is 0,65 cubic inches of oil/hour/ SCFM. That is $269 \cdot \frac{air\ Liters}{oil\ cm^3 hour}$.

Every month the graduated container of the oil mist generator is filled to the maximum level. The amount of integrated oil (q_i), which is also the monthly consumption of the generator unit, is measured as the difference between the maximum and the initial level.
A part of oil mist generated condenses in the piping distribution system and is being recovered through special container, and its monthly amount (r_i) is measured with graduate recipient. This oil has a physical and chemical good status to be recycled.
The oil mist lubrication system annual consumption ($Q_{oil\ -mist}$) is calculated according the equation (Eq.3.2)

$$Q_{oil\_mist} = \sum_{i=1}^{12} (q_i - r_i) \qquad \text{(Eq.3.2)}$$

$Q_{oil\ -mixt}$: amount of annual oil consumed of oil mist generator,

q_i : monthly amount of oil consumed of oil mist generator

r_i: monthly amount of oil mist condensed in the piping distribution system.

A part of the oil mist generated condenses in the supports of the machines and collected in container. Generally this oil is used. Its monthly amount (u_i) is measured with graduate recipient. The other part of oil mist generated is dispersed into the environment through leaks from the support of the machines and the bins. It's annual amount ($Q_{oil\text{-}dispersed}$) is calculated according to the equation (3).

$$Q_{oil\_dispersed} = \sum_{i=1}^{12} (q_i - r_i - u_i) \qquad \text{(Eq.3.3)}$$

3.3.1.3 Analysis of data

The amounts of lubrication oil consumption of both the method are compared in the Fig.3.5. The annual total oil consumed for the conventional oil sump system is 630 liters while that of OML systems is 781 liters, it's oil consumption is higher about 24%. This result is in contrast to a lot of articles and reports on oil mist lubrication [1, 6].

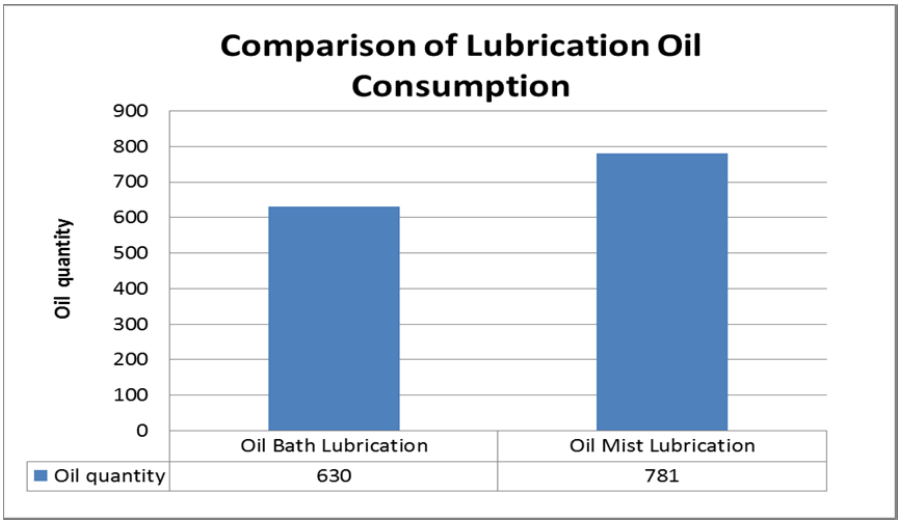

***Figure 3.5**: Comparison of oil consumption between the oil bath lubrication system and oil mist Lubrication systems.*

A critical aspect of oil mist lubrication systems is the dispersion into the environment of part of oil mist generated, about 46%. Fig.3.6 shows the repartition of the percentages of oil released into the environment, oil used and oil recycled. These percentage are calculated respect to annual quantity consumed by oil mist generator ($Q_{generator}$).

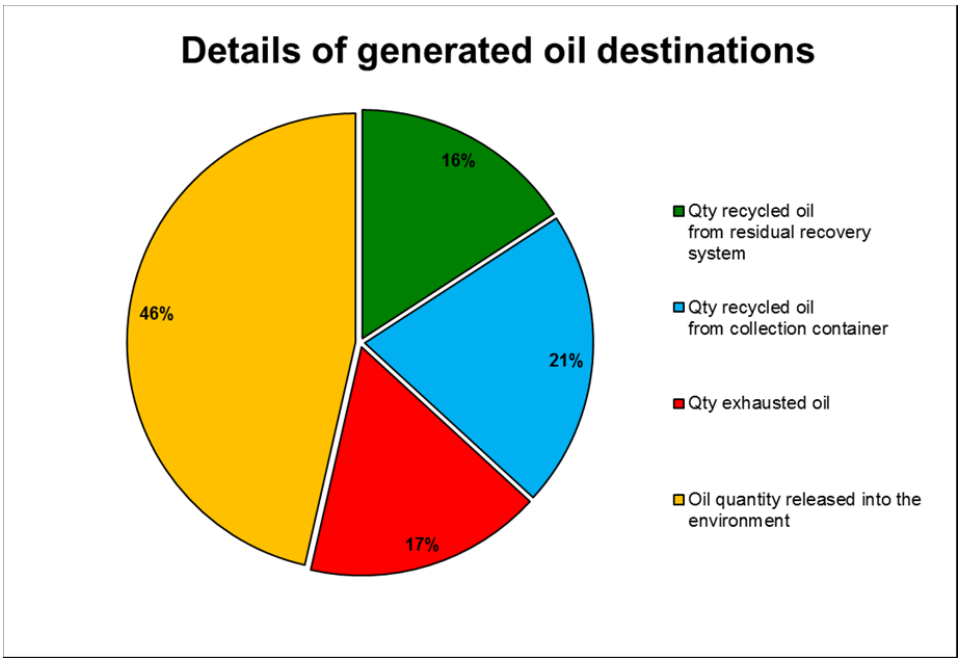

***Figure 3.6:** Destinations of the oil mist generated after the cycle of use.*

3.3.1.4 Synthesis and discussion

Retrofit the machine from conventional oil bath lubrication to oil mist lubrication system, have increased the plant oil consumption by 24%. Ensured that there are no accidental loss concerning the oil mist piping distribution system, this result is in contrast with what is reported in several publications [1; 2; 6; 7]. In over 46% of the oil mist generated is released in ambient. In the practice the dispersion into the environment of nearly 30% of oil mist generated is considered physiological. But in present case 46% is high and this may be due to pumps seal which are been design for oil bath lubrication.

It is important to make sure that this dispersion not introduces a risk to workers' health. Even if the industrial plant under study is not confined, the dispersion of 46% of oil mist generated in the environment need attention in the exposures of workers to oil mists [13;14]. An 8-h Time-Weighted-Average Occupational Exposure Limit (OEL-TWA) of 5mg/m^3 for oil mist is currently adopted by the US Occupational Safety and Health Administration, UK Health and Safety Executive, American Conference of Governmental Industrial Hygienists, and Taiwan government, with the exception of the Japan Society for Occupational Health adopting a lower exposure limit of 3 mg/m^3 [20]. 10 mg/m^3 for short term or 15-minute exposure [21].

3.4 Comparative study of rolling Bearing vibration under oil bath lubrication And oil mist lubrication in centrifugal pumps.

3.4.1 rolling bearings Lubrication

The lubrication of rolling bearings mainly serves one purpose: to avoid or at least reduce metal-to-metal contact between the rolling and sliding contact surfaces, i.e. to reduce friction and wear in the bearing. Conditions of elastohydrodynamic lubrication is the basic assumption behind bearing life calculations [8, 4, 9]. In the elastohydrodynamic lubrication regime, the oil film thickness is slightly higher than the combined surface roughness of the rolling elements and the raceways.

In the practice, the rolling bearings are not only subject to the elastohydrodynamic lubrication regime. In the industrial application the rolling bearings may operate under other lubrication regime such as boundary lubrication regime, mixed lubrication and especially the hydrodynamic lubrication which is actual the most diffused.
As the ratio between the oil film thickness and the combined surface roughness in the contact determines the lubrication mechanism, the vibration responses under the different lubrication regimes will be different.

3.4.1.1 Surface Roughness

Surface roughness is a significant source of vibration when its level is high compared with the lubricant film thickness generated between the rolling element raceway contacts (see Fig.3.7). Under this condition surface asperities can break through the lubricant film and interact with the opposing surface, resulting in metal-metal contact. The resulting vibration consists of a random sequence of small impulses which excite all the natural modes of the bearing and supporting structure. Surface roughness produces vibration predominantly at frequencies above sixty times the rotational speed of the bearing. Thus the high frequency part of the spectrum usually appears as a series of resonances [10].

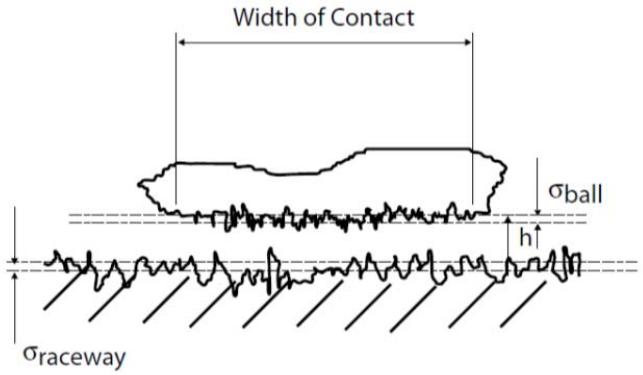

Figure 3.7: *Waviness and roughness of rolling surfaces. Figure redrawn from reference [1]*

A common parameter used to estimate the degree of asperity interaction is the lambda ratio (Λ). This is the ratio of lubricant film thickness to composite surface roughness and is given by the expression [28; 38; 39].

$$\Lambda = \frac{h}{\sqrt[2]{\sigma_b^2 + \sigma_r^2}} \qquad \text{(Eq.3.4)}$$

where Λ = degree of asperity interaction; h = the lubricant film thickness; σ_b = RMS roughness of the ball and σ_r = RMS roughness of the raceway.

3.4.1.2 Property changes and transitions in thin films

The change of the lubrication regime, involve the change in the lubricant thickness.

The properties of lubricant thin films change depending on their distance from the surface. When the thickness of the adsorbed film is comparable to the dimensions of the lubricant molecules themselves, the properties of the thin film is quite different than that of the bulk medium [22]. As shown in Fig.3.8, the effective viscosity, elasticity and relaxation time grows with diminishing thickness and diverges when the film thickness is sufficiently small. In this case, classical continuum considerations, which apply to the bulk phase, do not apply to thin films [22, 23].

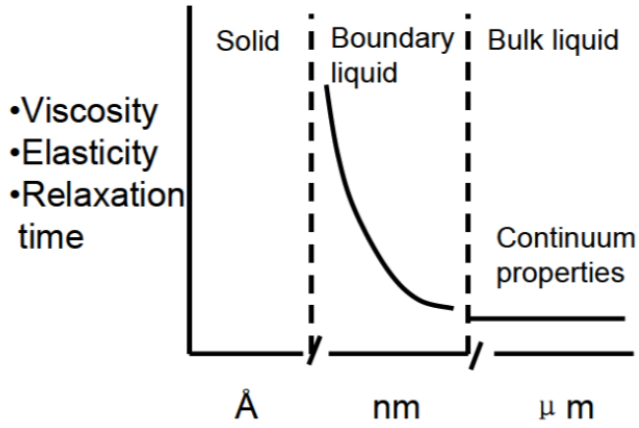

Figure 3.8: *Schematic diagram of how the effective viscosity, elasticity and relaxation change with thickness of a lubricant film. Figure redrawn from reference [13]*

3.4.1.3 Heat generation and Temperature

In rolling-contact bearings, at normal speed, the frictional heat generated at the ball-race contact can be given as follows [34]:

$$H_f = \omega_s M_s \qquad \text{(Eq.3.5)}$$

Where ω_s is the spin component and M_s the twisting moment required to cause slip. The bearing balls are an important heat flow path in the bearing and their conduction resistance has been extensively studied. Mizuta et al. [24] thoroughly studied the thermal conductance of the bearing balls and their effect on heat transfer. This study examined bearings rotating at speeds between 600 rpm and 4,000 rpm. They concluded that the bearing balls are the dominant heat carrier under an oil lubrication condition. Yovanovich in [25] and Bairi et al. in [26] concluded that bearing ball thermal resistance depends on axial force, bearing preload, thermal expansion effects, material properties, and contact patch area. Also important are boundary conditions on the bearing ball, such as lubricated, or in air, and whether or not the contact is considered to be perfect. A major assumption of Bairi et al. is that all the heat generated by frictional heating or a generalized heat flux is transferred out entirely by the bearing ball surface [26]. For any rolling element, the following heat-equilibrium situation can be applied:

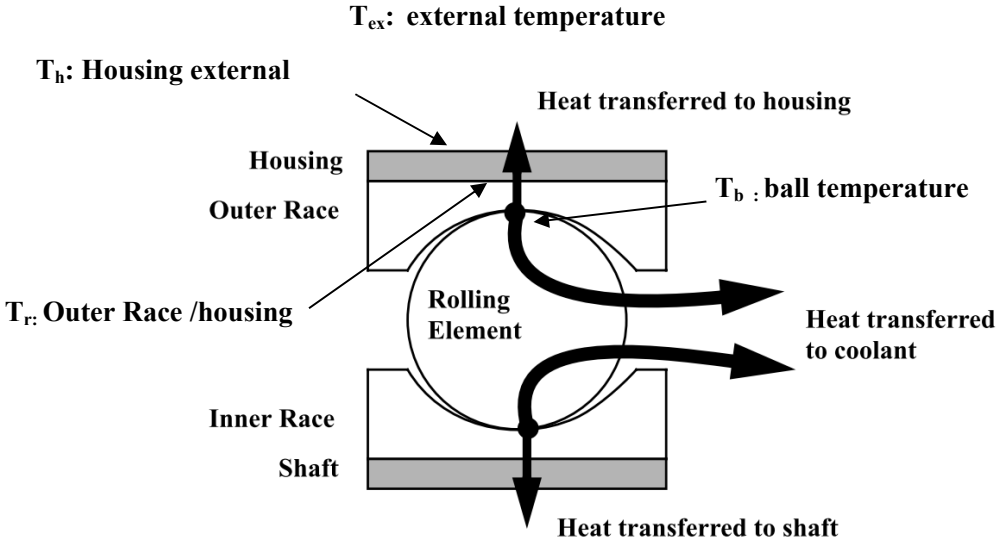

Figure 3.9: *Schematic of heat flow from rolling element/race contact to the external system.*

3.4.2 Generality of rolling bearing Vibration

3.4.2.1 Lubrication regimes and Vibration

Pure oil mist lubrication and conventional oil bath lubrication represent two different lubrication systems. The change of the lubrication systems, involve the change of lubrication regime, that means the change in the lubricant thickness. Pure oil mist lubrication is characterized by lubricant thin films and the conventional oil bath lubrication by the bulk medium. Fig.3.10 shows schematic representation of a Stribeck curve [22, 33] and its relation to lubrication regimes, vibration response.

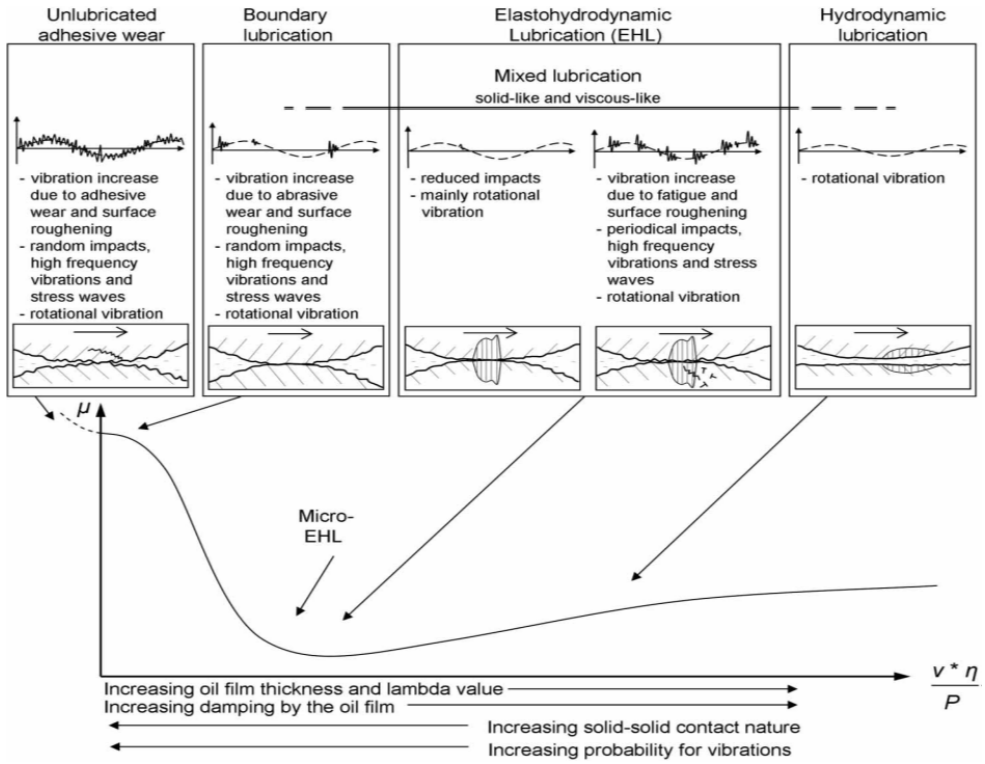

Figure 3.10*: Schematic representation of a Stribeck curve [22]and its relation to lubrication regimes, vibration response, and wear mechanism. Top: vibration response descriptions and schematics, in which the dashed line indicates rotational vibration (e.g. unbalance, bent shaft, and misalignment) and the solid line indicates transient vibration (e.g. impacts and stress waves).Middle: wear mechanism schematics. Bottom: Stribeck curve with coefficient of friction μ, velocity v, viscosity η, and load P.*

3.4.2.2 Generality of rolling bearing Vibration

Rolling contact bearings represents a complex vibration system whose components – i.e. rolling elements, inner raceway, outer raceway and cage – interact to generate complex vibration signatures. This argument has been fully dealt in the chapter 1. However it is useful to recall certain aspects. Although rolling bearings are manufactured using high precision machine tools and under strict cleanliness and quality controls, like any other manufactured part they will have degrees of imperfection and generate vibration as the surfaces interact through a combination of rolling and sliding [28]. A typical rolling element bearing can produce vibration from six primary types of dynamic forces:

irregularities of rolling surfaces; variations in stiffness; shock pulses when the lubrication layer is disrupted; friction forces; rotor self-oscillation forces; interactions with other components [29].

Due to the geometric restrictions in rolling bearings, different components have different rotational speeds and velocities. This is the main reason for excitations at different frequencies which are called “defect frequencies”. The vibration amplitudes at these frequencies are usually significantly higher than those at other frequencies when the component is defected.

3.4.2.3 Vibration related to lubrication problem

The vibration type links to lubrication problem is Shock Pulses when lubrication layer is disrupted. Surface roughness is a significant source of vibration when its level is high compared with the lubricant film thickness generated between the rolling element-raceway contacts. Under this condition surface asperities can break through the lubricant film and interact with the opposing surface, resulting in metal-to-metal contact. This produce the phenomena called shock pulses or squared noise [29, 30]. The resulting vibration consists of periodic or random shock pulses which excite two types of bearing element oscillations. Forced oscillations are excited by the leading front of the shock pulse. These are followed by damped natural oscillations. The impact at the leading edge of the shock pulse produces components across a wide range of frequencies. The second, damped oscillation appears in a narrow frequency band near the natural frequencies [29].

This problem products the cage noise.

3.4.3 Assessment of Rolling bearing lubrication condition based on values in envelope

Enveloping addresses the problem of isolating small but significant impulse perturbations. Applying to bearing monitoring these small impulse signals come from the accelerometer response to impulsive forces from bearing race defects, which indicate early signs of fatigue or insufficient lubrication. The early signs of fatigue of bearing

component can be identifying with his specific frequency in the spectrum as mention above.

In this study the interest is for the insufficient lubrication. The lubrication problem comes out from a type of vibration which are characterized by a typical envelope spectrum.

The bearing cage, mainly the metal cage, is the bearing component more sensible to lubrication problem. In fact, cages have wide contact surface with the balls. While the friction between the balls and the two rings are involute friction, that between the balls and the cage is the sliding friction. When the bearing with metal cages are stressed by lubrication problem, the cage makes a noise call "cage noise", which alerts the bad condition of lubrication (That are different from the cage defect).

Fig.3.11 shows an example of envelope vibration spectrum which is typical of insufficient lubrication problem. The insufficient lubrication generate some broad peaks in the low frequency range between 0 and 0,4 kHz approximately.

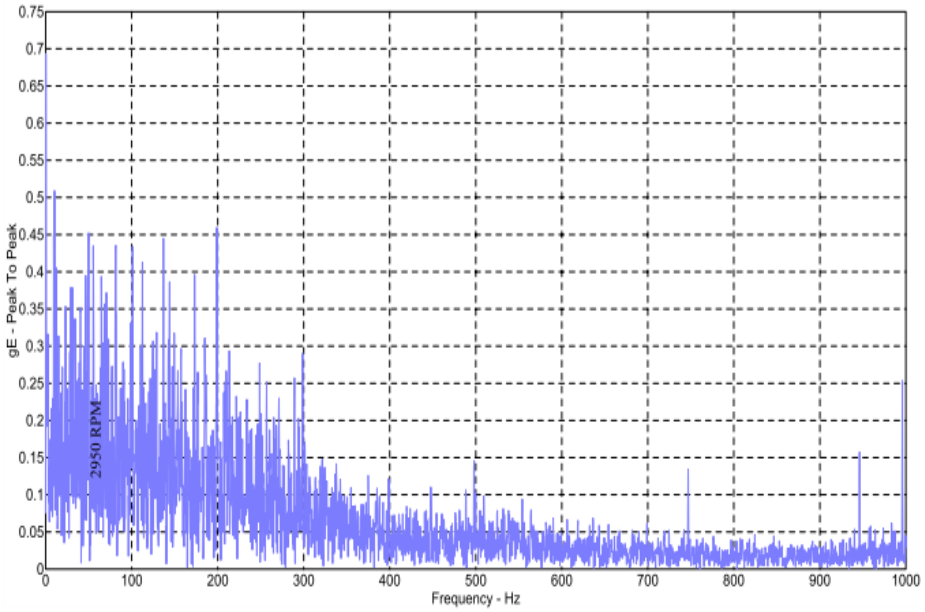

***Figure 3.11**: Typical vibration spectrum related to insufficient lubrication problem*

The lubrication problem comes out from envelope vibration spectrum analysis (and envelop values). If the bearings is not damages, a correction lubrication reports the spectrum in the normal condition. And it's important to note that this frequency range contains some natural frequencies of the bearings, the peaks can also report a bearing

preload for incorrect installation or excessive axial force, acting on the lubrication does not bring any change in the spectra.

The present study aim to made a comparison, between oil bath lubrication and pure oil mist lubrication in centrifugal pumps, basing on the vibration level measured in acceleration enveloping (gE) and the analysis of the relative spectrum.

3.5 Experimental Comparative study of rolling Bearing vibration under oil bath lubrication and oil mist lubrication

3.5.1 Experimental plant

This research work takes in count 27 centrifugal pumps. Our system is a part of real plants which include oil lubrication system: at first, conventional oil sump system, and then oil mist lubrication system. The instrumentation and data acquisition system is mobile: the vibration analyzer data collector is an SKF Microlog CMVA60, the accelerometer is SKF CMSS 793, the frequency of full scale is 1000 Hz, the envelope is obtained by means of the 3rd filter tool SKF Microlog CMVA60, the measurement is made in the shape of the envelope peak-to-peak.

The method of determining alarm settings is to trend vibration readings over time, establishing baseline values and alarm settings above baseline values.

3.5.1.1 Experimental variables

Three independents parameters are taken in consideration: bearing type, bearing load, and pump speed.

Bearing type

The machines involved in this study mount meanly two types of bearing as shown above in Fig.3.12:

- Single row deep groove ball bearings, with stamped metal cages,
- Single row angular contact ball bearings with massive brass cages. Bearing pairs arranged back-to-back.

Bearing load

We take into account the equivalent dynamic bearing load. It is defined as that hypothetical load, constant in magnitude and direction, acting radially on a radial bearing or axially and centrically on a thrust bearing which, if applied, would have the same influence on bearing life as the actual loads to which the bearing is subjected [ ]. This loads are get from the pumps design.

The study includes two types of pumps: overhung pumps and double-support pumps.

- For overhung pump we consider the thrust bearing support (Driver End). In this we consider that the deep groove bearing is not subject to heavy dynamic loads, as shown in Fig2.13-b in the next section.
- For double support pumps, we consider both the thrust bearing support; and deep groove bearing support which is mainly subjects to radial load.

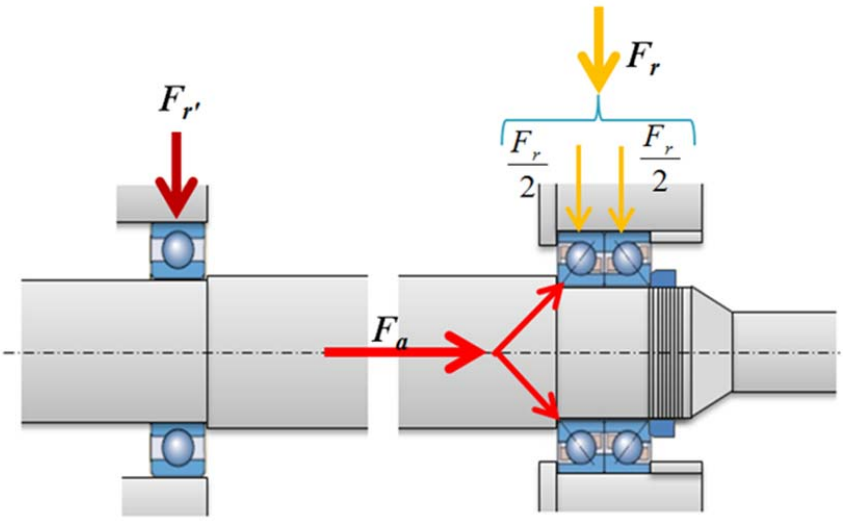

Figure 3.12: *schematic representation the loads on the pump bearings*

We interested in the equivalent dynamic on a single bearing P_u

Single row deep groove load

Assumption that : Fa'=0

$$P_u = F'_r \qquad \text{(Eq.3.6)}$$

Angular contact ball bearings

Angular contact ball bearings are mounted in pairs and arranged to back to back "O". Equivalent dynamic load on the bearing pair is given by normative ISO from the following expression (Eq.3.7):

$$P = 0{,}57F_r + 0{,}93F_a \text{ , when } \frac{F_a}{F_r} > 1{,}14 \qquad \text{(Eq.3.7)}$$

Where F_r is a radial load and F_a axial load.

The dynamic load is not equally distributed on the bearings pair, one bearing is more stressed than the other in particular with respect to the external axial load [SKF catalog]. In our study we are interested in evaluating the load on a single bearing, particularly the most loaded one. We make the assumption that the equivalent dynamic load on the most heavily loaded bearing *($P_{\,single\ bearing}$)* corresponds to the load on the bearing if it was mounted in singles.

Evaluation of the equivalent load on the most loaded single bearing N°1 :

$$P_{\,bearing\ pair} = 0{,}57\,F_r + 0{,}93F_a \qquad \text{(Eq.3.8)}$$

$$P_{\,bearing\ pair} = 2 \times 1{,}63 \times 0{,}35\,\frac{F_r}{2} + 1{,}63 \times 0{,}57F_a$$

$$P_{\,bearing\ pair} = 2 \times (1{,}63) \times 0{,}35\,\frac{F_r}{2} + 1{,}63 \times 0{,}57F_a$$

$$P_{\,bearing\ pair} = 1{,}63 \times \left(0{,}35\,\frac{F_r}{2} + 0{,}57F_a\right) + 0{,}285F_r$$

$$P_{\,bearing\ pair} = 1{,}63\,P_u + 0{,}285F_r$$

In the hypothesis $\frac{F_a}{F_r} \gg 1{,}14$

$$P_{\,bearing\ pair} \approx 1{,}63\,P_u \qquad \text{(Eq.3.9)}$$

Table 3.3 : *Synthesis bearing load*

Type of bearing	Assumption	Equivalent dynamic bearing load	Single bearing load
Single row deep groove ball bearings	*Load acts radially* $F_a \approx 0$	$P=F_r$	$P_u = F_r$
Single row angular contact ball bearings	$F_a/F_r >> 1{,}14$	$P = 0{,}57\ F_r + 0{,}93\ F_a$	$P_u = \frac{P}{1{,}63}$
Where : P = equivalent dynamic bearing load [kN], Fr = actual radial bearing load [kN] Fa = actual axial bearing load [kN]; Pu= equivalent dynamic single bearing load			

Pump speed

The pump speed *N* generally expressed in RPM. In this study, we take to a count a speed related to the bearing dimension which is defined according to the equation (Eq.3.10).

$$V = N \times D \qquad \text{(Eq.3.10)}$$

Where N is the pump speed [RPM], D the bearing bore diameter [mm]; V is expressed $[10^{-4}.\text{d.rpm}]$

3.5.1.2 Vibration data Acquisition and alarm thresholds setting

In this section a comparison based on vibration levels and spectrum analyses between those two kinds of lubrication is done in normal process industries. Other problems link to misalignment or unbalance have been excluded by previous analyses.

In fact each pump object of study is subjected to a testing procedure that allows to make an accurate determination on good initial condition of the machine. In particular must be satisfied the following considerations:

- New bearings mounted correctly,
- Exclusion of any problem link to misalignment , unbalance etc.…
- Exclusion of any process problem.

Therefore others significant problems are excluded, so that which can be observed is mainly due to pump normal process under a defined lubrication system.

Vibration acquisition

During each measurement round, in addition to the measures that allows to evaluate the condition of the pump bearings, also we acquired all the measurements on the machine train (motor + pump) in order to keep under control the whole set. The instrument (SKF Microlog GX60) and the acquisition procedures of vibration measurements are the same as those described in chapter 1.

The accelerometer was placed on the bearing house (pump support) in the horizontal direction, as shown in Fig. 3.13. The envelop filter selected from the SKF Condition Monitoring Microlog is the third filter HE3 (Frequency bands from 500-10.000 Hz).

Fig.3.13-a shows the envelop vibration acquisition points on a double support pump. These points are marked by blue circles (sensor). The blue color on both support means that we have taken into account both the acquisition in our study.

Fig.3.13-b shows the envelop vibration acquisition points on an overhung pump. The acquisition point on the thrust bearing support is marked by a blue circle while that on the radial bearing support is marked in orange. In the practice the dynamic load on the radial bearing in the overhung pump is not stressful, so the acquisition on the support radial bearing have not taken into account. In summary the acquisition points for our study are:

Type of pump	Number of pumps	Number of acquisition points
Double support pump	12	24
Overhung pump	15	15

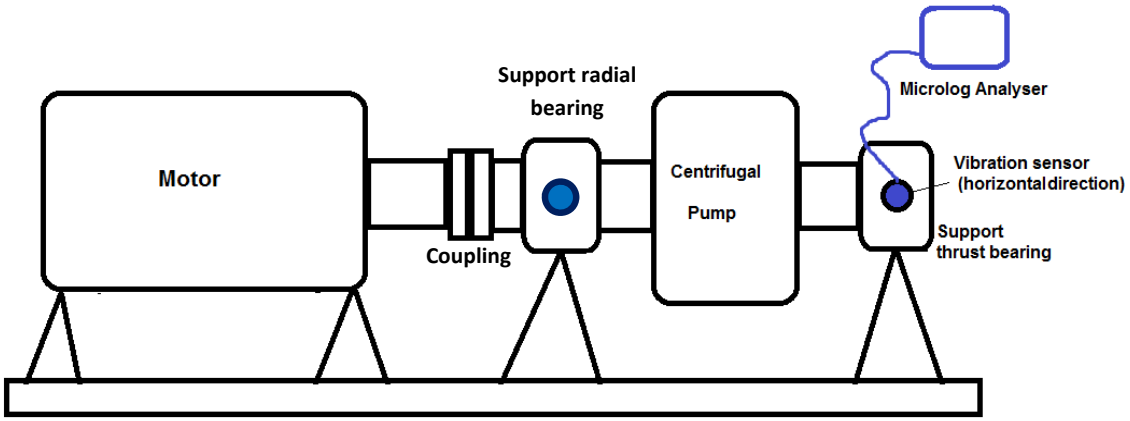

a) double support pump:
horizontal direction both on the thrust bearing support and on the radial bearing support

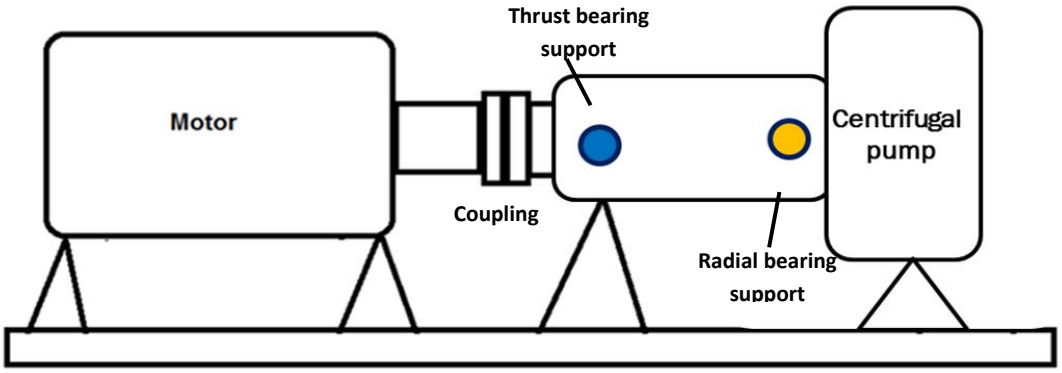

b) *overhung pump:*
horizontal direction both on the thrust bearing support and on the radial bearing support

Figure 3.13 *: Measurement points on the pumps*

Vibration alarm thresholds setting

- **Envelop vibration alarm thresholds under oil bath lubrication**

The vibration alarm thresholds have been set by the pumps historical vibration data. For each pump, from historical vibration data, vibration mean value *(ū)* and standard deviation **(σ)** are calculated. The machine possible conditions are the following:

- vibration overall value X_o least than $\bar{u} + 2\sigma$ ($X_o < \bar{u} + 2\sigma$) is considered to be good or satisfactory.
- vibration overall value between ū +2σ and $\bar{u} + 3\sigma$ ($\bar{u} + 2\sigma < X_o < \bar{u} + 3\sigma$) is considered to be unsatisfactory; therefore the machine is an alert condition.
- vibration overall value X_o more than $\bar{u} + 3\sigma$ ($X_o > \bar{u} + 3\sigma$) is considered to be unacceptable, the machine is in alarm condition.

- **Envelop vibration alarm thresholds under oil mist lubrication**

Envelop vibration alarm thresholds under oil mist lubrication have been set, basing on vibration mean value $(\bar{u})$ and standard deviation (σ) calculated for oil bath lubrication. However envelop vibration values may increase under Oil Mist lubrication. It is also necessary to known in which limit this increase be acceptable for the machine reliability. On the basis of similar cases, we assumed that this increasing is acceptable until *25%.* Consequently the machine possible conditions under Oil Mist lubrication are the following:

- The vibration value X_o, [for $Xo < 1{,}25\ (\bar{u} + 2\sigma)$] is considered to be good or satisfactory.
- The vibration value X_o, [for $1{,}25(\bar{u} + 2\sigma) < Xo < 1{,}25(\bar{u} + 3\sigma)$] is considered to be unsatisfactory; therefore the machine is an alert condition.
- The vibration value X_o, [for $Xo > 1{,}25\ (\bar{u} + 3\sigma)$] is considered to be unacceptable, the machine is in alarm condition.

3.5.1.3 Pump vibrations analysis and comparison

Vibration and bearing life data had been for 26 pumps of our plant. The first data acquisitions were made under OBL system (oil bath lubrication). For each pump, vibration severity and spectrum had been recovered for all the bearings life o until the planned maintenance (where the bearings are substituted by news ones). Later the same procedure was then made for each pump under OML system (oil mist lubrication).

Vibrations data (severity and spectrum) and the bearings 'life recovered under the two different lubrication system are been analysed and compared for each pump studied. The data related of the pumps are reported in the table 3.8.

The analysis of the 26 pumps allowed us to distinguish three different cases, and then to classify the pumps in 3 different categories:

- Case 1: the pumps retrofitted from OMB to OML show no change in both vibrations data and the bearing life.
- Case 2: the pumps retrofitted from OMB to OML show a slight increase in the vibrational level, but a significant increase in bearing life.
- Case 3: the pumps retrofitted from OMB to OML show a sharp increase in the vibrational level and a significant decrease in bearing service life.
- Case 4: very high increase of vibration of vibration level and immediate fault

Each one of the 4 cases will be illustrated in details by a specific example.

Case 1

The pump PS5 is a multistage centrifugal pump as shown in Fig.3.14. it have two bearing houses: the Support Radial Bearing (SRB) and the Support Thrust Bearing (STB)

It has been retrofitted from OBL to pure OML. That has not caused any increasing of vibration levels.

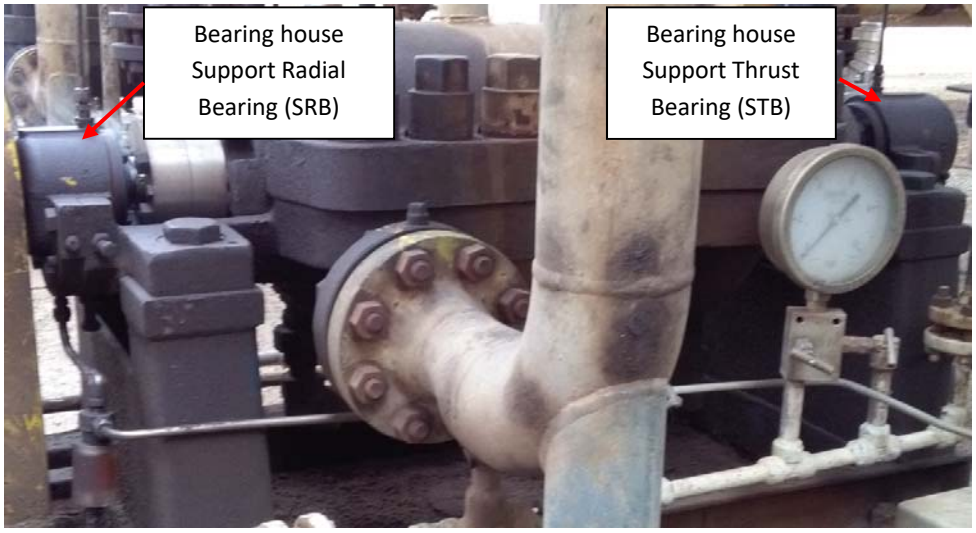

Figure 3.14 *: Multistage centrifugal pump PS5*

The vibration trend and waterfall are not shown any significant different in the two lubrication systems. The vibration spectrums analyses show the absence of lubrication problem in both the lubrication systems.

The Fig.3.15 shows the envelop vibration spectrum on STB under different lubrication systems. This support mounted two angular contact ball bearings (7405 BECBM), its equivalent dynamic load is 5,1 kN; so the single bearing load as defined above is P_u=3,13 kN. The Fig.3.15a shows the vibration spectrum under Oil bath lubrication and Fig.3.15b that under OML.

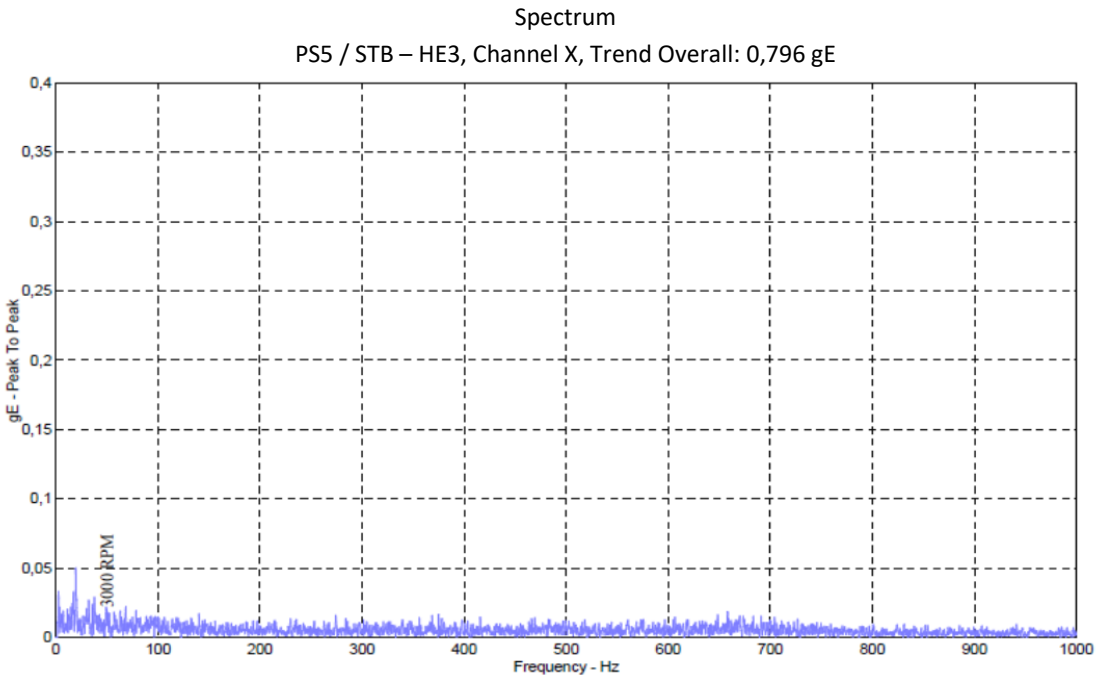

a)

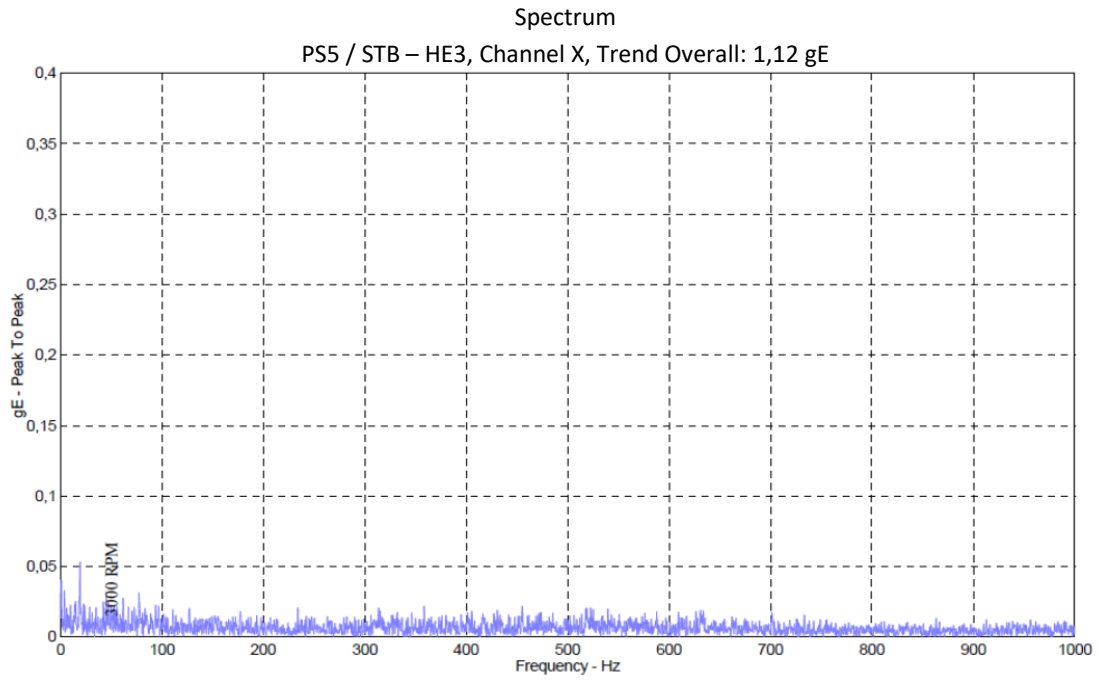

b)

Figure 3.15 : *Pump PS5- Envelop spectrum on the STB under different lubrication systems: a) under Oil bath lubrication and b) under Oil mist lubrication*

Both these vibration spectrums present a very low noise level (very normal condition in petrochemical application). In addition, they don't present any lubrication problem link to cage noise, they don't present any peak linked to bearing problem.
The vibration alarm thresholds are been setted from the pumps historical vibration data as reported in the table 3.4.

Table 3.4: *PS5- enveloped acceleration alarm.*

		PS5-STB vibration alarm based on historical data			
Storycal data under OBL		Alarm under OBL		Preset Alarm under OML	
Mean	**Std. Deviation**	gE unacceptable	gE unsatisfactory	gE unacceptable	gE unsatisfactory
$\bar{u}$	σ	$\bar{u}+3\sigma$	$\bar{u}+2\sigma$	$(\bar{u}+3\sigma)*1,25$	$(\bar{u}+2\sigma)*1,25$
0,91	0,22	1,57	1,35	1,96	1,69

The vibration spectrum overall value is 0,80 gE under oil bath lubrication and 1,12 gE under Oil Mist lubrication.

Fig.3.16 and Fig.3.17 show respectively the waterfalls and the vibration trends under the two different lubrication systems. It can be noted how Fig.3.16-a and Fig.3.16-b are similar. And how Fig.3.17-a and Fig.3.17-b are similar too. For both systems the vibration haven't been subject to significant change an operating time of 30000 hours.

Conclusion

Both with OBL and with OML, vibrational values remained normal and the bearings' life are more than 35,000 hours. During the period of the shutdown which occurs every four years, a general revision of the pump is carried out and all the bearings are substitutes by new ones.

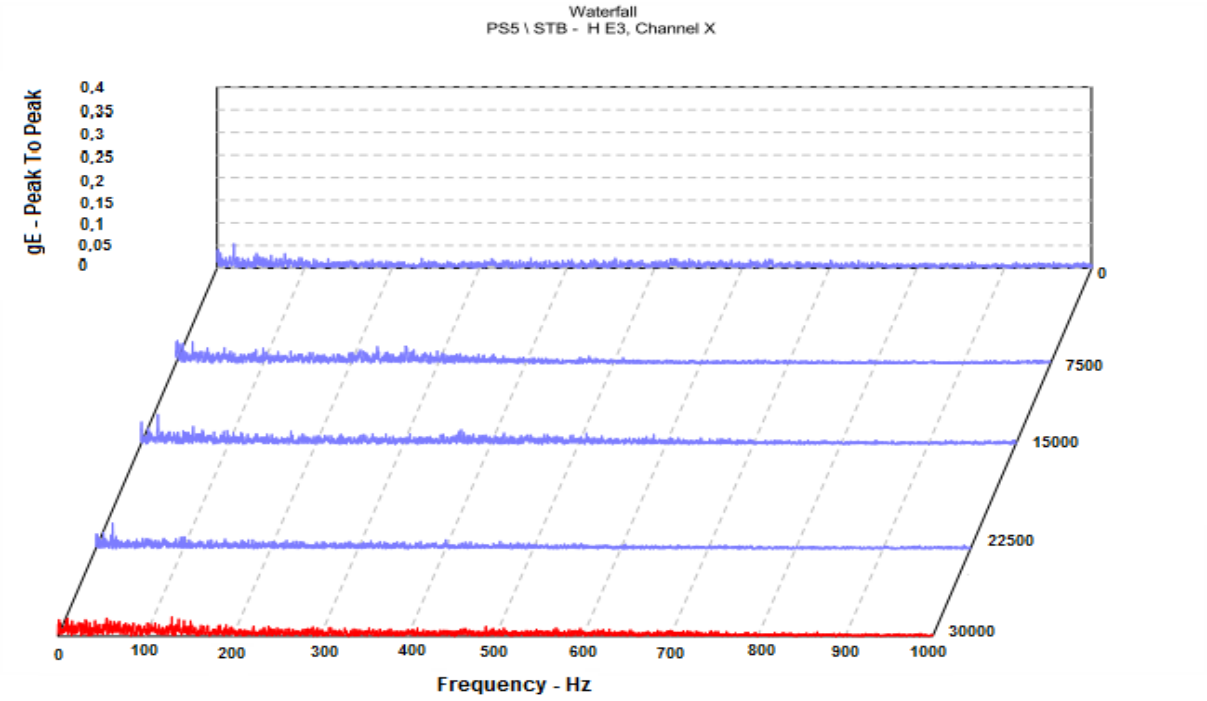

a)

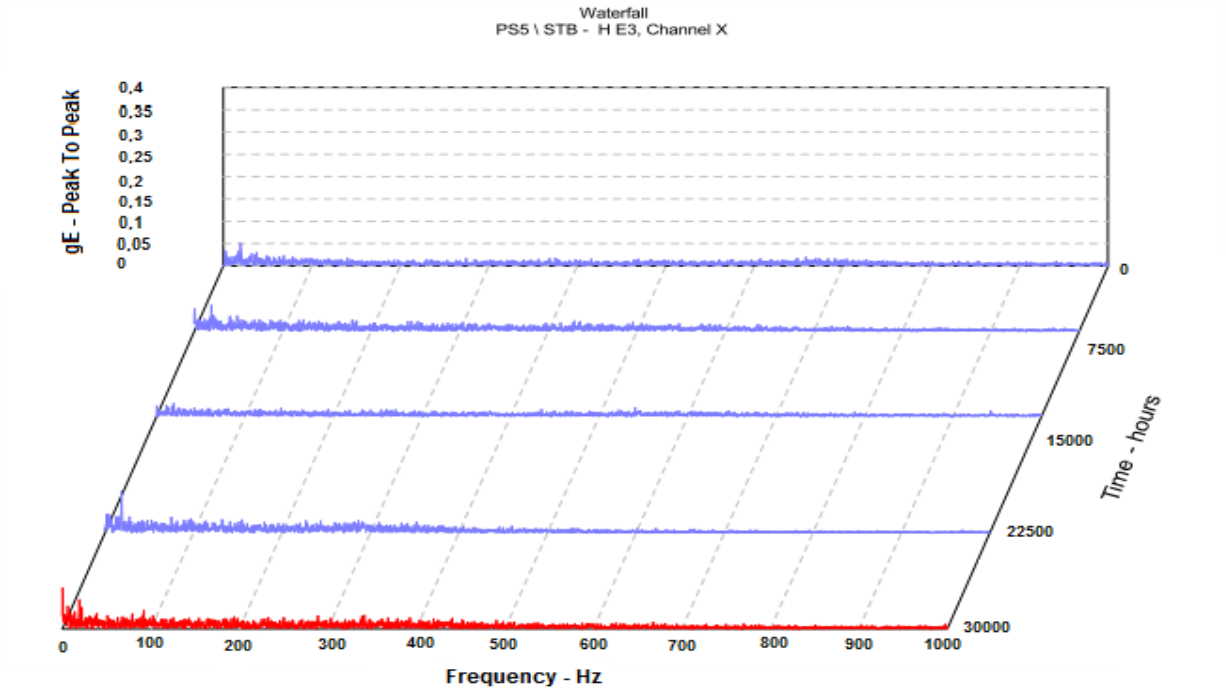

b)

Figure 3.16 : *Pump PS5- Envelop Waterfall on the STB under different lubrication systems: a) under Oil bath lubrication and b) under Oil mist lubrication*

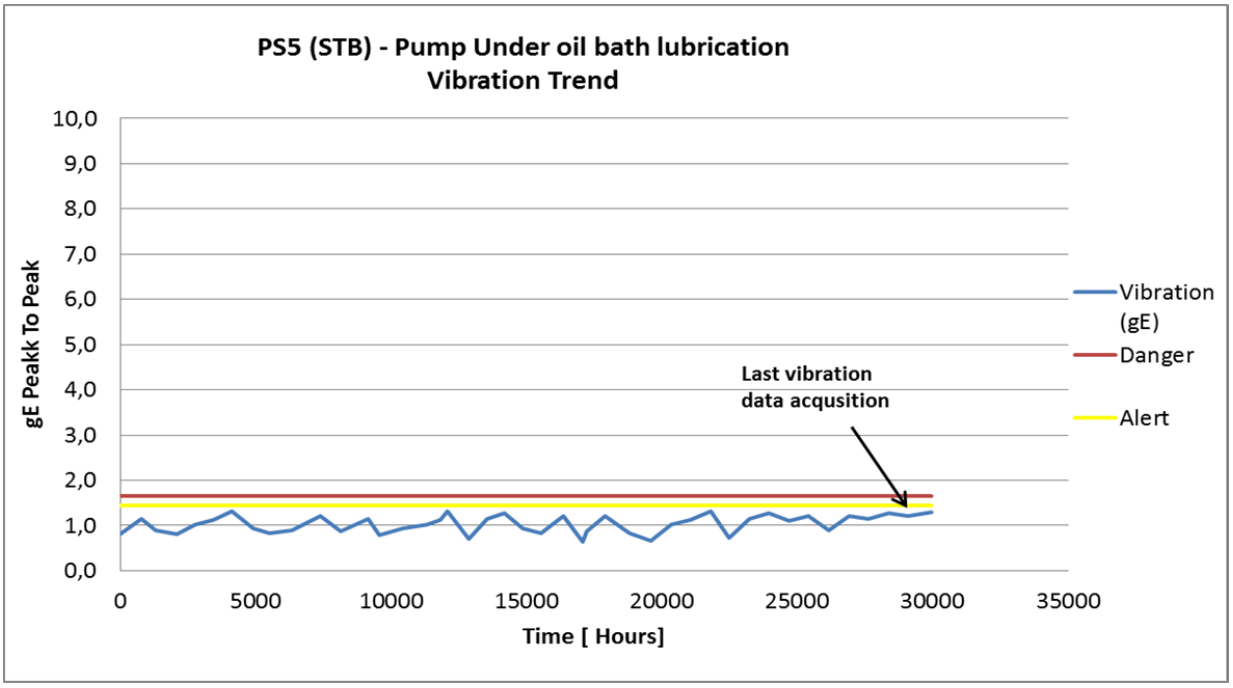

a)

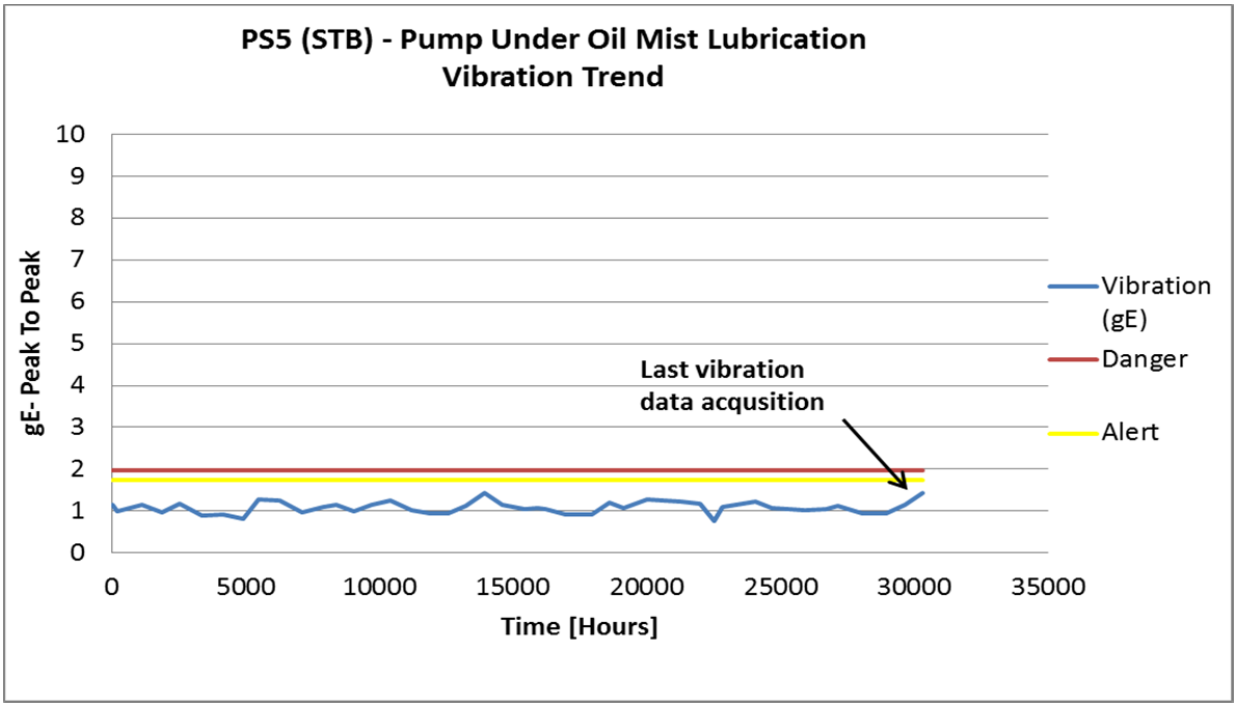

b)

Figure 3.17: *Pump PS5- Envelop vibration trend on the STB under different lubrication systems: a) under Oil bath lubrication and b) under Oil mist lubrication*

Case 2

The pump PS3 is an overhung centrifugal pump as shown in Fig.3.18. It has been retrofitted from oil bath to pure oil mist lubrication. That has not caused any increasing of vibration levels.

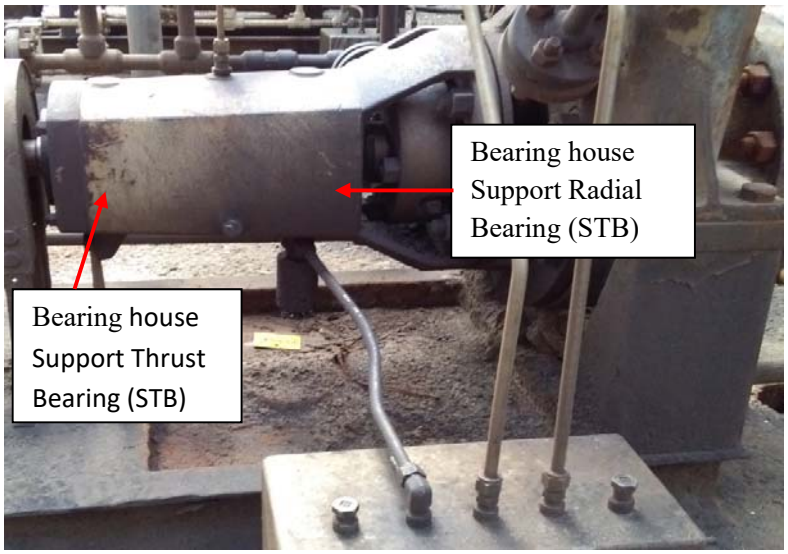

Figure 3.18: *Overhung centrifugal pump PS3*

The vibration trend and waterfall didn't show any significant different in the two lubrication systems. The vibration spectrums analyses show the absence of lubrication problem in both the lubrication systems.

Fig.3.18show the envelop vibration spectrum on STB of the pump PS3 under different lubrication systems. This support mounted two angular contact ball bearings (7311 BECBM), its equivalent dynamic load is 16,58 kN; so the single bearing load as defined above is P_u=10,17 kN. The Fig.3.19-a shows the vibration spectrums related to the first acquisition of new bearings under Oil bath lubrication and Fig.3.19-b that under Oil Mist lubrication.

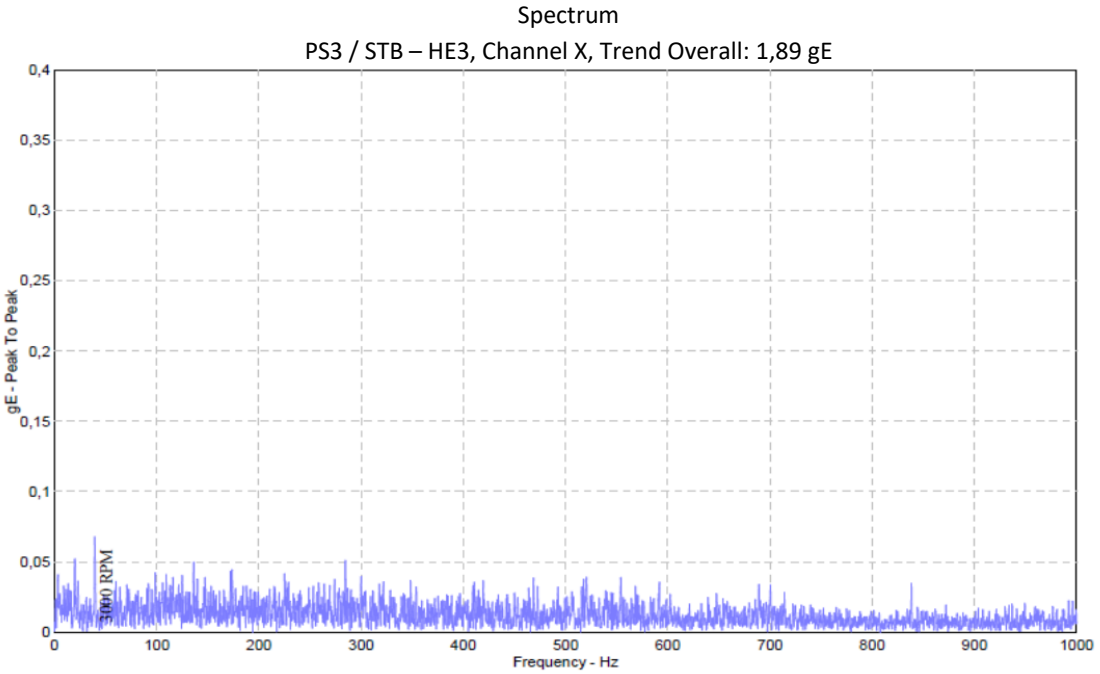

a)

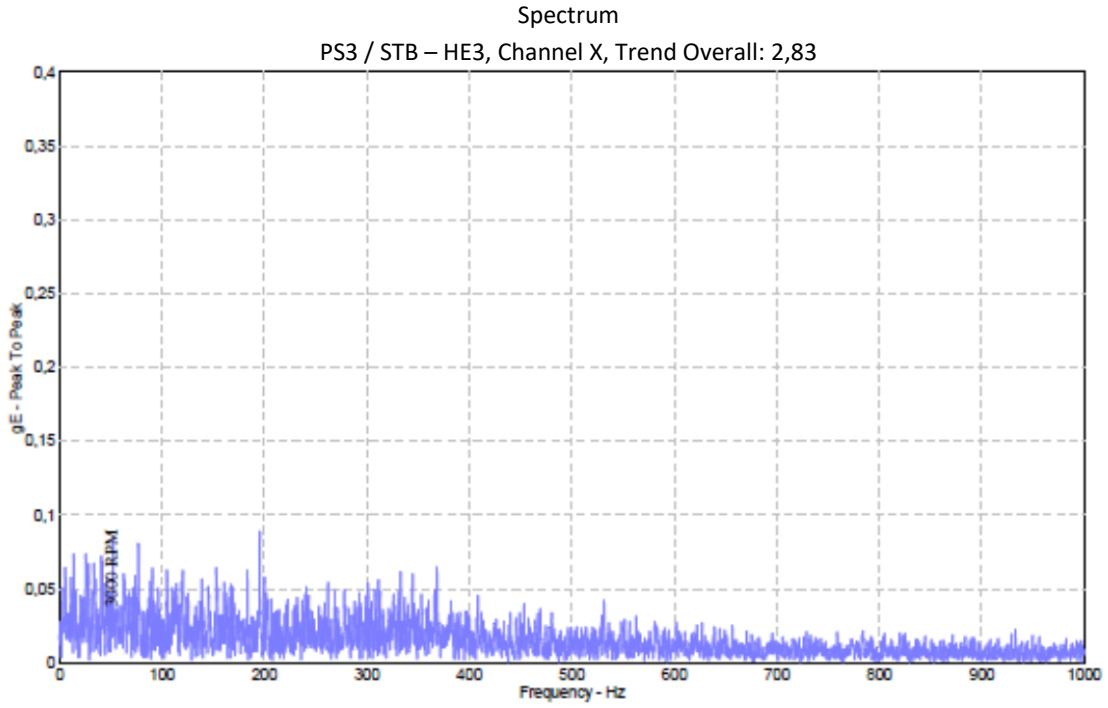

b)

Figure 3.19: *Pump PS5- Envelop spectrum on the STB under different lubrication systems: a) under Oil bath lubrication and b) under Oil mist lubrication*

Both these vibration spectrums present a normal noise level. The noise level under OML is slight higher than that under OBL. However none of them present any lubrication problem link to cage noise.

The vibration alarm thresholds are been stetted from the pumps historical vibration data, reported in the table 3.5.

Table 3.5: *PS3- enveloped acceleration alarm.*

		PS3-STB vibration alarm based on historical data			
Storycal data under OBL		Alarm under OBL		Preset Alarm under OML	
Mean	**Std. Deviation**	gE unacceptable	gE unsatisfactory	gE unacceptable	gE unsatisfactory
$\bar{u}$	σ	$\bar{u} +3\sigma$	$\bar{u} +2\sigma$	$(\bar{u} +3\sigma)*1,25$	$(\bar{u} +2\sigma)*1,25$
2,25	0,58	3,41	3,99	4,98	4,26

For new bearings, the vibration spectrum overall value is 1,89 gE under OBL and 2,83 gE under OML. In both of the case the machine operating condition is considered satisfactory because the vibrations overall values are less than their respective alert thresholds values.

Fig.3.19 shows that the bearings' life in the two cases are different. In Fig.3.19-a the bearing under OBL failures after 15.450 hours. While Fig.3.19-b shows that at the same operating conditions the bearing under OML reaches 23.880 hours without damage.

Conclusion

The vibration data (trend and waterfall) not shown any significant different in the two lubrication systems. But at the same operating conditions the bearings' life under OML is increased by 54%.

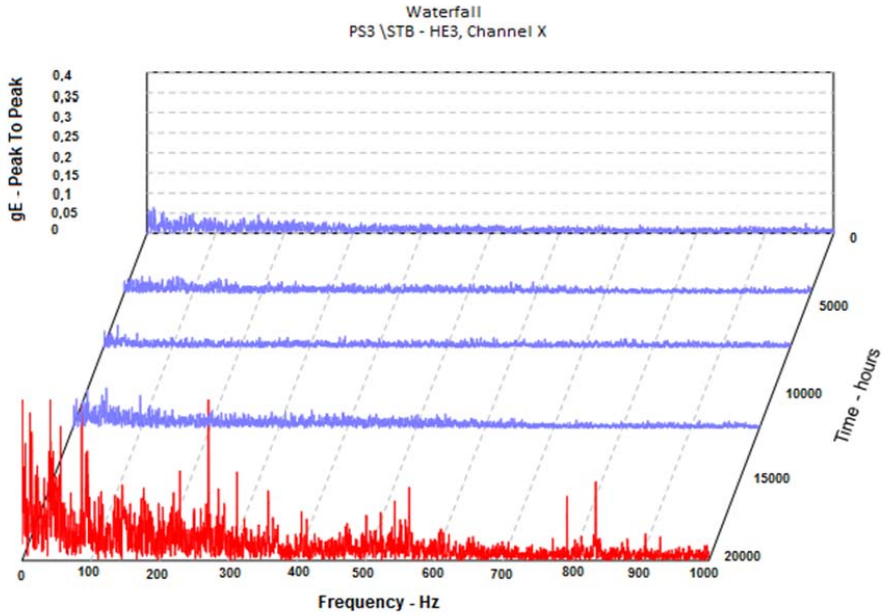

a)

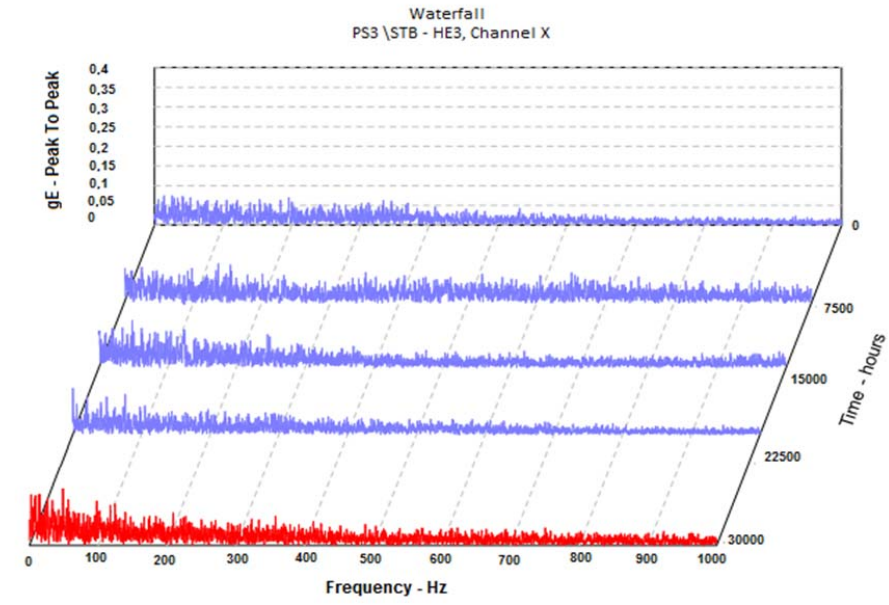

b)

Figure 3.20 : *Pump PS3- Envelop Waterfall on the STB under different lubrication systems: a) under Oil bath lubrication and b) under Oil mist lubrication*

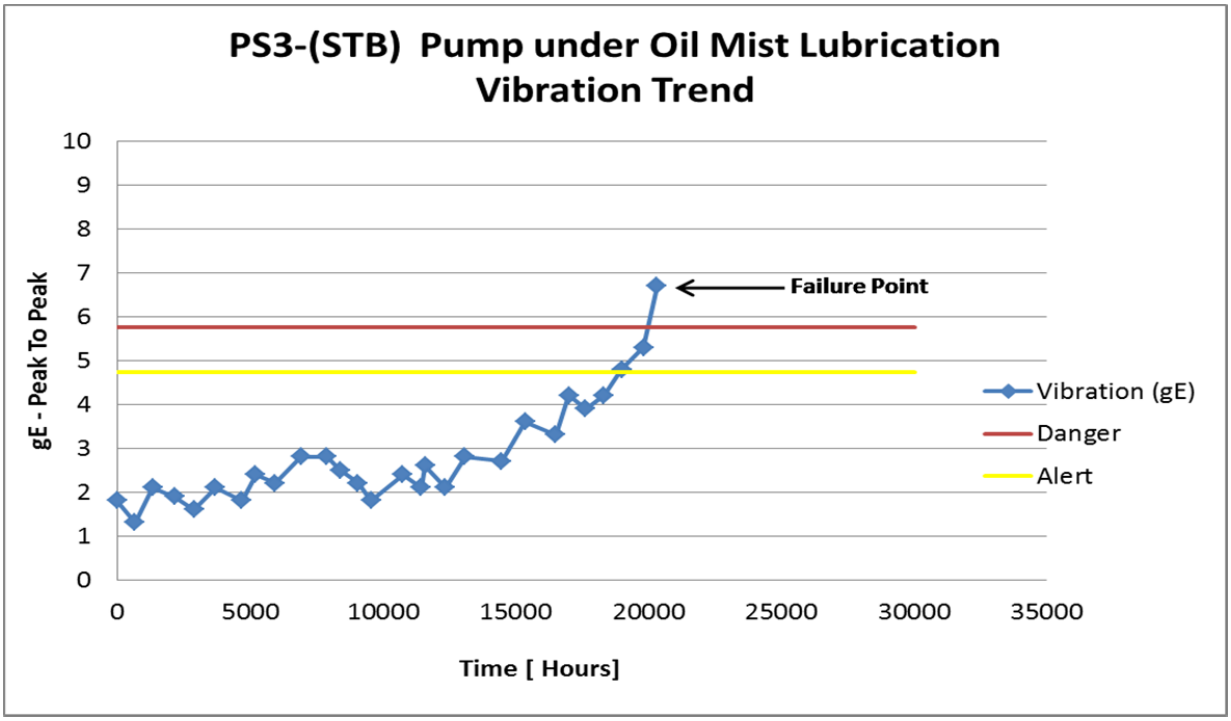

a)

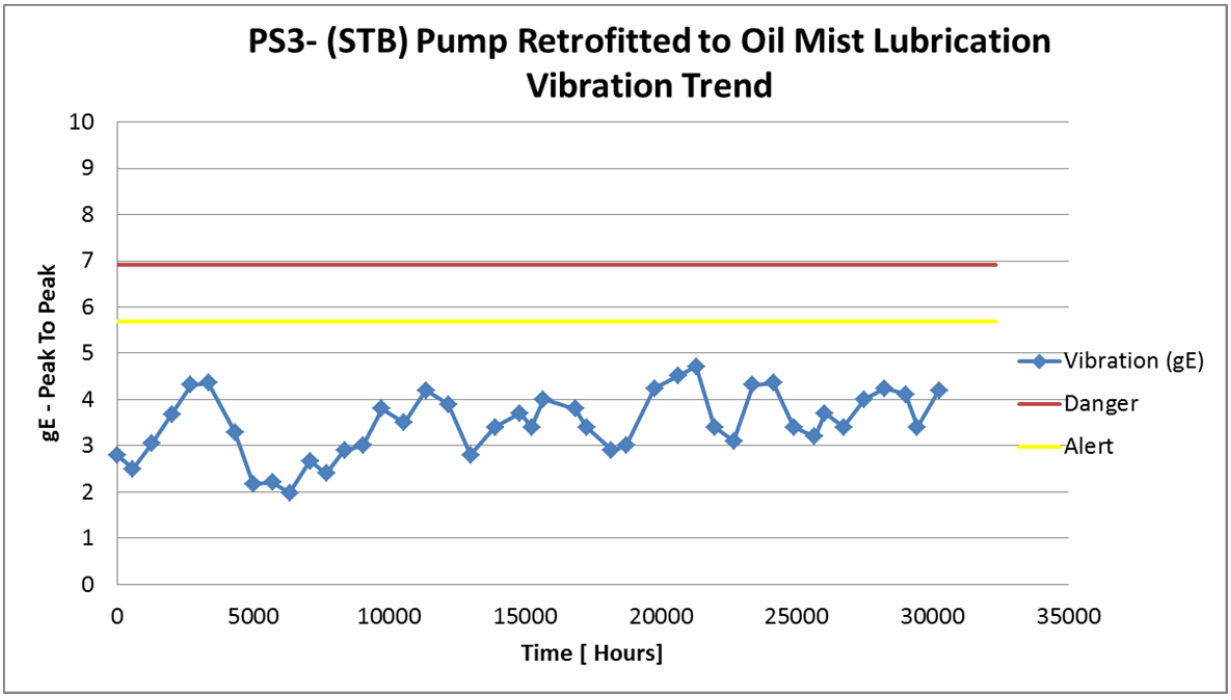

b)

Figure 3.21: *Pump PS3- Envelop vibration trend on the STB under different lubrication systems: a) under Oil bath lubrication and b) under Oil mist lubrication*

Case 3

The pump PS14 is a two stage centrifugal pump. Its drive end support, the Support Radial Bearing (SRB), is shown in Fig.3.22. This support mounted single row deep groove ball bearings (6317), its equivalent dynamic load is 27 kN; so the single bearing load as defined above is $P_u = 27$ kN.

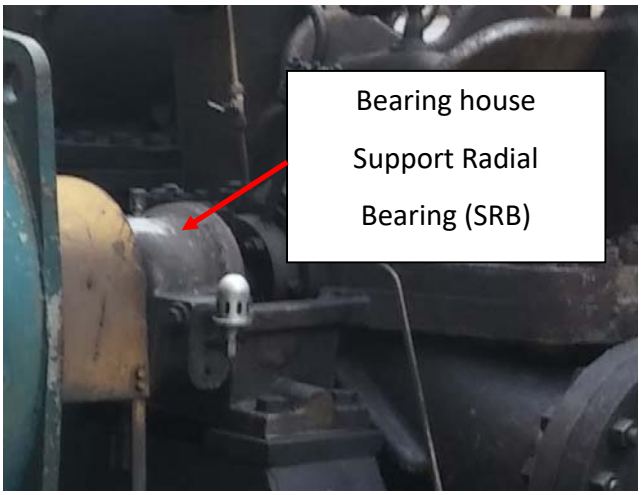

***Figure 3.22**: two stage centrifugal pump PS14*

The vibration alarm thresholds are been setted from the pumps historical vibration data, as reported in the table 3.6.

***Table 3.6:** PS14- enveloped acceleration alarm.*

		PS14-SRB vibration alarm based on historical data			
Storycal data under OBL		Alarm under OBL		Preset Alarm under OML	
Mean	**Std. Deviation**	gE unacceptable	gE unsatisfactory	gE unacceptable	gE unsatisfactory
$\bar{u}$	σ	$\bar{u} + 3\sigma$	$\bar{u} + 2\sigma$	$(\bar{u} + 3\sigma)*1,25$	$(\bar{u} + 2\sigma)*1,25$
3,45	0,58	5,19	4,61	6,48	5,76

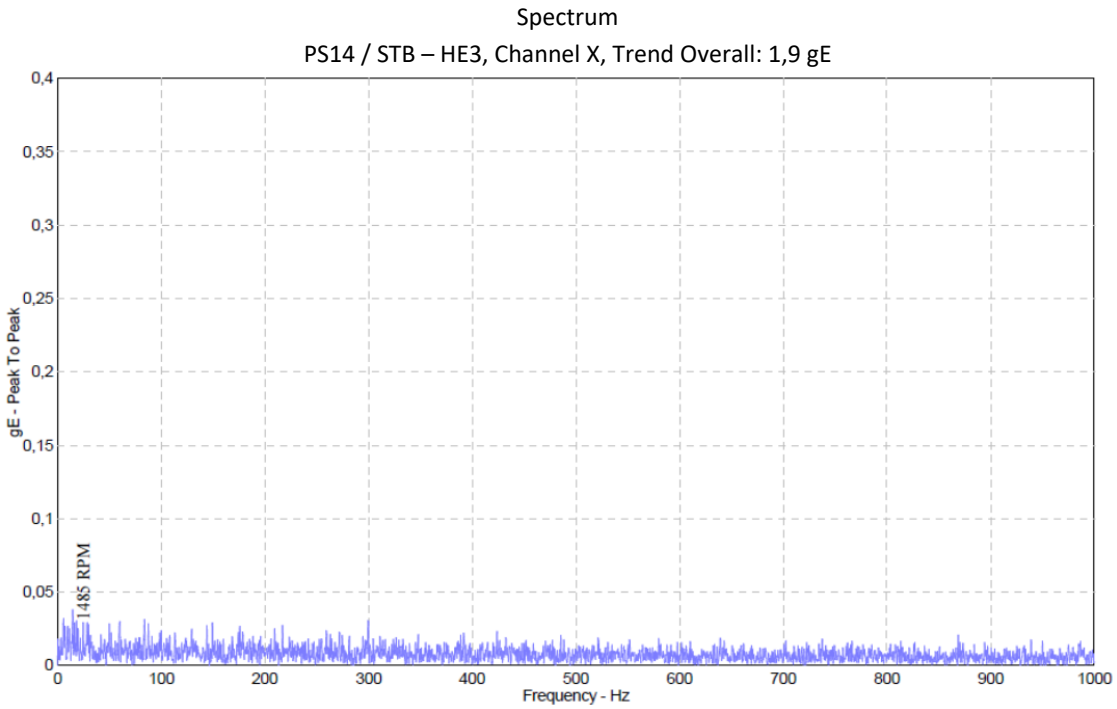

a)

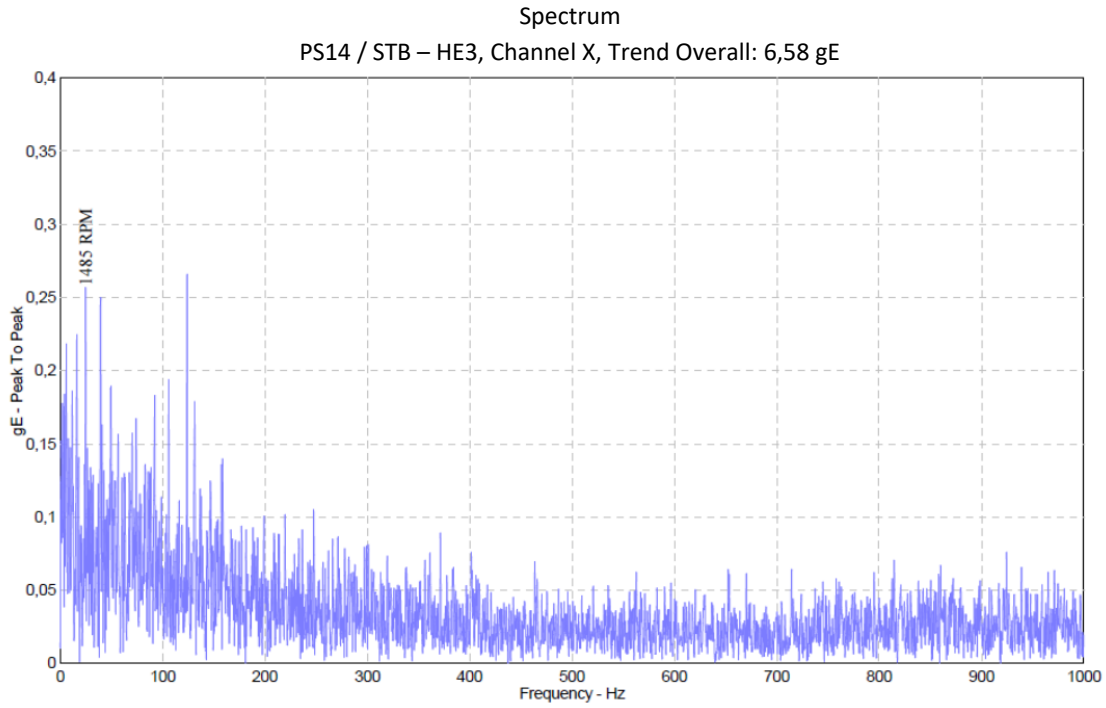

b)

Figure 3.23 : *Pump PS14- Envelop spectrum on the SRB under different lubrication systems: a) under Oil bath lubrication and b) under Oil mist lubrication*

Figure 3.23 shows the envelop vibration spectrum on SRB under different lubrication systems. For new bearings, in the first acquisition, the vibration spectrum overall value is 1,90 gE under OBL and 6,58 gE under OML.

From this figure we observe that despite of the pump operating condition has not changed, the retrofitting from OBL to pure OML has caused an increasing of vibration levels. The vibration spectrums under OBL in Fig. 3.23-a present a normal noise level, while the noise level under OML in Fig.3.23- b is very higher.

The waterfall comparison are made in Fig.3.24. The vibrational spectrum, in Fig.3.24-a, shows a basic noise level at the beginning of the bearing life. This noise grows slightly with normal bearing wear after long operation time up to reach unacceptable values on the occurrence of the break. In Fig.3.24- b, the vibrational spectrum shows strong noise from the beginning of new bearing life, persists over time and increases gradually until the bearing failure.

Even if the vibration increasing 25% has been considered normal under OML, in the present case the envelope overall values are increased over 100%. Envelope spectrums recorded from the new bearings shows deterioration to operation of the machine after the retrofitted pure oil mist lubrication. In fact the examination of the vibration spectrum exhibits a lubrication problem

Fig.3.24 shows that the bearings‘ life in the two cases has been different. In Fig.3.24-a the bearing under OBL failures after 17.330 hours, while Fig.3.24-b shows that at the same operating conditions the bearings’ life under OML decreases to 11.110 hours.

Conclusion

The vibration spectrum (and waterfall) show a significant different in the two lubrication systems. At the same operating conditions the bearings ‘life under OML is decreased by 38%.

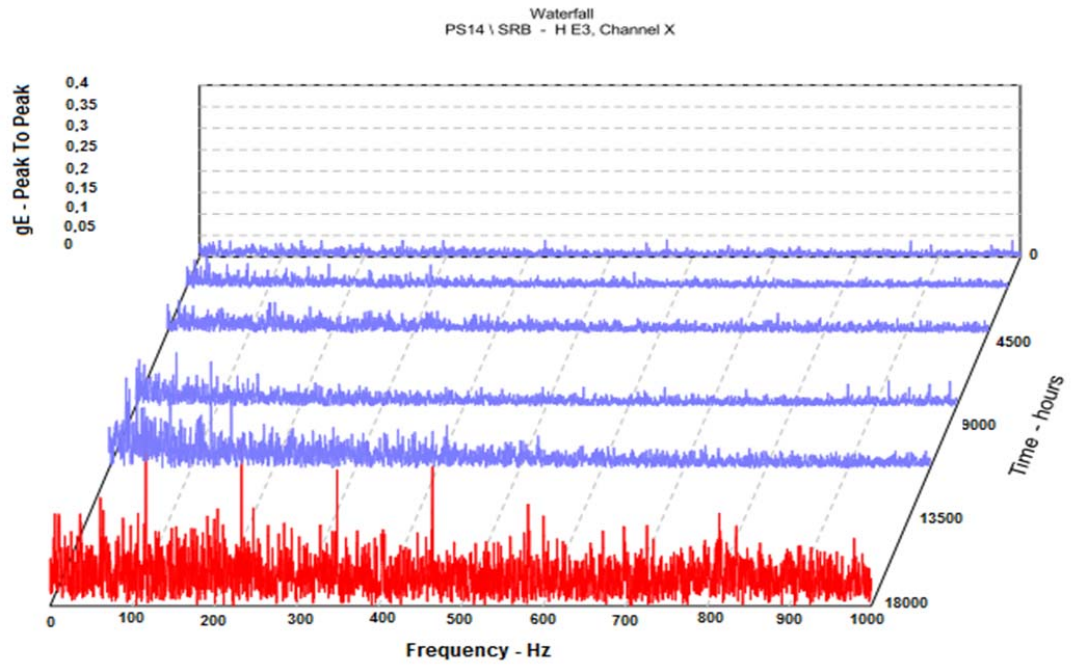

a)

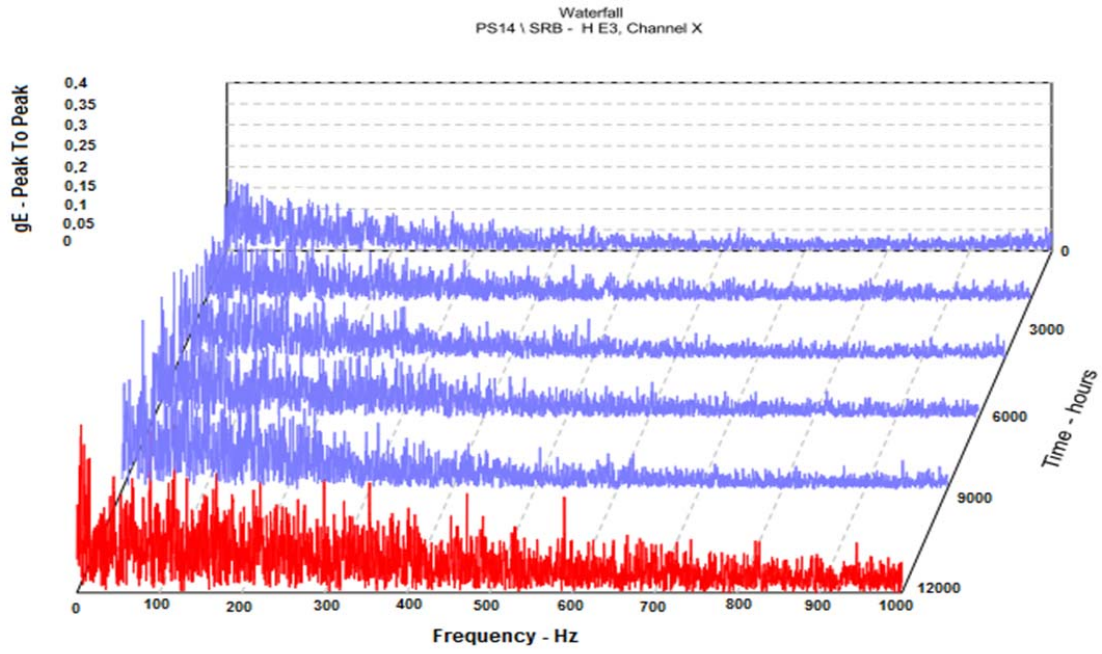

b)

Figure 3.24: *Pump PS14- Envelop Waterfall on the SRB under different lubrication systems: a) under Oil bath lubrication and b) under Oil mist lubrication*

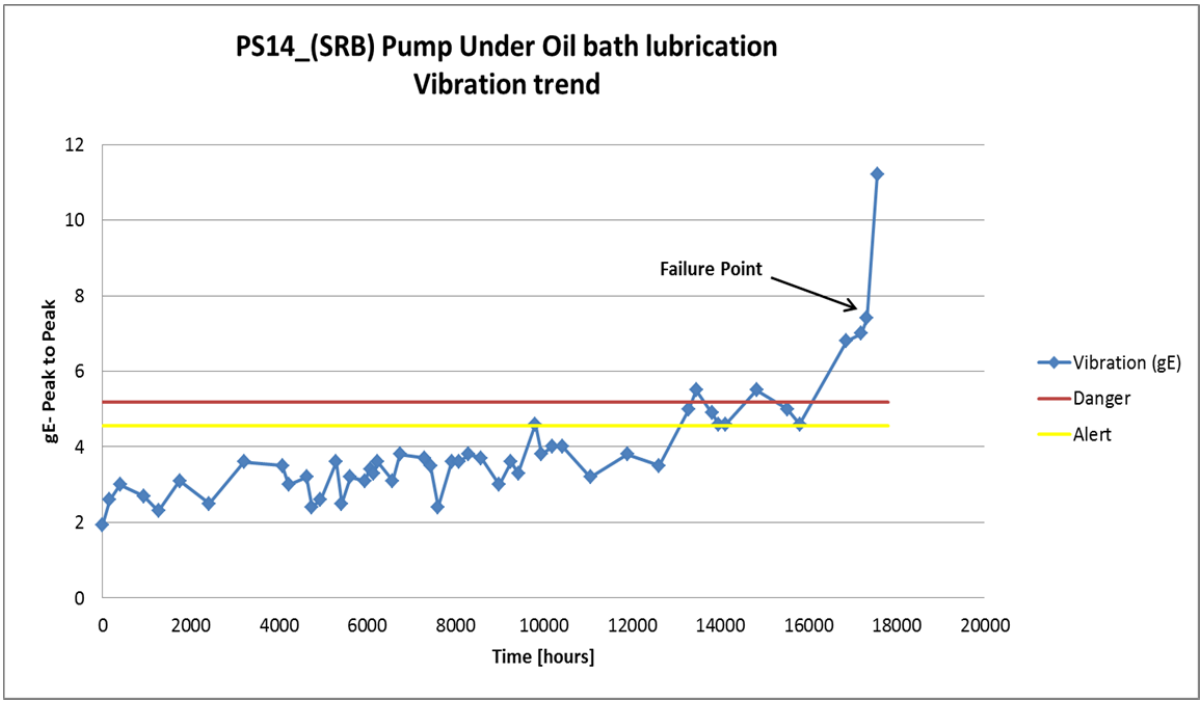

a)

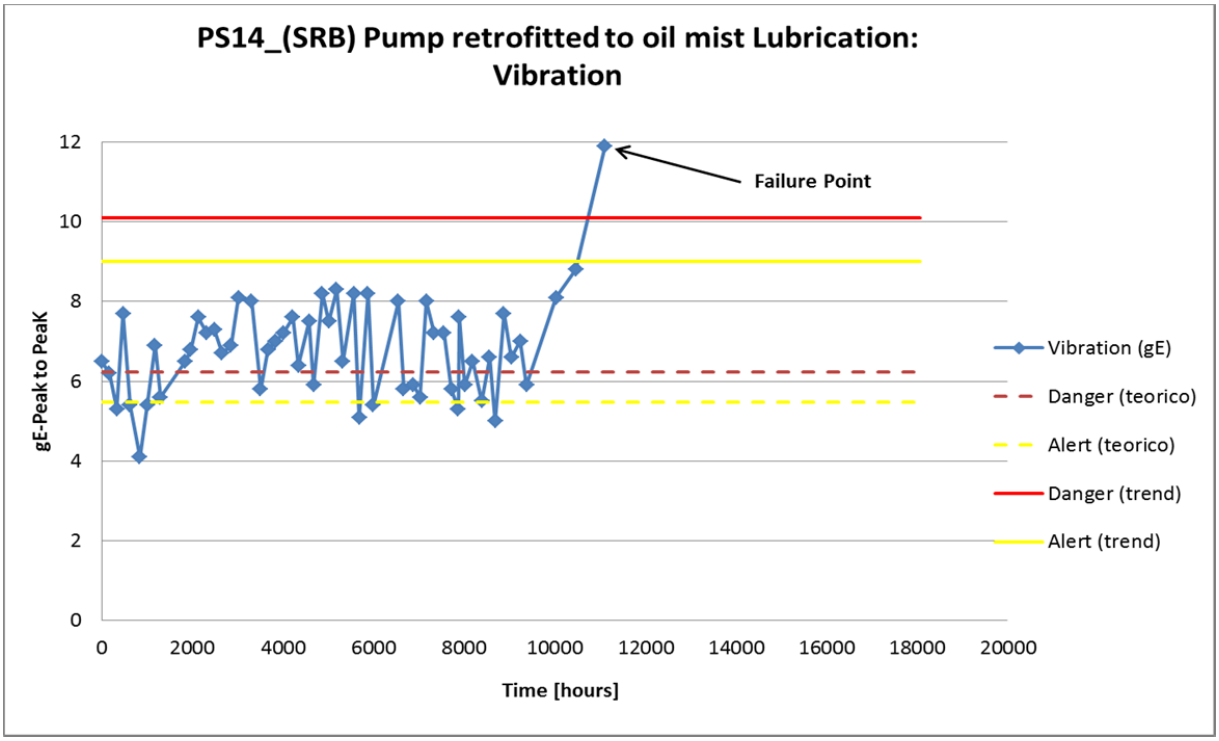

b)

***Figure 3.25**: Pump PS14- trend of Envelop global value on the SRB under different lubrication systems: a) under Oil bath lubrication and b) under Oil mist lubrication*

Case 4

The pump PS27 is a two stage centrifugal pump. The SRB is shown in the figure. This support mounted Self-aligning ball bearings (2317), its equivalent dynamic load is 40 kN. For this bearing the load acts radially. Its value of P_u *is* calculated *as a* "Single row deep groove ball bearings" which is defined above, so $P_u = 40$ kN.

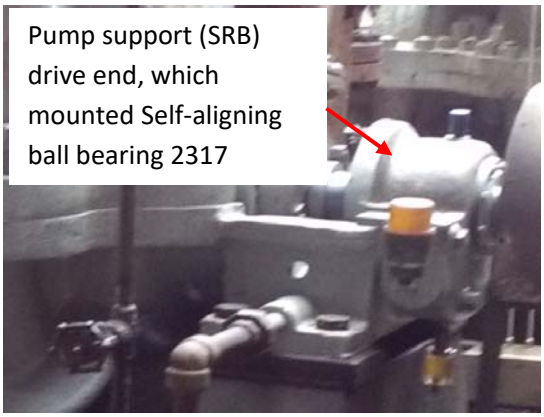

Figure 3.26: *Two stage centrifugal pump PS27*

Fig.3.27 shows the envelop vibration spectrum on PS27-SRB under different lubrication systems. For new bearings, in the first acquisition, the vibration spectrum overall value is 2,51 gE under OBL. After 48 hours working it had been retrofitted to OML. The vibration overall value increase suddenly to 14,15 gE and After 24 hours the bearing failure as show in Fig.3.27-b. In addition to a considerable increasing of the cage noise, it also highlights the presence of damage peak on the outer ring of the bearing.

Conclusion

The bearing failure after working only 24 hours. This confirm that the OML is not feasible in this case.

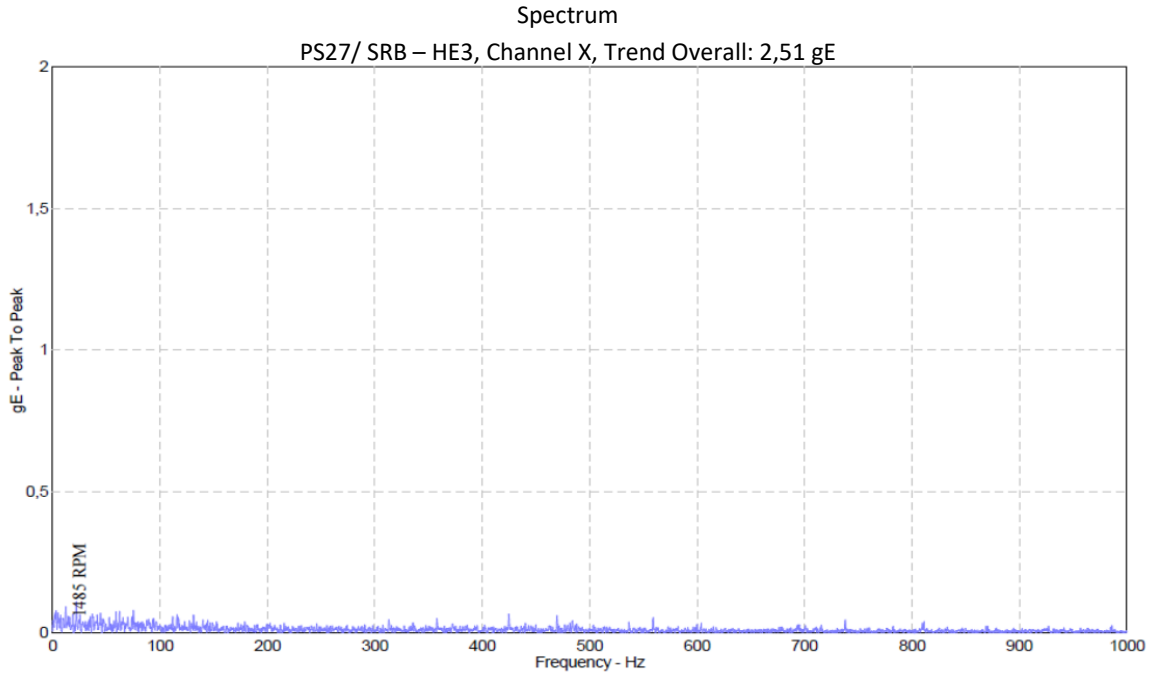

a)

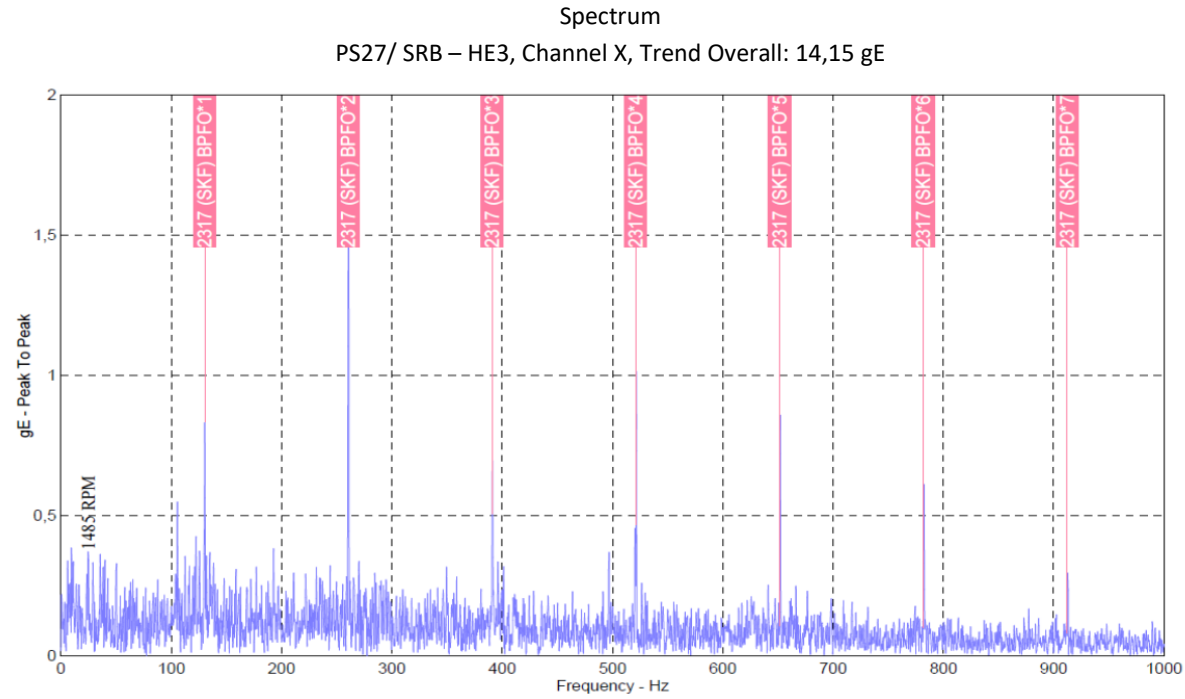

b)

Figure 2.27*: Pump PS14- Envelop spectrum on the SRB under different lubrication systems: a) under Oil bath lubrication and b)new bearing damage after 24 hours under Oil Mist Lubrication*

3.5.2 Set up and Definition lubrication factor (f_u)

As shown in the Fig.3.11 above, The Stribeck curve is used to represent the coefficient of friction f as a function of the variable μV/P , with μ dynamic viscosity, V peripheral speed and P diametrical load, for a bearing subjected to a fixed load in magnitude and direction . As far as concern the variable μV/P, it is interesting to note that the dynamic viscosity μ characterizes the lubricant (oil), while the peripheral speed V and diametrical load P characterize the lubricated system.

We will make a reliability analysis of the lubrication system based only on lubricated system characteristic. In this section, we intend to set up a parameter to evaluate the lubrication problem criticality. We define a factor f_u as the rate of lubricated system speed to the diametrical load.

$$f_u = \frac{V}{P_u} \qquad \text{(Eq.3-11)}$$

In this Eq.3-11 f_u [10^{-4}.mm.rpm/kN]; V [10^4.d.rpm] is the rotation speed and P_u [kN] a load support by a single bearing as defined above (section 3.3.1.1.2).

For each pump considered in this study, the factor f_u has calculated and reported un the table 2.8 with others characteristics.

- **Comparison with A. Shamim experiments [7].**

The angular contact ball bearings used in Shamim's test is B7012.TPA.P4.K5.UL.FAG. This bearing is subjected to different loads and rotation speed. Pure axial loads were applied to the witness, then the external radial load is negligible. Then applies the ISO standard for the individual bearings to calculate the bearing equivalent dynamic bearing load :

$P_{\text{single bearing}} = 0{,}35\ Fr + 0{,}57\ Fa$ when $Fa/Fr > 1{,}14$, as $Fr \approx 0$,

$P_u = P_{\text{single bearing}} = 0{,}57\ Fa$

The values so obtained may be used for the calculation f_u (it was to make a comparison of our data).

Table 3.7: *The factor* f_u *calculated from [7] experiment data.*

Test operating condition	Bore Diameter (mm)	Rotation speed (RPM)	Pure axial load [kN]	P_u [kN]	**Factor** f_u
1	60	1000	0,56	0,32	*18,80*
2	60	2000	0,56	0,32	*37,59*
3	60	1500	2,78	1,58	*5,68*
4	60	2000	5	2,85	*4,21*
5	60	1000	5	2,85	*2,11*
6	60	2400	18,9	10,77	*1,34*

Table 3.8: *The data related of the pumps studied*

Support side of Radial Bearing (SRB) *Overhung Pump (OP)*
Support side of Thrust Bearings (STB) *Double Support Pump (DSP)*

Pump Code	Pump type	Position	Bearing equivalente Load P [kN]	Bearing Load Pu [kN]	Rotation Speed N[rpm]	Bearing designation	bearing bore diameter	Bearings number	Oil bath				fu	Bearing life increase
											storic data	storic data		
									Mean	Std. Deviation	gE unacceptable	gE unsatisfactory		
									μ	σ	μ+3σ	μ+2σ		
PS1	OP	STB (1)	26,72	16,40	1475	7314	70	2	3,00	1,10	6,30	5,20	**0,63**	16%
PS2	OP	STB (1)	26,72	16,40	1475	7314	70	2					**0,63**	-12%
PS3	OP	STB (1)	16,58	10,17	2940	7311	55	2	2,25	0,58	3,99	3,41	**1,59**	53%
PS4	OP	STB (1)	16,58	10,17	2940	7311	55	2	3,52	0,68	5,56	4,88	**1,59**	46%
PS5	DSP	SRB (2)	2,7	2,7	2950	6307	35	1	0,91	0,30	1,81	1,51	**3,82**	0%
PS5	DSP	STB (1)	5,1	3,13	2950	7405	25	2	0,96	0,38	2,10	1,72	**2,36**	0%
PS6	DSP	SRB (2)	2,7	2,7	2950	6307	35	1	1,34	0,48	2,78	2,30	**3,82**	0%
PS6	DSP	STB (1)	5,1	3,13	2950	7405	25	2	1,89	0,38	3,03	2,65	**2,36**	5%
PS7	OP	STB (2)	14,78	9,07	2970	7311	55	2	1,75	0,66	3,74	3,07	**1,80**	38%
PS8	OP	STB (2)	14,78	9,07	2970	7311	55	2	2,26	0,70	4,36	3,66	**1,80**	41%
PS9	DSP	SRB (2)	24,8	24,8	1485	6317	85	1	3,17	0,79	5,54	4,75	**0,51**	-52%
PS9	DSP	STB (1)	46	28,22	1485	7317	85	2	3,25	0,75	5,50	4,75	**0,45**	-33%
PS10	DSP	SRB (2)	24,8	24,8	1485	6317	85	1	3,38	0,69	5,45	4,76	**0,51**	-28%
PS10	DSP	STB (1)	46	28,229	1485	7317	85	2	3,20	0,86	5,78	4,92	**0,45**	-25%
PS11	DSP	SRB (2)	24,8	24,8	1485	6317	85	1	3,20	0,81	5,63	4,82	**0,51**	-27%

PS11	DSP	STB (1)	46	28,22	1485	7317	85	2	2,10	0,97	5,01	4,04	**0,45**	-49%
PS12	OP	STB (1)	15,86	9,73	2950	7311	55	2	2,83	0,70	4,93	4,23	**1,67**	58%
PS13	OP	STB (1)	15,86	9,73	2950	7311	55	2	3,44	0,70	5,54	4,84	**1,67**	50%
PS14	DSP	SRB (2)	27	27	1485	6317	85	1	3,45	0,58	5,19	4,61	**0,47**	-31%
PS14	DSP	STB (1)	52,4	32,15	1485	7317	85	2	3,40	0,76	5,68	4,92	**0,39**	-38%
PS15	DSP	SRB (2)	27	27	1485	2317	85	1	2,20	0,81	4,63	3,82	**0,47**	-19%
PS15	DSP	STB (1)	52,4	32,15	1485	7317	85	2	2,90	0,62	4,76	4,14	**0,39**	-40%
PS16	DSP	SRB (2)	27	27	1500	6317	85	1	3,90	0,65	5,85	5,20	**0,47**	-29%
PS16	DSP	STB (1)	52,4	32,15	1500	7317	85	2	3,10	0,87	5,71	4,84	**0,40**	-26%
PS17	OP	STB (1)	18,31	11,23	2950	7312	60	2	1,57	0,55	3,22	2,67	**1,58**	33%
PS18	OP	STB (1)	18,31	11,23	2950	7312	60	2	2,71	0,27	3,52	3,25	**1,58**	29%
PS19	OP	STB (1)	16,5	10,12	2940	7311	55	2	3,00	0,51	4,53	4,02	**1,60**	113%
PS20	OP	STB (1)	16,5	10,12	2940	7311	55	2	2,76	0,62	4,62	4,00	**1,60**	74%
PS21	OP	STB (1)	20,12	12,34	2950	7313	65	2	1,80	0,42	3,06	2,64	**1,55**	-1%
PS22	OP	STB (1)	20,12	12,34	2950	7313	65	2	2,57	0,86	5,15	4,29	**1,55**	1%
PS23	OP	STB (1)			2950	7311	55	2	3,18	0,62	5,04	4,42	**1,56**	0%
PS24	DSP	SRB (2)	6,5	6,5	2970	2311	55	1	2,31	0,68	4,35	3,67	**2,51**	56%
PS24	DSP	STB (1)	13,86	8,50	2970	7311	55	2	2,57	0,61	4,40	3,79	**1,92**	56%
PS25	DSP	SRB (2)	6,5	6,5	2970	2311	55	1	2,58	0,83	5,07	4,24	**2,51**	80%
PS25	DSP	STB (1)	13,86	8,50	2970	7311	55	2	2,06	0,63	3,95	3,32	**1,92**	63%
PS26	DSP	SRB (2)	6,5	6,5	2970	2311	55	1	2,10	0,57	3,81	3,24	**2,51**	57%
PS26	DSP	STB (1)	13,86	8,50	2970	7311	55	2	2,89	0,81	5,32	4,51	**1,92**	57%
PS27	DSP	SRB (1)	40	40	1485	2317	85	1	-	-	-	-	**0,32**	
PS27	DSP	STB (2	81	49		7317	85	2	-	-	-	-	**0,27**	

3.5.3 Comparison between factors (f_u) and K (MRC Bearing Division of SFK Industries)

As mention in the section 2, the factor *K* is defined as equal to *DNP,* where *D*=bearing bore in mm, *N*= inner ring rpm, and *P*= load in pounds. If *K* does not exceed 10^9, oil mist is considered feasible [1]. Those two parameters are fundamentally different, by both aim to give an indices to valuate OML reliability. The factor ***K*** value has been converted ($K < K_{max}$ where $K_{max} = 445$ [10^{-4} mm.rpm. kN] to be confronted with factor f_u as show in the following Fig.3.28. In this figure condition factor ($K < K_{max}$) for which OML is considered feasible is represented by the entire area below the blue line. An additional evidence is indicated by the following conditions:

- For the condition where $f_u \geq 1$ [10^{-4}.mm.rpm/kN], the pumps retrofitting in OML has allowed to increase the bearing life. It is represented by the entire area above the green line.
- While for the condition where $f_u \leq 0{,}5$ [10^{-4}.mm.rpm/kN], the pumps retrofitting in OML has allowed to decrease the bearing life. It is represented by the entire area below the red line.

For the tests carried out according to different operating conditions by Shamim, the factor $f_u \geq 1$ [10^{-4}.mm.rpm/kN]. They represented by red triangles in Fig.3. This is fully in line with the study.

For two points which correspond to the pump PS27, $f_u \ll 0{,}5$ (and while the factor K is slightly higher than K_{max}), the OML is considered not feasible. Indeed the support P27/SRB has been damaged after 24 hours under OML.

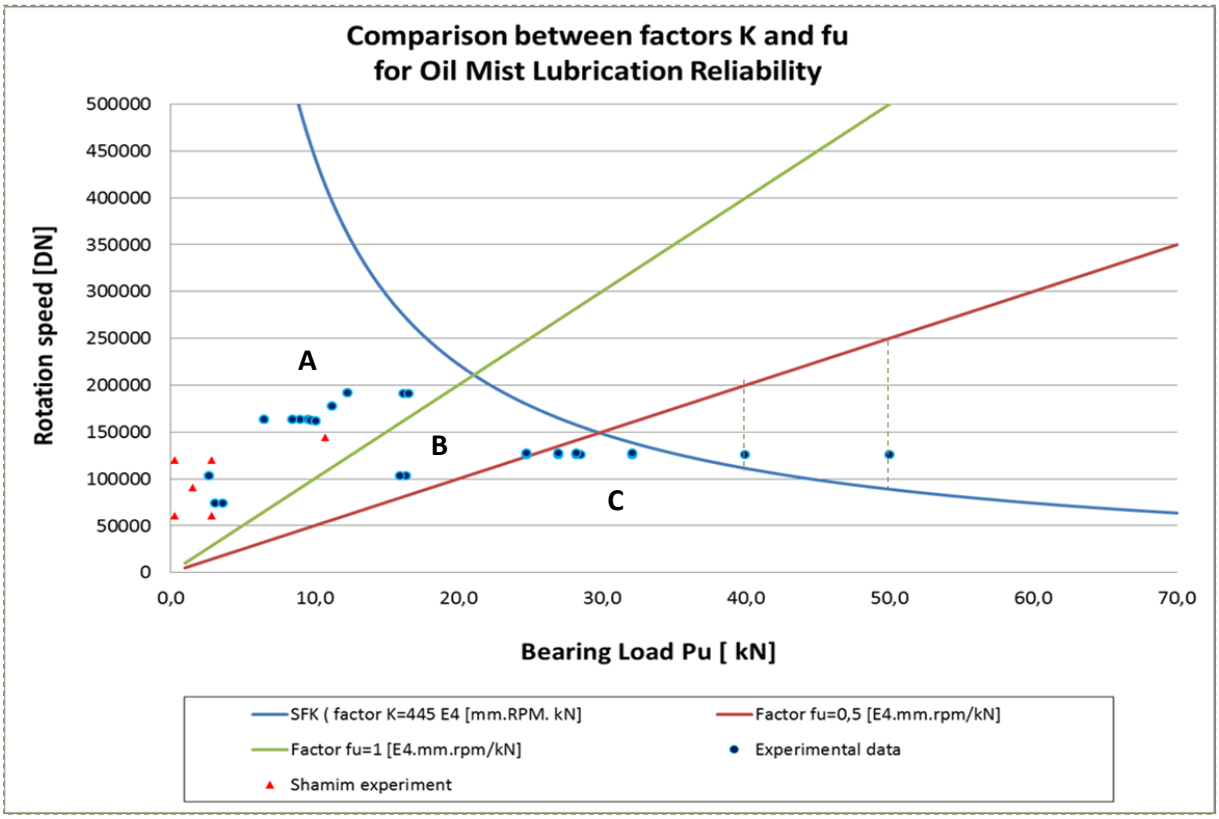

Figure 3.28: *Diagram of factor Comparison between factors f_u and K as function of load and the speed*

3.5.4 Synthesis and Discussion

The analysis allows us to highlight that after the retrofiring pumps support from the OBL system to OML system, three possible cases may happen:

Case A: the pumps retrofitted from OMB to OML show

- no change in both vibrations data and the bearing life. In both the conditions these parameters are considered to be very good.
- a slight increase in the vibrational level, but a significant increase in bearing life.

This case is represented by the pumps for which the factor $f_u > 1$ [10^{-4}.mm.rpm/kN].

Case B: the pumps retrofitted from OMB to OML show a sharp increase in the vibrational level and a significant decrease in bearing service life. This case is represented by the pumps for which the factor $\boldsymbol{f_u < 0,5}$ [10^{-4}.mm.rpm/kN].

Case C: the pumps retrofitted from OMB to OML show a sharp increase in the vibrational level and a significant decrease in bearing service life. it can be consider to be a transition condition between the case A and the case B**.** For this case only few pumps are been investigate. It needs further investigations to better define the different values of parameters corresponding to this transition condition. According to this study we can consider that this case is represented by the pumps for which the factor $\boldsymbol{f_u}$ is $0,55 < f_u < 1$ [10^{-4}.mm.rpm/kN].

Conclusion

In literature, the OML feasibility condition was established only by factor K < K_{max} defined by MRC Bearing Division of SFK Industries. But this was not sufficient condition to establish that the retrofitting pumps from OBL to OML will increase bearing life. The comparative study of rolling bearing vibration under OBL and OML in centrifugal pumps had been done and the following conclusions is derived:

Under equal operational conditions, the pumps bearings vibrations level may cause an increasing after the retrofitting from OBL to OML. This increasing is link to lubrication reliability and depends on the characteristics of the pump: the loads (P), the rotation speed (rpm) and the size of the bearing.

We have established in this study a factor $\boldsymbol{f_u}$, which is function of the parameters mentioned above, and used to establish a threshold of reliability.

- The bearings life increase for the pumps for which the factor $\boldsymbol{f_u} > \mathbf{1}$ [10^{-4}.mm.rpm/kN].
- The bearings life decrease for the pumps for which the factor $\boldsymbol{f_u} < \mathbf{0,5}$ [10^{-4}.mm.rpm/kN].
- A transition zone is observed when the factor $0,5 < \boldsymbol{f_u} < \mathbf{1}$ [10^{-4}.mm.rpm/kN].

The limited range of parameter values found in the plant under study did not allow us to estimate with more precision the value of factor $\boldsymbol{f_u}$ for the transition condition ($0,5 < \boldsymbol{f_u} < \mathbf{1}$ [10^{-4}.mm.rpm/kN]). This could be the subject of further work and future investigation for additional cases.

References

[1] Don Ehlert; "*Eliminating risks in bearing lubrication",* World Pumps July/August 2012, pp. 24-31.

[2] H.P. Bloch, "*Operating Principles and Systems Overview"*, Oil *Mist Lubrication Handbook*; 1987; pp. 9-15.

[**3]** H.P. Bloch, A. Shamim, *"Operating Principles and Systems Overview"*, *OIL MIST lubrication: Pratical Applications*, 2008 ; p. 9-14.

[**4]** H.P. Bloch, A. Shamim, *"The impact of Oil-Mist Lubrication",* chapter 1, *OIL MIST lubrication: Pratical Applications*, 2008 ; p. 1- 8.

[**5]** H.P. Bloch, "*The impact of Oil-Mist Lubrication",* chapter 1, *Oil Mist Lubrication Handbook* (1987), pp.

[6] Douglas C. Branham **,** *" Improving Machinery Reliability with Oil Mist Technology"*, – Lubrications System Company , Presented at IMC-2003 the 18th International Maintenance Conference

[7]. A. Shamim and C.F. Kettleborough, "*Tribological Performance Evaluation of Oil Mist Lubrication"*, *ASME Journal of Energy Resources Technology*, Vol. 116,No. 3, pp. 224–231, (1994)

[8]. Jeng, Y.-R., Gao, C.-C. "*Investigation of the ball-bearing temperature rise under an oil-air lubrication system",* Proceedings of the Institution of Mechanical Engineers, Part J:Journal of Engineering Tribology Volume 215, Issue 2, 2001, Pages 139-148.

[9] K. Ramesh, S.H. Yeo, Z.W. Zhong, Akinori Yui, "*Ultra-high-speed thermal behavior of a rolling element upon using oil–air mist lubrication***",** Journal of Materials Processing Technology 127 (2002) 191–198.

[10] Pinel, Stanley I.; Signer, Hans R.; Zaretsky, Erwin V.; "*Comparison Between Oil-Mist and Oil-Jet Lubrication of High-Speed, Small-Bore, Angular-Contact Ball Bearing***",** Tribology & Lubrication Technology; Apr 2011, Vol. 67 Issue 4, p32.

[11] K. Ramesh, S.H. Yeo, Z.W. Zhong, Akinori Yui, "*Ultra-high-speed grinding spindle characteristics upon using oil/air mist lubrication";* International Journal of Machine Tools and Manufacture, 2002.

[12]. Don Ehlert, " *Usa Getting The Facts On Oil Mist Lubrication",* 2011 *by Turbomachinery Laboratory*, Texas A&M University.

[13] Michalek, D.J., Hii, W.W.S., Sun, J., Gunter, K.L. and Sutherland, J.W. (2003). "*Experimental and Analytical Efforts to Characterize Cutting Fluid Mist Formation and Behavior in Machining"*. Appl. Occup. Environ. Hyg. 18: 842–854.

[14] Hsin-I Hsu, Mei-Ru Chen , Shih-Min Wang , Wong-Yi Chen, Ya-Fen Wang 4 , Li-Hao Young, Yih-Shiaw Huang, Chung Sik Yoon, Perng-Jy Tsai; "*Assessing Long-Term Oil Mist Exposures for Workers in a Fastener Manufacturing Industry Using the Bayesian Decision Analysis Technique";*

Aerosol and Air Quality Research, 12: 834–842, 2012.

[15] Russi, M., Dubrow, R., Flannery, J.T., Cullen, M.R. and Mayne, S.T. (1997). *"Occupational Exposure to Machining Fluids and Laryngeal Cancer Risk : Contrasting Results Using Two Separate Control Groups".* Am. J. Ind. Med. 31: 166–171.

[16] Kennedy, S.M., Chan, Y.M., Teschke, K. and Karlen, B. (1999). "*Change in Airway Responsiveness among Apprentices Exposed to Metalworking Fluids".* Am. J. Respir. Crit. Care Med. 159: 87–93.

[17] Kazerouni, N., Thomas, T.L., Petralia, S.A. and Hayes, R.B. (2000). "*Mortality among Workers Exposed to Cutting Oil Mist:* Update of Previous Reports. Am. J. Ind. Med. 38: 410–416.

[18] Jarvholm, B., Bake, B., Lavenius, B., Thiringer, G. and Vokmann, R. (1982). "*Respiratory Symptoms and Lung Function in Oil Mist-exposed Workers*." J. Occup. Med. 24: 473–479.

[19] Heyder, J., Gebhart, G., Rudolf, G., Schiller, C.F. and Stahlofen, W. (1986). "*Deposition of Particles in the Human Respiratory Tract in the Size Range 0.005−15 μm*". J. Aerosol Sci. 17: 811–825.

[20] Chen, M.R., Tsai, P.J., Chang, C.C., Shih, T.S., Lee, W.J. and Liao, P.C. (2007). *"Particle Size Distributions of Oil Mists in Workplace Atmospheres and Their Exposure Concentrations to Workers in a Fastener Manufacturing Industry".* J. Hazard. Mater. 146: 393–398

[21] The Canadian Association of Petroleum Producers (CAPP); *"Oil Mist Monitoring Protocol, 2004. Review 2010".*

[22]. Cho, Y. K.; Cai, L.; Granick, S., *"Molecular tribology of lubricants and additives"***.** Tribology International 1997**,** 30, (12), 889-894.

[23]. Jacobson, B**.** "*Thin film lubrication of real surfaces".* Tribol. Int., 2000, 33, 205–210.

[24]. Mizuta, K., et al. **"***Heat Transfer Characteristics Between Inner and Outer Rings of an Angular Ball Bearing*," Transactions of the JSME: Series B, Vol. 66, 2000, pp. 1162-1169.

[25]. Yovanovich, M.M., "*Thermal Constriction Resistance Between Contacting Metallic Paraboloids: Application to Instrument Bearings*," Heat Transfer and Spacecraft Thermal Control, edited by J.W. Lucas, Vol. 24, Progress in Aeronautics and Astronautics, AIAA, Reston, VA, 1971, pp. 337-358.

[26]. Bairi, A., Alilat N., Bauzin J.G., and Laraqi, N., "*Three-dimensional stationary thermal behavior of a bearing ball",* International Journal of Thermal Sciences, Vol. 43, 2004, pp. 561-568.

[27] Y. Hayashi, T. Akira, M. Osamu, "*High performance of mist cooled heat exchanger"***,** Proceedings of the international symposium on heat transfer, Beizing, 1988, pp. 612–622.

[28]. Dr. S. J. Lacey, "*An Overview of Bearing Vibration Analysis"*; Nov/Dec

2008 ME maintenance & asset management vol 23 no 6.

[29] A. V. Barkov and N. A. Barkova, "*Condition Assessment and Life Prediction of Rolling Element Bearings* - part 1 ", Sound and Vibration, June-1995, selected as their favorite vibration article of the past decade by Jack Mowry, editor/publisher and George Lang, associate editor, Sound & Vibration, January, 1997, 30th anniversary issue,
"The "Golden S&V" Awards - The Best of the Best".

[30] Tatsunobu M. and Banda N. "*Sound and Vibration in Rolling Bearings";*
Basic Technology Research and Development Center NSK; Motion & Control No. 6 -1999

[31]. Corrado Cesti, SKF Solution Factory Italy; "*I cuscinetti a rotolamento e le vibrazioni; L'analisi delle vibrazioni nella manutenzione predittiva";* 1996; pp.106-125..

[32]. SKF Reliability Systems, "*Acceleration Enveloping in Paper Machines***",** CM3024 (Revised 8-00), SKF Reliability Systems 4141 Ruffin Road San Diego, California 92123 USA,

[33]. J Halme∗ and P Andersson, "*Rolling contact fatigue and wear fundamentals for rolling bearing diagnostics".* Proc. IMechE Vol. 224 Part J: J. *Engineering Tribology*, October 2009, 377-389.

[34] T.A. Stolarski, "*Tribology in Machine Design",* Heinemann, Oxford, 1990, pp. 258-259.

[35] Michael Khonsari, Louisiana State University E.R. Booser, "*Guidelines for Oil Mist Lubrication",* Machinery Lubrication (9/2005).

[36]. *Oil lubrication*, SKF Bearing Maintenance Handbook; 1996; pp.234-247.

[37]G. Rodonò, R. Volpes, "*Trasmissione del calore moto dei fluidi; Fisica Tecnica"*, Vol 1, 1994. Facoltà Ingegneria di Palermo.

[38]. "*Elastohydrodynamic Lubrication"*, Engineering Tribology, Gwidon W., Andrew W. p 328,329.

[39]. T.E Tallian, "*On Competingg Failure modes in rolling contact"*, *ASLE Transactions*, Vol. 10, 1967,pp.418-439.

[40]. *"General" Alarm Guidelines for Enveloped Acceleration Measurements***,** SKF Condition Monitoring San Diego, CA.

Chapter 4

Balancing of multi-stage pump using the coupling hub

4 Balancing of multi-stage pump using the coupling hub

Abstract

Unbalance is found to be one of the most common causes of machinery vibrations in rotating systems in industrial plants. Dirt, wear, crashes, construction changes can all have a negative effect on balance of a machine. Removing the rotor and balancing it on a balancing machine is an option. However, to reduce at the minimum the downtime and to exclude the costs and risks of removing, transport and the remounting of the rotor, balancing the rotor on-site in the machine itself is, in many cases, the better option.

However balancing the rotor on-site is not possible for all type of machine, in particular for the pumps because their rotors are not accessible.

We present an experimental investigation to found some approach to balance on site a multistage-pump. To overcome the inaccessibility of pump rotor; the Coupling Hub fitted to the Pump (CHP) is assimilated to be part of the rotor. In determined cases, if the vibration measured on the Driver End Support (DES) is very higher than that measured on the Non Drive End Support (NDES), the CHP is considered to be the correction plan to apply on site balancing.

This method is verified experimentally in multistage pumps rotor balancing in an industrial plant. We use the Influence Coefficient Method. Two approaches are implicated. The Single Plane Balancing (SPB) using two supports vibrations measurements acquired with Eddy probe sensor. The other approach, which may be more simple and easy to apply, aim to apply the SPB using only one support vibrations measurements acquired with accelerometer. The results of the both the approaches are been compared.

4.1 Introduction

The rotor unbalance will not only cause rotor vibrations, but also transmit rotating forces to the bearings and to foundation structures. The force thus transmitted may cause damage to the machine parts and its foundation. If the transmitted force is large enough, it might affect even the neighbouring machines and structures. Therefore, it is necessary to remove the unbalance even that residual of a rotor, as much as possible, for its smooth running. Experimental estimation of the residual unbalance in rotor-bearing system is an age-old problem. From state of art of unbalance estimation, it can be calculated with fairly good accuracy [1,2,3,4]. Now the trend in the unbalance estimation is to reduce the number of test runs required, especially for the applications where the downtime is very expensive [5,6].

Rotating machines operating conditions can present a deterioration of vibration levels caused by the change of the equilibrium state of the machines due to wear, deformations, shifts to the assembled elements, deposition of material (dirk) on the rotor. Particularly the unbalance caused by deposition of material on the rotors happen very often in the multi-stage centrifugal pump used in heavy residual oils refining process. This origin of unbalance represents the more important part of their total unbalance. Balancing practice which needs to remove the rotor and balancing it on a balancing machine needs also to be planned and require the total shutdown of the machines. It cannot apply very often because of the high cost and the cost of missed production caused by the long downtime. It becomes important to develop new approach to make possible to apply the on-site balancing to the multi-stage centrifugal pump rotor.

The objective of the present study is to propose a method for on-site balancing of rotating machine such as multi-stage centrifugal pump, in order to reduce the number of unscheduled maintenance that requires the removing of rotor and others part of this machine. The proposed approaches are based on the method of influence coefficients which is recognized for its efficiency and for its ease of implementation in industrial context.

The first part presents the unbalance causes at rotors and rotating parts and an overview of basics theory of rotors balancing. It presents also the theoretical basis of the study. The unbalances in the rigid and flexible rotors. The theoretical development of Influence coefficient method for the flexible rotor balancing and its application.

The second part describes the on-site balancing approach of Multi-Stage Centrifugal Pump (MSCP). The problem definition and the description of theoretical approach for the resolution, the assumption of hypotheses to overcome the inaccessibility of pumps rotors for on-site balancing. The description of the two systems considered for the application of the theoretical approach of resolution.

In the thirds part , this document present an experimental study, application to industrial multi-stage pump. The pump and the vibration sensors and instruments are descripted in details. The balancing process of the pump based on the coupling hub are shown. The two different approaches for the two systems considered for balancing are studied and the results are then compared. These results allow to judge the effectiveness of such approaches to balancing multi-stage centrifugal pump in the industrial field.

A synthesis of the study is conducted, followed by a discussion before the conclusion.

4.2 Generality

4.2.1 Rotors and rotating parts Unbalance causes

Unbalance occurs in a rotating machine when the mass centerline and the geometric center do not coincide on each other. Unbalanced rotors generate vibrations which may damage their components. These vibrations are generally associated with the rotation frequency X [7]. In order to extend the life of the machine, vibration due to unbalance must be reduced to acceptable level. The unbalance can be caused by various defects that can have mechanical or thermal origin.

4.2.1.1 Mechanical unbalance

The mechanical unbalance can be due to various causes: loss of vane, rupture of a blade, etc.; a mounting change, erosion; deposition of material, creep etc.

Mass imbalance of rotors

Regardless of the care taken in the construction of machinery, it is not possible to align the axis of rotation with the center of gravity of each elementary portion of the rotor which characterises the imbalance. As a result, the rotating shaft is subjected to centrifugal forces which deform it. Imbalances generally come from machining defects, assembly or installation of the rotors. In operation, the rotors may then also deform under the effect of unsymmetrical overheating.

Loss of fin, rupture of a blade, etc.

When there is rupture and disappearance of a piece of the rotor, such as a fin, there is generally an instantaneous change of vibration. This evolution is better seen if it simultaneously monitors the amplitude and phase of vibration. The losses of blade also result in disturbances flowing (presence of repetitive pressure pulses).

Changing of the mounting

A sliding of the coupling plates results as in the previous example (loss of fin) by a sudden change of the synchronous vibrations of the rotation. This kind of incident is correlated to changes torsional loads (evolution of the torque transmitted during a charging socket).

Erosion. Deposition of material

The blades erosion can create an unbalance if the distribution is not symmetrical (which is quite common). The material deposition (dirt) occurs on the fans that operate in very dirty environments, such as blowers of fumes. Then there is a slow change in the vibration frequency of rotation, with occasional discontinuities when part of the deposit comes off under the effect of centrifugal forces.

Rotor Creep

When starting a machine after an extended shutdown period under certain conditions, one can observe high vibrations created by permanent deformation of the rotor due to: creep hot rotors even during short stop; creep cold rotors if they are very flexible and stopped a long time; etc.

4.2.1.2 Unbalance of thermal origin

Deformation of (turbine) rotors

When the rotors are not homogeneous, or when the temperature is not uniformly distributed, the rotors are deformed under the effect of thermal stresses. They deform asymmetrically, the centers of gravity shifts and the efforts vary.

Deformation of alternator rotors or electric motors

A non-homogeneity of the rotor may induce deformations. Because of the high energy dissipated by Joule effect or by hysteresis, it is necessary to cool the rotors. Any asymmetry rate (clogged ventilation channels and different losses of load) will result during a power variation by a variation of vibration.

The vibrations are then a function of the heating which depends on the intensity of the current in the rotor, but also the cooling fluid temperature, or its pressure.

Sliding and upset dilation of electric machines coils

If there is an obstacle to a bar expansion, or if the friction forces become high, the coil dilatation can no longer be freely and rotor twists. Is then observed in this case a change of the vibration level.

4.3 Overview of Basics Theory of Rotors Balancing

The balancing techniques use lumped mass models based on three approaches: the modal balancing method, the influence coefficient method and the unified approach. The modal balancing technique was developed by Bishop [8] and further investigated by several researchers [1,9,10,11]. In this method, the critical speed mode shapes of the rotor must be known from either theoretical or experimental measurements. It mean that this method requires knowledge of the modal base of the rotor, which involves the construction of an accurate digital model as well as the realization of a series of vibration measurements to determine the modal unbalance. Furthermore, identification techniques can be used to calculate this unbalance from various vibrations information [12,13]. Also, mass distribution must be determined from the geometry of the rotor. The problem of the modal balancing method is that its accuracy depends on the knowledge of the rotor mode shapes. So necessity to build a model that can accurately translate the dynamic behavior of the machine, which hinders their application because the machines are generally difficult to model.

The influence coefficients technique was presented by Goodman [14]. It has been improved and tested by several authors [15,16,17,18]. In general, this method requires an accurate measurement of vibration phase angle in order to produce acceptable results. The method of influence coefficients is more appropriate to balancing on site because it uses only the experimental information. The machine is described by measurement plans and corrective plans or balancing plans. For a given rotational speed, the sensitivity of the measurement planes with respect to the balancing planes characterizes the machine in response to the loads generated by the unbalance. This method involves the system linearity assumption. Goodman [19] widens the scope of the method by the use of a technique least squares which allows the inclusion of a number of measurement points greater than the number of balancing planes. Mahfoudh [20;21] improved the method by optimizing the choice of balancing planes and with

the possibility to weight the measurement planes. The implementation of the influence coefficients method remains simple but has a major disadvantage: the number of start-stops needed to characterize the machine. To overcome this problem, authors like Bigret, Knight et al. [22, 23] proposed numerical calculation of influence coefficients. But the difficulty of this method is equivalent to the modal method: we must have an accurate model of the system.

The unified approach of modal balancing method and the influence coefficient method was presented [24, 25] in order to retain their advantages and eliminate their disadvantages. Parkinson [24] shows that the method of influence coefficients applied to the first critical speed is equivalent to the modal method. All these methods consist in determining one or more unbalances correction which are manually carried on the rotor at a standstill. The correction is therefore fixed and can become ineffective in the case of evolutionary unbalances. This is why many authors have reflected on the possibility of correcting unbalance during operation of the machine. There are two categories of devices that modify the mass distribution of a rotating machine: the self-balancing devices and the active balancing devices.

The self-balancing devices principle is to use the centrifugal forces due to the rotation to move solids or liquids to predetermined positions that tend to equilibrate the system. Lee, Jinnouchi and Shimizu [26, 27, 28], presented a self-balancing devices. The theoretical and experimental studies show that the effectiveness is limited to supercritical speeds and that below the first critical speed, the effect is inverted and devices tends to unbalance the system. D.J. Rodrigues et al. [29] published their work which confirm what is said above. They [30] presented in the same year a simple model for a two-plane automatic ball balancer. The use of complex coordinates enabled the equations to be written in a compact form, and effects such as support anisotropy and rotor acceleration were also included. By symmetry properties they have demonstrated that operation above both critical frequencies is a necessary but not a sufficient condition for the stability of the balanced state. K. Green et al. [31] present a nonlinear bifurcation analysis of the dynamics of an automatic dynamic balancing mechanism for rotating machines. The principle of operation is to deploy two or more masses that are free to travel around a race at a fixed distance from the hub and, subsequently, balance any eccentricity in the rotor. Tadeusz [32] studies meanwhile phenomena that limit the effectiveness of self-balancing (friction, vibration of the frame ...) and shows that the perfect balancing is not possible with such systems. Real control of the positioning of balance weights therefore requires an external power source.

The active balancing devices address the vibrations of the machine in real time and use a power source to correct the imbalance.The first to be interested in the active balancing is Van De Vegte [33, 34]. He develops a device comprising two concentric discs equipped with a mass on their periphery. The relative positioning of the discs allows to generate an unbalance magnitude and appropriate phase. Bishop [35] took the technology developed by Van de Vegte and theoretically shows the possibility of a modal automatic balancing with balancing plane. Other original processes have been developed and presented in the literature. Furman [36] proposed the idea of a device with deformable elements on a disc. A radiant heating system would control their plastic deformation due to centrifugal forces to generate an imbalance. Zumbach [37] studies a thermal balancing principle of a rotating shaft line. The thermal unbalance is reduced by means of heating elements mounted on the circumference of the rotors. The reduction of vibrations at the bearings is shown in continuous operation. Jenkins [38] has developed an active balancing device suitable for large machines compartments discs are mounted on the couplings. Balancing is carried out by the mass transfer of fluids from one compartment to the other through the generation of a temperature gradient. Its effectiveness is limited by the positioning accuracy of correcting imbalances and the slow fluid transfers. In 2014 Hongwei Fan et al. [39] propose a new electromagnetic ring balancer for active mass imbalance compensation of rotating machinery. This type of active balancer maintains the balanced condition of machine by permanent magnets rather than clutch and external energy.

4.4 Unbalances in the Rigid and Flexible Rotors

We present the procedure of static and dynamic balancing of rotor. For dynamic balancing, rotors are classified in two major categories, e.g., balancing of the rigid and flexible rotors. In fact, the same shaft of a rotor can be considered as rigid if it is operating much below its first critical speed and the flexible when it is operating near or above the first critical speed. Basic principles of rigid and flexible rotor balancing are quite different. Necessary principles and theories for dynamic are descripted in detail [40]. In general, a rigid rotor can be balanced by putting correction masses in two balancing planes, however, flexible rotor can be balanced by N_{planes} balancing planes, where N_{planes} is the number of flexible modes need to be balanced. Often, it is suggested to balance flexible rotor by (N_{planes} +2) balancing planes (i.e., to balance rigid rotor modes by 2 planes at low speeds and to balance flexible rotor modes by N planes at high speeds).

4.4.1 Unbalance in a Single Plane

Such unbalance occurs in gear wheels, grinding wheels, single stage compressors, blades of wind mills, the propeller of aircraft engines, etc. Fig.4.1 shows a rigid thin disc with the single plane unbalance. Where O is the centre of rotation of the disc and G is the centre of gravity of the rotor. The eccentricity, e , is defined as a distance between the centre of rotation and the centre of gravity, in practice the tolerable eccentricity would be of the order of μm (however, it will very much depend upon the type of applications). The unbalance in the disc is defined as in the equation (Eq.4.1)

$$U = me \qquad \text{(Eq.4.1)}$$

Where U is the unbalance with a unit of kg-m or g-mm, m is mass of disc, e is the eccentricity in the disc (length OG in Figure 1).

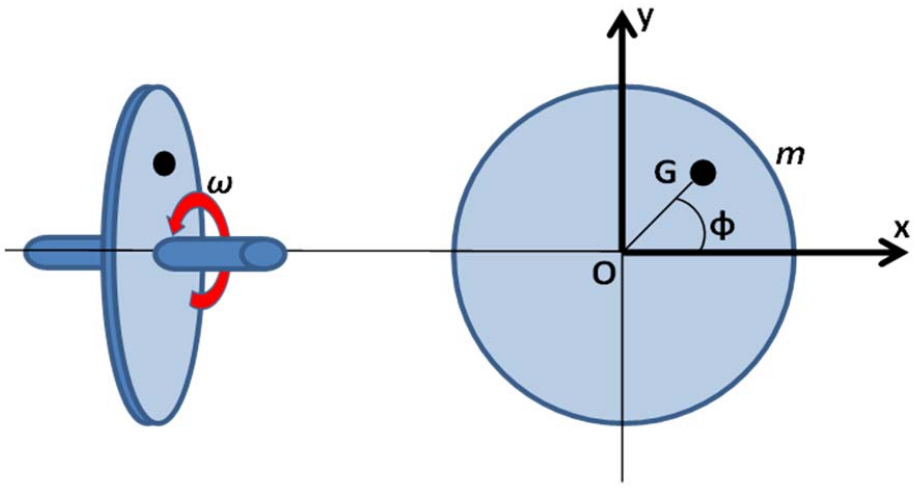

Figure 4.1: Unbalance in single plane

The unbalance force, for a single plane disc as shown in Fig.4.1, is given by the equation (Eq.4.2).

$$F = m{\omega_s}^2 e \qquad \text{(Eq.4.2)}$$

where ω is the spin speed of the rotor. Even if the order of eccentricity is very less for large rotors, which generally runs at high speed, the effect of unbalance force could be devastating. The unbalance in a single plane is corrected using a static balancing. The correction mass, m_c, at a radius of r, is given by the equation (Eq.4.3)

$$m_c = \left(\frac{e}{r}\right) m \qquad \text{(Eq.4.3)}$$

The correction should be placed 180° away from unbalance mass m_u. Such a correction is called a single plane balancing of the rotor, which eliminates the inertia forces transmitted to the foundation (or bearing).

4.4.2 Unbalances in Two or More Planes

4.4.2.1 Unbalance in a rigid rotor system

Fig.4.2 shows two types of unbalance in a rigid rotor system. The rotor consists of a rigid rotor and a massless elastic shaft. First type of unbalance (Fig.4.2a) illustrates the static unbalance, which is the state represented by a geometric eccentricity, *e*, of the center of a gravity of a rotor from the centerline or rotational axis of the shaft. The unbalance produces a centrifugal force proportional to the square of the rotational speed. This static unbalance can be detected without operating the rotor since the unbalance is always directed downward if the shaft is supported horizontally by bearings having little friction. Theoretically, it is similar to the single plane unbalance described above, except the unbalance in uniformly distributed along the length of the rigid rotor. Second type of unbalance (Fig.4.2b) shows the couple unbalance, which is the state represented by the angular misalignment of the principal axis of mass moment of inertia of the rotor with respect to the centerline or rotational axis of the shaft. The magnitude of the couple unbalance is determined by the angle as shown in the figure. This type of unbalance cannot be detected without rotating the shaft. Since the centre of gravity lies on the axis of rotation of the rotor, it could be in stable position at any orientation of the rotor, unlike the static unbalance. Fig.4.2 (a and b) shows these unbalances as models with one and two concentrated masses, respectively. That means static unbalance can be balanced by a single plane balancing and couple unbalance has to be balanced with two balancing planes. With the above definition now the dynamic unbalance in a rigid rotor means the state with both the static and couple unbalances. (i.e., combination of Fig.4.2a and 4.2b). However, for such a case also two-plane balancing will be enough.

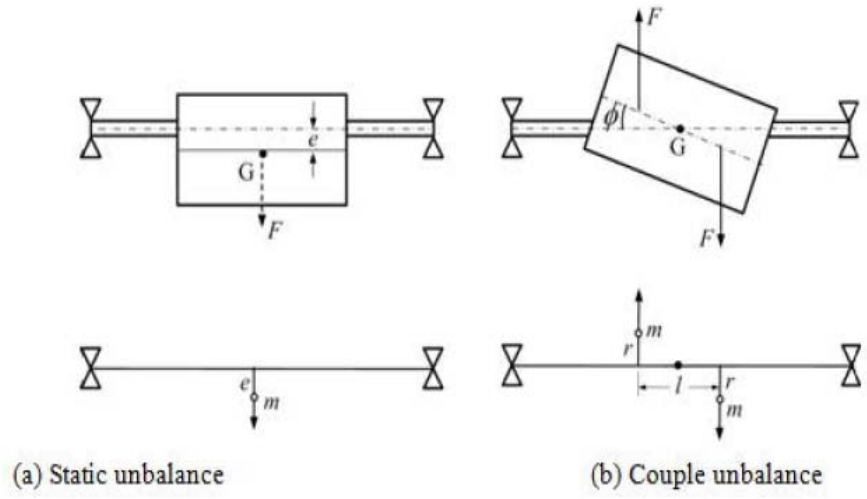

Figure 4.2: Unbalances in a long rigid rotor system [40]

Some basic principle of rigid rotor balancing will be outlined and this will pay the way to understand balancing methods for practical rotors.

- **Static Balancing (Two plane balancing)**

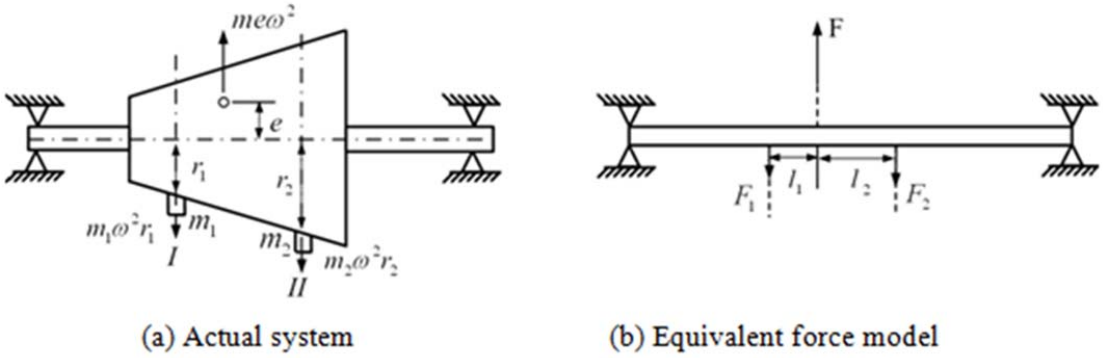

Figure 4.3: Static Balancing two plane

We represent eccentricities and centrifugal forces as vectors, for which both magnitude and direction are necessary.

$$F_I + F_{II} = F \qquad \text{and} \qquad F_I l_1 = F_{II} l_2 \quad \text{(Eq.4.4)}$$

where l_1 and l_2 are shown in Fig.4.3-b.

- **Couple unbalance**

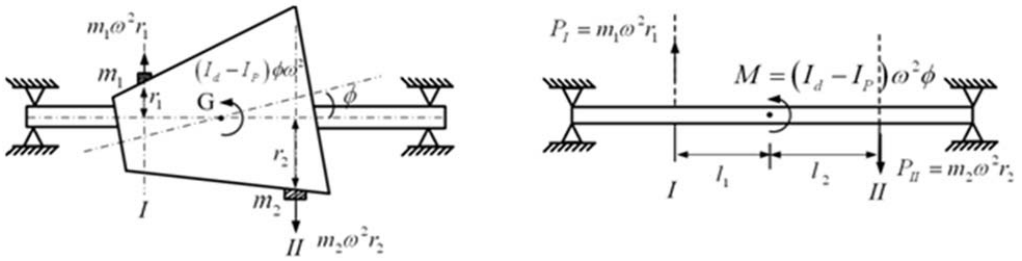

Figure 4.4: Couple unbalance

The moment $M = (I_d - I_p)\omega^2\phi$ due to couple unbalance can be replaced equivalently by a couple of forces $P = M/d$, which is separated by the distance d. We add correction masses m_1 and m_2 to cancel moment M by the centrifugal forces $P_I = m_1\omega^2 r_1$ and $P_{II} = m_2\omega^2 r_2$ (Fig.4.4). For this case the following relationships must hold

$$P_I l_1 + P_{II} l_2 = M \quad \text{(6-a)} \qquad \text{and} \qquad P_I = P_{II} \quad \text{(6-b)} \qquad \text{(Eq.4.5)}$$

The latter is the condition to prevent a new static unbalance due to the addition of m_1 and m_2. Vectorially they should be $\vec{P}_1 = -\vec{P}_2$. Equations (6-a and 6-b) give

$$P_I = P_{II} = \frac{M}{l_1 + l_2} \qquad \text{(Eq.4.6)}$$

It is assumed here that we know the plane of couple unbalancing.

- **Dynamic unbalance**

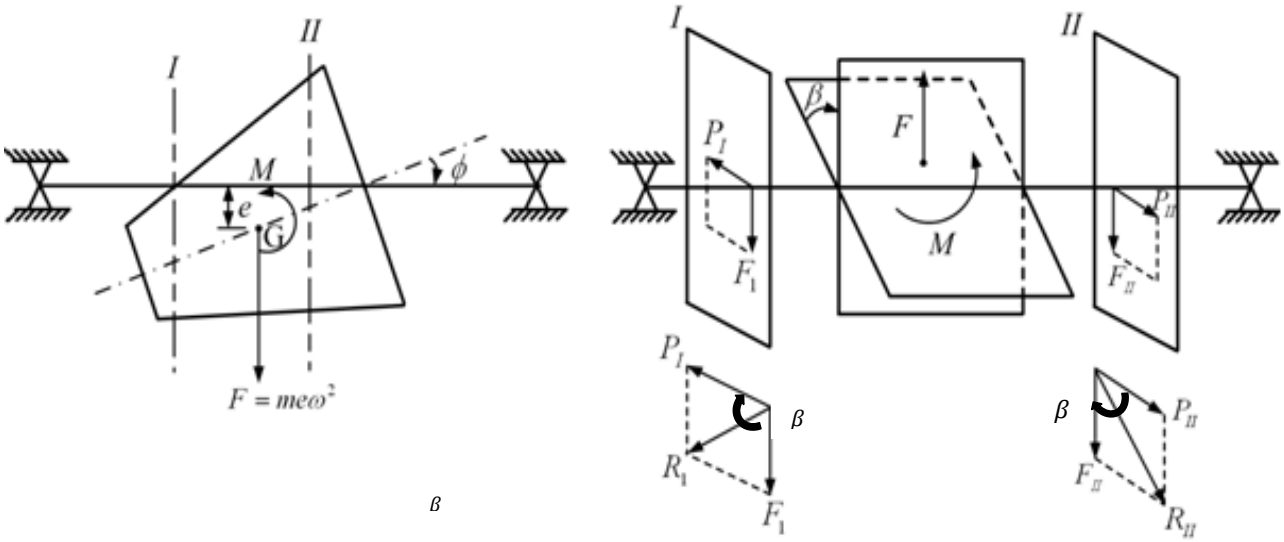

Figure 4.5: *Static and couple unbalance*

The static and couple unbalances effects i.e. force and moments may not be in the same plane; however, they will be perpendicular to the bearing axis (Fig. 4.5). The balancing is attained by adding correction weights in the correction forces $\vec{R}_I$ and $\vec{R}_{II}$ determined by the following vector relationship (Eq.4.7). See Fig. 4.5.

$$\vec{R}_I = \vec{P}_I + \vec{F}_I \qquad \text{and} \qquad \vec{R}_{II} = \vec{P}_{II} + \vec{F}_{II} \qquad \text{(Eq.4.7)}$$

4.4.2.2 Unbalance in a flexible rotor system

The unbalances in a continuous rotor (i.e., a flexible rotor with distributed mass) is shown in Fig.4.6.

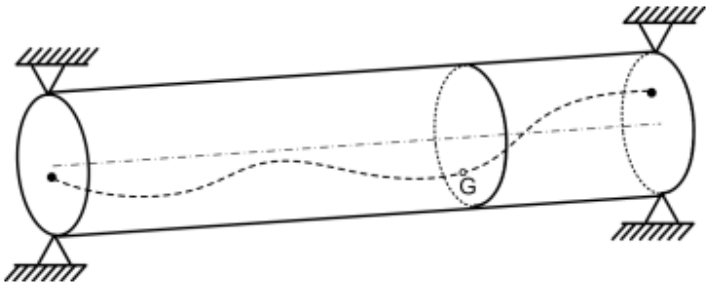

Figure 4.6: *Variation of the unbalance in continuous flexible rotor [40]*

The balancing technique of rigid rotors mentioned earlier is applicable only when the operating range is far below the first critical speed. We cannot use it when the rotor deforms in high-speed range. In fact, as long as the rotor experiences no deformations or has appreciably small displacements, i.e. it remains as a rigid rotor, the balancing procedure discussed earlier is effective. Once the rotor bends while approaching a critical speed, the bend center line whirls around and additional centrifugal forces are set-up and the rigid rotor balancing becomes ineffective (sometimes rigid rotor balancing worsens bending mode whirl amplitude). In this case eccentricity and its angular orientation may change in three-dimension continuously from one end of the shaft to another. It is require *P* plane balancing, where and generally for balancing up to m^{th} mode $P \geq 2+m$, for $m > 2$.

Various types of practical balancing techniques for flexible rotors have been proposed (early mention above) [8 to 18]. One of the most representative balancing methods: the influence coefficient method, which is largely employed in industrial sector, is explained in the next section.

4.4.3 Influence coefficient method for the flexible rotor balancing

In the present section we dealt with the influence coefficient method for the flexible rotor balancing in which case influence coefficients themselves depend upon the speed at which the rotor is being operated. Hence, influence coefficients obtained at one speed will no longer be valid for other speeds. The Fig. 4.7 shows the effect of deflection in various modes of the shaft on influence coefficients. It can be seen that they depend upon shaft speeds (especially near critical speeds).

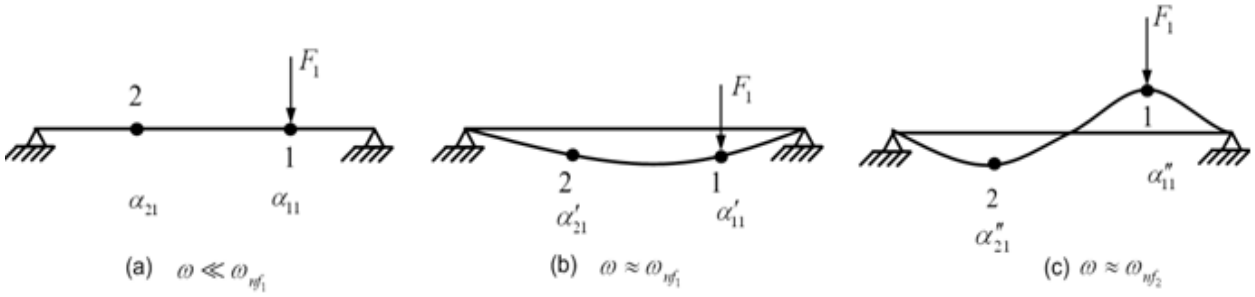

Figure 4.7: *Effect of mode shapes on influence coefficients*

The method of influence coefficients is a reverse type of method: the construction of a matrix model of the structure is made of sensitivity to experimental measurements unbalance. It applies to balancing

rotors assumed to be linear, rigid or flexible, non-amortized or depreciated. Its objective is to cancel the vibrations of a number of measurement points, by decomposing the imbalance to correct in certain number of balancing planes as shown in Fig.4.8. These vibrations can be canceled for one or more operating speeds, called balancing speed.

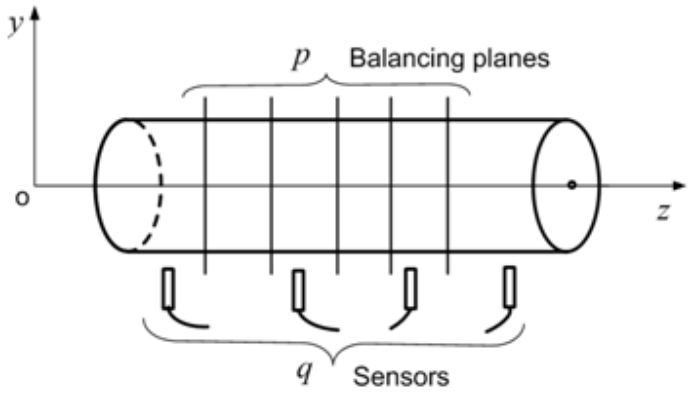

Figure 4.8: *A rotor system with measurement locations and balancing planes*

4.4.3.1 Definition of influence coefficient

Let us choose p number of balancing planes (where mass can be added or chipped-off), and q number is measuring planes; generally it is two; i.e. at bearing planes. First the distributed unbalance is *e (z)* is replaced by the concentrated unbalance $\vec{e}_1$, $\vec{e}_2$, …., $\vec{e}_p$ approximately. Let the unbalance, $U=m_u.e$ in each of the balancing planes be $\vec{U}_1$, $\vec{U}_2$,… $\vec{U}_p$. The method is based on the assumption of linearity of the system. For a given speed ω_1 this results in the relationship:

$$\{W(\omega_1)\}_{\boldsymbol{q\times 1}} = \left[\boldsymbol{C^{(1)}}\right]_{\boldsymbol{q\times p}}\left\{\boldsymbol{U^{(1)}}\right\}_{\boldsymbol{p\times 1}} \qquad \text{(Eq.4.8)}$$

Or

$$\begin{Bmatrix} \vec{W}_1 \\ \vec{W}_2 \\ . \\ . \\ . \\ \vec{W}_q \end{Bmatrix} = \begin{bmatrix} \boldsymbol{C_{11}^{(1)}} & \boldsymbol{C_{12}^{(1)}} & \cdots & \boldsymbol{C_{1p}^{(1)}} \\ \boldsymbol{C_{21}^{(1)}} & \boldsymbol{C_{22}^{(1)}} & \cdots & \boldsymbol{C_{2p}^{(1)}} \\ . & . & \cdots & . \\ . & . & \cdots & . \\ . & . & \cdots & . \\ \boldsymbol{C_{q1}^{(1)}} & \boldsymbol{C_{q2}^{(1)}} & \cdots & \boldsymbol{C_{qp}^{(1)}} \end{bmatrix} \begin{Bmatrix} \vec{\boldsymbol{U}}_{\boldsymbol{1}}^{\boldsymbol{(1)}} \\ \vec{\boldsymbol{U}}_{\boldsymbol{2}}^{\boldsymbol{(1)}} \\ . \\ . \\ . \\ \vec{\boldsymbol{U}}_{\boldsymbol{p}}^{\boldsymbol{(1)}} \end{Bmatrix} \qquad \text{(Eq.4.9)}$$

where *w* is the vibration measurement at the measuring plane and subscripts in matrices and vectors represent their sizes.

Determination of influence coefficients

The coefficients in column *j* of the matrix [$C^{(1)}$] are determined by taking the ratio of vibrations $\{We\}$ resulting in the addition of a test unbalance Ue_j in the balancing planes *j*, and test unbalance.

$$C_{ij} = \frac{W_{ij} - W_i}{Ue_j} \qquad \text{(Eq.4.10-a)}$$

Where :

W_i is the vector of initial vibration measured by the sensor i

W_{ij} is the vector of vibration measured by the sensor i after adding a trial masse m_j on the plane *j*.

Ue_j is the test unbalance created by adding a trial masse m_j on the plane *j*.

If the trial masses are all fixe to equal distance from the rotation axis, the coefficients can be calculated by the equation Eq.4.12-b.

$$C_{ij}^{(1)} = \frac{W_{ij} - W_i}{m_j} \qquad \text{(Eq.4.10-b)}$$

C_{ij} means how much the vibration on the sensor i is influenced by the imbalance on the plane *j*. Then you need to do many experimental tests as they are the imbalance plans. In each test, I find one column of the matrix [$C^{(1)}$].

The major part of the machine have a single operating speed. Then this matrix constructed for a only speed is sufficient. But, for the machine that they operate at different speeds, it is necessary construct similar matrix for each speed. So if you register at different ω I find similar columns of other matrices. These are grouped together to construct a larger matrix [C]. And I get:

$$\{\boldsymbol{W}\} = [\boldsymbol{C}]\{\boldsymbol{U}\} \qquad \text{(Eq.4.11)}$$

Or $$\{W(\boldsymbol{\omega})\}_{\boldsymbol{qn}\times\boldsymbol{1}} = [\boldsymbol{C}(\boldsymbol{\omega})]_{\boldsymbol{qn}\times\boldsymbol{p}}\{\boldsymbol{U}\}_{\boldsymbol{p}\times\boldsymbol{1}} \qquad \text{(Eq.4.12)}$$

Where:

{U}: the vector of initial unbalance unknown which size is p

{W}: the vector initial vibrations which size is $q \times n$

[C]: the matrix of influence coefficient which size is $(q \times n) \times p$

*p:*number of balancing planes,

q: number of measurement points of vibration

n: number of balancing speed.

To account for the phase and the amplitude variable, complex quantities are used. The matrix *[C]* is of the form:

$$[\boldsymbol{C}] = \begin{bmatrix} \boldsymbol{C_{11}^{(1)}} & \boldsymbol{C_{12}^{(1)}} & & & & \boldsymbol{C_{1p}^{(1)}} \\ \boldsymbol{C_{21}^{(1)}} & \boldsymbol{C_{22}^{(1)}} & \cdot & \cdot & \cdots & \boldsymbol{C_{2p}^{(1)}} \\ \cdots & \cdots & \cdot & \cdot & \cdot & \cdot \\ \cdots & \cdots & \cdots & \cdot & \cdot & \cdot \\ \cdots & \cdots & \cdot & \cdots & \cdot & \cdot \\ \boldsymbol{C_{q1}^{(1)}} & \boldsymbol{C_{q2}^{(1)}} & \cdot & \cdot & \cdots & \boldsymbol{C_{qp}^{(1)}} \\ \boldsymbol{C_{11}^{(2)}} & \boldsymbol{C_{21}^{(2)}} & \cdot & \cdots & \cdots & \boldsymbol{C_{1p}^{(2)}} \\ \cdots & \cdots & \cdots & \cdot & \cdot & \cdot \\ \cdots & \cdots & \cdot & \cdots & \cdot & \cdot \\ \cdots & \cdots & \cdot & \cdot & \cdots & \cdot \\ \boldsymbol{C_{q1}^{(2)}} & \boldsymbol{C_{q2}^{(2)}} & \cdot & \cdot & \cdot & \boldsymbol{C_{qp}^{(2)}} \\ \cdots & \cdots & \cdot & \cdot & \cdot & \cdot \\ \cdots & \cdots & \cdots & \cdot & \cdot & \cdot \\ \cdots & \cdots & \cdot & \cdots & \cdot & \cdot \\ \boldsymbol{C_{11}^{(n)}} & \boldsymbol{C_{12}^{(n)}} & \cdot & \cdot & \cdots & \boldsymbol{C_{1p}^{(n)}} \\ \boldsymbol{C_{21}^{(n)}} & \boldsymbol{C_{22}^{(n)}} & \cdot & \cdot & \cdot & \boldsymbol{C_{2p}^{(n)}} \\ \cdots & \cdots & \cdots & \cdot & \cdot & \cdots \\ \cdots & \cdots & \cdot & \cdots & \cdot & \cdots \\ \cdots & \cdots & \cdot & \cdot & \cdots & \cdots \\ \boldsymbol{C_{q1}^{(n)}} & \boldsymbol{C_{q2}^{(n)}} & & & & \boldsymbol{C_{qp}^{(n)}} \end{bmatrix}$$

The amplitude unbalance is generally expressed in kg.m or g.cm. The measured vibration can be displacements or accelerations respectively expressed in mm or m/s^2 and in velocity expressed in mm/s in some industrial case.

4.4.3.2 Determination unbalance correction

Three cases then appear:

- $p=qn$: The matrix [C] is invertible; the solution is unique. Balancing then returns to solve:

  $$\{\boldsymbol{U_c}\} = -\{\boldsymbol{U}\} = -[\boldsymbol{C}]^{-1}\{\boldsymbol{W}\} \quad \text{(Eq.4.13)}$$

  Where U_c is the vector of desired correction unbalanced.

- $p>qn$: This case is not encountered in practice because the plans available for balancing are rarer than plans available for measurement.
- $p<qn$: The matrix [C] is rectangular and is thus not invertible. they have to use a specific method to minimize residual vibrations.

Minimizing least squares

The least square method is used to minimize vibrations at discrete points when the matrix [C] is rectangular. The methods presented in [19; 20, 21] minimizes the quadratic norm of the residual vibration. The vector of the residual vibrations $\{\varepsilon\}$ is such that:

$$\{\boldsymbol{\varepsilon}\} = [\boldsymbol{C}]\{\boldsymbol{U_c}\} + \{\boldsymbol{W}\} \quad \text{(Eq.4.15)}$$

If $\{\boldsymbol{U_c}\}$ is solution to least squares, then $\{\boldsymbol{U_c}\}$ achieves the minimum of the function:

$$\boldsymbol{\phi}(\boldsymbol{U}) = ([\boldsymbol{C}]^*\{\boldsymbol{U}\} + \{\boldsymbol{W}\}^*)^{\boldsymbol{t}}([\boldsymbol{C}]\{\boldsymbol{U}\} + \{\boldsymbol{W}\}) \quad \text{(Eq.4.16)}$$

$$\boldsymbol{\phi}(\boldsymbol{U}) = \{\boldsymbol{U}\}^{\boldsymbol{t}}[\boldsymbol{C}^*]^{\boldsymbol{t}}[\boldsymbol{C}]\{\boldsymbol{U}\} + \mathbf{2}\{\boldsymbol{U}\}^{\boldsymbol{t}}[\boldsymbol{C}^*]^{\boldsymbol{t}}\{\boldsymbol{W}\} + \{\boldsymbol{W}^*\}^{\boldsymbol{t}}\{\boldsymbol{W}\} \quad \text{(Eq.4.17)}$$

Where the symbol * is the conjugate.

Then the gradient $\boldsymbol{\phi}(\mathbf{U})$ vanishes at $\{\mathbf{U_c}\}$:

$$\mathbf{grad}\ \boldsymbol{\phi}(\boldsymbol{U_C}) = \mathbf{2}[\boldsymbol{C}^*]^{\boldsymbol{t}}[\boldsymbol{C}]\{\boldsymbol{U_c}\} + \mathbf{2}[\boldsymbol{C}^*]^{\boldsymbol{t}}\{\boldsymbol{W}\} = \mathbf{0} \quad \text{(Eq.4.18)}$$

$$[\boldsymbol{C}^*]^{\boldsymbol{t}}[\boldsymbol{C}]\{\boldsymbol{U_c}\} = -[\boldsymbol{C}^*]^{\boldsymbol{t}}\{\boldsymbol{W}\}$$

Unbalance correction obtained is expressed the following equation (Eq.3.19):

$$\{\mathbf{U_c}\} = -\{[\boldsymbol{C}^*]^{\boldsymbol{t}}[\boldsymbol{C}]\}^{-\mathbf{1}}\,[\boldsymbol{C}^*]^{\boldsymbol{t}}\{\boldsymbol{W}\} \quad \text{(Eq.4.19)}$$

The application of the unbalanced $\{U_c\}$ in the balancing planes reduces vibrations in the measuring plane.

In practice, the behavior of the system is measured by accelerometers or displacement sensors. In the case of accelerometers, the measure actually represents the acceleration of the structure while the one that comes from the eddy current displacement sensors is not necessarily in the image of the movement of the structure. Indeed, these sensors are sensitive to the heterogeneity of the material as well as displacement at a low enough speed so that the rotor can be considered rigid. The run-out vector {R} which results is then subtracted (in terms of vectors) to minimize the displacements. The unbalance correction is given by the equation (Eq.4.20).

$$\{\mathbf{U_c}\} = -\{[\boldsymbol{C}^*]^t[\boldsymbol{C}]\}^{-1}\,[\boldsymbol{C}^*]^t\{\boldsymbol{W}-\boldsymbol{R}\} \qquad \text{(Eq.4.20)}$$

4.4.3.3 Influence coefficient method Application to Normal Balancing Process

We call "*normal balancing procedure*" the balancing operation in which the correction plans are actually part of the rotor. In the balancing practice in which the rotor is remove and balancing on a balancing machine, all the rotor correction plans are accessible to set the weights. In the on-site balancing only part of the rotor may accessible, but it is sufficient to set weights. It is important to note that in both these practices, the weights are directly set on rotor part.

Technical approaches for rotor on-site balancing

The Single Plane Balancing SPB and the Two-Plane of Balancing (TPB) based on ICM are the technical approaches most used in industrial sector for machine rotor on-site balancing.

For rigid rotors the TPB method works well for more balancing problems. Also arrow and overhung rotors are balanced using the two-planes approach. But for these rotors this method can be difficult to be applied directly because narrow and overhung rotors are often dominated by static unbalance. As shown above (section 2.3.2.1) any two-plane dynamic balance solution can be separated into a static and couple component. Therefore, it is proposed [41] to eliminate the static unbalance first, before trying to correct the couple.

For flexible rotors, as it has been mention above, the deflection curves changes depending on the rotational speed. However actually in industrial plant, the major part of machine work at constant speed. Therefore the balancing of long flexible rotors can be fortunately reduced to the balancing problem at operational speed. In this condition, for long flexible rotors balancing, the SPB and the TPB based on ICM is considered also useful, as the static correction can be applied in the center of the rotor (near the center of gravity) which reduces (satisfactory vibration) the rotor flex near its first critical speed, before trying to correct the couple.

In all these cases of balancing, a necessary condition is the accessibility to the rotor and its rotating parts such as blades.

Limits of "normal of balancing approaches" respect to industrial production needs

The application of this approaches require that the rotors parts (blades, ..) are accessible to set the weights. The needs of the industrial production is to reduce to a minimum the downtime of the machines. The rotor on-site balancing is the approach to achieve this objective when it is question to solve machine rotor unbalance problem. While this approach can be applied with success in some rotating machine such fan, it cannot be applied to the centrifugal pump in general, and multi-stage centrifugal pumps in particular, because their rotor parts are accessible only by removing the rotor. Therefore the balancing solution is to remove the rotor and balance it on a balancing machine. But this solution, have high cost in terms of maintenance and production missing because the work requires some days (7 to 10), during which the production process involved is reduced or stopped in some cases. It is preferable to plan this solution to be performed during the plant scheduled shutdowns.

When a pump is subject to frequent rotor unbalance and is fundamental for the production process, or has very high maintenance costs, this solution can become unsustainable. It is therefore necessary to find a new approach to return the machines in the acceptable operating conditions as quickly as possible.

The objective of this study is to present a new approach of rotor one- site balancing method applied to multi-stage centrifugal pumps to reduce to a minimum the downtimes and consequently the costs.

4.4.4 Rotor On-site balancing approach applied to Multi-Stage Centrifugal Pump

The multi-stage centrifugal pump considered in this study is used in heavy petrochemical product process in an industrial plant. This machine is frequently subject to unbalance problem because a dirt from the product adheres to the rotor (impeller) and goes to alter the balance state of the rotor. This situation therefore creates unacceptable vibration levels.

4.4.4.1 Problem definition and theoretical approach to resolution

In fact the product in question is a residue of a first stage of refining the crude oil which is reused for feeding a second phase. This product is very viscous and is fed at a temperature of 306 ° C. For local unfavourable conditions a dirt from the product can adhere to the blades causing a phenomenon of unbalance of the pump rotor. The Fig.4.9 schematise the pump rotor. The weight of dirt which causes the unbalance is represented by the red point.

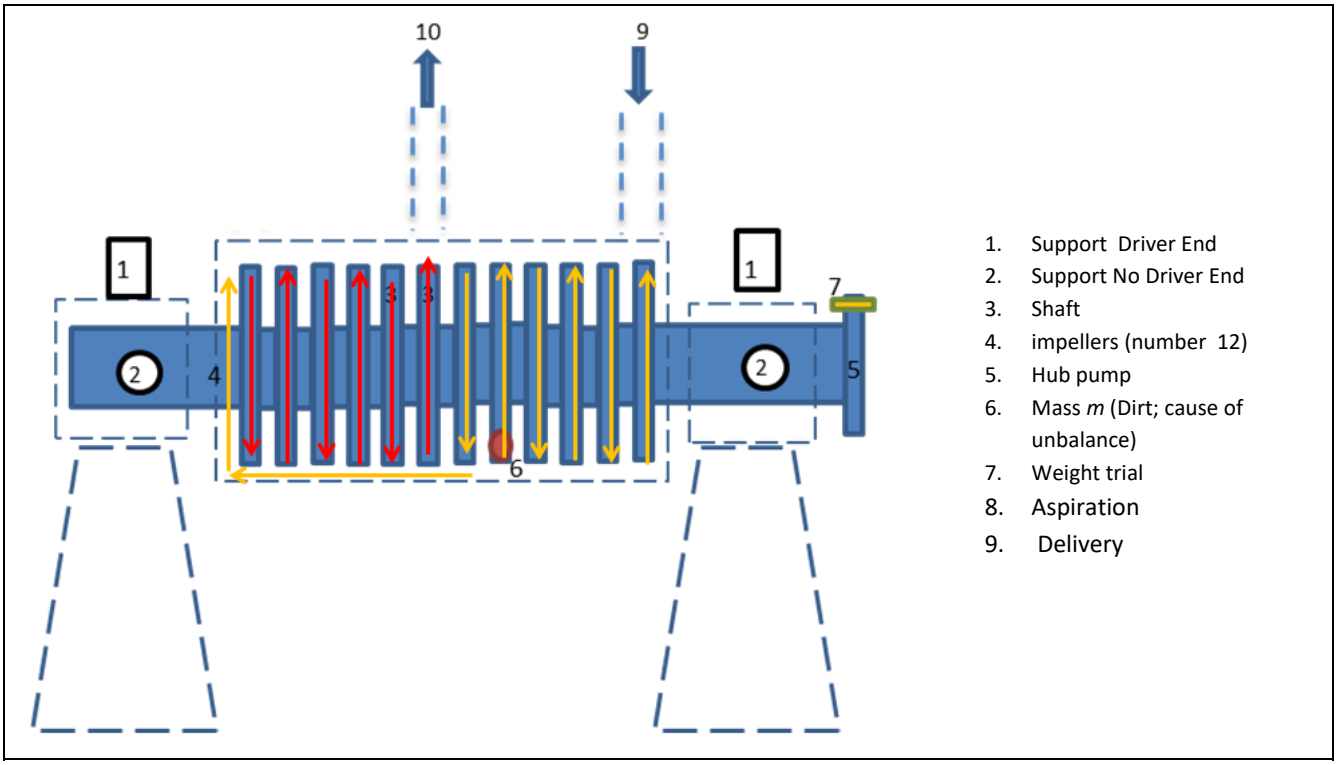

***Figure 4.9**: Schematic representation of Multi-stage Centrifugal Pump unbalanced*

4.4.4.2 Theoretical approach

The pump in a state of unbalance

The Fig.4.10 shows the schematic representation of the forces generated by the unbalance state. Where:

$F = m\omega^2$ is the force of inertia created by the mass of m (Product attached on the impeller) ,
R_{NDE} is the reaction force to the force F on the NDE support and R_{DE} the reaction force to the force F on the DE support.

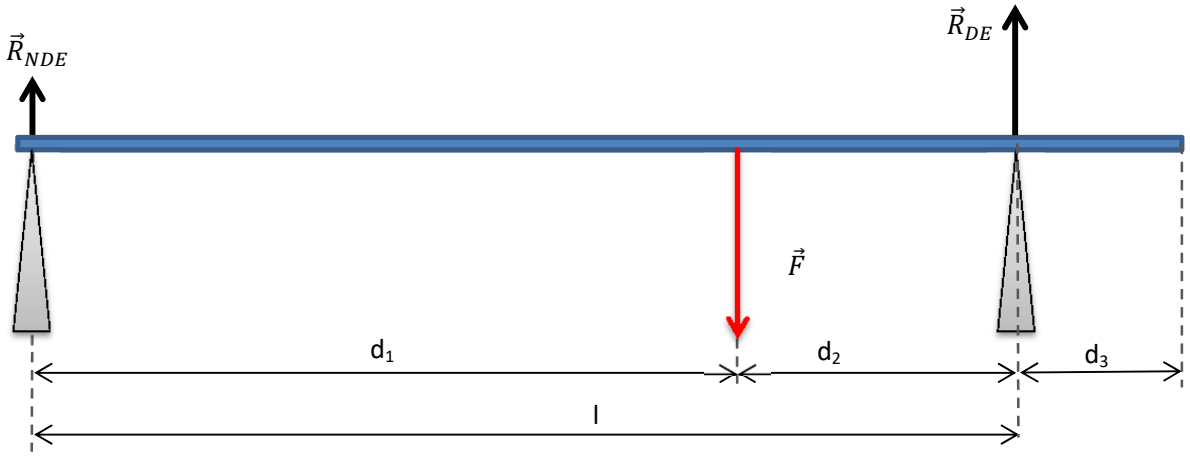

Figure 4.10: *Schematic representation of the forces due to the unbalance of the pump*

Force balance

$$\vec{F} = \vec{R}_{NDE} + \vec{R}_{DE} \qquad \text{(Eq.4.21)}$$

Moments Balance

The balance of moments around the support point on the support DE is described in equation (Eq.4.22) and that around the support point on the support NDE is described in equation (Eq.3.23) .

$$\left.\begin{array}{ll} R_{NDE}\,l = F d_2 & (\text{Eq. 4.22}) \\ R_{DE}\,l = F d_1 & (\text{Eq. 4.23}) \end{array}\right\} \Rightarrow \quad \frac{R_{DE}}{R_{NDE}} = \frac{d_1}{d_2} \qquad \text{(Eq.4.24)}$$

The equation (Eq.4.24), established from the equations (Eq.4.22) and (Eq.4.23) shows that the rapport between the reaction on the two supports $\frac{R_{DE}}{R_{NDE}}$ is equal to $\frac{d_1}{d_2}$, the inverse of the ratio of their respective distances from the point of application of the force *F*.

We assume the vibration magnitude on a support is proportional to the reaction force on this support. Therefore $\frac{R_{DE}}{R_{NDE}} = \frac{V_{DE}}{V_{NDE}}$. Where $\boldsymbol{V_{DE}}$: Vibration amplitude on support DE; $\boldsymbol{V_{NDE}}$: Vibration amplitude on support NDE.

Theoretical consideration for the pump balancing

This part discusses the theoretical possibility to balance the pump (return the vibration normal) applying the mass correction only by an end of the rotor (i.e. the coupling hub). The Fig.4.11 presents the schematic representation of the forces present in the pump balancing.

F is the force of inertia created by the mass of m (Product attached on the impeller), $Z = mr\omega^2$ correction force (where m is the correction weight and r the distance from shaft center).

R'_{NDE} is a new the reaction force on the NDE support after adding the force Z and R'_{DE} the new reaction force on the DE support

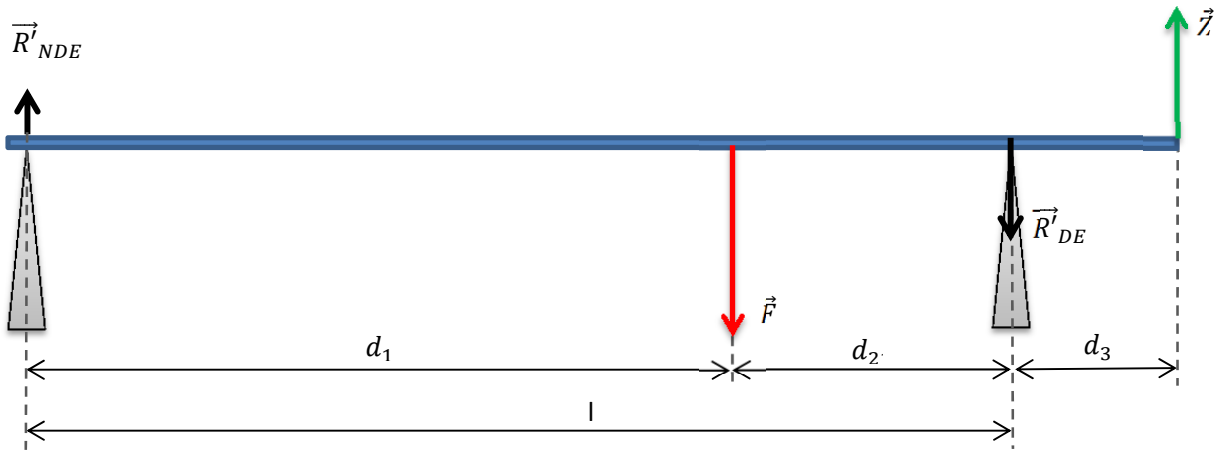

Figure 4.11: *Schematic representation of the forces present in the pump balancing*

Position the T correction force to the extreme (opposite versus of the force F) creates a couple on the rotor. But our aim is to define the balancing condition that brings the vibration measurements the norm nevertheless.

Force balance

$$\vec{F} + \vec{Z} + \vec{R'}_{NDE} + \vec{R'}_{NDE} = \vec{0} \qquad \text{(Eq.4.25)}$$

Moments Balance

After adding the correction force Z , the balance of moments around the support point on the support DE is described in equation (6) and that around the support point on the support NDE is described in equation (7).

$$\begin{cases} R'_{NDE} l = Fd_2 + Zd_3 \quad \text{(Eq. 4.26)} \\ R'_{DE} l = Fd_1 - Z(l + d_3) \quad \text{(Eq. 4.27)} \end{cases} \Rightarrow \begin{cases} R'_{NDE} = \dfrac{Fb + Zd_3}{l} \\ R'_{DE} = \dfrac{Fd_1 - Z(l + d_3)}{l} \end{cases}$$

$$\Rightarrow \begin{cases} R'_{NDE} = \dfrac{Fd_2}{l} + \dfrac{d_3}{l} Z \qquad (Eq. 4.28) \\ R'_{DE} = \dfrac{Fd_1}{l} - \dfrac{(l + d_3)}{l} Z \ (Eq. 4.29) \end{cases}$$

F is a fixed datum linked to the state of unbalance.

The data *c* and *l* are known from the machine design. In general $d_3 \ll l$, the ratio $\frac{d_3}{l}$ is of the order of tenths ($\frac{d_3}{l} \approx 0{,}1$). This means that:

- $R'_{NDE}\ (Z)$ grows slowly in function of Z.
- $-\frac{(l+d_3)}{l} \approx -1{,}1$; which means that $R'_{DE}\ (Z)$ decreases faster in function of Z.

Depending on the relationship between a and b, we can distinguish two cases:

- **Case 1 :** $d_1 < d_3$

In the case 1, $\frac{R_{DE}}{R_{NDE}} = \frac{d_1}{d_3} < 1$. In others terms $R_{DE} < R_{NDE}$. This case is represented in Fig.4.12.

Noting that $R'_{NDE}\ (T)$ is increasing, it is impossible to decrease the sensitivity of reaction force R'_{NDE} to bring back the rate of vibration normal.

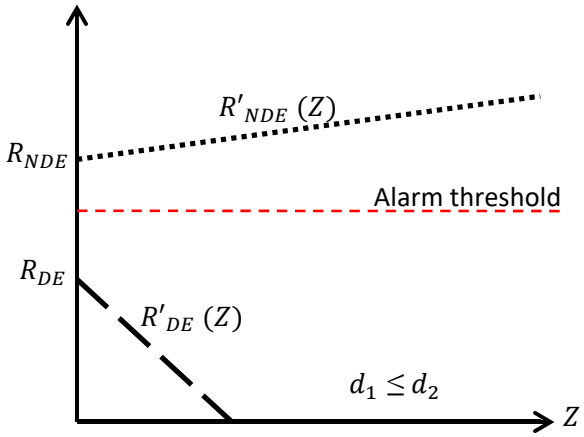

Figure 4.12: *Representation of the reaction forces as a function of the correction force if* $d_1 \leq d_2$

- **Case 2 :** $d_1 > d_2$

The case 2 is represented in the figure x, $\frac{R_{DE}}{R_{NDE}} = \frac{d_1}{d_2} > 1$, in others terms $R_{DE} > R_{NDE}$.

In this case, we must distinguish two sub-cases:

- **Case 2-1 : where R_{DE} is slightly higher than R_{NDE} => d_1 *is slightly higher than* d_2**

When not only the vibration induced on the DE support is higher than the alarm threshold, but also that on the NDE support is higher than the alarm threshold or very close. This case is resubmitted in Fig.4.13 a.

Noting that $R'_{NDE}(0) = R_{NDE}$ and that $R'_{NDE}(Z)$ is increasing:

- If the vibration on the NDE support is higher than the alarm threshold, it will be impossible to bring back the strength of reaction R'_{NDE} to bring back to normal.
- If the vibration on the NDE support is close to the alarm threshold, R'_{NDE} will grow with the increase of T and cause a vibration higher than the alarm threshold before R_{DE} decreases enough to bring back the rate of vibration in the norm on the DE support.

- **Case 2-2: where R_{DE} is very higher than R_{NDE} (or when $\frac{R_{DE}}{R_{NDE}} = \frac{V_{DE}}{V_{NDE}} \geq 2.$) => $d_1 >> d_2$**

Noting that :

- $R'_{NDE}(Z)$ is increasing very slowly,
- $R'_{NE}(Z)$ decrease fast

R'_{DE} will decrease with the increase of T and bring back the vibration magnitude in the mormal on the DE support, before R'_{NDE} increase enough to cause vibration higher than the alarm threshold. This case is shown in Fig.4.13 b.

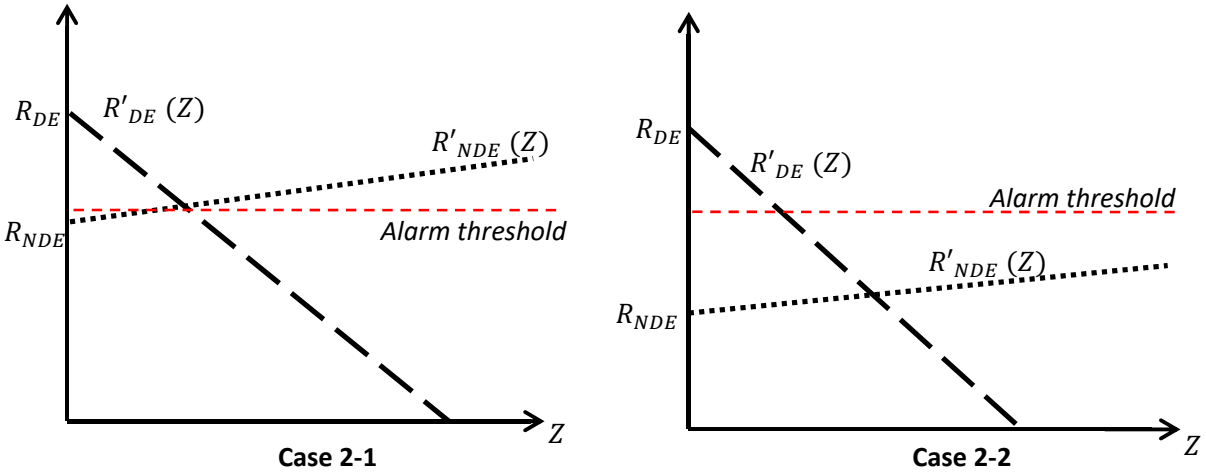

Figure 4. 13: *Representation of the reaction forces as a function of the correction force if* $d_1 > d_3$

4.4.4.3 Solving approaches

An approach for the multi-stage pump rotor on- site balancing must considered the greatest constraint that the pump impellers are inaccessible for the reasons explained above. However, to overcome this constraint, we can make the following important observation on multi-stage pump frequent unbalances :

The machine vibration induced by the unbalance caused by the dirt on the pump is very higher on the support 1 (DE) of the pump with respect to support 2 (DNE). This observation allows us to make the following assumptions:

- It is hypothesized the dirt from the product is adhered to an impeller nearest to the pump support DE on which we measured the high magnitude of vibration.

- The Coupling Hub fitted to the Pump **(CHP)** is considered to be part of the pump rotor (the component indicated with the N° 5 on the figure 9). Therefore it will be assimilated to be a rotor accessible part so the unbalance correction plan (plan where to set the correction weight).

- The first approach consist to apply the ICM considering1balancing plane and 2 vibration measure points. This mean that the system which must be balance includes the Multi-stage Centrifugal Pump rotor and the CHP. With reference to Fig.4.9, this system includes components 3, 4 (12 impellers), 6 and 5.
- The second approach consist to apply the ICM considering 1balancing plane and considering the influence coefficient from only one measure point. In the case where R'_{DE} is very higher than R'_{NDE} (As in the Case 2-2 defined above), in additional to first approach , we propose a second approach. So the single-plane balancing method basing on the influence coefficients from only the support (DE) where the highest vibration has been measure.

The second approach aim to simplify the rotor one site balancing respect to the first one. Therefore the comparative study of those two approaches is necessary to verify if they can be optional.

The first approach

The system rotor + coupling hub is considered as a flexible rotor. As illustrated in Fig.4.9 above, the pump is a double supports which represent 2 different points for vibration acquisition. The correction plane is the plane *P*. The pump rotates at a constant speed. So the number of vibration measure points q=2, the number of balancing plane $p=1$ and the number of balancing speed $n=1$.

[C]: The matrix of influence coefficient size is (2×1)

$$[\mathrm{C}] = \begin{bmatrix} c_{11} \\ c_{21} \end{bmatrix}$$

The coefficients in column *1* of the matrix [C] are determined by taking the ratio of vibrations {We} resulting in the addition of a test unbalance u_{t1} in the balancing plane *1*, and test unbalance.

As shown in Fig.3.9, the support DE will be called support *1* and the support no driver end support*2*.

$$c_{11} = \frac{We_1 - W_1}{u_{t1}} \quad ; \quad c_{21} = \frac{We_2 - W_2}{u_{t1}}$$

To take into account the modules and phase of vectors, the coefficients are expressed in complex numbers. The matrix [C] is rectangular and is thus not invertible. They have to use a specific method to minimize residual vibrations. Unbalance correction obtained in this case is descript in the following equation ($Eq.4.30$) :

$$\mathrm{u_c} = -\left\{\begin{bmatrix} c_{11}^* \\ c_{21}^* \end{bmatrix}^t \begin{bmatrix} c_{11} \\ c_{21} \end{bmatrix}\right\}^{-1} \begin{bmatrix} c_{11}^* \\ c_{21}^* \end{bmatrix}^t \begin{Bmatrix} W_1 \\ W_2 \end{Bmatrix}$$

$$\boldsymbol{u_c} = -\frac{\boldsymbol{c_{11}^* W_1 + c_{21}^* W_2}}{\boldsymbol{c_{11}^* c_{11} + c_{21}^* c_{21}}} \qquad (Eq.4.30\ )$$

The second approach

The vibration acquisition point considered on the pump is the support DE. The correction plane is the plane P. The pump rotates at constant speed, so the number of balancing speed *n*=1. The number of vibration measure points *q*=1, the number of balancing plane *p=1* and the influence coefficient is $c_{11} = \frac{We_1 - W_1}{u_{t1}}$;

Unbalance correction obtained in this case is descript in the following equation ($Eq.4.31$) :

$$\boldsymbol{u_c} = (c_{11}^* c_{11})^{-1}(c_{11}^* W_1)$$

$$\boldsymbol{u_c} = \frac{\boldsymbol{c_{11}^* W_1}}{\boldsymbol{c_{11}^* c_{11}}} \qquad (Eq.4.31)$$

4.5 Experimental study: Application to industrial multi-stage pump

This section presents the on-site balancing of the MSCP (12 stage). The MSCP considered in this experimental study is used in heavy petrochemical product process in an industrial plant. This machine is frequently subject to unbalance problem because the dirt from the product adheres to the rotor (impeller) and goes to alter the balance state of the rotor. This situation therefore creates unacceptable vibration levels .

4.5.1 Description of the pump

4.5.1.1 Description of the pump

This pump is driven by an electric motor via a multiplied speed, as shown in Fig. 4.14. The motor is three-phase type which power is equal to1700 kW, and its rotation speed is 1492 rev/min. The multiplier has a transmission ratio of approximately 3.2. therefore the pump rotation speed is equal to 4783 rev/min. On the multiplier fourth proximity sensors (Eddy Probe) are mounted on the supports in the vertical direction.

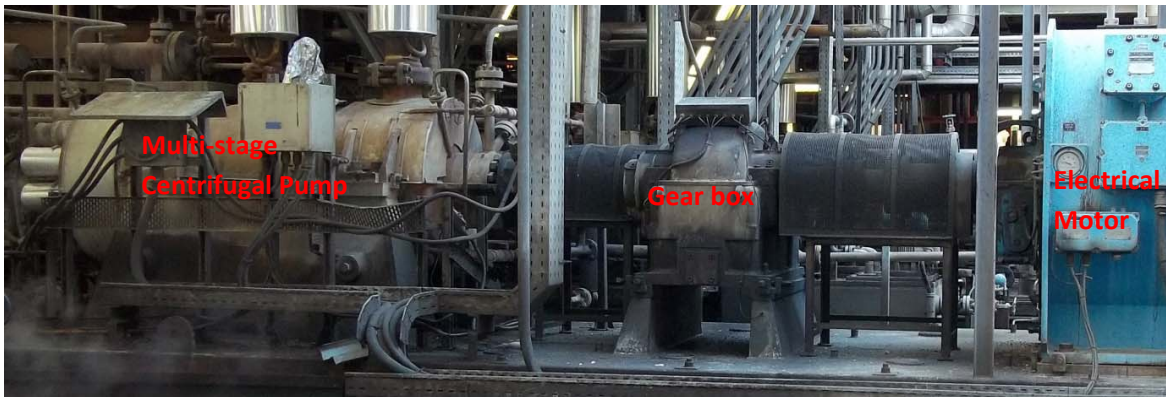

Figure 4.14: *Global view of motor , gear box and pump*

4.5.1.2 Pump Description

The pump is subject to frequent unbalance linked to the dirt form the product of exercise. In fact the product in question is a residue (vacuum residue) of a first stage of refining the crude oil which is reused for feeding a second phase. The product is very viscous and is fed at a temperature of 306 °C. For local unfavourable conditions a dirt adheres to rotor impellers causing a phenomenon of unbalance of the rotor. With reference of Fig.3.9, the pump has 12 impellers. We can consider them in numerical order from N°1 to N°12 starting from the support 1(support DE) to support 2 (support NDE). The pump is designed to allows the product passes progressively from stage 1 to 6, the corresponding steps from the impeller N°1 to N°6. From the stage 6 the product is sent to the impeller N°12 which corresponds to the stage 7 and then the impeller N°11which corresponds to the stage 8 and progressively until the impeller N°7 which corresponds to the stage 12. This design is aimed primarily to reduce the pump axial thrust.

The length of the steel shaft of the MSCP is l=3297 mm. The shaft is brought by two cylindrical hydrodynamic bearings. The maximum residual imbalance is 10,9 g.cm. The rotors weight is 218 kg. The pumped liquid is vacuum residue, its capacity 120 m^3. The pump speed is 4783 RPM .

Table 4.1: *Pump Allowable vibration.*

	Allowable vibration
Normal	40 µm peak to peak
Alarm	54 µm peak to peak
Shutdown	70 µm peak to peak

4.5.1.3 Description of the Eddy-Current sensors

The pumps is monitoring online with eddy probes which measure shaft motion in axial direction *z* on the support *NDE* and in direction *X'* and *Y'* for each of the two supports as shown in Fig.4.15. Displacements of the shaft are measured in micro with detection peak-to-peak.

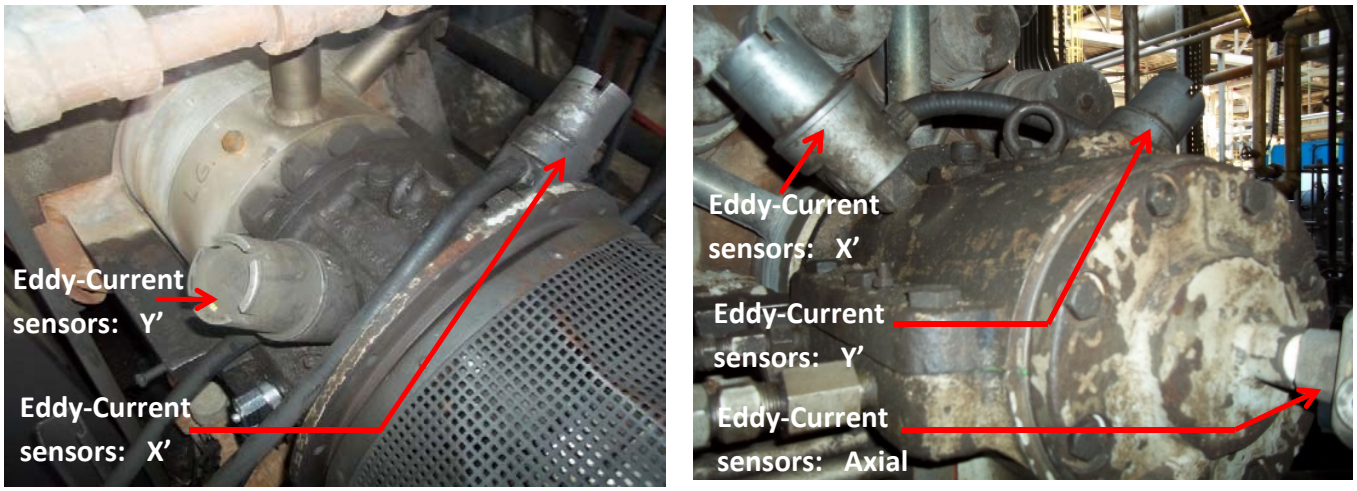

a) Pump support DE b) Pump support NDE

Figure 4.15: *Pump Supports*

The eddy-current sensors have been descripted in the chapter 1.

4.5.1.4 Description of the joint

The shaft of the pump is connected to the gear box by a Meta-stream coupling as shown in Fig.4.16. The CHP, which is extern, is consider as an accessible plane of the pump rotor where we can set the imbalance correction weight. This hub is connected to the coupling block by 10 bolts at regular distance

and angle (36 degrees). Then the weight is added on the hub by increasing the weight of the bolt and screw together at one or two precise positions.

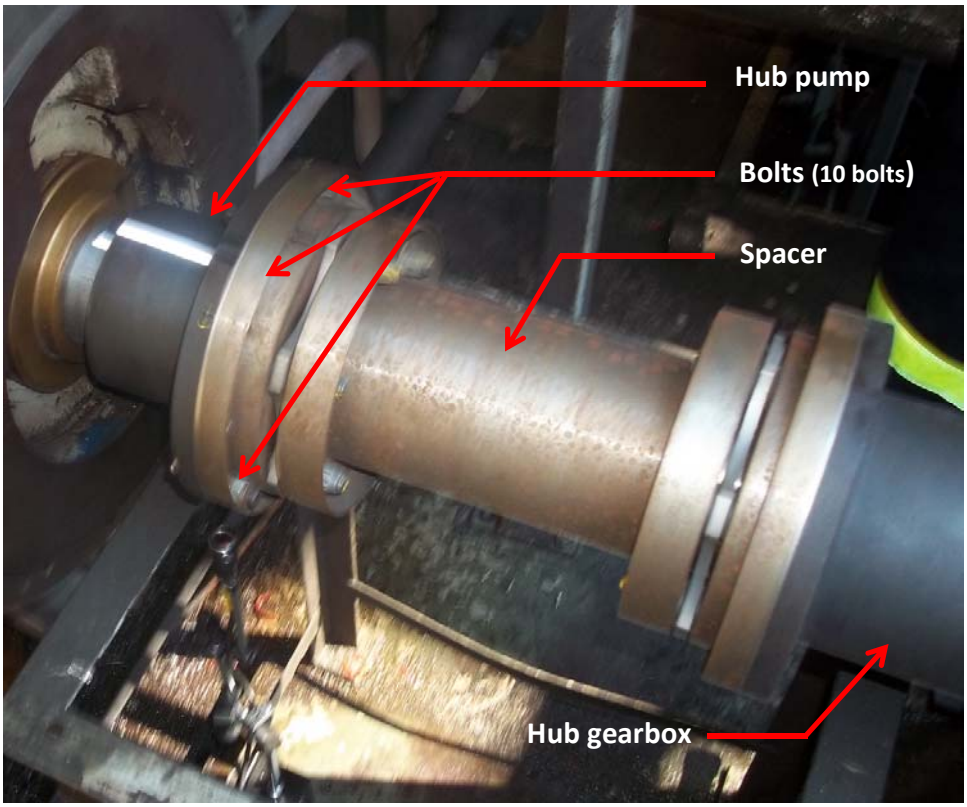

Figure 4.16: *Description METASTREAM Coupling*

4.5.1.5 Microlog description

SKF Microlg GX with functionality: two channel route measurements, and one-or two-plane static or dynamic couple balancing applications.

- **SKF Microlog application modules**

SKF Microlog Analyzer GX series (CMXA 75) presented in Fig.4.17 is an portable instrument with a wide range of application specific firmware modules:

- *Run up Coast down*: The Run up Coast down module analyses data from machines where noise or vibration levels are changing with speed, time or load (applications that cause transient phenomena) to establish the critical/ resonant speeds of a machine.

Figure 4.17: *SKF Microlog Analyzer GX*

- *Frequency Response Function:* The Frequency Response Function (FRF) module is designed to enable a user to quickly establish a structure's properties (accelerance, apparent mass, mobility, impedance stiffness or compliance). Color coding of the FRF indicates the selectable level of coherence. A key feature of this module is its ability to automatically detect and reject double hits.
- *Bump Test*: A Bump (rap) Test is an impact test carried out to excite the machine and measure its natural frequencies. This helps to determine if resonance is responsible for high noise or vibration levels or if there is a potential machinery problem.
- *Data Recorder:* Signals from sensors connected to the SKF Microlog GX series are digitally recorded and stored as standard .wav files allowing a user to listen to and filter signals. These files can also be sent via email or transferred directly to SKF's Analysis and Reporting module for post-processing. Using the storage capacity of SD cards allows a user to record many hours of continuous raw data for analysis at a later date or upon return to the office.
- *Analysis and Reporting module*: The Analysis and Reporting module is a PC based software application for transferring, displaying and analysing data generated by the application modules of the SKF Microlog GX series. Once uploaded, data is automatically displayed in the application's main window, and a single mouse click is all that is needed to view the data in a powerful, interactive graphical plot.
- *Balancing:* The Balancing application resolves single-plane, two-plane and static-couple balances (three planes) with high precision.

- **SKF Microlog balancing module**

This module allows precision balancing of rotating machinery across a wide range of speeds. The Balancing application resolves single-plane, two-plane and static-couple balances (three planes) with high precision. Clear, comprehensive setup menus and easy-to-follow display screens with graphical data representations combined with the ability to set an acceptance limit ensure easy operation as shown in Fig. 4.18. The SKF Microlog GX series can accept a variety of trigger signals including key phasors, tachometers and strobes.

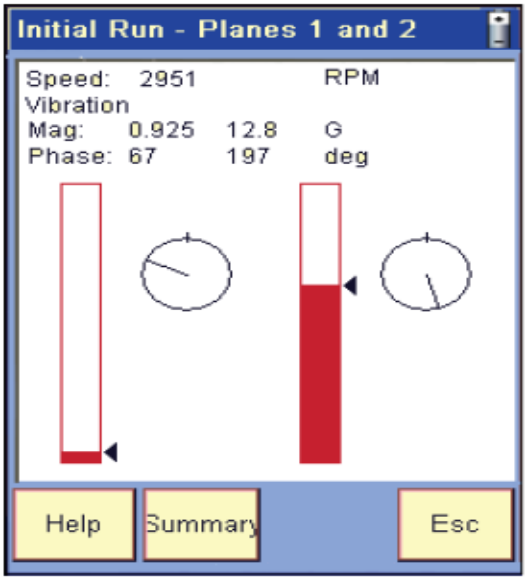

Figure 4.18: *Graphical data representations in Balancing application resolving two-plane balancing*

Polar Vector plots show vibration amplitude and phase. Phase is the angular difference between a known mark on a rotating shaft and the shaft's vibration signal. Vibration and phase readings are taken to establish the magnitude and position of the unbalance force. On screen instructions advise where to attach the correct amount of compensation weight – or where and how much material to remove. The SKF Microlog GX as other SKF microlog version such as CMVA 55 Microlog [41], is capable of solving any dynamic balancing problem using the static couple approach. In the balancing process, it is important to note that the trial weight must produce a significant change (either 30° in phase or 30% in the amplitude of vibration) in order for the computations to be accurate. This is referred to as the 30-30 rule.

4.5.2 Experimentation

4.5.2.1 Determine the state of the machine and establish that unbalance is the actual problem

We determined the state of the machine vibration is inacceptable, and it is established that unbalance is the problem. In facts on the spectrum shown in Fig.4.19, the peak detected at the frequency corresponding to the rotation speed are very high (61.69 µm in direction *X'* and 72,78 µm in direction *Y'*) than any other peak. It is thus the main cause of high vibration.

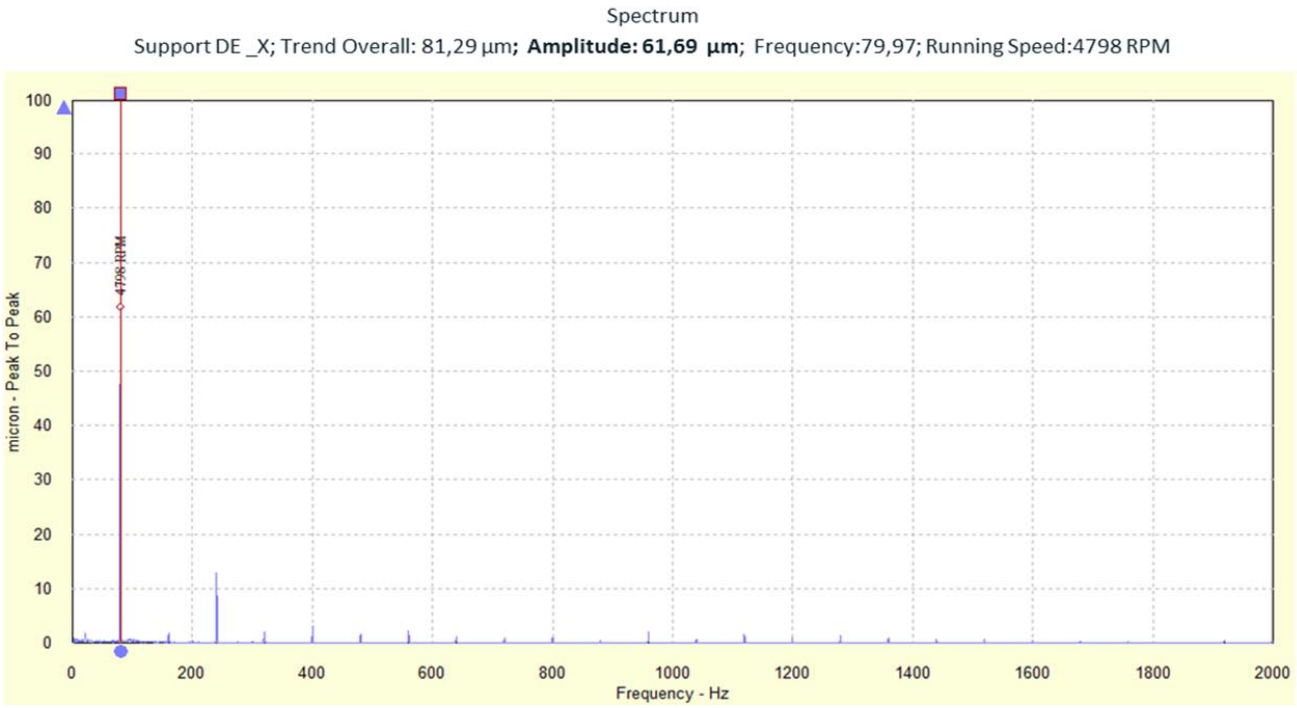

a) *Vibration Spectrum on support-DE in direction X'*

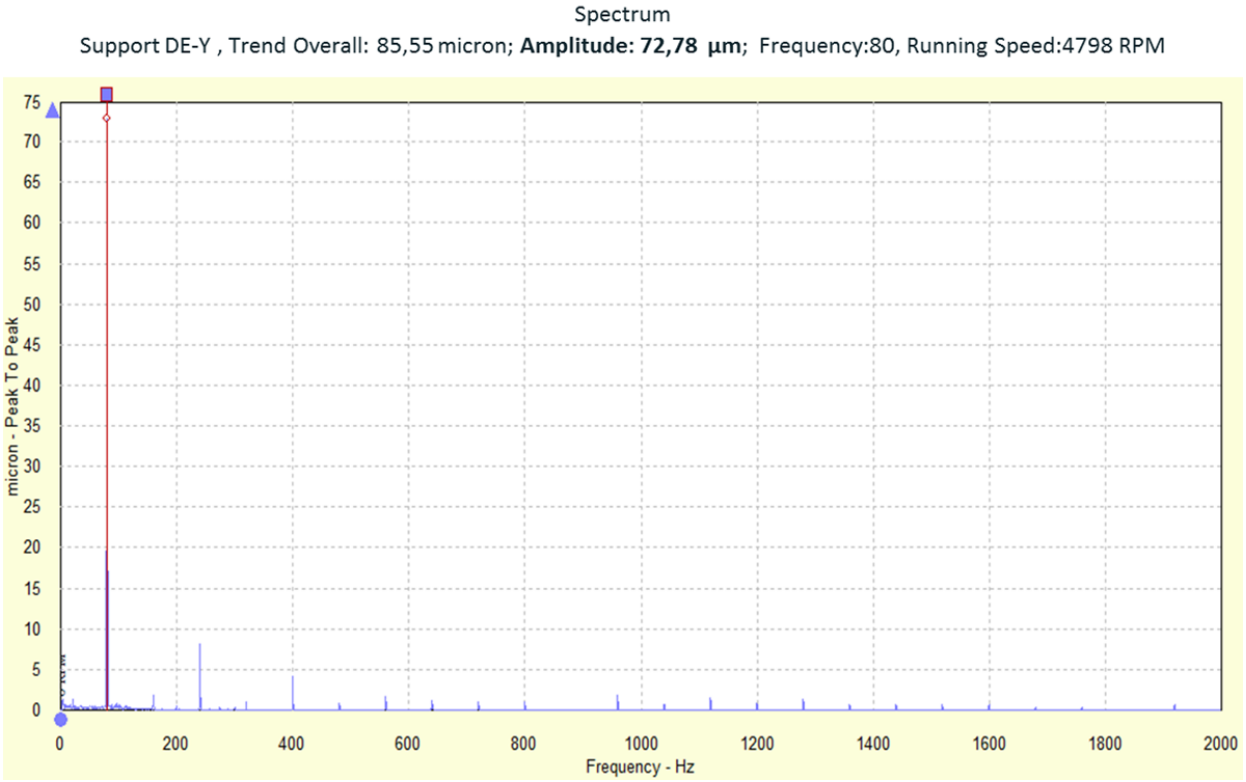

b) *Vibration Spectrum on support-DE in direction Y'*

Figure 4.19: *Vibration Spectrum on support-DE showing the unbalance*

4.5.2.2 Two different approaches of Balancing Procedure

The aim of this study is to establish a method of balancing of multistage centrifugal pumps in site without access to the rotating rotor. The first approach we present, takes into account the vibration of both pump supports. It use one plane and two vibration acquisition supports. It will be called procedure for "*Single - Plane Balancing and two support*" using Influence Coefficient Method.

The second approach has for objective to simplify the problem of unbalance of the double support pump to that of only one vibration acquisition support. It is considered only the support that has the highest vibrational value (as formulated in the assumptions made in section 4-1-1). It is the "*Single - Plane Balancing and one support*" using Influence Coefficient Method.

The acquisition of the measures for both the balancing approaches were doing simultaneously.

The first approach: Balancing the System rotor + coupling hub.

We use the *procedure for single - plane balancing and two support using Influence Coefficient Method*. The Microlog connected to the eddy probes and the Keyphasor allow you to read vibration amplitudes (V) and the phase (θ). This parameters enables you to write the vibration rotating vectors with complex numbers ($\overrightarrow{\boldsymbol{W}} = \boldsymbol{We^{j\theta}}$). That will be used in a special program prepared in excel for the calculations relating to the application of Influence Coefficient Method.

Device for vibrations and phases measurement

To apply the balance with one plan and two supports of vibrations measurement, it is sufficient one point of acquisition of each support. Since we have a pump that equipped with 4 sensors (2 by support), we will profit to compare the results of the two-way acquisition *X'* and *Y'*. So we Consider the pair of sensors Eddy-Current sensors X' of supports DE and NDE, and the pair sensors Eddy- Current sensors Y' of supports DE and NDE. As normal procedure the instrument Microlog connected to the pair of sensors Eddy-Current sensors X' (and then to the pair of sensors Eddy-Current sensors Y) from a room, and to a keyphasor for reading of the phases. From the readings vibration of values in micro and phase, each vector rotary of vibration can be written in complex number form: $\boldsymbol{W = We^{j\theta}}$. And the application of *ICM* is possible.

The second approach :

For the second approach we use the procedure for single plane balancing and single support using ICM. It is a balancing procedure on one plane and one vibration acquisition point, being interested only support DE. The instrument Microlog has a program designed for balancing on the single plane which also implies a single point of acquisition of vibration.

An accelerometer with magnetic base is fixed on the support DE and a key phasor are connected to the instrument Microlog to connect vibration and phase (The lag phase is the angle from the reflective tape on the rotor (hub pump) to the vibration vector, for each vibration vector). The reflective tape is attached to the hub of the coupling in correspondence of a bolt in such a way that the ten bolt of the hub correspond each to a well precise angle (0 °, 36 °, 72 °, 108 °, ..., 360 °).

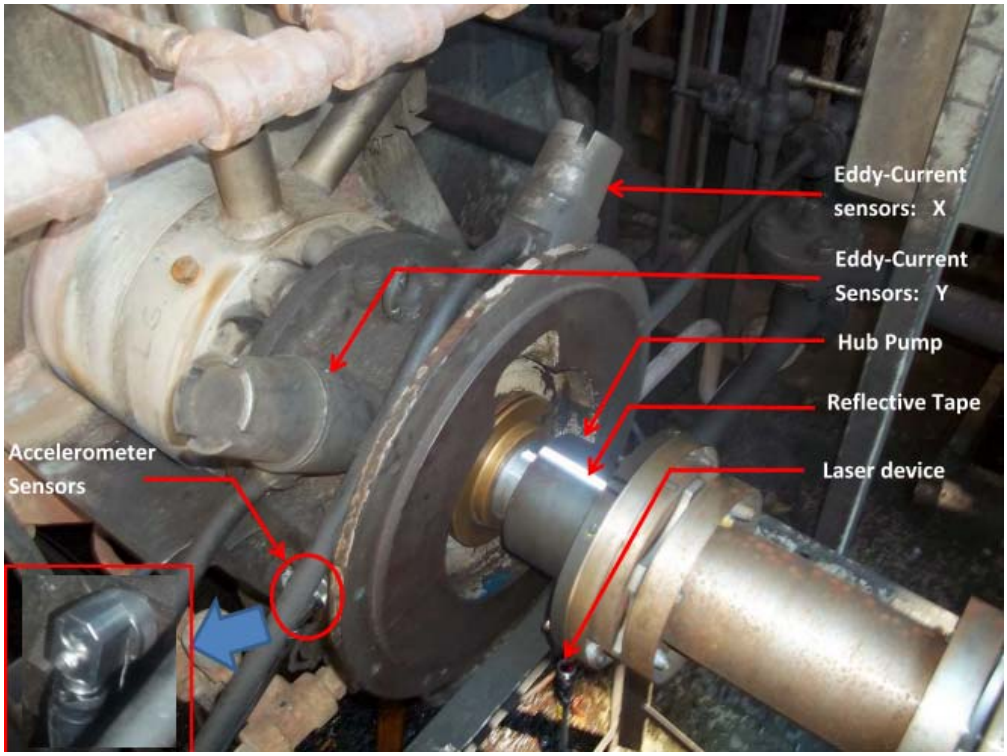

Figure 4.20: *Device for vibrations and phases measurement*

Procedure for Single - Plane Balancing Using Influence Coefficient Method

The procedure for SPB using *ICM* is synthesised in the following steps.

1) Installation of the measuring device (adhesive tape and laser and sensors). With the machine at rest, a reflective tape is attached on the rotor. A key phasor (laser device) is installed under

the rotor in such a way that the laser can reflect on the tape once during the rotation of the rotor as shown in Fig.4.20 above.

2) Run the machine at the selected speed (4978 RPM) and measure the synchronous vibration amplitude and phase lag of the tacho pulse to the next peak of the synchronous vibration signal.
3) Stop the rotor and attach a trial mass at an angle from the Reflective Tape, using the same convention as step 2.
4) Start the rotor and record its vibration amplitude and phase measured at the same speed as step #2.
5) Determine the size of the correction mass and its position on the rotor.
6) Remove the trial weight and add the calculated correction mass.
7) Start the rotor and record its vibration amplitude and phase at the same speed
8) If the new vibration data is within an acceptable range, then the balancing job is complete; otherwise, either a trim balance is required (back to Step #4) or unbalance may not be the problem.

4.5.2.3 First approach : Measures one plane and two supports

Vibration measurements were carried out on the support DE and that NDE. As shown in Fig.4.15, each pump support has two eddy probe radial sensors in the directions *X'* and *Y'*. The resulting vibration measurements and the correction weights calculated are reported in the tables 4.2 and 4.3.

Acquisition point in direction X'

Table 4.2: *Vibration initial measurement in direction X' and the trial weight*

Direction	**W_1 (Support DE _vibration vector)**		**W_2 (Support NDE _vibration vector)**		**U_e (**trial mass)	
	Modulo (µm)	Phase (degrees)	Modulo (µm)	Phase (degrees)	Modulo (g)	Position (degree)
X'	61,69	128	13,72	308	10	144

Table 4.3: *Vibration measurement in direction X' after adding trial and the correction weights calculated*

Direction	**W_{e1}** (Support DE _vibration vector with trial mass)		**W_{e2}** (Support NDE _vibration vector with trial mass)		**Correction weigh**	
	Module (µm)	Phase (degrees)	Modulo (µm)	Phase (degrees)	Weigh (g)	Position (degree)
X'	31,45	129	10,5	308	**20,64**	**145**

Acquisition point in direction Y'

Table 4.4: *Vibration initial measurement in direction Y' and the trial weight*

Direction	**V_1** **(Support DE _vibration vector)**		**V_2** **(Support NDE _vibration vector)**		**U_e** **(**trial mass)	
	Modulo (µm)	Phase (degrees)	Modulo (µm)	Phase (degrees)	Modulo (g)	Position (degree)
Y	72,11	218	12,01	38	10	144

Table 4.5: *Vibration measurements in direction Y' after adding trial and the correction weights calculated*

Direction	**W_{e1}** (Support DE _vibration vector with trial mass)		**W_{e2}** (Support NDE _vibration vector with trial mass)		**Correction weigh**	
	Module (µm)	Phase (degrees)	Modulo (µm)	Phase (degrees)	Weigh (g)	Position (degree)
Y	36,97	218	15,55	38	**19,98**	**145**

Correction according to the first approach: single-plane and two support

The mass and the angle of the correction weight has been calculated using the equation (27). Considering that the weight for unbalance correction is attacked as part of bolts of the coupling hub, we

calculated the distribution of equivalent masses as part of the two bolts closer. That is to say from position 145°, so the bolts closer are 144° ($\frac{8}{10}\pi$) and 180° (π) as expressed by the equation (Eq.4.28)

$$\boldsymbol{U_c e^{\frac{806}{1000}\pi j} = U_{c1} e^{\frac{8}{10}\pi j} + U_{c2} e^{\pi j}} \qquad \text{(Eq.4.28)}$$

Where U_{c1} and U_{c2} are the mass of correction weight corresponding respectively to the position at 144° and 180 °. This correction weights are been calculated and reported in the tables 4.6.

Table 4.6: *Correction weights in the first approach: single-plane and two support*

Direction	U_c			U_{c1}			U_{c2}		
	Module (g)	Phase (degree)	Phase (radian)	Modulo (g)	Phase (degree)	Phase (radian)	Modulo (g)	Phase (degree)	Phase (radian)
X'	20,64	145	$\frac{806}{1000}\pi$	20,14	144	$\frac{8}{10}\pi$	0,61	180	π
Y'	19,98	145	$\frac{806}{1000}\pi$	19,50	144	$\frac{8}{10}\pi$	0,59	180	π

4.5.2.4 Second approach : Measures one plane and one support approach

On the support DE, there are two sensors Eddy probe in the radial directions X' and Y'. The resulting vibration measurements and the correction weights calculated are reported in the table 4.7.

Eddy probe in the radial directions *X'*

Table 4.7: *Vibration initial measurement and the trial weight*

Sensors	W_1 (Support DE _vibration vector)		Ue (trial mass)	
	Modulo (µm)	Phase (degrees)	Weigh (g)	Position (degree)
Eddy Probe X'	61,69	128	10	144

Table 4.8: *Vibration measurements after adding trial and correction weight calculated*

Sensors	**W_{e1} (Support DE _vibration vector)**		**Correction weigh calculed**	
	Modulo (µm)	Phase (degree)	Weigh (g)	Position (degree)
Eddy Probe X'	31,45	129	**20,39**	**145**

Eddy probe in the radial directions Y'

Table 4.9: *Vibration initial measurement and the trial weight*

Sensors	**W_1 (Support DE _vibration vector)**		**Ue (trial mass)**	
	Modulo	Phase (degrees)	Weigh (g)	Position (degree)
Eddy Probe Y'	72,11 (µm)	218	10	144

Table 4.11: *Vibration measurements after adding trial and correction weight calculated*

Sensors	**We1 (Support DE _vibration vector)**		**Correction weigh calculed**	
	Modulo (µm)	Phase (degree)	Weigh (g)	Position (degree)
Eddy Probe Y'	36,97	218	**20,51**	**145**

Accelerometer in horizontal direction

Table 4.12: *Vibration initial measurement and the trial weight*

Sensors	**W_1 (Support DE _vibration vector)**		**Ue (trial mass)**	
	Modulo (mm/s)	Phase (degree)	Weigh (g)	Position (degree)
Accelerometer	2,89	83	10	144

Table 4.13: *Vibration measurements after adding trial and correction weight calculated*

Sensors	**We1 (Support DE _vibration vector)**		**Correction weigh calculed**	
	Modulo (mm/s)	Phase (degree)	Weigh (g)	Position (degree)
Accelerometer	1,51	83	**20,93**	**145**

In accordance with the method described above, the mass of correction weights U_{c1} and U_{c2} corresponding respectively to the position at 144° and 180 ° are been calculated and reported in the table.

Table 4.14: Correction weights in one plane

Direction	**U_c**		**U_{c1}**		**U_{c2}**	
	Module (g)	**Phase (degree)**	**Module (g)**	**Phase (degree)**	**Module (g)**	**Phase (degree)**
Accelerometer	20,93	145	20,43	144	0,62	180
Eddy Probe X'	20,39	145	19,90	144	0,60	180
Eddy Probe Y'	20,51	145	20,02	144	0,61	180

4.5.2.5 Actual correction weight adding

Observing the data reported in tables 4.6 and 4.14, we can note that the values of U_{C2} are much lower than those of the U_{c1} ($U_{c2} \approx 0{,}03\ U_{c1}$). This is due to the fact that the theoretical position correction at 145 ° is almost equal to that of the bolt positioned at 144 °. Consequently, considering the difference between 145 ° and 144 ° negligible, we will fix the correction weight U_c at position 144 °.

In addition we observe that the values of U_c calculated for the different approaches and different sensors are not perfectly equal, but their difference is less than 5% ($\frac{\Delta U_c}{\overline{U_C}} < 5\%$).

To balance the rotor, we considered the correction weight resulting from the calculations based on vibration measures by the accelerometer in second approach: measures one plane and one support approach: $U_c = 20{,}9$ g.

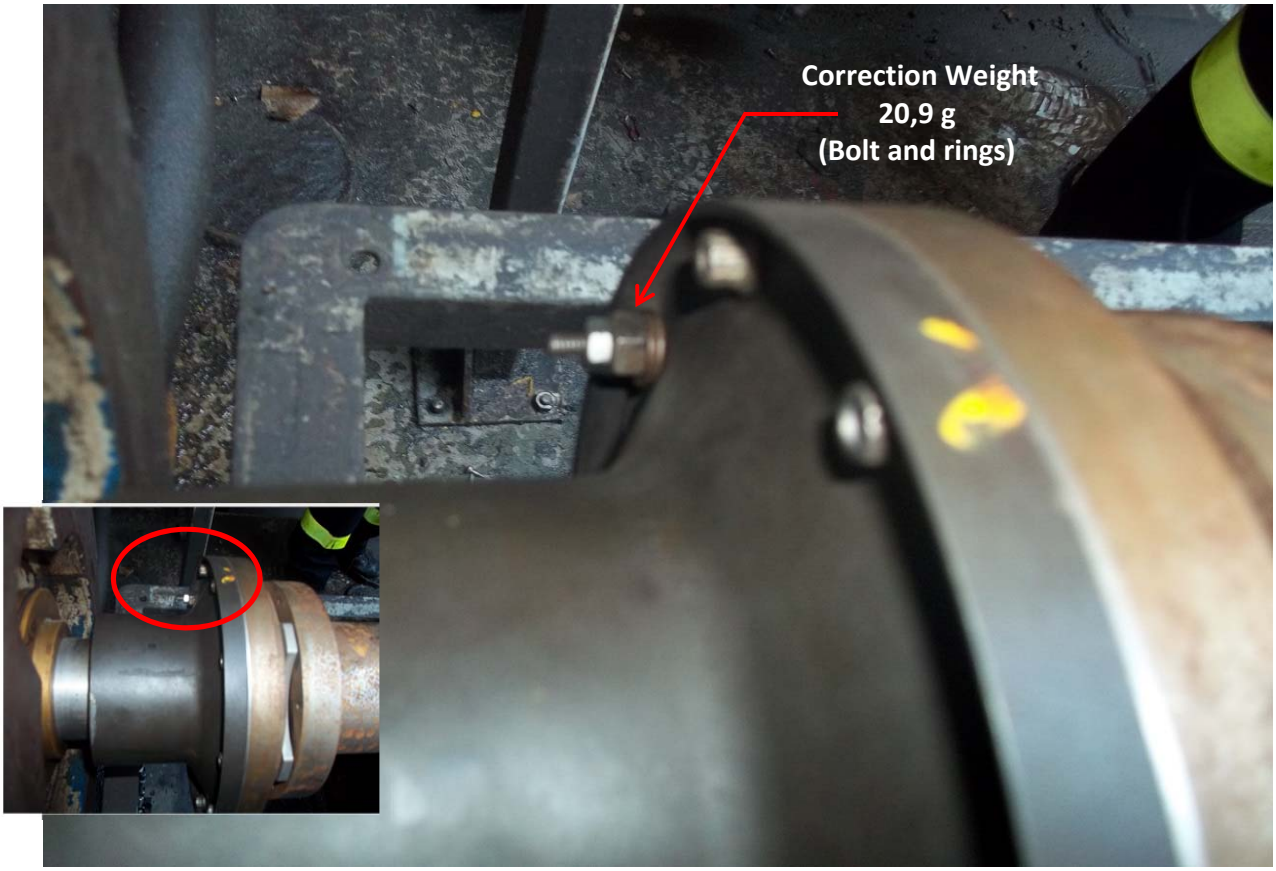

Figure 4.21: *Addition of the correction weight*

The Fig.4.21 shows, the actual weight of correction (20,90 g) attacked to the position 144 ° angle.

Residual vibration after addition of the correction weight

The residual vibrations measured on the support DE by the accelerometer and the two sensors Eddy probe in directions *X'* and *Y'*, and those measured on the support NDE by the two sensors Eddy probe in *X'* and *Y'* directions are given in Table 4.15.

Table 4.15: *Residual vibration values measured after correction weight Addition*

Direction	**W_{c1}**
Sensors	Modulo
Accelerometer	0,51 (mm/s)
Eddy Probe X'	13,97 (µm)
Eddy Probe Y'	19,26 (µm)

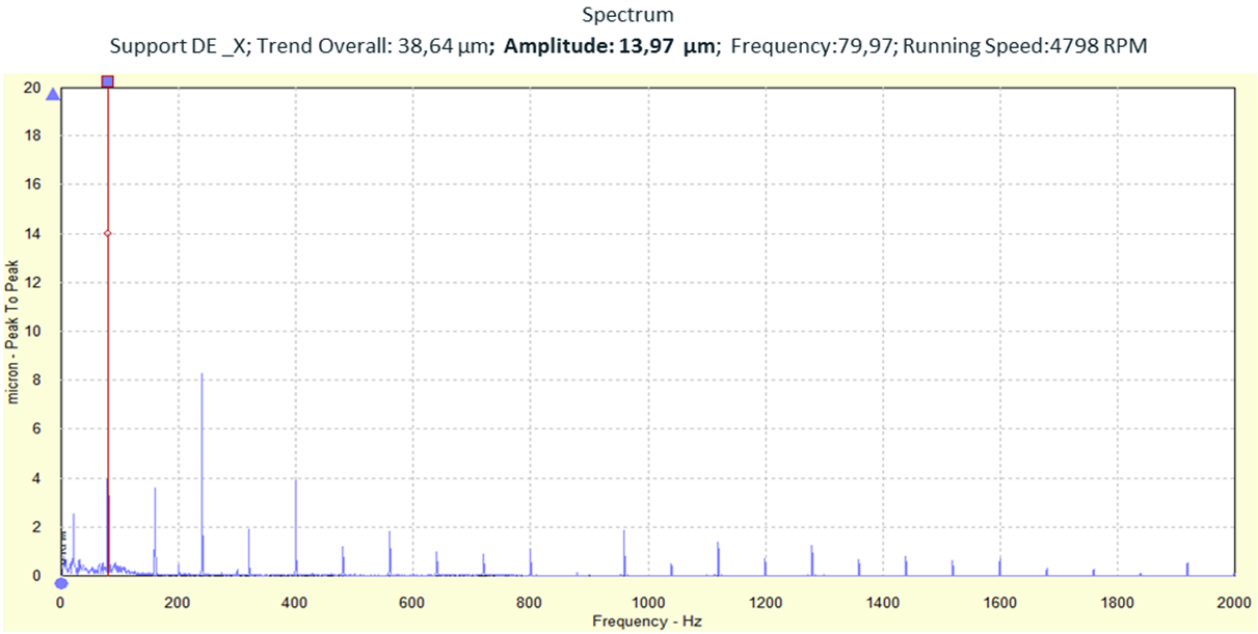

a) Vibration Spectrum on support-DE in direction X' after Adding the correction weight

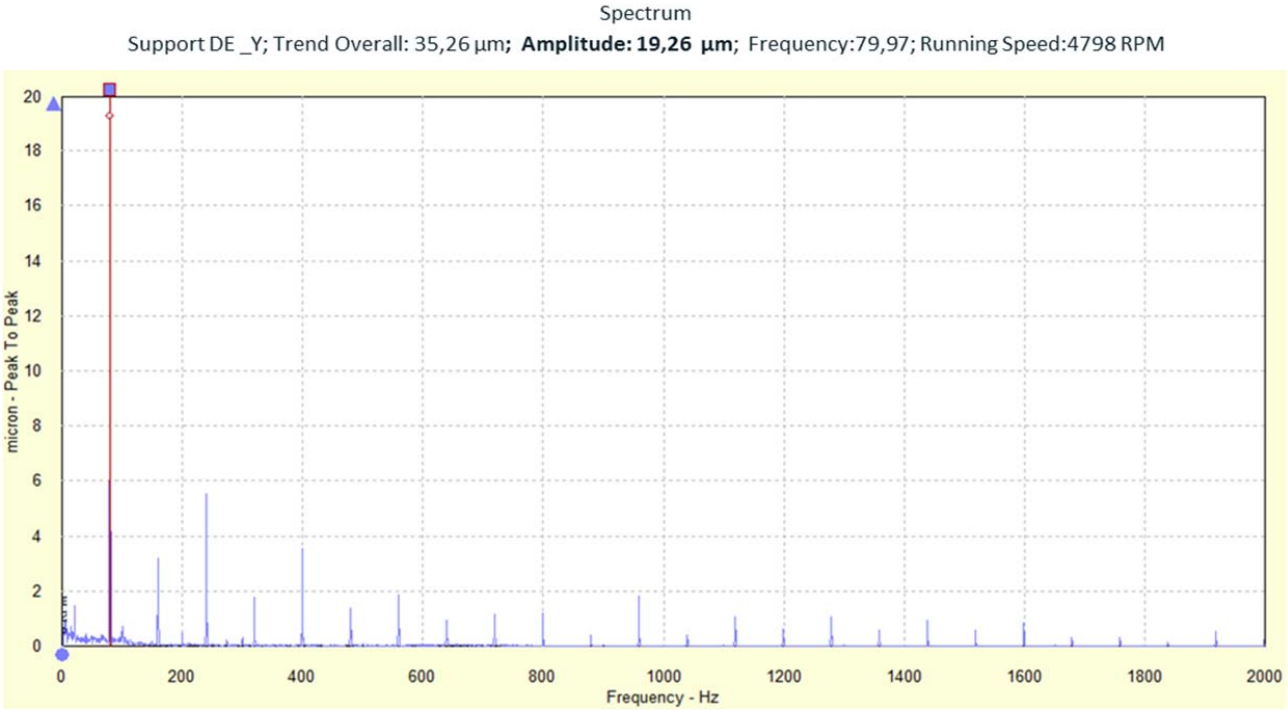

b) Vibration Spectrum on support-DE in direction Y after Adding the correction weight

Figure 4.23: *Vibration Spectrums on support-DE Adding the correction weight*

Verification

The pump rotor balancing obtained by adding a correction weight to the CHP has permitted to reduce considerably vibration level which is turn to be normal. However it is important to verify that the added weight did not increase pump axial vibration and not cause any problem to the gear box vibrations.

Pump axial vibration

The pump axial vibration values have not undergone any substantial change as reported in table 4.16. These vibrations had measured with eddy probe sensors as shown above in Fig.4.15-b. The values remained normal even after the balancing.

Table 4.16*: Pump axial vibration values before and after balancing*

Vibration measure point		Vibration value (µm) Before balancing	Vibration value (µm) After balancing	**Vibration change**
2	Support NDE	5,3	5,1	-3,7%

Gear box vibrations

As reported in table 4.17, the gearbox vibration values have not undergone any substantial change. These vibrations had measured with eddy probe sensors. The values remained normal even after the balancing. The added weight did not affect the reliability of the gearbox.

Table 4.17: *vibration values on the gearbox before and after balancing*

Vibration measure point		**Vibration value (µm) Before balancing**	**Vibration value (µm) After balancing**	**Vibration change**
4	Shaft 2 _SDE	34,57	35,06	1,4%
3	Shaft 2 _SNDE	-	-	-
1	Shaft 1_SDE	10,93	10,75	-1,65%
2	Shaft 1_SNDE	4,38	4,31	-1,60%
Shaft 1 : shaft of the Gear box, connected to the motor shaft by a coupling *Shaft 2* **:** shaft of the Gear box, connected to the pump shaft by a coupling				

4.5.2.6 Synthesis

The objective of this study is to demonstrate, at first, on the basis of the hypotheses done above (section 3.1.1) that the multi-stage centrifugal pump unbalance can be solved using the CHP. This has been done using ICM with the approach " 1 Plane Balancing and two support" (Approach 1) which consists in considered 2 vibration measure points and one correction plane (CHP).
In a second step, this study showed that in the same hypotheses of unbalance, the balancing done using ICM and the approach of "One Plane Balancing and one support" (Approach 2), in which the vibration measure point is the support DE, provides nearly the same result as the approach1.
The imbalance correction weights are almost equal for the two approaches.

For the approach1: the calculated value of the correction weight is 20,64 g according to the vibrations measured with sensors Eddy Probe in the direction *X'*, and 19,98 g according to those in the *Y'* direction.

For the approach 2: the calculated value of the correction weight is 20,39 g according to the vibrations measured with sensors Eddy Probe in the direction *X'* and 20,51 g according to those in the direction *Y'*. In addition the value calculated using the accelerometer in the horizontal direction is 20,93 g. Compared to the average of the first two values the difference is about 2%.

This allows us to say that the approach 2 can validly replace the approach 1 in the hypotheses established. The approach 2 has the advantage to be relatively more simple and more easily applicable. Whereas many machines are not equipped with fixed sensors (for cost reason), this result shows how the approach 2 can be useful.

Advantage:

1. The rotor unbalance problem of double pump support can be solved from one support in the hypothesis established.
2. In the approach 2, eddy probe sensors and accelerometer, did the same result. The sensors eddy probe are fixed sensors, which are mounted only on certain critical machines for cost reason. The accelerometer is a sensor movable that is attacked (by magnetic base) to the pump support and therefore can be used for any pump.

4.5.3 Discussion

The imbalance involves variation of vibrations amplitudes. For pump with double supports, from the point of view of vibrations, it can occur three possible cases of imbalance:

case 1) $\frac{V_{DE}}{V_{NDE}} \leq 1$; case 2-a) $1 < \frac{V_{DE}}{V_{NDE}} < 2$; case 2-b) $2 \leq \frac{V_{DE}}{V_{NDE}}$

where : V_{DE}: Vibration amplitude on support drive end ; V_{NDE}: Vibration amplitude on support non-drive end.

Our hypothesis is based on the case 2-b), in which the amplitude of the vibrations measured on the pumps support near the coupling is at least 2 times higher than that measured on the other support.

The others two cases of unbalance (1 and 2-a) have not been investigated formally. However it is clear from theoretical study that in the case 1 a corrective action on CHP cannot solve the imbalance problem; in this case you need a "normal balancing method". On the contrary, in the case 2-a, the corrective action on CHP could reduce the imbalance effect and may have the desired effect but also the opposite.

In the cases of imbalance occurred on the *MSCP* subject of this study, more than 85% of the rotor unbalance were caused by the dirt, and almost always the vibrations that result are in conformity with the case 2-b. Whereas this method avoids at least five days to stop, so avoids missing production which is approximately 50,000€/day, and the maintenance cost € 20,000, the saving make in each intervention is **270,000 €.**

The approach set out in this study allows to solve the unbalance due to exercise product dirt in the shortest possible time, reducing the time required to an hour on average. It allows you to bring the machine in acceptable reliability conditions. But it not replaces definitely the normal balancing which is made eventually necessary in the unbalance cases due to wear, deformations, shifts to the assembled elements…, and in the context of a general review planned.

Conclusion

The rotating machinery vibration problems remain a concern despite progress in recent years in their design. The imbalances are an important cause. The literature review highlights the interest of designing balancing approaches that reduce the machines downtime so that to minimize the production loss generated in industrial plants.

This study established a method of on-site balancing of MSCP, which ordinarily can't be balanced on site because the rotor is only accessible with the disassembly of the pump. Nevertheless we demonstrate that in determined hypothesis of unbalanced condition ($2 \leq \frac{W_{DE}}{W_{NDE}}$), we can take the CHP as compensation plane, and we obtain a good success. In the MSCP, this hypothesis occurs in the greater part of the cases of unbalance problem (over 85%) frequently caused the dirt.

Two approaches had been adopted: the "One Plane Balancing and two support " approach and the "One Plane Balancing and one support " approach. Both of them are efficient. The second approach has the advantage to be relatively more simple and more easily applicable.

References

[1] W. Kellenberger, *"Should a flexible rotor be balanced in n or (n+2) planes?"* Journal of Engineering for Industry ASME 94 (2) (1972) 548–560.

[2] J. Drechsler; *"Processing surplus information in computer aided balancing of large flexible rotors";* Institution of Mechanical Engineers Conference on Vibrations in Rotating Machinery, Cambridge, 1980; UK, 65-70.

[3] P. Gnilka; *"Modal balancing of flexible rotors without test runs: an experimental investigation".* 1983 Journal of Vibration 90, 157-172.

[4] J.M. Krodkiewski, J. Ding and N. Zhang. *"Identification of unbalance change using a non-linear mathematical model for rotor bearing systems";* 1994 Journal of Vibration 169, 685-698.

[5] S. Edwards, A.W. Lees and M.I. "*Experimental Identification of Excitation and Support Parameters of a Flexible Rotor-Bearings-Foundation System from a Single Run-Down";*Friswell 2000 Journal of Sound and Vibration, 232(5), 963-992.

[6] R. Tiwari, *"Conditioning of Regression Matrices for Simultaneous Estimation of the Residual Unbalance and Bearing Dynamic Parameters";* 2005, Mechanical System and Signal Processing.

[7] Jacques MOREL ; *"Surveillance Vibratoire Et Maintenance Prédictive"*, Département surveillance diagnostic maintenance à EDF, Division recherches et développement Référence R6100 (2002)

[8] R.E.D. Bishop, G.M.L. Gladwell, The vibration and balancing of an unbalanced rotor, Journal of Mechanical Engineering Science 1 (1) (1959) 66–67.

[9] S. Saito, T. Azuma, "*Balancing of flexible rotors by the complex modal method",* Journal of Vibration, Acoustics Stress and Reliability in Design ASME 105(1983) 94–100.

[10] Shimada, K. Fujisawa, F., "*Balancing method of multi-span, multi-bearings rotor system".* Bulletin of the JSME, 1980, 23(185) 1894 1898.

[11] Saito, S. and Azuma, T., "*Balancing of flexible rotors by the complex modal method".* ASME Journal of

Vibration, Acoustics, Stress and Reliability in Design, 1983, 105, 94 100.

[12] Gnielka P., "*Modal Balancing of Flexible Rotors without Test Runs : an Experimental Investigation"*, Journal of Sound and Vibration, 1993, Vol. 90, N°2, pp. 157-172.

[13] Markert R., "*Modal Balancing of Flexible Rotors with Data Acquisition from Non-stationary Run-up and Run-down".* International Modal Analysis Conference, 6 th , Kissimmee (FL), feb. 1-4 1988, Vol. 1, pp. 210-216.

[14] T.P. Goodman, "*A least-square method for computing balance corrections",* Journal of Engineering For Industry Series ASME 86 (3) (1964) 273–279.

[15] J.W. Lund, J. Tonnesen, " *Analysis and experiments on multi-plane balancing of flexible rotors",* Journal of Engineering for Industry ASME (1972) 233–242.

[16] J.M. Tessarzik, R.H. Badgley, W.J. Anderson, "*Flexible rotor balancing by the exact point–speed influence coefficient method",* Journal of Engineering for Industry Series B ASME 94 (1) (1974) 148–158.

[17]. Tessarzik, J. M. and Badgley, R. H., "*Experimental evaluation of the exact point-speed and least-squares procedures for flexible rotor balancing by the influence coefficient method".* ASME Journal of Engineering for Industry', Series B, 1974, 96(2) 633-643

[18]. Tessarzik, J. M., Badgley, R. H. and Fleming, D. P., "*Experimental evaluation of multiplane-multispeed rotor balancing through multiple critical speeds".* ASME Journal of Engineering for Industry, 1976, 988 998.

[19] Goodman T. P., A Least-Squares "*Method for Computing Balance Corrections"*, ASME Journal of Engineering for Industry, August 1964, pp.273-279.

[20] Mahfoudh j., Der Hagopian J., Cadoux J., "*Equilibrage Multiplans-Multivitesses avec des contraintes Imposées sur les déplacements",* Matériaux Mécanique Electricité, sept. 1988, N°427, pp. 38-42.

[21] Mahfoudh J., " *Contribution à l'équilibrage de machines tournantes"*, Thèse de doctorat de l'INSA-Lyon, 1990, 139 p.

[22] Bigret R., Karajani p., Vialard s., Chevalier R., "*Machines tournantes. Détermination des coefficients d'influence par les caractéristiques modales* , Revue française de mécanique, 1995, N°4, pp. 277-283.

[23] Chevalier R., Bigret R., Karajani P., Vialard s., "*Equilibrage des machines tournantes par coefficients d'influence à l'aide de modèles numériques"* , Revue française de mécanique, 1995, N°4, pp. 285-292.

[24] A.G. Parkinson, M.S Darlow, A.J. Smalley*, "A theoretical introduction to the development of unified approach to flexible rotor balancing"*, Journal of Sound and Vibration 68 (4) (1980) 489–506.

[25] S.G. Tan, X.X Wang, "*A theoretical introduction to low speed balancing of flexible rotors: unification and development of the modal balancing and influence coefficients techniques"*, Journal of Sound and Vibration 168 (3) (1993) 385–394.

[26] Lee J., Van Moorhem W. K., "*Analytical and Experimental Analysis of a Self-compensating Dynamic Balancer in a Rotating Mechanism,* ASME Journal *of Dynamic Systems, Measurement and Control*, sept. 1996, Vol. 118, pp. 468-475.

[27] Jinouchi Y., Araki y., Inoue J., Ohtsuka Y., Tan c., "*Static Balancing and Transient Response of Multiball-type Automatic Balancer"*, Asia-Pacific Vibration Conférence, Session Rotordynamics, Kytakyushu, Nov. 1993, pp. 493-498.

[28] Shimizu S., Lee H. S., "*Basic study of Self-automatic Balancer for High Speed Spindles"*, London : Institution of Mechanical Engineers, 1992, preprint IMechE C432/050, pp. 569-574.

[29] D.J. Rodrigues a , A.R. Champneys a, M.I. Friswell , R.E. Wilson; "*Experimental investigation of a single-plane automatic balancing mechanism for a rigid rotor"*; Journal of Sound and Vibration 330 (2011) , pp 385–403

[30] D.J. Rodrigues a , A.R. Champneys a, M.I. Friswell , R.E. Wilson; "*Two-plane automatic balancing: A symmetry breaking analysis"*; International Journal of Non-Linear Mechanics 46 (2011) , pp 1139-1154.

[31] K. Green, A.R. Champneys, N.J. Lieven, "*Bifurcation analysis of an automatic dynamic balancing*

mechanism for eccentric rotors"; Journal of Sound and Vibration 291 (2006), pp 861–881.

[32] TADEUSZ M., "*Position Error Occurence in Self-balancers used on Rigid Rotors of Rotating Machinery",* Mechanical and Machine Theory, 1988, Vol.23, N°1, pp. 71-78.

[33] Van De Vegte J., Lake R. T., *"Balancing of Rotating Systems during Operation",* Journal of Sound and Vibration, 1978, Vol. 57, N°2, pp. 225-235.

[34] Van De Vegte J., "*Balancing of Flexible Rotors during Operation"*, Journal of Mechanical Engineering Science, 1981, Vol. 23, N° 5, pp. 257-261.

[35] Bishop R. E. D., "*On the Possibility of Balancing Rotating Flexible Shafts"*, Journal of Mechanical Engineering Science, 1982, Vol. 24, N° 4, pp. 215-220.

[36] Furman B. J., " *a New, Thermally Controlled, Non-contact Rotor Balancing Method"*, ASME Journal of Mechanical Design, 1994, Vol. 116, pp. 823-832.

[37] Zumbach M., Schweitzer g., Schoellhorn K., "*On-Line Thermal Balancing Technique for a Large Turbo-Generator"*, ASME Journal of Vibration and Acoustics, 1992, Vol. 114, N° 1, pp. 60-66.

[38] JENKINS L. S., Vibration "*Performance of a Westinghouse RCP during Continuous Changes in Mass Unbalance at the Pump Coupling",* EPRI Eighth International Workshop on Main Collant Pumps, Pittsburgh (Pennsylvania, US), Sept. 25-27, 1996, 20 p.

[39] Hongwei f., Minqing J., Renchao W., Heng Liu, Jingjuan Zhi; "*New electromagnetic ring balancer for active imbalance compensation of rotating machinery";* Journal of Sound and Vibration 333 (2014), pp 3837–3858.

[40] R. Tiwari, "*Dynamic Balancing Of Rotors",* Department of Mechanical Engineering Indian Institute of Technology Guwahati 781039,

[41] John Harrell, "*Precision Balancing with the CMVA 55 Microlog"* , SKF Reliability Systems 4141 Ruffin Road San Diego, California 92123 USA, CM3028, 1999